REPORT DOCUMENTATION PAGE

Form Approved OMB NO. 0704-0188

1. REPORT DATE (DD-MM-YYYY)	2. REPORT TYPE	3. DATES COVERED (From - To)
27-08-2015	Manuscript	-

4. TITLE AND SUBTITLE	5a. CONTRACT NUMBER
Interspecies Scaling in Blast Pulmonary Trauma	W911NF-10-1-0526
	5b. GRANT NUMBER
	5c. PROGRAM ELEMENT NUMBER
	611103

6. AUTHORS	5d. PROJECT NUMBER
GW Wood, MB Panzer, CA Cox, CR Bass	
	5e. TASK NUMBER
	5f. WORK UNIT NUMBER

7. PERFORMING ORGANIZATION NAMES AND ADDRESSES	8. PERFORMING ORGANIZATION REPORT NUMBER
University of Pennsylvania 3451 Walnut Street, Suite P-221 Philadelphia, PA 19104 -6205	

9. SPONSORING/MONITORING AGENCY NAME(S) AND ADDRESS (ES)	10. SPONSOR/MONITOR'S ACRONYM(S)
U.S. Army Research Office P.O. Box 12211 Research Triangle Park, NC 27709-2211	ARO
	11. SPONSOR/MONITOR'S REPORT NUMBER(S)
	58155-LS-MUR.101

12. DISTRIBUTION AVAILIBILITY STATEMENT

Approved for public release; distribution is unlimited.

13. SUPPLEMENTARY NOTES

The views, opinions and/or findings contained in this report are those of the author(s) and should not contrued as an official Department of the Army position, policy or decision, unless so designated by other documentation.

14. ABSTRACT

Between October 2001 and May 2012 approximately 70% of U.S. military personnel killed in action and 75% wounded in action were the direct result of exposure to an explosion. As of 2008, it was estimated that nearly 20% of all Operation Iraqi Freedom and Operation Enduring Freedom (OIF/OEF) veterans had sustained some form of traumatic brain injury (TBI). Blast exposure is also a civilian problem due to widespread availability of explosives and the increased usage of explosives in terrorist attacks on civilians. Before 2005, blast injury research focused on the pulmonary system and the other air-containing organs which have been shown to be susceptible to blast

15. SUBJECT TERMS

Interspecies scaling, blast, pulmonary trauma

16. SECURITY CLASSIFICATION OF:			17. LIMITATION OF ABSTRACT	15. NUMBER OF PAGES	19a. NAME OF RESPONSIBLE PERSON
a. REPORT	b. ABSTRACT	c. THIS PAGE	UU		David Meaney
UU	UU	UU			19b. TELEPHONE NUMBER
					215-573-3155

Interspecies Scaling in Blast Pulmonary Trauma

ABSTRACT

Between October 2001 and May 2012 approximately 70% of U.S. military personnel killed in action and 75% wounded in action were the direct result of exposure to an explosion. As of 2008, it was estimated that nearly 20% of all Operation Iraqi Freedom and Operation Enduring Freedom (OIF/OEF) veterans had sustained some form of traumatic brain injury (TBI). Blast exposure is also a civilian problem due to widespread availability of explosives and the increased usage of explosives in terrorist attacks on civilians. Before 2005, blast injury research focused on the pulmonary system and the other air-containing organs which have been shown to be susceptible to blast overpressure injury. A shift in injury pattern during recent conflicts is characterized by decreased incidence of pulmonary injuries relative to TBI thought to be associated with blast exposure. This increase in observation of blast TBI has resulted in a large research effort to understand mechanisms and thresholds. However, due to the relatively sudden shift, much of this research is being conducted without a proper understanding and consideration of blast mechanics and interspecies scaling effects.

This dissertation used experimental and computational finite element (FE) analysis to investigate some of the important questions surrounding blast TBI research. These key issues include the effects of body armor usage on blast trauma risk, the effect of interspecies differences on in vivo animal model research, and the effects of interspecies scaling on current and future in vivo animal model experimentation for blast trauma. An experimental investigation was conducted to determine the effects of modern thoracic body armor usage on blast pressure exposure seen in the lungs and gut. To improve FE modeling capabilities, brain tissue mechanics in common blast TBI animal model species were investigated experimentally and computationally to determine viscoelastic constitutive behavior and measure interspecies variation of the brain properties. To improve our understanding of blast pulmonary trauma risk and appropriate interspecies scaling a meta-analysis of blast pulmonary literature was conducted to update interspecies scaling and injury risk models. Finally, to derive interspecies scaling and injury risk models for blast neurotrauma endpoints a meta-analysis of existing experimental data was used.

This dissertation makes major contributions to the field of injury biomechanics and blast injury research. Research presented in this dissertation showed that modern thoracic body armor can lower the risk of pulmonary injury from blast exposure by attenuating and altering blast overpressure. The study shows that the use of soft body armor can attenuate peak overpressure levels by a factor of up to 14 in the tested range and results in the pulmonary injury threshold being similar to that for neurotrauma. The use of hard body armor can attenuate peak overpressure levels by a factor of up to 57 in the tested range and results in the threshold for pulmonary injury occurring at higher levels than that of neurotrauma. This finding is important, as it helps to explain the recent shift in injury types observed and highlights the importance of continued widespread usage of body armor not only for ballistic protection but for protection from blast as well.

This dissertation also shows the importance of interspecies scaling for investigation of blast neurotrauma. This work looks at existing in vivo animal model data to derive appropriate scaling across a wide range of brain size. Appropriate scaling for apnea occurrence and fatality for blast isolated to the head was found to be approximately equal to a characteristic length scaling of brain size, assuming spherical brain shape. Power law scaling for overpressure duration, based on a ratio of brain mass to a human brain mass, was found to have a scaling exponent, α, of 0.336 for apnea risk. Similarly, for neurotrauma fatality risk, scaling exponents were found to be 0.316 and 0.080 for overpressure duration and and peak overpressure scaling, respectively. By combining the interspecies scaling developed and existing tests data, injury risk models were derived for short overpressure duration blast exposures. The contributions and conclusions of this dissertation serve to inform the injury biomechanics field and to improve future research efforts. The consideration by researchers of the recommendations presented in this dissertation for in vivo animal model testing will serve to maximize the value gained from experimentation and improve our understanding of blast injury mechanisms and thresholds. The injury risk

models presented in this work help to improve our ability to prevent, diagnose, and treat blast neurotrauma.

Interspecies Scaling in Blast Neurotrauma

by

Garrett Wayne Wood

Department of Biomedical Engineering
Duke University

Date:_____

Approved:

_____
Cameron R. Bass, Supervisor

_____
Barry S. Myers

_____
Roger W. Nightingale

_____
Edward J. Shaughnessy

_____
Bruce P. Capehart

Dissertation submitted in partial fulfillment of
the requirements for the degree of Doctor
of Philosophy in the Department of
Biomedical Engineering in the Graduate School
of Duke University

2015

ABSTRACT

Interspecies Scaling in Blast Neurotrauma

by

Garrett Wayne Wood

Department of Biomedical Engineering
Duke University

Date:_____
Approved:

_____
Cameron R. Bass, Supervisor

_____
Barry S. Myers

_____
Roger W. Nightingale

_____
Edward J. Shaughnessy

_____
Bruce P. Capehart

An abstract of a dissertation submitted in partial
fulfillment of the requirements for the degree
of Doctor of Philosophy in the Department of
Biomedical Engineering in the Graduate School of
Duke University

2015

Abstract

Between October 2001 and May 2012 approximately 70% of U.S. military personnel killed in action and 75% wounded in action were the direct result of exposure to an explosion. As of 2008, it was estimated that nearly 20% of all Operation Iraqi Freedom and Operation Enduring Freedom (OIF/OEF) veterans had sustained some form of traumatic brain injury (TBI). Blast exposure is also a civilian problem due to widespread availability of explosives and the increased usage of explosives in terrorist attacks on civilians. Before 2005, blast injury research focused on the pulmonary system and the other air-containing organs which have been shown to be susceptible to blast overpressure injury. A shift in injury pattern during recent conflicts is characterized by decreased incidence of pulmonary injuries relative to TBI thought to be associated with blast exposure. This increase in observation of blast TBI has resulted in a large research effort to understand mechanisms and thresholds. However, due to the relatively sudden shift, much of this research is being conducted without a proper understanding and consideration of blast mechanics and interspecies scaling effects.

This dissertation used experimental and computational finite element (FE) analysis to investigate some of the important questions surrounding blast TBI research. These key issues include the effects of body armor usage on blast trauma risk, the effect of interspecies differences on in vivo animal model research, and the effects of

interspecies scaling on current and future in vivo animal model experimentation for blast trauma. An experimental investigation was conducted to determine the effects of modern thoracic body armor usage on blast pressure exposure seen in the lungs and gut. To improve FE modeling capabilities, brain tissue mechanics in common blast TBI animal model species were investigated experimentally and computationally to determine viscoelastic constitutive behavior and measure interspecies variation of the brain properties. To improve our understanding of blast pulmonary trauma risk and appropriate interspecies scaling a meta-analysis of blast pulmonary literature was conducted to update interspecies scaling and injury risk models. Finally, to derive interspecies scaling and injury risk models for blast neurotrauma endpoints a meta-analysis of existing experimental data was used.

This dissertation makes major contributions to the field of injury biomechanics and blast injury research. Research presented in this dissertation showed that modern thoracic body armor can lower the risk of pulmonary injury from blast exposure by attenuating and altering blast overpressure. The study shows that the use of soft body armor can attenuate peak overpressure levels by a factor of up to 14 in the tested range and results in the pulmonary injury threshold being similar to that for neurotrauma. The use of hard body armor can attenuate peak overpressure levels by a factor of up to 57 in the tested range and results in the threshold for pulmonary injury occurring at higher levels than that of neurotrauma. This finding is important, as it helps to explain

the recent shift in injury types observed and highlights the importance of continued widespread usage of body armor not only for ballistic protection but for protection from blast as well.

This dissertation also shows the importance of interspecies scaling for investigation of blast neurotrauma. This work looks at existing in vivo animal model data to derive appropriate scaling across a wide range of brain size. Appropriate scaling for apnea occurrence and fatality for blast isolated to the head was found to be approximately equal to a characteristic length scaling of brain size, assuming spherical brain shape. Power law scaling for overpressure duration, based on a ratio of brain mass to a human brain mass, was found to have a scaling exponent, α, of 0.336 for apnea risk. Similarly, for neurotrauma fatality risk, scaling exponents were found to be 0.316 and 0.080 for overpressure duration and and peak overpressure scaling, respectively. By combining the interspecies scaling developed and existing tests data, injury risk models were derived for short overpressure duration blast exposures.

The contributions and conclusions of this dissertation serve to inform the injury biomechanics field and to improve future research efforts. The consideration by researchers of the recommendations presented in this dissertation for in vivo animal model testing will serve to maximize the value gained from experimentation and improve our understanding of blast injury mechanisms and thresholds. The injury risk

models presented in this work help to improve our ability to prevent, diagnose, and

treat blast neurotrauma.

Dedication

This dissertation is dedicated the most beautiful and patient woman that I know, my wife Jessica. I likely would not have survived graduate school without her support. No matter how tough and frustrating the work in this dissertation was, she was always there as my #1 supporter and cheerleader. Jessica, I love you and appreciate everything that you do.

Contents

List of Tables

List of Figures

Acknowledgements

I wish to acknowledge my advisor and mentor, Dale Bass, for his endless advice and guidance through my graduate career. I'll be eternally grateful for all of the wisdom and sage advice he has provided to me. His passion and enthusiasm for science and research has motivated and inspired me. I would also like to acknowledge my other advisors for their guidance. Thank you to Bruce Capehart for your clinical perspective along with your friendship. Thank you to Roger Nightingale for your advice and help since my undergraduate days long ago. I greatly appreciate Edward Shaughnessy and Barry Myers for sharing some of your knowledge and allowing me honor to work with you.

I've been blessed with a wonderful group of people in the Injury Biomechanics Lab here at Duke. A big thank you to Kyle Matthews and Jason Kait for keeping things running. Thank you to all of my labmates for your help and friendship over the last few years. Thank you to Matthew Panzer for your help and guidance in my early graduate career. I'd like to specially acknowledge Brian Bigler for all of your FE expertise and help completing my dissertation work.

I would like to acknowledge my family for all of the support and encouragement they have given me to pursue and complete my PhD. Without the guidance of my parents, Andy and Lisa, I wouldn't be where I am today and I can't thank you enough. I would especially like to thank my grandparents and my brother and sister, A.J. and

Candice, for their encouragement to pursue my academic goals and for their never ending love and support. Thank you to the Nances for your confidence in me and support. The rest of my family and close friends have stayed with me through this long PhD journey and I thank them for that. Most of all I want to acknowledge my wife Jessica for your understanding and sacrifice through my long nights in the lab and missed suppers. There is no way I could thank all of those I've mentioned enough and I will be forever grateful.

Chapter 1 - Introduction

1.1 Statement of the Problem

Military conflict has long been a driving force in injury biomechanics research. That focus has changed as the nature of conflicts and tactics have changed. Recently, potentially injurious exposures to U.S. personnel in Operation Iraqi Freedom (OIF) and Operation Enduring Freedom (OEF) have been dominated by improvised explosive devices (IEDs) and other explosive munitions (Taber et al. 2006). As of 2008, approximately 81% of all OIF/OEF injuries were the result of exposure to blast (Owens et al. 2008). According to the U.S. Department of Defense, 7 of 10 killed in action and 3 of 4 wounded in action between October 2001 and May 2012 were the result of explosions (Statistics 2012). Many of these injuries were classified as traumatic brain injury (TBI). Approximately 88.5% of blast related injuries treated at Walter Reed Army Medical Center included some form of closed-head injury (Warden 2006). As of 2008 it was estimated that approximately 19% or 320,000 OIF/OEF veterans had sustained a TBI (Tanielian et al. 2008). In 2011 a total of 32,591 U.S. service members sustained some form of TBI (Bagalman 2013). Realistically, the actual numbers of TBI are likely higher due to under-detection and under-reporting.

The problem of blast-related injury is not solely a military issue alone. Civilians exposed to explosive events are often at a higher risk of injury due to the lack of protective clothing and equipment. In Iraq and Afghanistan alone between October of

2001 and July of 2011, 3,238 civilian fatalities were attributed to blast (SIAD). The use of explosives by various groups targeting civilians has increased across the world. For example, between 2001 and 2011 a few select large scale terrorist bombings account for 575 civilian fatalities in Bali, Indonesia (Brolén et al. 2007), Baghdad, Iraq (SIAD), Istanbul, Turkey (Rodoplu et al. 2004), Madrid, Spain (Gómez et al. 2007), London, England (Lockey et al. 2005), and six separate events in Israel (Mekel et al. 2009).

There has been a recent increase in observation of TBI, with an apparent corresponding decrease in blast injuries to the pulmonary system (Owens et al. 2008). It is theorized that this is a direct result of widespread usage of improved personnel protective equipment and clothing. High areal density ballistic protective vests and especially those included hard ceramic inserts are thought to significantly decrease the blast wave seen by the thorax. This was the source of some controversy, unknown prior to 2010, and is definitively addressed in this dissertation. Alternatively, current military helmet design provides relatively little protection against blast pressure, especially at the open face. This allows for the observation of blast head injury in cases where extensive pulmonary injury would have resulted in fatality or otherwise would have been priority in patient care. The blast pressure attenuation capabilities of modern thoracic body armor is assessed as part of this dissertation.

There are many challenges associated with blast neurotrauma research, especially when deriving human data from epidemiology. Blast is highly directional

and it is often difficult to recreate the details surrounding an explosive event. Modeling

or simulating the blast dosage that resulted in known injury to personnel is a tool to

assess human tolerance and predict the outcome of future events. However, recreating a

blast event requires close approximations of details including explosive charge size,

distance from the charge (standoff), personal protective equipment, and any immediate

injury response such as loss of consciousness (LOC) or apnea.

Further complicating blast neurotrauma research is the difficulty in reliably

identifying blast-related TBI in humans, especially for mild severity, and separating

organic neurotrauma from comorbid physical and psychiatric conditions. Though mild,

moderate, and severe blast TBI and fatality are clear and have been recreated in a lab

setting with animal models (Rafaels et al. 2011, Rafaels et al. 2012), there is no universal

agreement on the pathologic relationship between blast TBI in animal models and mild

TBI occurring in military personnel (e.g. Bell 2008). In addition, diagnoses of blast

neurotrauma is often masked or clouded by other blast effects such as injury to

additional organ systems, penetrating trauma, and blunt trauma. The brain is especially

difficult to assess due to the contribution of post-injury inflammatory response to acute

and chronic tissue injury (Denes et al. 2010).

In military settings, the presence of post traumatic stress disorder (PTSD) or

comorbid PTSD adds to the difficulties associated with neurotrauma diagnoses

(Capehart et al. 2012). It has been shown that PTSD can occur in the combat

environment with and without mild TBI (Zatzick et al. 2010). PTSD in addition to mild

TBI has also been shown to increase post-concussive symptoms (Brenner et al. 2010).

The overlapping symptomology between PTSD and mild TBI has resulted in

misdiagnosis (Stein et al. 2009). Other comorbid psychiatric conditions like major

depression and alcohol or drug abuse are often associated with PTSD and TBI diagnoses

(Seal et al. 2011). To improve the identification of blast neurotrauma advances in

imaging, histochemical measures, and biomarkers are essential.

One of the largest areas of uncertainty in blast neurotrauma research is

interspecies scaling of blast effects. One of the most important tools we have in blast

injury research is relating pathophysiological response in an in vivo animal model to the

expected human response (Bass et al. 2012). Scaling establishes a dose-response

relationship between animals and humans. Methodologically, we must ensure that the

proper blast dose is being administered to replicate the desired human equivalent

exposure. Without appropriate scaling, there is no way to establish human injury

criteria from in vivo animal models. Without interspecies scaling there is no way to

verify that the blast dosage in the model represents that of interest or even corresponds

to a level realistically seen in combat or other blast exposure scenarios.

The current uncertainty in blast neurotrauma scaling leads to some major

questions in research. What scaling is appropriate for the use of animal models for blast

neurotrauma? How well does current literature model appropriate blast exposure

levels? What can be concluded about injury risk and interspecies scaling from current

blast injury literature? This dissertation seeks to discuss and answer these questions.

1.2 Clinical Relevance

As already discussed, blast related neurotrauma is an important problem for the

injury biomechanics field and our understanding of closed-head blast injury is limited.

A better understanding of blast trauma is important clinically, for improved diagnosis,

categorization, and treatments. Traumatic brain injury is typically categorized as mild,

moderate, or severe. A description of graded TBI as defined by the U.S. Department of

Veterans Affairs is presented in Table 1-1 (Bagalman 2013).

Table 1-1: Identifying characteristics of graded TBI (Bagalman 2014).

	Mild	Moderate	Severe
Loss of Consciousness (LOC)	< 30 minutes	30 minutes – 24 hours	> 24 hours
Post-traumatic amnesia	< 1 day	1 – 7 days	> 7 days
Glasgow Coma Scale (GCS)	13 - 15	9 - 12	3 – 8

Mild TBI is associated with sleep disturbance, anxiety, irritability, concentration

difficulties, and cognitive impairments (Capehart et al. 2012). Moderate TBI is further

associated with extended LOC and posttraumatic amnesia. Severe TBI also results in

extended LOC, a larger period of amnesia, and is often associated with coma. As

discussed, the diagnosis of mild TBI is especially complicated by comorbid disorders

like anxiety disorder, depression, and substance abuse (Masel et al. 2010). A patient

subject to blast and reporting symptoms such as insomnia, irritability, and loss of

concentration are difficult to diagnose. Proper diagnosis is vital to providing the proper treatment in a timely manner to maximize positive outcomes. These challenges highlight the importance of focused research on proper human equivalent exposures to further our understanding of injury mechanisms and injury endpoints to improve diagnosis and treatment.

1.3 Specific Aims

This dissertation seeks to discuss some of the large questions in current blast injury research. The work seeks to improve the utility and application of existing research, especially that involving in vivo animal models. This will be achieved through the experimental and computational research techniques. The specific aims of this dissertation include:

1. Experimentally investigate the ability of modern ballistic body armor to protect the human thorax from primary blast loading, and evaluate its contribution to the decreased observation of blast pulmonary injury and increased observation of blast neurotrauma in military settings.

2. Complete a meta-analysis of the existing blast brain and pulmonary injury literature to collect response and pathophysiology data to augment data available at Duke, and to examine existing techniques and potential scaling procedures based on available input parameters including blast overpressure

and overpressure duration and available pathophysiological response to derive injury criteria.

3. Conduct tissue mechanical characterization of common in vivo animal model species across size scales from both lissencephalic and gyrencephalic species to supplement existing tissue property data.

The major contributions of this work will be to develop and provide appropriate interspecies scaling for blast trauma applications. Additionally, this dissertation will assess the current body of blast injury research to highlight weaknesses and challenges and provide recommendations to improve blast injury research methodology to maximize the useful information produced. he results of this work serve to aid in the experimental design, present blast injury criteria, and help to improve clinical ability to assess risk and design appropriate protective equipment for blast exposure.

Chapter 2 - Literature Review

2.1 Blast Physics

The physics associated with blast is different from that associated with lower rate blunt impact which widely studied in injury biomechanics. Injurious blunt impact to the head typically has realtively large momentum transfer over 5-100ms, while short duration injurious blasts can have small momentum transfer over 1-5ms. This section describes the basic production of shock waves and how they interact with bodies. Also discussed within this section is the characterization of shock waves for use in blast research and common experimental techniques to produce blast loading.

2.1.1 Characterization and Measurement of Shock Waves from Blast

The term shock wave and blast wave will be used interchangeably for the purpose of this discussion, meaning propagation of a shock wave through air from an explosive source. Blast waves have some basic characteristics including a wave front that is moving faster than the speed of sound in the material (generally air or water) and a near discontinuous pressure, density, and temperature change called shock. These waves are associated with large accelerations and velocities of gas particles, but the local particle velocity is much smaller than the wave propagation that occurs across the material (Iremonger 1997). Idealized simple pressure waves are most often used for blast injury research. These types of waves occur in the free-field or in properly designed experimental apparatus without the presence of reflecting surfaces. This type

of waveform is often used to easily describe and reproduce blast dosage consistently.

The introduction of structures and reflecting surfaces that are common in real-world

scenarios produces a more complex waveform that is more difficult to characterize. A

representation of a simple and complex waveform as presented in Figure 2-1.
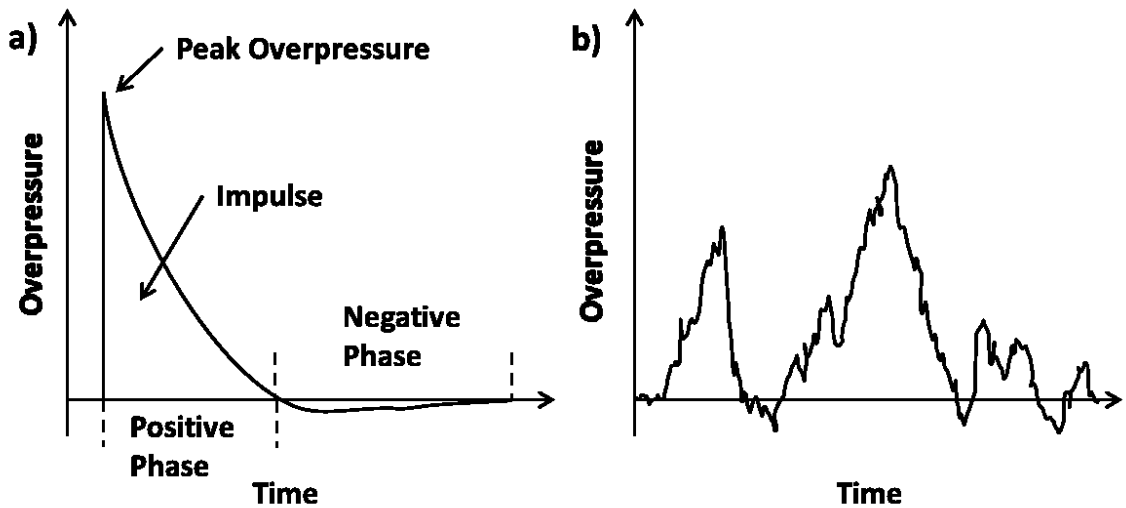
**Figure 2-1: Representation of blast pressure waveforms a) simple Friedlander and b) a
more difficult to characterize complex wave generally resulting in greater pressure
impulse.**

The idealized, simple pressure-time history shown in Figure 2-1a is referred to as

a Friedlander pressure waveform (Iremonger 1997). When measured at a fixed standoff

distance from the initiation of the blast, the pressure time history has a near

discontinuous jump followed by exponential decay. This is known as the positive

phase. After a zero crossing, the pressure time history becomes negative before

returning to ambient pressure. The waveform can be described by several important

characteristics. The peak overpressure is the maximum value of pressure seen at this

9

location. The overpressure duration is the length of time over which the positive phase

of the pressure wave occurs. Finally, the overpressure impulse is a measure of the

energy contained within the blast wave and is the integral of the positive phase in

pressure and time. The impulse and peak of the negative phase of the blast wave is

small relative to the positive phase for common blast exposures and properly designed

research tools. The simple waveform can be described by the Friedlander equation

presented below (Equation 2-1).

$$P(t) = P_{max}\left(1 - \frac{t}{\Delta t}\right)e^{-\frac{t}{\alpha}}$$
　　　　　　　　　　　　　　Equation 2-1

Where Pmax is the peak overpressure, Δt is the overpressure duration, α is the decay

coefficient, and t is the time after arrival of the shock. With increased standoff distance

from an explosive charge, the peak pressure decreases while the overpressure duration

generally increases. Peak pressure, overpressure duration, and impulse are the most

common descriptors of the waveform for blast research purposes.

Measurement technique is an important consideration for blast research. This

includes consistent methodology and reporting of the measurement of pressure waves

(Bass et al. 2012). Measurement of a moving (shocked) pressure wave can be made in

two primary ways. The first is incident, or side-on, measurement where the direction of

wave travel is parallel to the sensor surface. Alternatively, reflected, or face-on,

measurements can be made where the direction of wave travel is perpendicular to the

sensor surface. These two orientations are depicted in Figure 2-2.
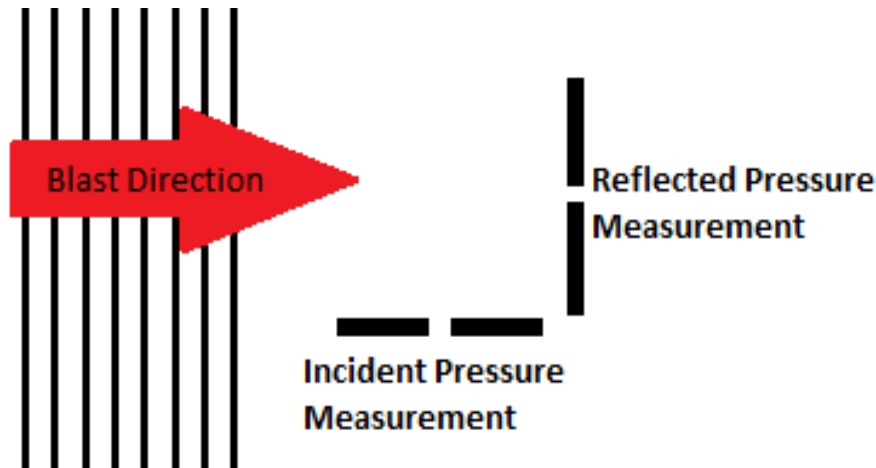
Figure 2-2: Incident versus reflected pressure measurement orientations. Reflected measurement results in 2 to 8 times higher magnitude when ideal gas is assumed.

Correct identification and reporting of measurement type is vital since reflected measurements result in a different magnitude for the same blast wave. The measured pressure magnitude for reflected waves is 2 to 8 times higher when ideal gas is assumed and can exceed 20 times higher when deviations from ideal gas occur (Iremonger 1997). Assuming ideal gas behavior and utilizing conservation of energy and momentum, shock conditions can be applied to derive a relation between incident and reflected pressure (Equation 2-2).

$$\frac{\widehat{P}_{Ref}}{\widehat{P}_{Inc}} = \frac{P_{Ref}-P_{Atm}}{P_{Inc}-P_{Atm}} = \frac{\left[2\frac{\gamma-1}{\gamma+1}+1\right]\frac{P_{Inc}}{P_{Atm}}+1}{\left(\frac{\gamma-1}{\gamma+1}\right)\frac{P_{Inc}}{P_{Atm}}+1} \qquad \textbf{Equation 2-2}$$

Where P_{ref} is the reflected overpressure, P_{inc} is the incident overpressure, P_{atm} is the atmospheric or ambient pressure, and γ is the heat capacity ratio for the gas. For shock in air this relation can be further simplified to Equation 2-3.

$$\widehat{P}_{Ref} = 2\widehat{P}_{Inc}\frac{7P_{Atm}+4\widehat{P}_{Inc}}{7P_{Atm}+\widehat{P}_{Inc}} \qquad \textbf{Equation 2-3}$$

This is referred to as the Rankine-Hugoniot relations and can be used to convert incident to reflected pressure and vice versa (Iremonger 1997).

Insufficient description of the pressure measurement methodology used, or completely ignoring the effects, makes the interpretation of some research result challenging or impossible. Some studies directly compare incident measurements in the free-field to reflected measurements on the surface or within a test object and misleadingly report this as pressure amplification or enhancement (Moss et al. 2009, Alley et al. 2011). Incident pressure measurement without an object impeding the flow is generally desired as it is independent of the size or shape objects in the blast field. However, the incident pressure measurement does not include the dynamic component of the pressure wave which may be important if the wave is not Friedlander in form.

2.1.2 Free-Field Testing

Free-field testing is the use of high explosives to generate blast waves for research. High explosives are characterized by detonation with supersonic combustion of the constituents. High explosives used are commonly trinitrotoluene (TNT), pentaerythritol tetranitrate (PETN), or other plastic explosives such as C-4, Semtex or Composition B. High explosives are rated by their equivalent weight of TNT and that is how they will be described in this dissertation. Charge weight and standoff distance can be used to determine the characteristics of the resulting ideal blast wave. Free-field testing is often performed with no reflecting structures or barriers to minimize

reflections and complexity of the resulting wave as this is shown to exacerbate injury (Richmond et al. 1985, Panzer et al. 2012d).

When explosives are isolated from the ground or other objects, the air blast wave travels away from the charge in a spherical manner. Typically in blast research the charge is placed in one of two different configurations. The charge may be placed on the ground where the resulting blast wave is essentially hemispherical and is typical of the threat from an IED or roadside explosive placed on the ground or shallowly buried. Alternatively, the charge may be suspended above the ground. In this case the spherical wave interacts with the ground to form reflections. These reflections travel faster than the incident wave and intersect to form a triple point and a mach stem. Within the region of the mach stem the peak pressure is approximately double that of the incident wave due to the ground reflection interaction (Iremonger 1997). A diagram of the wave interactions from a suspended charge are shown in Figure 2-3. To avoid uncertainties with ground interactions the blast pressure dose at the test location should be reported for suspended charges.
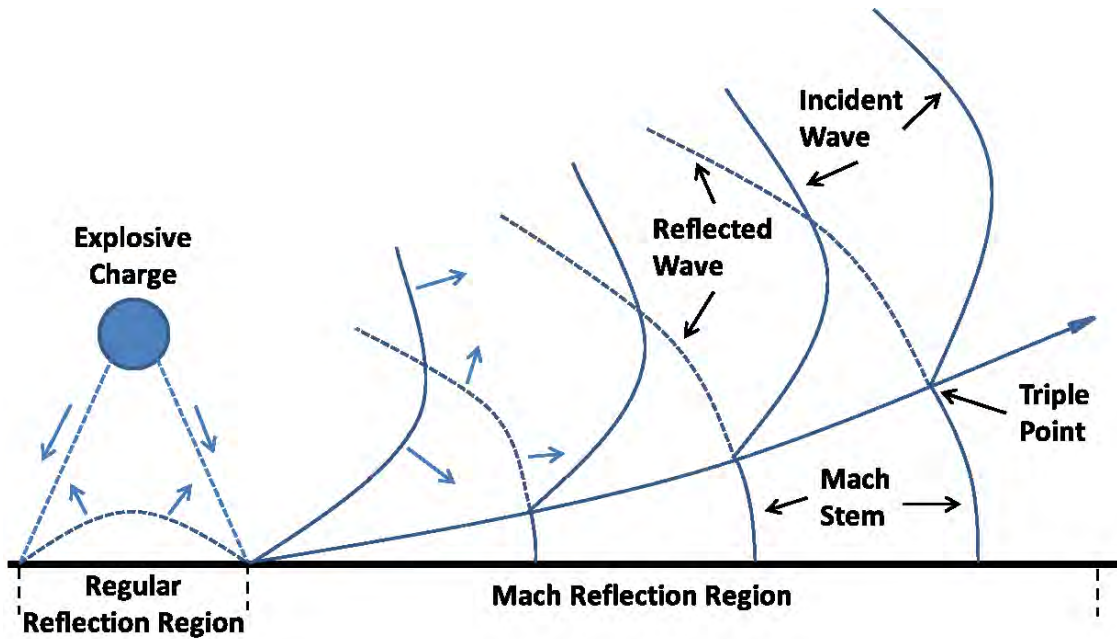
Figure 2-3: Blast wave form and interactions from a suspended explosive charge. Overpressure exposure can be complicated by interactions with the ground [adapted from (Bass et al. 2012)].

The peak pressure and overpressure duration are uniquely determined by the size of the charge and standoff distance. A single set of empirical blast curves determine these characteristics. The blast scaling law dictates that distance and time of the blast scale with the cubed root of the charge weight. Additionally, the peak pressure is constant for a given scaled distance (Baker 1973). This is referred to as Hopkinson scaling and is described by the set of three equations below.

Scaled Distance:	$Z = {R}/{W^{1/3}}$	**Equation 2-4**
Scaled Duration:	$\tau = {t}/{W^{1/3}}$	**Equation 2-5**
Scaled Impulse:	$\xi = {I}/{W^{1/3}}$	**Equation 2-6**

Where R is the standoff distance (meters), W is the equivalent TNT charge weight (kg), t is the overpressure duration (ms), and I is the incident impulse (kPa-ms). This scaling can be used to calculate blast parameters given sufficient data. Hopkinson scaling is validated over a very large range of charge size.

The advantage to using free-field testing techniques is that it provides an complete representation and replication of blast events. However, free-field testing is relatively expensive, time-consuming, dangerous, and it is often difficult to isolate the effects of primary blast for research purposes.

2.1.3 Shock Tube Testing

A more commonly used laboratory tool for the generation of blast waves is the shock tube (Figure 2-4). Gas-driven shock tubes can be designed and tuned to create a wide range of blast wave conditions. The experimental apparatus is composed of a long tube with two sections divided by a frangible membrane. One section, the driver, is filled with high pressure gas until the diaphragm separating it from the driven section spontaneously or is manually burst. The large difference in pressure sends a normal shock wave into the low pressure driven section.

The rupture of the membrane between the high pressure driver and low pressure driven section creates a compression wave which travels into the stationary driven gas. The local speed of sound increases within the compression wave causing the tail end of the compression wave to catch the front end resulting in a buildup and shock formation.

15

Simultaneously, an expansion wave travels back into the high pressure driver gas and

reflects off of the back wall of the tube. This expansion wave then travels down the

driven section forming an expansion fan that erodes the pressure wave. This interaction

is necessary to form the simple Friedlander waveform. If the driver section is too long

compared to the driven section, or a gas with a low speed of sound is used, the

expansion fan has insufficient time/distance to catch up to the wavefront. This results in

a pressure waveform with a plateau, containing greater impulse for a given peak

pressure and overpressure duration. A simple shock tube schematic is presented along

with representative Friedlander and plateaued waveforms in Figure 2-4.
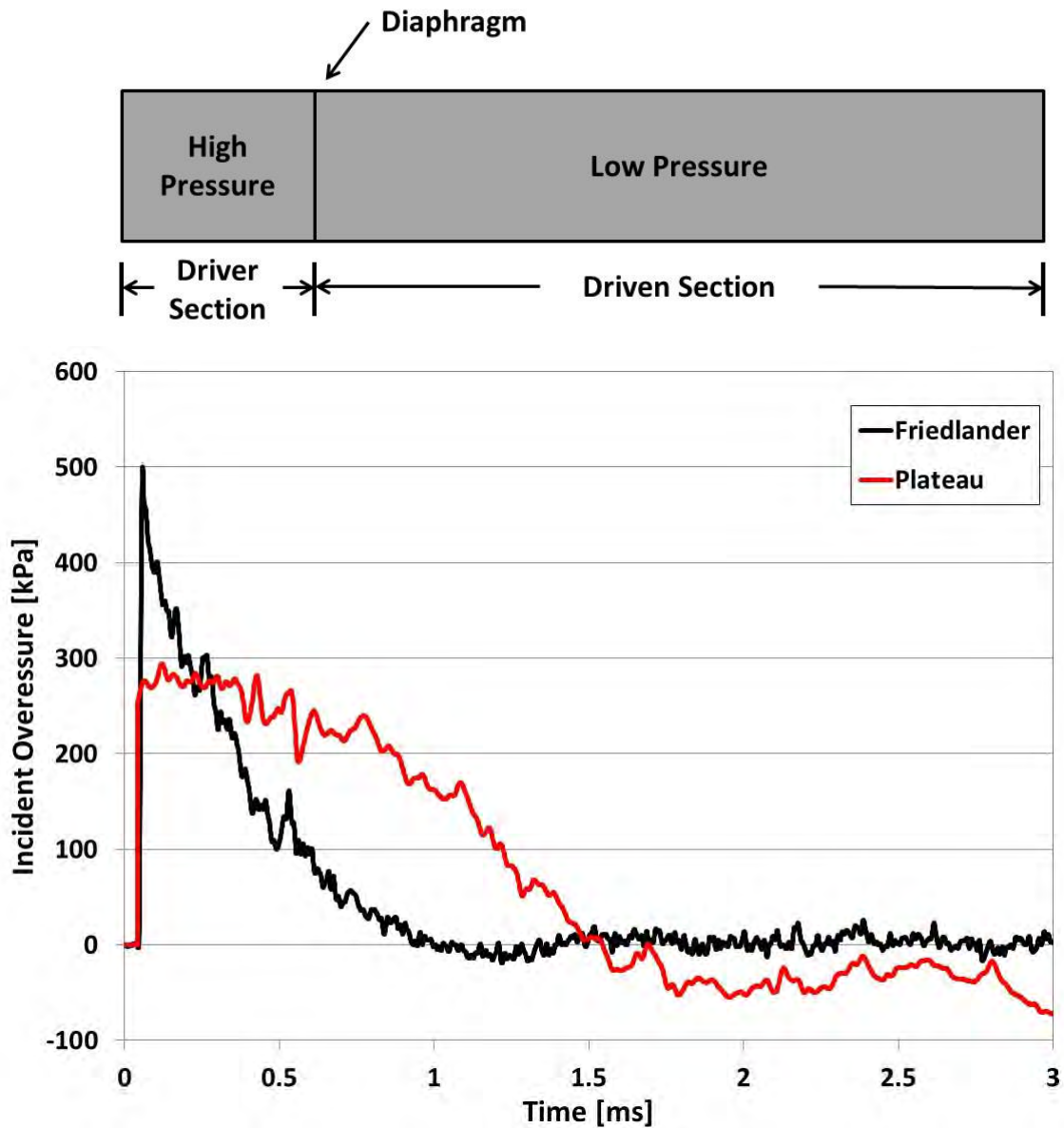
Figure 2-4: Simple shock tube schematic and typical Friedlander and plateaued waves. Pleateaued waves may result from insufficient driven length and contain higher pressure impulse.

There are many considerations when designing a shock tube to meet a certain

blast level or be used on a specific test specimen. As a rule-of-thumb, to ensure laminar

flow at the tube exit, the driven section of the tube must be at least 10 times as long as

the driver section (Celander et al. 1955a, Sharma et al. 1996). The peak pressure output

of the tube is modulated by the burst pressure of the diaphragm separating the driver

and driven sections. This can be achieved either through the modification of diaphragm

thickness (Celander et al. 1955a) or by manual rupture of the diaphragm at the desire

burst pressure (Richmond et al. 1966). Overpressure duration is modulated by changes

in the length of the driver section or through selection of the driver gas. Extending the

driver section or using driver gases with lower sound speeds results in a longer positive

phase duration. It is important to note that the manipulation of peak pressure and

overpressure duration are not independent, and increases in peak pressure through

diaphragm manipulation often result in longer durations while extending the driver

length not only extends overpressure duration but lowers the peak pressure.

There are two major configurations of shock tubes for blast testing. Closed-

ended shock tubes cap the end of the driven section creating a closed system or

containing small vents to relieve the high pressure gas (Richmond et al. 1959, Damon et

al. 1966, Bogo et al. 1971). This creates strong reflections traveling back up the tube after

the initial incident wave reaches the closed end. This configuration helps to ensure a

planar incident wav but may result in a complex waveform with long overpressure

duration and high impulse. Alternatively, the driven section remains open to the

ambient. In this case an almost spherical wave exits the tube end and an expansion

wave propagates back into the tube. The open-ended case is more commonly used in research today (Rafaels et al. 2012, Shridharani et al. 2012b, Yu et al. 2012).

With open-ended shock tubes there are options for placement location of the test specimen. Primarily, there lies a choice between placement outside of the tube exit or within the driven section of the shock tube. This is a subject of controversy and has been experimentally investigated by Yu (Yu et al. 2014). Placement within the shock tube is advantageous as it ensures a planar wave, but may have nonideal positive phase impulse. There are also potential concerns with confinement effects if the inner diameter of the tube is not large enough relative to the test specimen as well as reflections from the tube walls creating a complex wave interaction. The benefits of placement outside of the tube exit are that these confinement and wave reflection effects are avoided. However, care must be taken to limit the effects of the expansion wave ruining planarity and the exposure to momentum dominated blast wind. These effects are minimized by placing test specimens close to the midline and exit of the driven section.

There are many benefits to using gas-driven shock tubes for blast research including but not limited to the fact that they are clean, well-controlled, cheap, repeatable, and safer than free-field testing. Shock tubes are not suitable if thermal or other blast effects are desired, but these effects are generally small for ideal blasts outside the blast fireball. Finally, shock tube and free-field blast physics are

complicated, therefore special knowledge and care must be taken to simulate the desired

blast dosage.

2.2 Blast Injury

Blast injuries have been reported for over 400 years. The possibility of injury

from blast without penetrating or blunt trauma was a much debated topic around World

War I (Mott 1919). The bulk of significant research has taken place during and following

World War II beginning with Zuckerman (Zuckerman et al. 1940). This section will

discuss the categories of blast injury. Also, this section will outline the history of blast

injury research, including blast scaling and injury criteria.

2.2.1 Categorization

The interaction of a body with blast is complicated with multiple effects possible,

beyond overpressure exposure. Blast injuries are generally separated into four

categories (White et al. 1971):

Primary Blast Injury: Primary injuries are those resulting from the direct effects of

overpressure. Gas-filled organs are most susceptible to this type of injury (e.g. lungs,

stomach, tympanic membrane) due to the tissue-gas interface and its interaction with

the overpressure wave (Maynard et al. 1997). Primary blast neurotrauma is thought to

occur as a result of the direct interaction of the pressure wave with the tissue of the head

and brain.

Secondary Blast Injury: Secondary injuries are those resulting from penetration or impact related to the blast event. This is commonly the result of high-velocity fragments such as shell casings or debris. These high energy impacts and penetration may result in internal bleeding.

Tertiary Blast Injury: Tertiary injuries are those resulting from transferred momentum or damage to the surrounding structure. These injuries are commonly a result of body translation from blast wind and the ensuing impact. Injuries can also result from the failure of nearby structures. Tertiary injuries are characterized by blunt or crushing mechanisms.

Quaternary Blast Injury: Quaternary injuries are those resulting from exposure to blast byproducts beyond those in primary, secondary and tertiary injuries. This includes asphyxiation, exposure to harmful gases, burns and radiation poisoning among others.

The focus of the work in this dissertation is primary blast. The biomechanics of secondary and tertiary blast are closely related to other widely studied fields such as automotive, sports, and wound ballistics. Due to the extensive body of work in these fields, the effects and mechanisms related to secondary and tertiary blast are better

understood. It is often difficult to isolate primary blast effects, especially in human epidemiology where other blast injury types are present. The term "blast injury" is generally applied to all types associated with explosions (Champion et al. 2009), but will refer to primary blast injury in this work.

2.2.2 History of Research

Fatality from primary blast exposure was reported as early at the 1500's (Pare et al. 1585). Reports of injury and death in combat without obvious blunt impact also exist from the early 19th century (Larry 1812, Kincaid 1830). Primary blast injury, especially in the lungs, certainly occurred with the widespread usage of high explosives in military conflicts following the American Civil War. During WWI there were extensive reports of injuries to service personnel in trenches caused by overhead explosions. Blast TBI symptoms were prevalent (headache, memory loss, nausea, anxiety) and were associated with the unprecedented usage of high explosive artillery and mortar fire (Panzer et al. 2012a). There was debate whether this was a physical injury (commotio cerebri) or a psychiatric condition only ("shell shock") (Mott 1916, Mott 1919). The debate was temporarily won by the proponents that the symptomology could be explained as a psychiatric condition only.

The first significant work focused on the etiology of blast followed WWI. The work of Hooker investigated blast loading from guns, mortars, and explosives (Hooker 1924). In vivo animal models were used including cats, dogs, rabbits, and frogs to assess

injury. The primary injury observed was to the lungs with extensive hemorrhaging

occurring at the higher blast levels. There was no neurotrauma reported in the presence

of fatal pulmonary trauma (Hooker 1924).

In the 1940's Zuckerman and collaborators carried out extensive research on

primary blast across a wide range of species. It was concluded that pulmonary injury

was a result of overpressure interaction with the chest wall. The effects of different

materials (rubber, plaster, steel) for thoracic protection from blast was tested

(Zuckerman 1940). The effect of animal size on the required lethal dose of blast was also

investigated for the first time (Fisher et al. 1941). Work was also done to investigate the

effects of blast on the head in animals with and without pulmonary protection but

results of EEG measurements in the cerebral cortex showed no abnormalities

immediately post-blast even in the presence of severe pulmonary damage (Krohn et al.

1941, Krohn et al. 1942).

Following WWII the primary focus of blast injury research changed. There was a

significant research push to understand the mechanisms of lung injury from primary

blast but the focus was on nuclear blast effects. Clemedson was a pioneer of much of

our understanding of pulmonary blast injury mechanisms and along with his colleagues

was one of the first to extensively use gas driven shock tubes (Celander et al. 1955a).

They focused on how blast waves interact with the body and concluded that lung injury

was caused by an impedance mismatch of the air-containing organs with the

surrounding tissues and depends on pressure, overpressure duration, and waveform (Clemedson et al. 1955). This was in opposition to the existing hypothesis that lung injury was caused by high pressure gas entering the respiratory system and intestinal tracts resulting in tissue damage (Anonymous 1915).

From the mid 1950's to the mid 1980's the Lovelace Foundation, located at Kirtland Air Force Base in New Mexico, conducted blast injury research. Led primarily by White and Richmond, the most comprehensive and extensive testing on the effects of blast was carried out. The goal of this research effort was to develop injury risk criteria for nuclear blast injury. A wide range of animal model species were exposed to nuclear blast, characterized by long durations (>10ms) and large pressure impulse. Additionally, tests with high explosives and varied shock tubes were used to supplement the free-field data (Richmond et al. 1962b, Richmond et al. 1966). The extensive data from mouse to cattle size constitutes the basis of blast animal test data we have today. They created injury criteria, and provided data that is essential for recent injury criteria development (e.g. Bass et al. 2008, Rafaels et al. 2010). The work at the Lovelace Foundation provided the basis for many of the current areas of focus and controversy in blast research; long versus short overpressure duration, repeated blast, complex versus ideal waves, personal protective equipment effects, and large versus small animal species behavior.

In the 1980's and 1990's there was a major shift in the focus of blast injury research. Much more emphasis was placed on sub-lethal levels of blast and was largely motivated by occupational health considerations for exposure to artillery firings and shoulder fired rockets (e.g. Dodd et al. 1989). Lung injury thresholds for repeated low level blast was studied in sheep and was characterized by minor hemorrhaging of the larynx, gastrointestinal tract, and lungs that were below the threshold to require treatment (Dodd et al. 1989, Yang et al. 1996). Repeated exposure to low level blast from artillery and breaching charges was also studied to determine appropriate limitations on exposure (Stuhmiller et al. 2008).

Historically, primary blast injury to the head constituted a small minority of research work because fatalities directly attributed to head injuries were not observed compared with demonstrable fatalities from injuries to the air-containing organs. Before the late 1990's, the primary blast neurotrauma results that were seen appeared to be transient. For example, in a study of behavioral effects of blast in rhesus monkeys, immediate neurologic impairment was seen on audio and visual task performance at blast levels resulting in 50% lethality from pulmonary injury. However, these neurological and cognitive deficits were temporary and performance returned to normal by 4 hours post-blast (Bogo et al. 1971).

Before recent conflicts, there was little reporting of primary blast injuries. The bulk of recognized blast-related casualties were attributed to ballistic penetration or

explosive fragmentation. In the late 1990's published work began to suggest that primary blast was in fact responsible for neurotrauma. In a study of 665 patients subjected to blast, 30% showed signs of neurologic disorder (Cernak et al. 1999). Others also observed that primary blast led to mild neurological disorders in military personnel (Trudeau et al. 1998).

With the onset of U.S. military conflicts in Iraq and Afghanistan, casualties were dominated by closed-head injuries from the high rate of exposure to IEDs and other explosives (Taber et al. 2006, Warden 2006). The high incidence of this type of injury was unexpected base on previous clinical experience and research and led to a big push to understand primary blast neurotrauma. The focus of blast injury research now shifted to the understanding of neurological response, mechanism, and threshold to primary blast. Injury outcomes from altered cellular and biochemical processes up to behavioral changes were observed at dosage levels below pulmonary lethality. Some studies created measurable injury outcomes from primary blast exposure; cellular responses (neuronal degeneration, activated microglia and astrocytes, axonal transport disruption, increased nitric oxide generation) (Kaur et al. 1995, Cernak et al. 1996, Saljo et al. 2000, Säljö et al. 2001, Saljo et al. 2002, Moochhala et al. 2004), brain bleeding (Rafaels et al. 2011, Rafaels et al. 2012), and behavioral outcomes such as a decline in active avoidance response (Cernak et al. 2001a, Risling et al. 2002). Alternatively, some studies quantified blast dosage in terms of; intracranial pressure (Chavko et al. 2007,

Chavko et al. 2011, Leonardi et al. 2011, Shridharani et al. 2012b), skull deformation (Bolander et al. 2011), and head kinematics (Shridharani et al. 2012b). A wide range of blast dose with consistent methodology has been used to determine injury risk for injury endpoints like fatality and brain bleeding (Rafaels et al. 2011, Rafaels et al. 2012). However, much of the recent research is focused on measuring or replicating injury outcome rather than relating the outcome to a realistic blast dosage.

2.2.3 Existing Blast Scaling

Primary blast research relies heavily upon in vivo animal models and therefore an understanding of interspecies scaling is of great importance. Scaling will describe a relationship between human and model exposure that produces a biomechanical response resulting in equivalent pathophysiological response. The first work to report an increase in blast tolerance with larger species developed a primitive scaling for 50% lethality which accounted for body mass (Fisher et al. 1941).

Later, the most well-known and widely used interspecies scaling for blast trauma was developed by Bowen for primary blast pulmonary injury (Bowen et al. 1965). This scaling was derived from a lumped-mass thoracic model using dimensional analysis to relate lung pressure between different animals. Constant tissue density and moduli were assumed for simplicity. The scaling was reduced to a simple model for the scaling of overpressure duration, Δt, by the animal body mass, M_{body}, relative to a 70kg human reference, $M_{body,ref}$.

$$\Delta t_{scaled} = \Delta t \left(\frac{M_{body,ref}}{M_{body}} \right)^{1/3} \qquad\qquad \textbf{Equation 2-7}$$

This is essentially a length scaling with assumed spherical geometric similarity in body shape from the animal to that of a human. This suggests that the relative size of the subject to the blast wave should remain constant from animal model to humans.

Of special consideration with Bowen's scaling is the fact that species clearly fell into one of two groups for fatality risk, "large" or "small". The small animal group (i.e. mouse, rat, rabbit) had significantly lower pulmonary tolerance to blast than the large animal group (i.e. dog, ferret, pig). These differences were attributed to major differences in pulmonary anatomy. Those species who fell into the small animal group has much lower normalized lung value and higher lung density when compared to the large animal group (Bowen et al. 1965). Humans are assumed to fall within the large animal group based on body size and pulmonary anatomy. Bowen's small and large animal pulmonary lethality risk curves are presented in Figure 2-5.
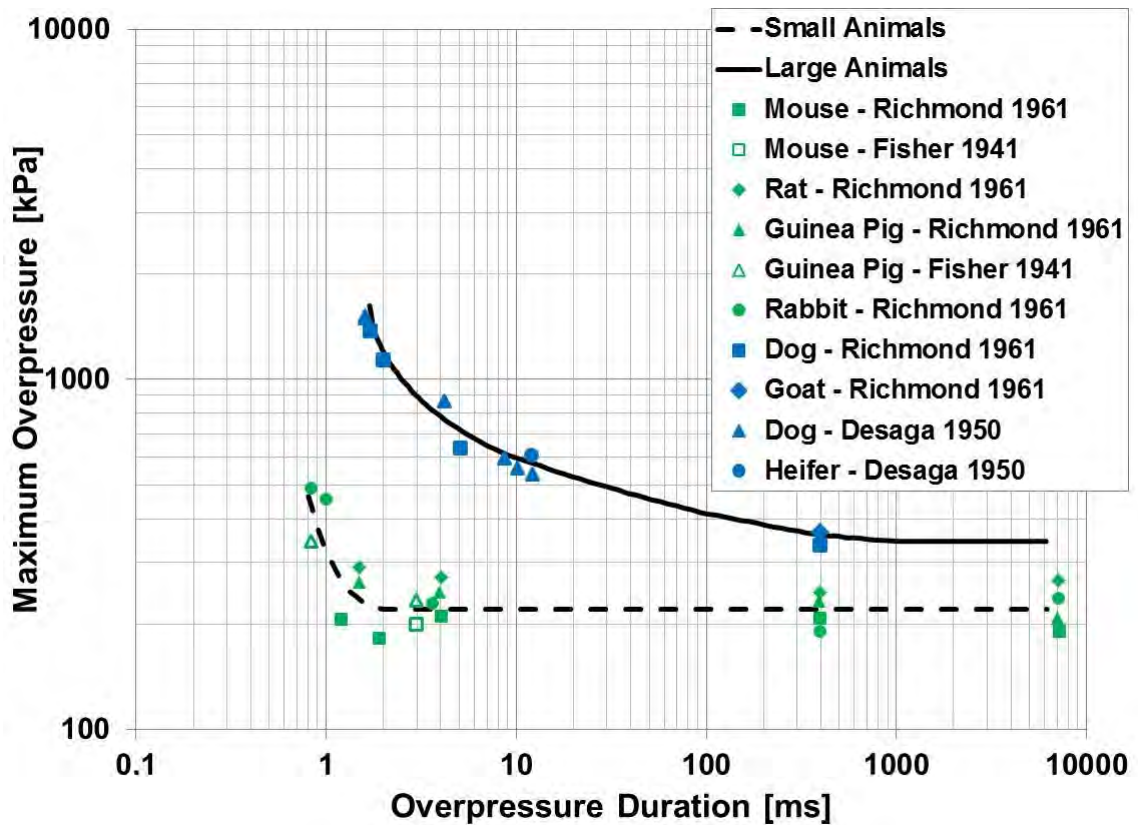
Figure 2-5: Bowen's small and large animal pulmonary lethality risk curves show clear categorical separation with small animals being more susceptible to blast pulmonary injury [adapted from (Bass et al. 2012)].

This scaling model was later validated with extensive empirical data from

hundreds of blast animal experiments (Bowen et al. 1968). Surprisingly, this scaling is of

the same for of that later developed for automobile blunt impact injury (Eppinger et al.

1984).

More recently, work by Panzer investigated interspecies scaling for blast

neurotrauma applications (Panzer 2012). A finite element computational study was

conducted to look at the effect of head size on the biomechanical response of brain to

blast impact. A simplified head/brain model was scaled to 5 different sizes representing

a range of models from the size of a mouse up to humans. These models were exposed

to a wide range of blast severity and volumetric and deviatoric mechanical response of

the brain was assessed, and a scaling model was developed based on the peak brain

pressure and peak brain shear strain results. The study showed that peak strain and

peak acceleration were both higher in the smaller heads over the entire range of blast

conditions. Input peak pressure was found to dominate the resulting peak brain

pressure while blast duration dominated the peak brain strain results. Peak strains

increased by 50% when halving the head size (Panzer 2012). Peak pressure scaling was

found to be negligible and overpressure duration scaling was derived of the same

simple form as Bowen (Bowen et al. 1965). Interspecies scaling of overpressure

duration, based upon a brain mass ratio, was used to match biomechanical output

between all head sizes according to Equation 2-8.

$$\Delta t_{scaled} = \Delta t \left(\frac{M_{brain}}{M_{brain,ref}} \right)^{0.248} \qquad \text{Equation 2-8}$$

2.2.4 Injury Criteria

One of the main goals of injury biomechanics research is the development of

injury criteria predict injury on a probabilistic basis. This is helpful for the development

of protective equipment, provides guidelines for risk, and informs decisions on

occupational health policies on acceptable exposure. Injury criteria for primary blast

help us to understand the relationship between dose and pathophysiological response.

The most widely used injury criteria for primary blast exposure are those developed by Bowen and colleagues for pulmonary injury risk (Bowen et al. 1968). These risk models derived from a wide range of animal model species are based on nearly 2000 in vivo blast tests with sharp rising pressure signatures. The interspecies scaling derived by Bowen was used to convert all blast doses to a human equivalent level. Risk lines for fatality and injury threshold, dependent upon peak overpressure and overpressure duration were presented and are commonly referred to as the "Bowen curves" (Bowen et al. 1968).
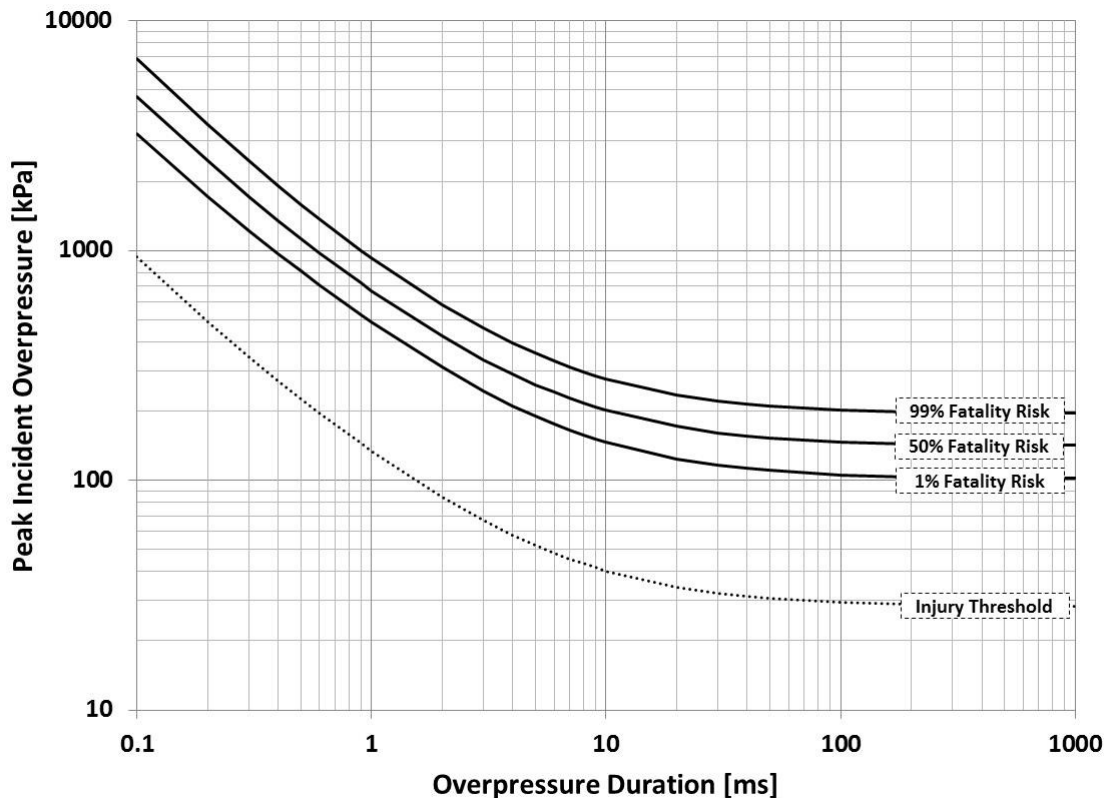
Figure 2-6: Bowen curves for pulmonary injury risk from primary blast with a reflecting surface show increased injury risk with increasing peak pressure and

duration. Injury risk is independent of overpressure duration at long durations (Bowen et al. 1968).

For short durations (<10ms) risk is highly dependent upon blast duration and peak pressure (Figure 2-6), risk increases as overpressure duration or peak pressure increase. At longer durations (> 30ms) risk is peak pressure dependent only. Despite being over 40 years old these criteria are still widely used as the standard for blast pulmonary injury.

Recently, Bowen's curves for pulmonary injury risk were updated with a more extensive experimental database of large animal tests. Bass and colleagues considered short overpressure duration (Bass et al. 2008) and long overpressure duration (Rafaels et al. 2010) separately. For low-momentum, short overpressure duration (< 30ms) exposures, injury is assumed to result from localized spalling of alveolar tissue due to the impedance mismatch between tissue and air (Cooper 1996). This short duration condition is representative of conventional high explosives less than 500kg in charge weight (IEDs, mines, artillery, etc.). The Bass group, like Bowen, found that injury response is highly dependent upon peak pressure and overpressure duration. For long overpressure duration (> 10ms) the injury is associated with diffuse pulmonary injury resulting from a large momentum transfer to the thorax causing lung compression (Cooper 1996). There is a limited effect of overpressure duration on injury risk at these durations. This type of exposure results from large high explosive charges (> 2000kg) in the form of truck bombs or conventional military bombs, or thermobaric and nuclear

weapons. The pulmonary 50% lethality risk for short (Bass et al. 2008) and long (Rafaels et al. 2010) durations are shown in Figure 2-7.
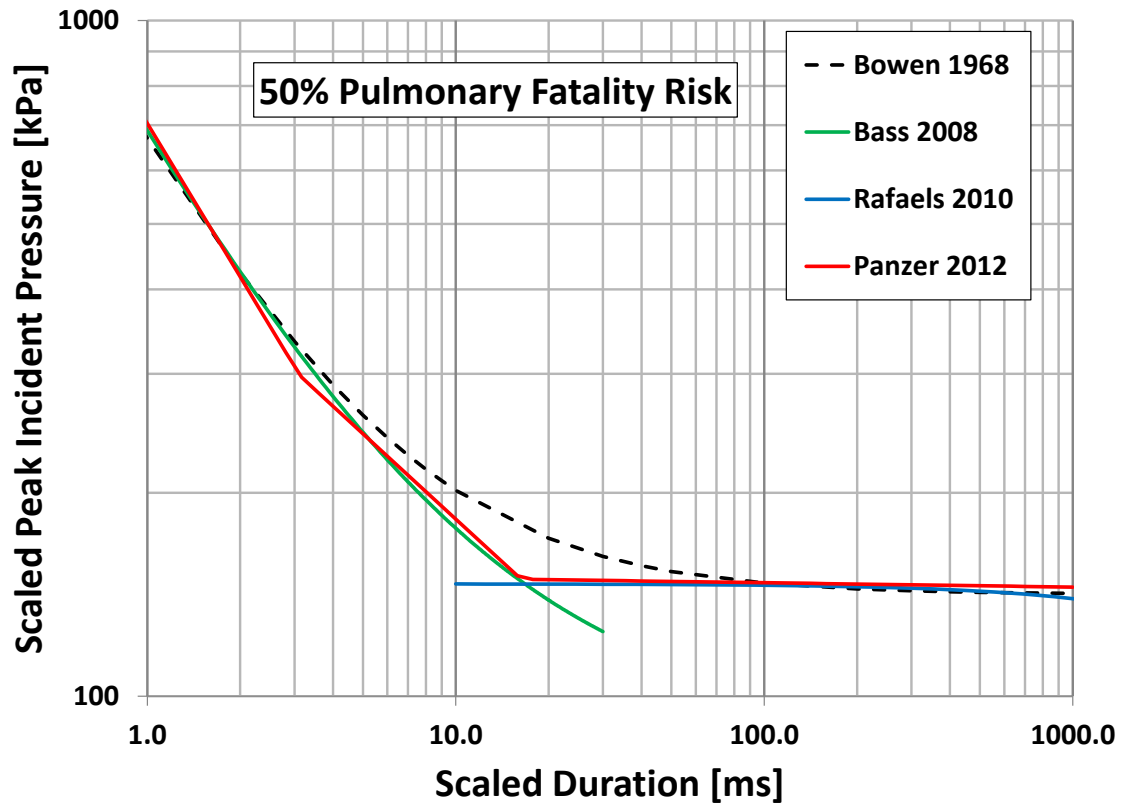
Figure 2-7: Comparison of existing pulmonary fatality injury criteria shows similar behavior at long and short durations with a transition occurring at approximately 20ms.

Further work on pulmonary injury risk in large animals was conducted by

Panzer and considered short and long overpressure duration together (Panzer et al.

2012c). A piece-wise linear model form was used to describe injury risk dependent

upon peak pressure and overpressure duration based on existing injury data from

literature. The model breakpoints indicate a shift from the short to long overpressure

duration injury mechanisms. This study also examined the effect of repeated blast

exposure and determined an increased injury risk with increasing number of exposures

at the same level. Injury risk models were derived for pulmonary lethality, pulmonary

injury, and non-auditory injury which may occur to the upper respiratory tract or

gastrointestinal tract (Panzer et al. 2012c). The 50% pulmonary lethality risk is presented

in Figure 2-7.

 For pure primary blast neurotrauma, there is far less experimental data

compared with pulmonary experimentation making development of injury criteria more

challenging. However, there have been studies investigating single or a small group of

different species over a large enough exposure range to develop injury risk models.

 The first risk function for blast neurotrauma with exposure isolated to the head

was conducted with rabbits (Rafaels et al. 2011). Animals were provided with steel

thoracic protection and pressure exposure to the thorax well below the threshold for

significant pulmonary injury was confirmed. This shock tube study exposed 12 rabbits

to blast levels ranging from 200 -1100kPa and 3-6ms scaled durations. Bowen scaling

was used to convert exposure levels to a human equivalent. Apnea was observed at

higher blast levels and the animals required ventilator support. 5 of the 12 specimens

failed to survive the 4-hour post-blast period. A logistic risk function was fit to the

survival data across the range of blast levels. Peak pressure and overpressure duration

were monotonically related for this specific shock tube, therefore risk was fit to peak

pressure only. 50% fatality risk for the rabbits (Rafaels et al. 2011) was compared to the

50% fatality risk from pulmonary injury in an unprotected thorax (Bass et al. 2008) and is

shown in Figure 2-8.
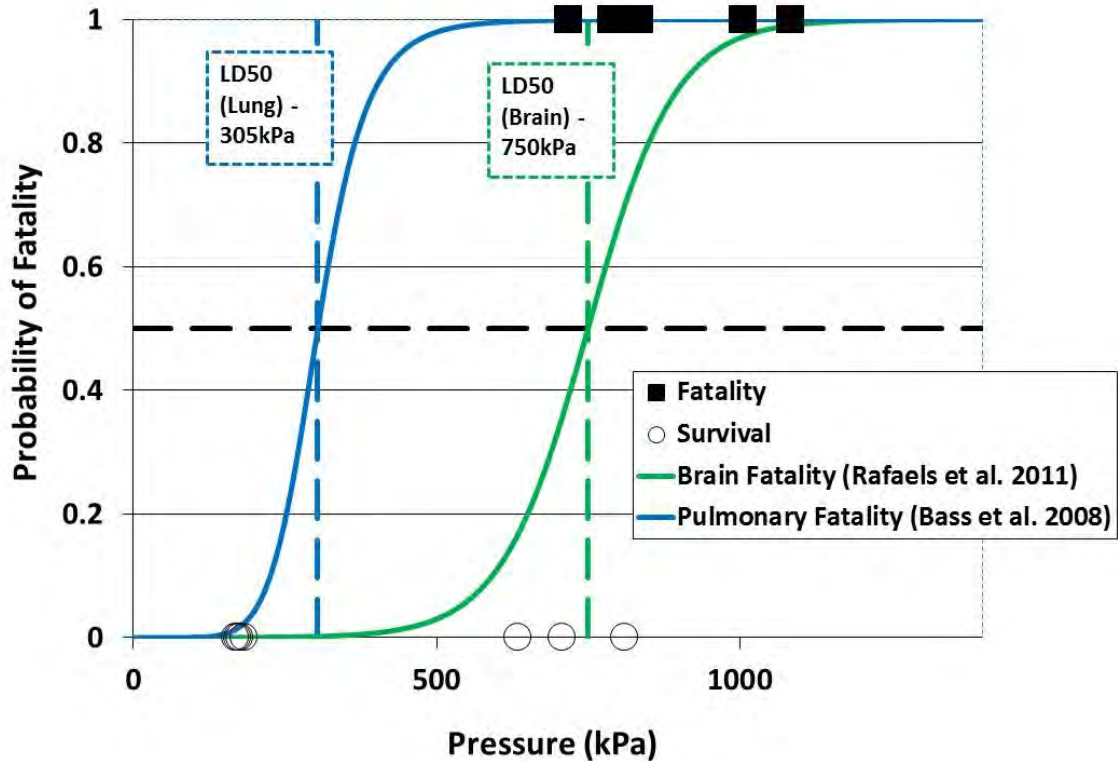
**Figure 2-8: 50% neurotrauma fatality risk from in vivo rabbit testing occurs at higher
peak overpressure levels than 50% pulmonary fatality risk (Rafaels et al. 2011).**

Results show that the risk of fatalities from blast damage to the pulmonary

system is greater than the risk of fatalities from primary blast than the brain. Along the

characteristic pressure-duration line of the shock tube used, 50% risk of brain fatality

was 750kPa compared to 305kPa for pulmonary.

Later, Rafaels conducted a more extensive test series on 70 thorax protected ferrets (Rafaels et al. 2012). Shock tube exposures ranged from 100-840kPa and 2-15ms scaled durations. The goal was to evaluate moderate to severe brain injury. Injury endpoints such as apnea and brain bleeding were observed. Nearly half of the animals experienced apnea and 6 of the 70 ferrets dies from the exposure. Scaled ferret data combined with previously published rabbit data (Rafaels et al. 2011) was used to develop a pressure and overpressure duration dependent fatality risk model for blast neurotrauma (Rafaels et al. 2012), which is shown in Figure 2-9.
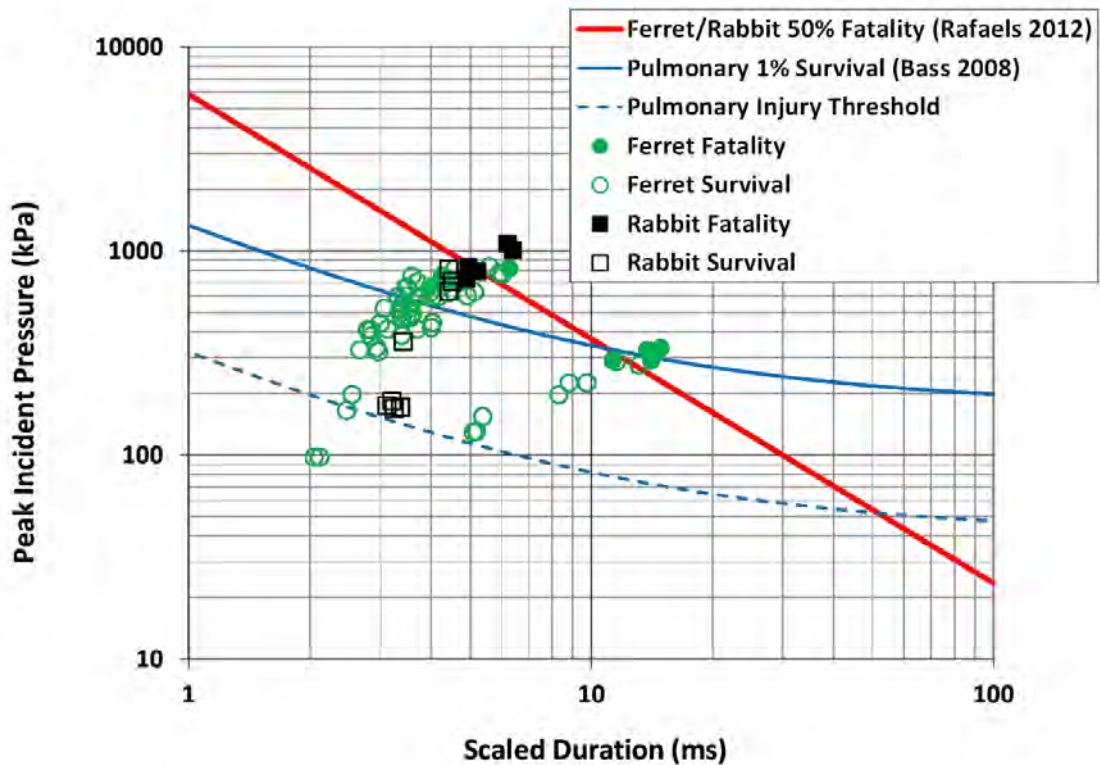
Figure 2-9: A combined blast neurotrauma 50% fatality risk model for rabbit and ferret occurs at higher blast dosage levels than 1% pulmonary risk (Rafaels et al. 2012).

Additional risk functions were derived for mild, moderate/severe brain bleeding, and apnea. Those models are presented in Figure 2-10. Rafaels observed that the blast level corresponding to mild brain injury is comparable to or even less than the levels associated with the onset of pulmonary injury (Rafaels et al. 2012). This is of great interest for blast neurotrauma research as such mild brain hemorrhaging may be difficult to detect with current clinical imaging techniques and may explain some of the symptoms of mild TBI occurring at levels below those widely thought to cause blast brain injury.
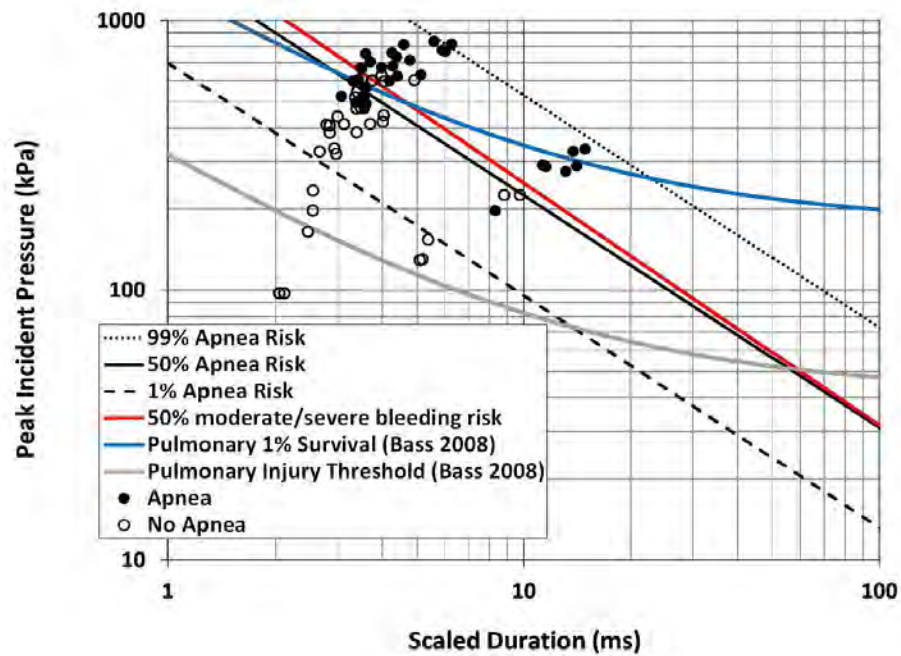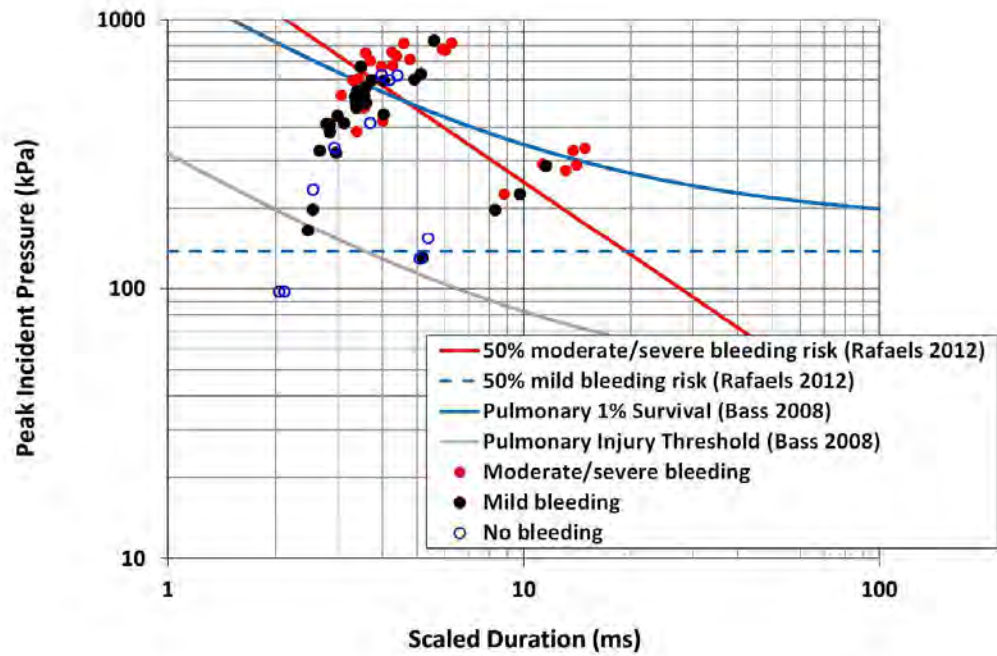
Figure 2-10: Ferret blast neurotrauma risk models for graded brain bleeding and apnea show that mild brain bleeding may occur at blast levels below the pulmonary injury threshold (Rafaels et al. 2012).

2.3 Neuroanatomy and Mechanics

An understanding of neuroanatomy is important for assessing and predicting injury through both experimental and computational finite element methods. This section will present applicable neuroanatomical macrostructure and microstructure of the mammalian brain with a focus on humans. This will be followed by a discussion on the mechanics of brain tissue including a summary of existing literature along with strengths and weaknesses in providing the necessary mechanics for modeling and interspecies comparison.

2.3.1 Neuroanatomy

The brain is the largest nervous organ and is responsible for the function of every body system. The brain governs sensory processing, motor processing, higher mental function, and regulation of body systems. The brain is divided into 5 regions with their own function and unique microstructure. The 5 brain regions are labeled in Figure 2-11 with the substructures of the basal ganglia (caudate nucleus, globus pallidus, putamen) labeled. The important substructures and primary functions of the different regions are presented in Table 2-1.
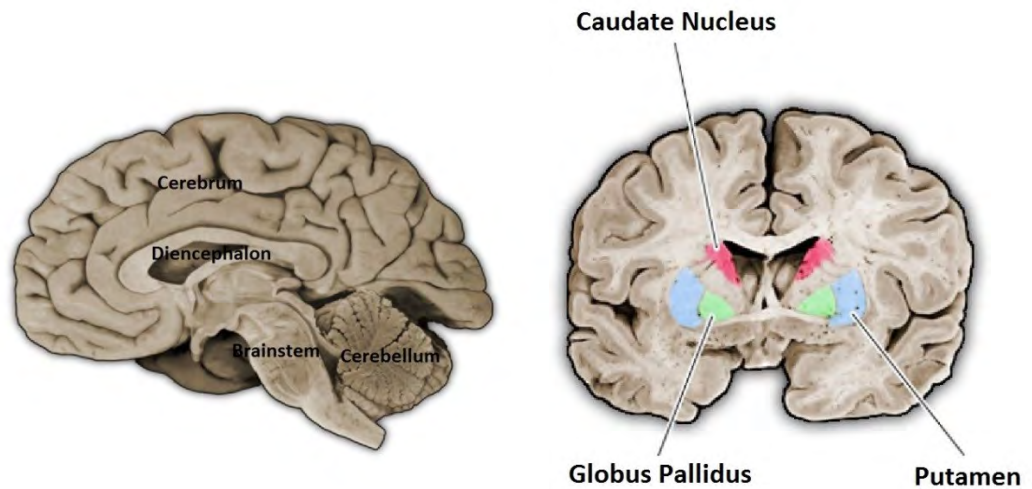
Figure 2-11: 5 regions of the mammalian brain (Wikimedia Commons).

Table 2-1: Substructures and functions of the 5 brain regions (Purves et al. 2008).

Region	Substructures	Function
Cerebrum	Cerebral Cortex	- Higher brain function (learning, memory, emotion, sensory processing)
Basal Ganglia	Caudate Nucleus, Globus Pallidus, Putamen	- Connection for motor impulses from brain stem to cerebral cortex
Diencephalon	Thalamus. Hypothalamus	- Connection for sensory impulses to the CNS - Regulates visceral activities to maintain homeostasis
Cerebellum		- Fine muscle control and posture - Sensory information integrator from peripheral nervous system
Brain Stem	Midbrain, Pons, Medulla oblongata	- Vasomotor, cardiac, and respiratory control centers - Sleep, respiration, equilibrium signaling - Head and eye reflexes

The largest region of the brain is the cerebrum and is composed of two hemispheres separated by the corpus callosum. In humans and in many other large mammals the surface of the cerebrum is convoluted by gyri and sulci. This brain folding is referred to as gyrencephaly. The brains of many small mammals are far less convoluted, or not at all, and are referred to as lissencephalic. The cerebrum is divided into four lobes. The lobes are portrayed in Figure 2-12 and their major associated functions are provided in Table 2-2. The function of the different lobes is important to injury biomechanics as the type of deficit may be a result of localized injury within the cerebrum.
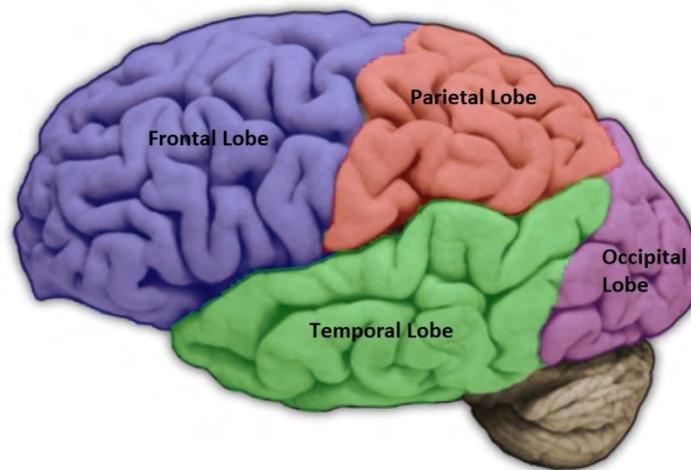
Figure 2-12: Four lobes of the human cerebrum (Wikimedia Commons).

Table 2-2: Major functions of the lobes of the human cerebrum (Purves et al. 2008).

Lobe	Major Functions
Frontal	- Reasoning - Motor Skills - High Level Cognition - Expressive Language
Parietal	- Sensory Information
Temporal	- Speech and Language - Memory
Occipital	- Visual

The cerebral cortex makes up part of the cerebrum. The cortex is 2-5mm thick in humans and is made up of the folded surface of the cerebrum (Shier et al. 2007). The cerebral cortex is mostly comprised of gray matter with neuronal cell bodies and their dendrites and glial cells. The term gray matter is owed to the color of the tissue when fixed. The cerebral cortex is where many of the higher brain functions take place. Most of the remaining cerebrum is made up of white matter. The white matter contains glial cells and axons and provides a pathway for signals to travel between different areas of gray matter.

Other important brain substructures for injury biomechanics are the ventricles. The ventricles are interconnected cerebrospinal fluid filled (CSF) cavities within the cerebrum that produce CSF. It is theorized that they may serve as shear decouplers between areas of the cerebral cortex to protect from tissue damage during head motion

(Viano et al. 1997). These structures may also serve as an impedance mismatch during high strain rate events like those associated with blast. This could lead to localized injury surrounding the ventricles, much like that seen in spalling of alveolar tissue in blast pulmonary trauma.

The brain is covered in a three layer structure called the meninges. The meninges act as a barrier and maintain a CSF layer between the skull and brain. The outermost and strongest layer is the dura mater. It is attached to the inner surface of the skull. Interior to the dura mater is the arachnoid mater. This layer is a thin tissue membrane resembling a spider web and is connected to the inside surface of the dura. The innermost layer lies between the arachnoid mater and the brain tissue surface and is the pia mater. The pia mater is rich in vasculature and lines the sulci and fissures of the brain surface. Of importance is the area between the pia and arachnoid mater called the subarachnoid space. It is filled with CSF and is important for the function of the blood brain barrier. Neurotrauma may lead to bleeding in and around these layers referred to subdural and subarachnoid hemorrhages.

The microstructure of the brain is comprised of two main cell types, neurons and neuroglia (Shier et al. 2007). There are approximately 85 billion neurons in the human brain (Azevedo et al. 2009). Neurons are made up of a cell body with numerous protruding structures as shown in Figure 2-13. Axons transmit electrical impulses from the cell body and stimulate other neurons or terminate into cells outside of the central

nervous system (muscles, etc.). Each neuron typically has only one axon but it may

terminate into more than one target cell. Axons vary greatly in length from less than

1mm up to greater than 1m and are covered in a myelin sheath to improve conductivity.

Dendrites are the receiver for signals from other neurons and branch from the neuronal

cell body.
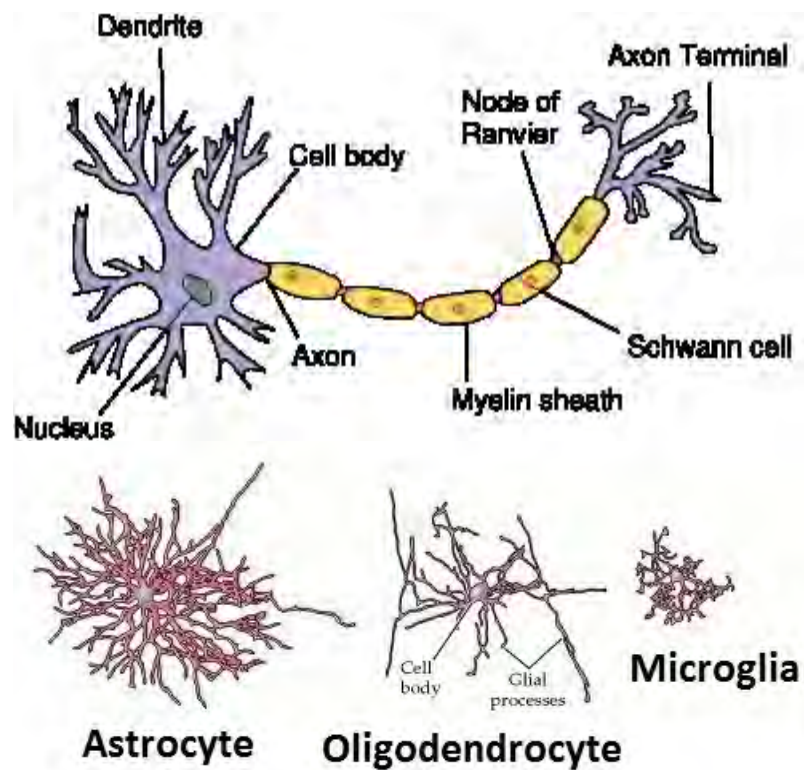
Figure 2-13: Basic structure of the neuron and neuroglia (Wikimedia Commons).

There are approximately the same number of neuroglia and neurons within the

human brain (Azevedo et al. 2009). There are three types of neuroglia as shown in

Figure 2-13. The most common type are astrocytes which serve to support the cells of

the blood brain barrier. Astrocytes are also an essential part of the scarring and repair

process within the brain. The function of microglia is to clear damaged neurons and foreign material from brain tissue. Microglia are an important part of the inflammation and immune response of the brain. Finally, oligodendrocytes form the myelin sheath to insulate the length of axons. This increases the conduction speed and therefore loss of the myelin sheath leads to diminished axonal function. This loss of myelin sheath is characteristic of some neurodegenerative diseases such as multiple sclerosis.

The brain microstructure is important for the study of neurotrauma biomechanics. The orientation and grouping of axons changes the mechanical response of tissue and presumably the mechanical injury threshold (Bain et al. 2000). High strain rate stretching like that associated with blast can lead to damage to axons and surrounding structures. This is commonly referred to as diffuse axonal injury (DAI) and can result in axonal swelling and initiate axonal death cascades (Smith et al. 2000). Considering these factors, the brain microstructure is likely an important factor for low strain amplitude, high strain rate injuries assumed to come from primary blast exposure.

An understanding of neuroanatomy and functional neuroanatomy as injuries to different areas and substructures change how injury manifests. Knowledge of brain function may allow us to better pinpoint areas where injury occurs. Further, injury to different areas of the brain may result in varied long-term outcome. For example, injuries to the front lobe may be non-life threatening but result in deficits in cognition and personality, while injuries to the cerebellum may impair motor coordination and

balance. Alternatively, injuries of similar magnitude to the brain stem may be fatal. In addition, it's likely important that we consider the biomechanics of the brain/skull interface as well as the cerebrum/ventricle interface when attempting to understand the injury mechanism for blast

2.3.2 Brain Tissue Characterization

Accurate mechanical characterization of brain tissue is important for the modeling of injury, especially in finite element models since existing FE models of the head rely on accurate material properties to provide biofidelic response (Moss et al. 2009, Taylor et al. 2009, Panzer et al. 2012b). FE models are valuable tools for the detailed assessment of injury mechanisms, but model biofidelity is often limited by a lack of mechanical data for biological tissue at relevant strain rates (Yang et al. 2006, Panzer et al. 2012b). The sensitivity of a FE head model for blast to changes in material properties has been investigated (Panzer 2012). In this study both the deviatoric (viscoelastic) and volumetric (density, speed of sound) properties of brain tissue were varied. Small changes in brain pressure response were observed relative to the size of changes in brain properties. The viscoelastic properties were found to be important for the prediction of tissue strain response. An order of magnitude difference in peak Von Mises stress was observed for the same blast conditions when comparing the brain material properties used in several published FE models (Zhang et al. 2001, Moss et al. 2009, Panzer et al. 2012b).

There is a limited understanding of the injury mechanism and tissue level

thresholds for blast. Electrophysiological impairment in guinea pig optic nerve axons

has been observed at 18% strain (Bain et al. 2000). In organotypic slice cultures, the

threshold for cortical cell death was found to be between 10 and 20% strain and also

strain rate dependent (Elkin et al. 2007b). So, it is likely that blast neurotrauma is strain

and strain rate dependent.

Brain tissue mechanics research has primarily focused on injuries that occur at

automotive or physiological rate. These rates are much lower than those interesting for

blast, with most research at frequencies less than 100Hz. Early work on brain tissue

showed primarily elastic and nearly incompressible behavior under cyclic dilatational

loading up to 100Hz. Resulting estimates of shear properties saw viscoelastic (VE)

material behavior with complex moduli of approximately 20kPa at rates up to 120Hz

(Galford et al. 1970, Metz et al. 1970). More recent work has shown brain to be much

softer (with a complex modulus between 0.3 and 2kPa), nonlinearly viscoelastic, and to

exhibit interspecies differences (Cheng et al. 2008, Chatelin et al. 2010). Bulk elastic

properties of brain measured at ultrasonic frequencies are as much as 1000 times stiffer

than the shear properties presented most commonly in literature (Lippert et al. 2004). It

is clear that the behavior of brain tissue is rate dependent and tissue properties derived

for automotive and blunt impact injury may not be suitable for blast applications. The

47

wide variation in complex shear modulus and the loss angle, tanδ, of tests on

mammalian brains are shown in Figure 2-14 and Figure 2-15, respectively.
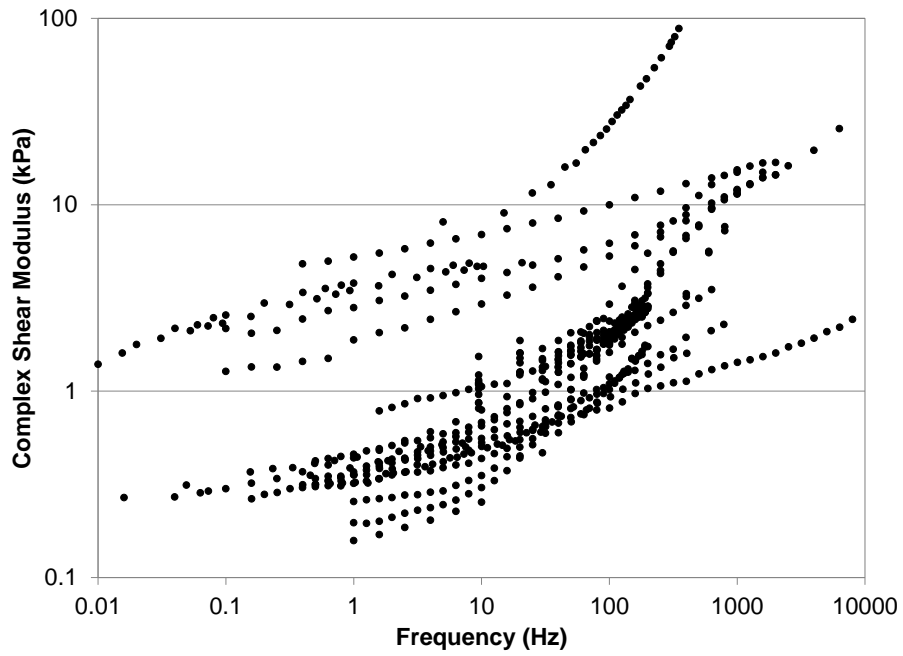
Figure 2-14: Published values of complex shear modulus for brain tissue from several mammalian species varies over two orders of magnitude.
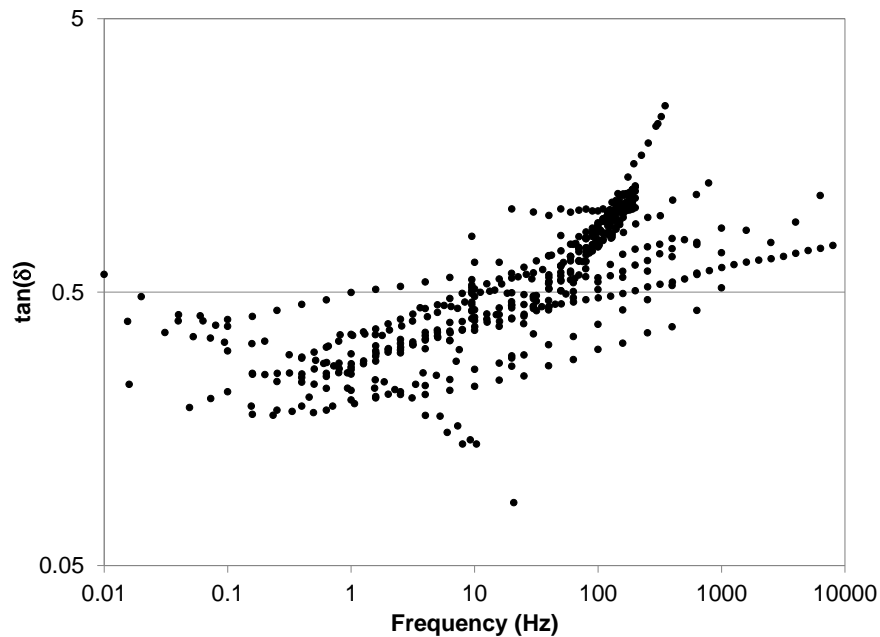
Figure 2-15: Published values of tanδ for brain tissue from several mammalian species shows frequency dependence and high variation.

Brain tissue has been shown to exhibit regional differences in mechanical properties. The complex shear modulus has been shown to be significantly higher in the brain stem over the cortex in pigs (Arbogast et al. 1997). Likewise, in pigs regional differences in shear modulus have been measured between cortical gray matter of the corpus callosum and thalamus (Coats et al. 2006). In rats, differences in tissue stiffness between hippocampus substructures (Elkin et al. 2007a) and regions of a sagittal slice (Finan et al. 2012) have been observed. Many have shown there to be differences in shear properties of white and gray matter as well (Prange et al. 2000, Nicolle et al. 2004, Johnson et al. 2013).

Several studies have investigated both regional and local tissue anisotropy in mammalian brains (Arbogast et al. 1998, Elkin et al. 2011, Finan et al. 2012, Feng et al. 2013). Small directional dependence within gray matter of anatomical structures has observed (Elkin et al. 2009). More significant anisotropy was measured in the porcine brain stem with stiffness differences at small strains (Arbogast and Margulies 1998).

Of possible significance in animal model research for neurotrauma, age-related differences have been shown in some studies. Age-dependent stiffness has been shown in the rat hippocampus (Elkin et al. 2009) and cortex (Gefen et al. 2003, Shulyakov et al. 2011). In pigs a significant difference in complex shear modulus of the cerebrum was found between neonatal and mature animals (Thibault et al. 1998).

A wide range of methodologies have been used to characterize brain tissue mechanics. The bulk of tissue mechanics literature has tested specimens in vitro, or removed from the skull. This has the advantage of allowing multiple types of specimen geometry and testing mode. With in vitro tests it is common to cut tissue into the shape of cylinders (Arbogast and Margulies 1997, Bilston et al. 1997, Darvish et al. 2001) or cubes (Estes et al. 1970, Coats and Margulies 2006). Unconfined platen compression was a popular technique for testing brain tissue, especially in early research, as it is a simple test with relatively simple analytical solutions available to characterize the response (Estes and McElhaney 1970, Galford et al. 1970, Miller et al. 1997). Testing of brain tissue in oscillatory shear is the most common testing method due not only to the ease of

testing but also due to the specific interest in shear properties of brain, which will be further discussed later (Fallenstein et al. 1969, Shuck et al. 1972, Arbogast and Margulies 1997, Brands et al. 1999). A final and much less common in vitro testing method is Hopkinson-Bar testing. This testing methodology was developed to test material, primarily orders of magnitude stiffer than brain, at very high strain rates. While this testing method is capable of the strain rates which we desire for blast applications it is made very difficult due to the soft behavior of brain tissue. Published data using this method report very large strain magnitudes up to 75% which is outside of the amplitude we are interested in (Pervin et al. 2009, Nie et al. 2013).

A common testing method for in vivo and in situ brain tests is indentation (Wang et al. 1972, Gefen et al. 2004, Elias et al. 2012). Indentation at low to moderate depths is non-destructive and can be used in living animals through a small burr hole in the skull. Indentation is also valuable for in vitro tests, especially to measure local properties and differences between substructures (Elkin et al. 2007a, Finan et al. 2012). However, due to complex geometries and insufficient analytical solutions, it is often necessary to utilize inverse finite element analysis techniques to derive constitutive models from indentation tests. Another relatively new and promising technique that has been used for brain tissue characterization is magnetic resonance elastography (MRE) (Feng et al. 2013, Johnson et al. 2013). This method uses magnetic resonance imaging on a tissue subjected to vibrations to measure tissue properties. This methodology is completely

non-destructive and non-invasive so it may be used in living animals or humans. With

living tissue in an undisturbed state it can most accurately measure the underlying

mechanics. The results of MRE analysis of brain tissue also compare well with other in

vivo and in situ characterizations.

Testing of brain tissue in vivo (in a living animal) or in situ (in a post-mortem

intact skull) holds advantages of the common in vitro testing. In vivo tests model the

living state we are truly interested in for injury modeling, but have drawbacks such as

difficulties dealing with living subjects and dynamic physiological response during

testing (Fallenstein et al. 1969, Wang and Wineman 1972, Gefen and Margulies 2004). In

situ testing configurations model the tissue in its native environment but avoid the

complications associated with living tissue (Elias and Spector 2012). In vivo/in situ

testing also avoids the creep behavior that the very soft brain tissue exhibits in

unconstrained testing. In a study of the cerebral cortex of pigs, there was no difference

seen between the mechanical properties of brain in vivo and in situ, while differences in

the long term relaxation behavior were observed for in vitro tests (Gefen and Margulies

2004). In vitro tests are still valuable when investigating deep structures or areas of the

brain that are not accessible without removal from the skull.

An area of possible concern with existing literature that warrants consideration is

the strain levels at which brain tissue are irreversibly damaged. It's been shown that at

finite strains non-recoverable changes in material properties can be introduced (Darvish

and Crandall 2001). It is important for testing with tissue this soft to diligently check for tissue damage due to testing and modify methodologies accordingly. It's likely that in some studies preconditioning strains are resulting in irreversible tissue damage that alters the measured tissue properties and may have an adverse effect on the biofidelity of the resulting models.

A range of material model forms have been used to describe brain tissue. Parametric FE studies have shown that the choice of constitutive model has a large effect on the pressure and shear response of brain for blunt impact simulations (Darvish et al. 2002, Horgan et al. 2003). Both deviatoric (shear stiffness, VE) and bulk (density, speed of sound, acoustic impedance) tissue properties are important for blast applications as wave transmission must be modeled (Panzer 2012). The brain's high bulk modulus relative to its shear modulus means that the tissue is more likely to deform in shear when loaded (Arbogast and Margulies 1997). The bulk properties of brain are often assumed to be approximated by those of water and the focus of research has been on measuring and modeling the deviatoric response.

Brain tissue is most commonly characterized as a VE material. The simplest formulation used is that of linear VE (Brands et al. 1999, Nicolle et al. 2004, Elias and Spector 2012, Feng et al. 2013). This model assumes a linearly elastic response and a viscous relaxation response independent of strain level and is likely only valid for small strains. Quasilinear viscoelasticity (QLV) is also widely used to characterize brain along

with many soft biological tissues (Miller and Chinzei 1997, Prange et al. 2000, Darvish and Crandall 2001). This model form assumes a separable relaxation and elastic response with the relaxation behavior being independent of strain level. The assumptions of QLV eventually breakdown but the model has been shown to be valid up to 10% strain in brain tissue (Darvish and Crandall 2001). Beyond QLV are fully non-linear VE models of brain mechanics (Bilston et al. 1997, Darvish and Crandall 2001, Takhounts et al. 2003). This type of model likely most accurately models the tissue behavior up to large strains and high strain rates and is capable of modeling nonlinear elastic and viscous behavior. However, this material model requires a much more extensive set of test data and is often too expensive experimentally and computationally to use.

Work has been done to look at the application ranges over which these VE models suitably model the tissue response. Assumptions for LVE and QLV models are known to breakdown at high strains. Modeling of experimental data from bovine and human brain tissue showed LVE to be valid up to approximately 0.2 strain and QLV to be acceptable up to approximately 0.5 strain, beyond which a fully non-linear model was necessary (Takhounts et al. 2003).

A final area of research and of special importance when considering scaling for animal models is interspecies differences in brain mechanics. Experimental data exists for brain tissue from a range of mammalian species including; human (Estes and

McElhaney 1970, Galford and McElhaney 1970, Johnson et al. 2013), porcine (Arbogast

and Margulies 1997, Prange et al. 2000, Coats and Margulies 2006), bovine (Bilston et al.

1997, Darvish and Crandall 2001, Nie et al. 2013), rat (Gefen et al. 2003, Elias and Spector

2012, Finan et al. 2012), and rhesus monkey (Fallenstein et al. 1969, Estes and McElhaney

1970). Bovine and porcine models are the most common with a recent increase in the

number of studies using rats. Some studies have shown mechanical differences between

monkey and human (Galford and McElhaney 1970) as well as pig and human (Prange et

al. 2000). Alternatively, studies have observed no difference between pig and human

(Nicolle et al. 2004). Also, MRE results have shown no difference in tissue behavior

between mouse (Atay et al. 2008) and rat (Vappou et al. 2008) brain. Limited work has

been published on mice and ferrets which are of special interest as common blast animal

models and will be further investigated as part of this dissertation. Experimental data

for complex shear modulus and tanδ divided into the three most common species are

presented in Figure 2-16 and Figure 2-17, respectively.
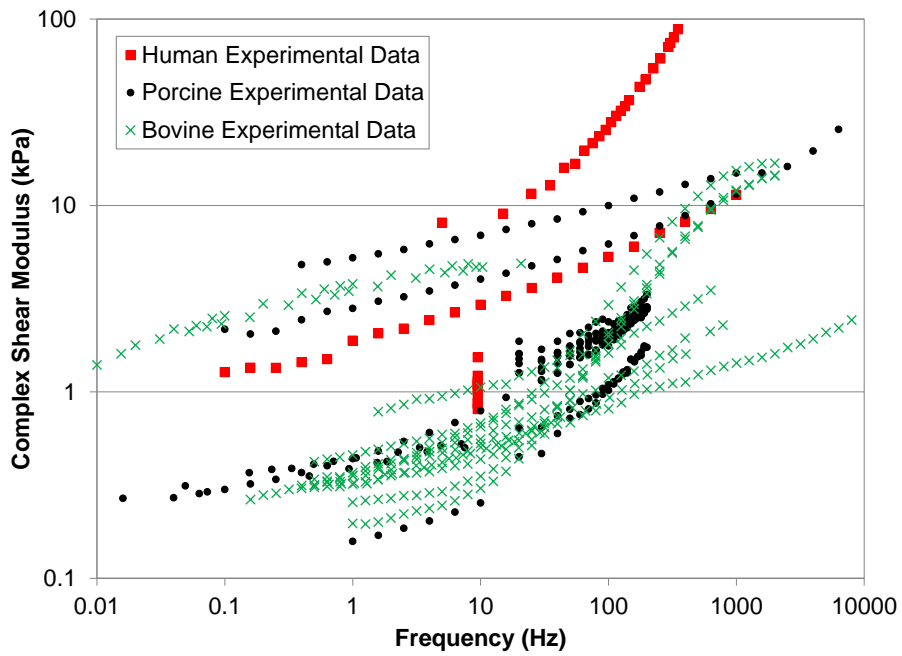
Figure 2-16: An interspecies comparison of complex shear modulus of mammalian brain tissue shows no clear species dependence.
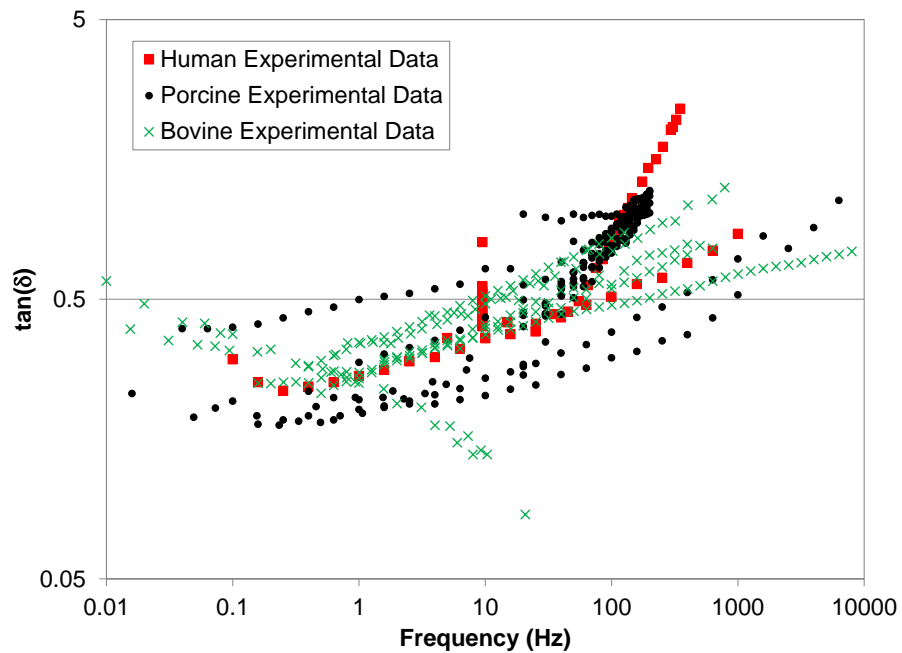
Figure 2-17: An interspecies comparison of tanδ of mammalian brain tissue shows no clear species dependence.

Many challenges exist with the mechanical characterization of brain tissue. Due to the high metabolic requirement of brain tissue it begins to break down very quickly post-mortem and significant degradation of tissue mechanics occurs after approximately 6 hours (Gefen et al. 2004, Garo et al. 2007). Testing of tissue in vivo is desired to maximize the accuracy of measurements and biofidelity of the resulting models. This is made difficult by the sensitivity of the tissue to injury and inaccessibility due to the skull. In in vivo animal models the effects of circulation and pulse also complicate sensitive testing (Fallenstein et al. 1969, Gefen and Margulies 2004). Recent advances such as MRE make in vivo characterization easier but this new technique is not without its own problems to be resolved and therefore limited experimental data has been produced to date. Due to significant differences in methodology large differences in measured tissue behavior exist. As can be seen in Figure 2-14 and Figure 2-15, order of magnitude differences in complex shear modulus and tanδ have been published. Brain tissue is very soft and nearly incompressible, highly viscoelastic, and anisotropic. This makes it hard to not only test but to analytically and computationally model for FE simulation tools (Chatelin et al. 2010, Panzer et al. 2012b, Panzer et al. 2013).

2.4 Comparative Anatomy and Scaling

An understanding of some of the major differences in comparative anatomy between mammalian species commonly used for blast research is important for development of interspecies scaling. This section will first look at the basics of

biomechanical scaling used across injury biomechanics research. Then an overview of

comparative anatomy will be presented, with a focus on mammals, especially those used

for blast research. Finally, this section will discuss simple scaling and allometric

relations between species that may help explain interspecies differences in blast injury

tolerance.

2.4.1 Biomechanical Scaling

Scaling has long been used in injury biomechanics research to either normalize

test data among different species to a standard species or size, or to extend experimental

data to a larger or smaller size (Melvin 1995). These scaling techniques are commonly

derived through dimensional analysis using three fundamental quantities; characteristic

length (body, head, etc.), tissue mass density, and tissue stiffness (Ommaya et al. 1967,

Melvin 1995, Eppinger et al. 1999). These scaling relations allow us to scale the dose so

that a given physical response (i.e. acceleration, force, strain) is matched across species.

Some of these biomechanical scaling models are presented in Table 2-3.

Table 2-3: Biomechanical scaling relations for scaling dose to match output response (Panzer et al. 2014).

Length scale	$\lambda_L = L_1/L_2$
Mass density scale	$\lambda_\rho = \rho_1/\rho_2 = 1$
Modulus of elasticity scale	$\lambda_E = E_1/E_2$
Mass scale	$\lambda_m = m_1/m_2 = \lambda_L{}^3$
Time scale	$\lambda_T = T_1/T_2 = \lambda_L/\sqrt{\lambda_E}$
Velocity scale	$\lambda_V = V_1/V_2 = \sqrt{\lambda_E}$
Acceleration scale	$\lambda_a = a_1/a_2 = \lambda_E/\lambda_L$
Force scale	$\lambda_F = F_1/F_2 = \lambda_L{}^2\lambda_E$
Moment scale	$\lambda_F = M_1/M_2 = \lambda_L{}^3\lambda_E$
HIC scale	$\lambda_{HIC} = HIC_1/HIC_2 = \lambda_A{}^{2.5}\lambda_T = \lambda_E{}^2/\lambda_L{}^{1.5}$
Head angular acceleration scale	$\lambda_\Omega = \Omega_1/\Omega_2 = \lambda_m{}^{-2/3} = \lambda_L{}^{-2}$

Where subscripts 1 and 2 refer to the subjects to be scaled to and from, respectively

The use of a characteristic length generally assumes geometric similarity between subjects or species and mass densities of tissues are generally assumed to be constant. These scaling relations are widely used for injury biomechanics, especially in automobile injury research. For example, pediatric neck injury criteria have been derived from scaled pediatric porcine data (Eppinger et al. 1999). For the study of blunt trauma,

scaled angular head acceleration has been scaled to match peak brain shear strain from

rhesus monkey experiments to a human equivalent dose (Ommaya et al. 1967).

Similarly, head angular acceleration was used to develop rotation injury criterion for

human diffuse axonal injury from in vivo primate injury model data (Margulies et al.

1992). One major limitation of these scaling techniques is that there is no consideration

of differences in physiology and pathological injury manifestation between subjects or

species.

2.4.2 Comparative Neuroanatomy and Allometry

There are large differences in body size, morphology, organ structure, and

physiology between common blast animal model species. The large anatomical and

physiological differences must be accounted for if we are to compare injury response

across species and to humans. However, there are many similarities, at least within

mammals. Mammals display similar central nervous system microstructure and

organization of brain regions is consistent, while differences in relative size and shape

exist. Differences across species often times are described by simple scaling relations.

Allometry is the study of such scaling relations that empirically derives power

law relationships between parameters of interest, often as a function of body mass

(Equation 2-9). Sucessful scaling relations produce a straight line when displayed on a

log-log graph, and the slope of this line, α, describes the general behavior of the

parameter. These allometric, power law scaling relations predict the parameter value, X,

using body mass and a scaling exponent, α. The constant, b, is associated with a subset of species, often applying to a majority of mammals. An allometric model with a slope greater than 1 indicates that the parameter's relative size increases in larger species, for example bone mass which must increase at a greater rate than body mass to support the body (Lindstedt et al. 1981). A slope equal to 1 indicates that the parameter has the same relative size across body mass, such as lung mass in mammals (Calder 1981). A slope less than 1 indicates that the parameter has a relatively smaller size in larger species, such as brain mass which constitutes a smaller portion of total body mass in large species (Armstrong 1982). Some research areas use allometry extensively such as in comparative anatomy (Lindstedt and Calder 1981), animal care (Kleiber et al. 1961, Hofman 1983), and pharmacokinetics research (Boxenbaum 1982, Mordenti 1985). This type of empirical scaling is valuable, especially when analytical or experimental derivation of scaling is not possible.

$$X = bMass_{body}^{\alpha} \hspace{4cm} \textbf{Equation 2-9}$$

Previously derived and validated blast injury scaling for pulmonary injury was found to be dependent on total body mass of the animal (Bowen et al. 1968). This would suggest that blast neurotrauma scaling should show dependence on mass of the head or brain. There are orders of magnitude differences in brain mass from less than 1g in mice to greater than 1kg in humans, and the relative sizes of popular blast animal model brains are presented in Figure 2-18.
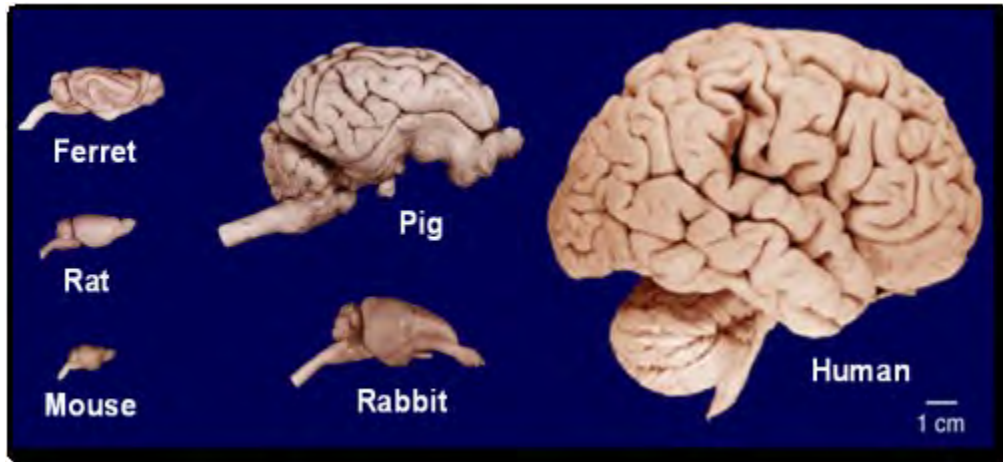
Figure 2-18: Relative brain size and surface structure of common animal model species shows large differences in brain size and degree of cortical folding [adapted from Wisconsin Brain Collection].

The variation in brain size across species has been extensively studied through body size allometry (Kleiber et al. 1961, Lindstedt et al. 1981, Boxenbaum 1982). Among vertebrates, mammals typically have the largest brains relative to body size, as much as 10 times larger than reptiles (Northcutt 2002). Primates and carnivores are above average among mammals, artiodactylas (pigs) and ungulates (horses) are about average, while rodents and lagomorphs (rabbits) are below average (van Dongen 1998a). A representation of mammal species brain size versus body size in presented in Figure 2-19 along with the allometric scaling line. A metric to quantify the variation of brain mass in a specific species from that predicted by allometry has been developed. This metric is referred to as the encephalization quotient and is greater than 1 in species with unexpected large brains (i.e. humans and other primates) and less than 1 in species with unexpected small brains (van Dongen 1998a). Brain mass is known to be factor in

62

concussive tolerance to rotational acceleration (Ommaya et al. 1971). It stands to reason

that brain mass it therefore a large factor in blast neurotrauma.
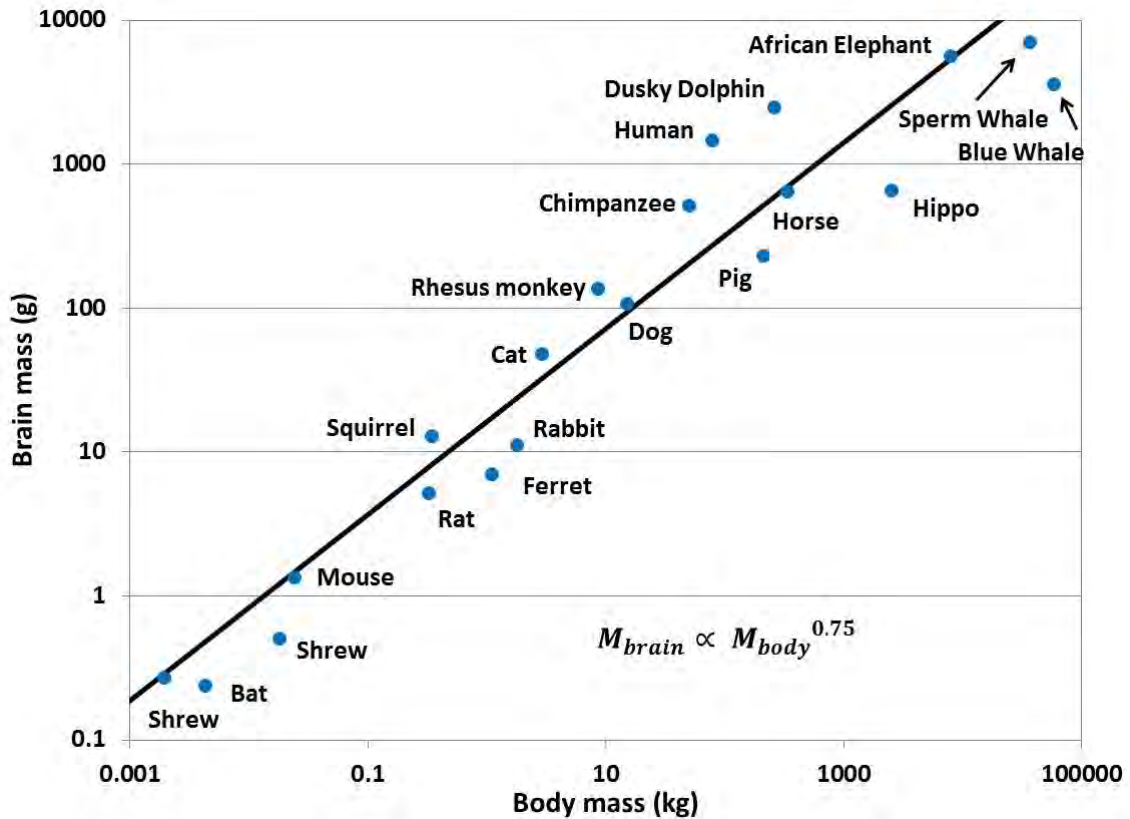
Figure 2-19: Brain mass versus body mass for the full range of mammal body size, with the resulting allometric scaling line. Species falling above the line indicate larger than predicted brain mass while below the line indicates smaller than predicted brain mass (van Dongen 1998a).

Beyond brain size there are clear differences in morphology between mammalian

brains, especially on the cortical surface. The folding of the cortical surface is referred to

as gyrencephaly and the surface convolutions may be an important biomechanical

difference between species (Bass et al. 2012). In Figure 2-18, there is a range of brain

folding from the mouse which is primarily smooth, or lissencephalic, up to the human

which is highly folded. In general mammals with a brain mass less than 5g are

lissencephalic while those with brain mass greater than 50g are gyrencephalic, with a

few exceptions (Van Dongen 1998). This increased cortical surface area is associated

with a potential for higher brain function. The biomechanical role of cortical folding is

not yet clear but a computational model has shown the presence of folding may decrease

brain tissue strain during inertial loading (Ho et al. 2009). The effect of surface

convolutions at blast rates is unknown. The degree of gyrencephaly is often described

an index of folding, which is the ratio of total cortical surface area to that of an

equivalent sized smooth brain (Hofman 1985). This index of folding is approximately 1

in lissencephalic species and can exceed 5 in some marine mammals, in humans it's

approximately 2.8 (Van Dongen 1998). The index of folding as a function of body mass,

for several mammalian species of interest, is presented in Figure 2-20.
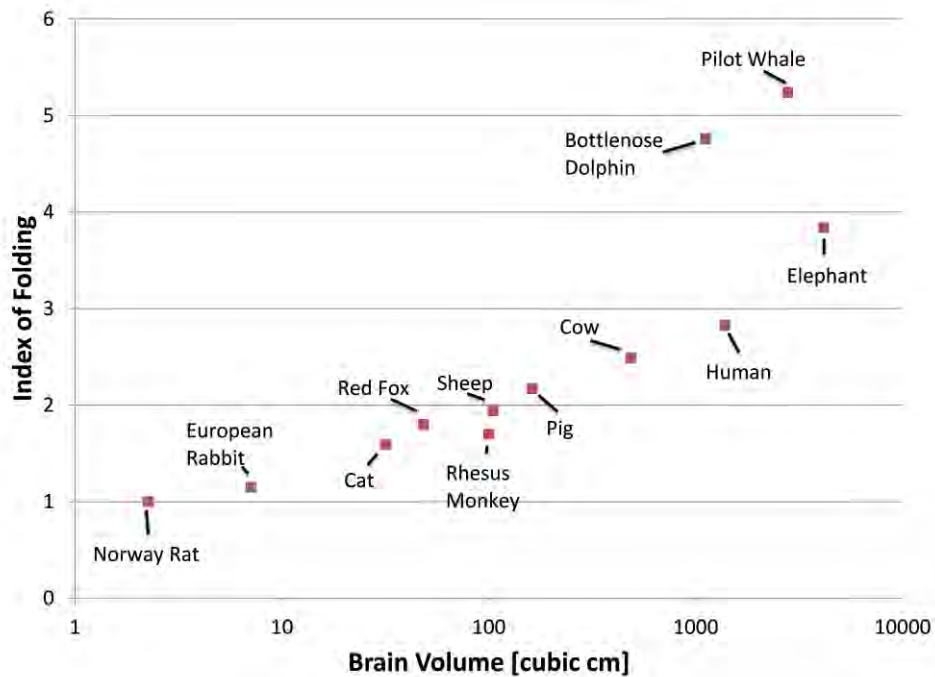
Figure 2-20: Index of folding for representative mammal species over a large range of body mass. Index of folding = 1 indicates lissencephalic brain (Hofman 1985).

There are additional differences in brain anatomy that may contribute to differences in injury tolerance but cannot necessarily be described by simple scaling relations. Large variations in skull thickness and morphology exist between the species commonly used for blast neurotrauma research. Some species like pigs have highly variable skull thickness depending upon region while species like mice are pretty consistent across the skull. Skull thickness in pigs can vary from approximately 12mm in the frontal and parietal down to 5mm in the temporal region for 60kg animals. In humans, skull thickness is much more consistent, varying from approximately 7mm in the frontal and occipital to 5mm thick in the parietal region (Lynnerup 2001). Skull

65

thickness does not however, reliably scale across mammals according to body size. The effect that skull thickness has on blast injury tolerance in unknown, but it is reasonable to expect it plays a role in pressure attenuation and local deformation at the brain surface.

Absolute and relative size of brain substructures also varies in mammals. The cortical thickness has been observed to increase with brain size but with large variation. The relative size of brain structures (i.e. amygdala, hippocampus, ventricles) vary but cannot be described by simple scaling across a large range of mammals. There have also been measurements of differences in brain microstructure. While glial cell mass has been shown to vary little, neuronal cell mass increases with increasing brain mass (Mota et al. 2014). Likewise an investigation of variation in cell size across types found that quickly dividing cells that make up most of the body exhibit consisten size, while slowly dividing cells like neurons and adipocytes seem to scale with body size (Savage et al. 2007). Additionally, a decrease in neuronal density has been shown in increasing brain size (Hofman 1983). These factors that do not scale across body size predictably are hard to account for with simply scaling models. This could mean that scaling models may not be appropriate for all mammals, with different scaling models required for species qualitatively different, like lissencephalic and gyrencephalic.

Beyond obvious differences in brain size and morphology there exists significant physiological differences between mammalian species. Like with some of the size and

morphology measures discussed there are some clear body mass dependent

physiological parameters that can be described by allometry. These relations are

important when utilizing animal models and especially important in pharmacokinetics

research when trying to relate animal physiological response to that in humans

(Boxenbaum 1984, Mordenti 1986).

Most allometric physiological relations fall into one of three categories based on

their behavior related to body mass. The first group is capacity parameters. The

parameters within this category are those usually associated with maintenance and

physiological support of the body. Parameters such as organ mass, lung tidal volume,

and blood volume fall within this category and usually scale with an exponent of

approximately 1 (Lindstedt et al. 1981). This means that the value of these parameters

relative to the body size of the animal stays constant as animal body mass increases.

A second group is volume-rate parameters. These make up a large portion of

allometric research and have to do with the rate at which things flow or are used up

within the body. Parameters like metabolic rate, cardiac output, and minute respiratory

volume fall into this category and scale with an exponent of approximately 0.75 (Kleiber

et al. 1961, Hofman 1983). This group of parameters displays a decrease in relative value

with increasing body mass.

The final major category is cycle lengths and frequencies. This group scales with

an exponent of approximately 0.25 and is often referred to as physiological time

(Lindstedt and Calder 1981, Boxenbaum 1982). Parameters such as breath duration, heartbeat duration, and lifespan fall within this category. One implication is that mammals have approximately the same number of total breaths and heartbeats in their lifetime (Boxenbaum 1982). Physiological time may be an important factor in the scaling of response between animal models as it describes the characteristic time period over which things happen within a species. It is possible that this can explain differences in injury response due to the rate of blast relative to the physiological time in the animal, as well as change injury time course in difference species.

Chapter 3 - Viscoelastic Properties of Hybrid III Head Skin

Anthropomorphic testing devices (ATDs) are a common and valuable tool for the study of injury biomechanics. These human surrogates allow us to measure the mechanics resulting from a given input and correlate with known human injury tolerance. An understanding of the mechanical behavior of all parts of the test device is crucial for assessing its biofidelity and maximizing its research value. This chapter presents an experimental viscoelastic characterization of the rubber skin covering used in Hybrid III ATDs. This chapter was originally published as a manuscript (Wood et al., 2010. Viscoelastic Properties of Hybrid III Head Skin. SAE International Journal of Materials and Manufacturing. 3(1):186-193.) and is adapted for this dissertation by permission of the publisher.

3.1 Introduction

The Hybrid III anthropomorphic testing device (ATD or dummy) has been widely used in automotive biomechanics testing as a robust human surrogate for assessing the potential for human injury (Mertz 1985). The dummy has also been utilized for biomechanics research in sports injury (Pellman et al. 2003) and military injury (Hayda et al. 2004, Bass et al. 2005). Finite element models of the Hybrid III have been developed to enable numerical simulation of motor vehicle accidents (Yang et al. 1992, Moss et al. 1997) and federal motor vehicle safety standards. Finite element

dummy models are useful as they are generally less complex than human body models, and can be validated experimentally with repeated tests. To produce accurate Hybrid III simulation results over a range of input scenarios, the model must use appropriate material properties that have been characterized over the wide range of strain and strain rates that the dummy will experience during an impact or event. In this regard, the properties of skin materials play an important role in the dummy response during a blunt impact scenario, as the bulk of the compliance in ATD heads is in the skin. Accordingly, simulation of this impact requires material properties derived from experimental data encompassing this regime of loading.

Viscoelastic material testing of rubbers may be performed using tension (Dickie et al. 1971, Song et al. 2004), compression (Moreland et al. 1994, Shergold et al. 2006) and shear (Wu et al. 2000) loading. Indentation testing coupled with finite element analysis has also been used to determine viscoelastic behavior (Chua et al. 2009). To determine the viscoelastic behavior of the rubber skin material, compression loading was chosen. A common method for compression testing of rubber is testing a sample between two flat platens and using a prescribed compressive displacement while measuring the force generated by the compression (Gent et al. 1970, Wu et al. 2003). In this setup, the end conditions of the sample have an effect on the stress distribution in the sample and on the measured response (Gent and Meinecke 1970). It has been shown in Hybrid III head test applications, such as head drop, that surface treatment with lubricants has

70

significant influence of acceleration based injury metrics (Mertz 1985). The mechanical

effect of end conditions can also be controlled by lubrication of the sample contact

surfaces (Gent and Meinecke 1970, Walley et al. 1989, Shergold et al. 2006). Lubrication

reduces the effective stiffness of the material by reducing the constraints applied to the

ends of the sample, and thus gives a better measure of the material properties in pure

compression.

Most rubbers have nonlinear viscoelastic properties (Schapery 2000). There have

been many approaches to modeling the behavior of time-dependent materials such as

rubber and biological tissue (Fung 1981). Integral-type viscoelastic models are

commonly used as they can be easy to implement for complex loading and nonlinear

behavior materials (Green et al. 1959, Pipkin et al. 1968). Quasi-linear viscoelasticity

(QLV) is a common viscoelastic theory used to characterize biological materials and

polymers that have nonlinear elastic responses, as it reduces constitutive model

complexity by separating the nonlinear elastic response from a linear temporal response

(Fung 1981, Funk et al. 2000). A fully nonlinear viscoelastic model, where the elastic and

temporal responses cannot be considered independent, can be considerably more

complex and require a large number of tests to fully characterize the model (Schapery

2000, van Dommelen et al. 2006).

The goal of this study was to characterize the viscoelastic material properties of

the Hybrid III head skin. A nonlinear viscoelastic model with separable temporal and

elastic responses (similar to QLV) was used to model the material. The viscoelastic

model developed in this study will be used in finite element models of the Hybrid III to

increase the accuracy of the response during blunt impact to the dummy head.

3.2 Methods

3.2.1 Experimental Setup

Cylindrical samples from a newly manufactured Hybrid III head skin (Denton

ATD, Rochester Hills, MI) were cut from both lateral aspects of the head using a 0.5 inch

diameter rubber punch mounted in a press. The samples were cut slowly with minimal

force to minimize compression of the material (ASTM 2007). Nine samples with a

length/diameter ratio of one were chosen for testing, with four samples taken from the

left side of the head and five taken from the right side. Viable area on the head skin

from which consistent samples could be taken was limited by the surface curvature.

Each sample was measured using digital calipers to determine the height and the

diameter of the sample, with the diameter measured at a midlevel between the top and

bottom surfaces. The average ± standard deviation (SD) of the sample height (l0) and

sample diameter (D0) were 10.55 mm ± 0.62 and 9.97 mm ± 0.18, respectively. The left

side samples were 1 mm shorter than the right side samples (p = 0.0035), and 0.3 mm

wider than the right side samples (p = 0.0012).

Tests were performed by compressing each sample between two flat platens

mounted to a servohydraulic testing system (MTS, Eden Prairie, MN). To minimize

friction between the sample and the platens, petroleum jelly (Unilever, London, UK) was applied to both surfaces of the sample in contact with the platens during testing (Gent et al. 1970, Walley et al. 1989, Shergold et al. 2006). Minimal thickness of lubrication was used to avoid contribution to the overall height of the sample.

Samples were compressed using displacement control. Displacement inputs were based upon engineering strain as defined by the ratio of change in height (Δl) to the initial height ($l0$) of the sample. Zero strain was defined by the height of the sample under a 1N initial load. This initial load was to ensure the proper contact of the bottom and top surfaces of the sample without substantial displacement from its initial unstressed height. Subsequent tests for each individual sample were separated by a period of at least 24 hours.

Each sample was subjected to separate step-hold tests to engineering strain levels of 10%, 20% and 30% compression. Each strain level was held for 60 s to study the relaxation behavior of the material. Displacement rates were set to the maximum velocity allowed by the system to study material response for the shortest available duration. The rise time for each step was approximately 40 ms. An additional series of step-hold tests were done on each sample four times at the same strain level to assess the repeatability of the testing, and to ensure that the material was not being damaged from testing. Each sample was then tested at constant engineering strain rate up to 30%

engineering strain over four different strain rates. The constant strain rates were 0.1%,

1%, 10%, and 100% 1/s.

Displacement and force data was recorded at 10 kHz using data acquisition

software (LabVIEW, National Instruments). The resulting data was filtered and

decimated using MATLAB (MathWorks) to perform model fitting and optimization

done using Excel Solver (Microsoft).

3.2.2 Modeling/Analysis

The stress response, $\sigma(\lambda, t)$, was analyzed for each test using a convolution

integral of the form in Equation 3-1.

$$\sigma(\lambda, t) = \int_0^t G_{red}(t - \tau) \frac{d\sigma^e}{d\lambda} \frac{d\lambda}{d\tau} d\tau \qquad \textbf{Equation 3-1}$$

where Gred is the reduced relaxation function, σe is the instantaneous elastic function, λ

is the stretch ($\lambda = 1 + \Delta l/l_0$), t is the time, τ is a dummy variable for integration, and σ is

the material true stress ($\sigma = F/A = \lambda[F/A_0]$).

The reduced relaxation function is based on a series of Maxwell elements, and

expressed as the Prony series (Equation 3-2).

$$G_{red}(t) = G_\infty + \sum_{n=1}^{5} G_n e^{\frac{-t}{\tau_n}} \quad \sum G_i = 1 \qquad \textbf{Equation 3-2}$$

where G∞ is the steady-state relaxation coefficient and τn are the time constants

corresponding to each of the relaxation coefficients, Gn. In this study, five terms in the

Prony series were used, with time constants, τn, constrained to decade values 100s, 10s,

1s, 100ms, and 10 ms (Lucas et al. 2008). The convolution integral, Eq. (1), was

numerically integrated in terms of instantaneous elastic parameters, and relaxation

coefficients (Darvish et al. 1999). This technique allowed for the evaluation of the

convolution integral using an arbitrary displacement input based on displacement time-

history of each test rather than a idealized step-hold displacement (Darvish and al.

1999). A generalized reduced gradient technique was used to find an optimal solution

for instantaneous elastic parameters and the relaxation coefficients (Excel Solver,

Microsoft).

Reduced relaxation coefficients and instantaneous elastic function parameters

were simultaneously optimized by minimizing the sum of the squared errors for all 54

step-hold tests together. Multiple hyperelastic models were considered for the

instantaneous elastic function, including Neo-Hookean, Mooney-Rivlin, 1-term Ogden,

and 2-term Ogden models. The functional forms of each of the hyperelastic models in

uniaxial compression are shown in Table 3-1 in order of increasing complexity.

Complete sets of relaxation and instantaneous elastic parameters were optimized for

each of the elastic models. Quality of viscoelastic model fit was assessed using a sum of

squared errors (SSE) metric.

Table 3-1: Functional forms of hyperelastic models in uniaxial compression.

Model	Stress (True) – Stretch
Neo-Hookean	$\sigma = \mu(\lambda^2 - \lambda^{-1})$
Mooney-Rivlin	$\sigma = \mu_1(\lambda^2 - \lambda^{-1}) + \mu_2(\lambda^{-2} - \lambda^1)$
One-term Ogden	$\sigma = \mu(\lambda^\alpha - \lambda^{-\frac{\alpha}{2}})$
Two-term Ogden	$\sigma = \mu_1\left(\lambda^{\alpha_1} - \lambda^{-\frac{\alpha_1}{2}}\right) + \mu_2(\lambda^{\alpha_2} - \lambda^{-\frac{\alpha_2}{2}})$

3.3 Results

Plots of representative material behavior during the step-hold relaxation testing

and constant strain rate testing are shown in Figure 3-1. The relaxation tests (Figure

3-1A) showed typical viscoelastic behavior where the magnitude of compressive stress

decreases with time during the duration of constant applied displacement. For the

constant strain rate tests (Figure 3-1B), the material response was noticeably nonlinear

and stiffening with increasing compressive strain. Additionally, there was a marked

increase in material stiffness with increasing applied strain rate.
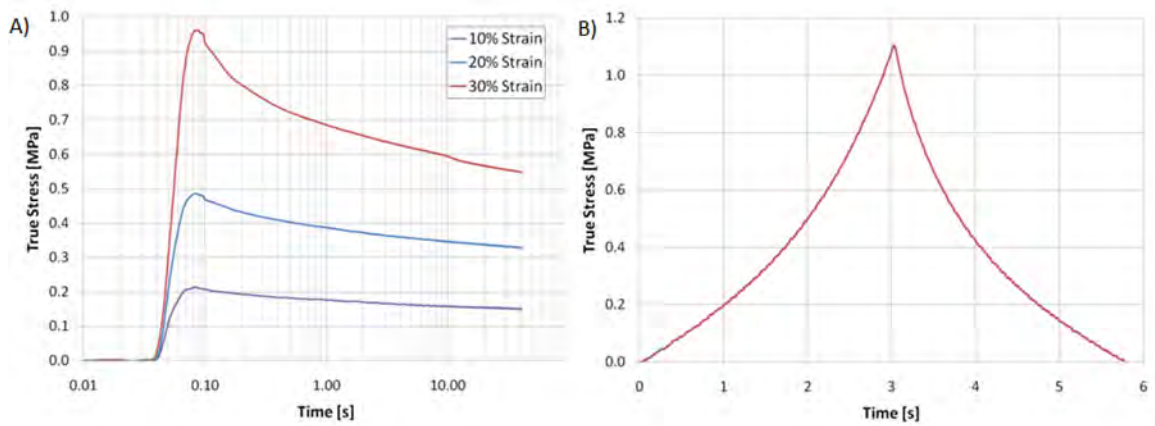
Figure 3-1: Representative true stress responses from A) step-hold relaxation tests, and B) constant strain rate tests.

Step-hold tests were repeated four times to ensure the repeatability of the stress response of the material. A representative series of four step-hold tests on a single sample is shown in Figure 3-2. The repeated testing up to 30% strain shows slight differences in long-term response, with normalized stress levels at 60 seconds varying by less than 10% of their mean. Importantly, the material shows no progressive decrease in stress-time response with number of tests, ensuring that no material damage occurred up to this strain level.
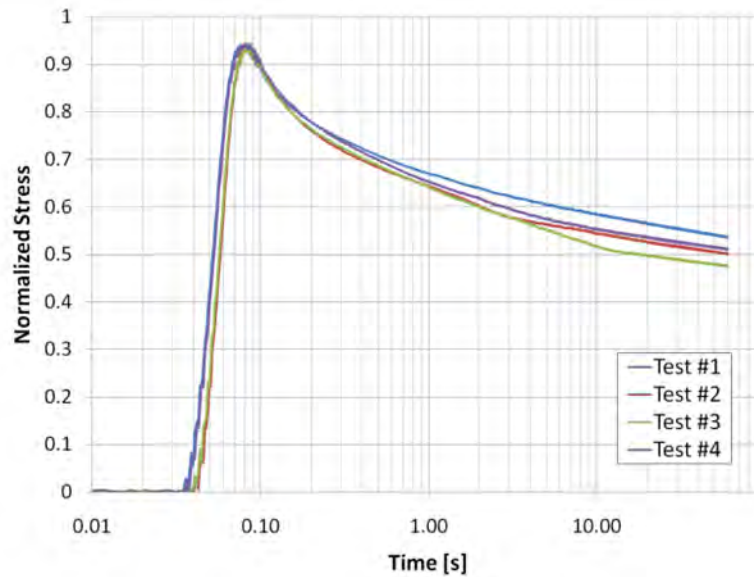
Figure 3-2: Representative true stress responses of a single sample for repeated 30% strain step-hold shows no progressive material damage.

Figure 3-3 shows the average normalized force response for each of the strain levels with ± 1 standard deviation error bars. To compare the mean relaxation responses at the three different strain levels, Student t-test was performed (α=0.05, p < 0.05 is statistically significant) using the final relaxation level at 60 s. No statistical difference was found between the average relaxation response of the 10% and 20% compressive strain data (p = 0.1067); However, the 30% strain relaxation response was statistically different than both the 10% and 20% strain levels responses (p < 0.001). This suggests that the separability assumptions were valid for the head skin material up to 20% compressive strain.
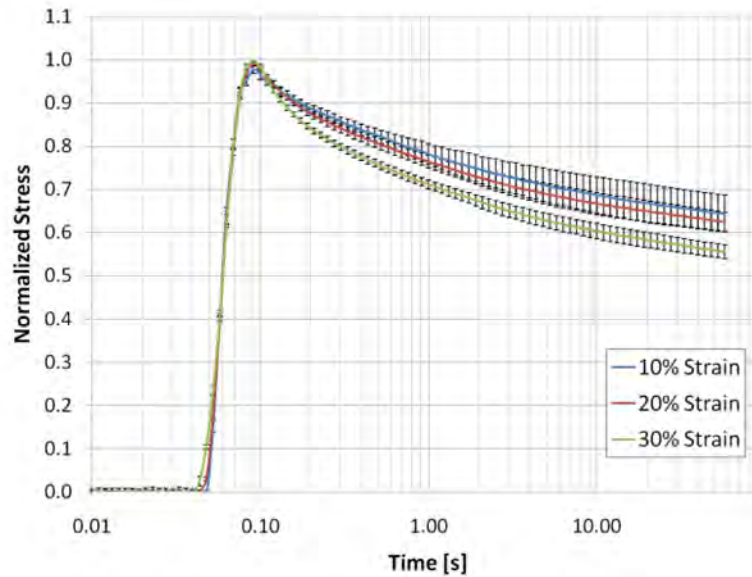
Figure 3-3: Normalized true stress response of complete set of step-hold tests shows altered relaxation behavior at 30% strain. Solid lines represent average normalized true stress at each level and bar are representative of ± 1 SD corridors.

The reduced relaxation function and instantaneous elastic function for each

elastic model were fit using the complete set of step-hold data. The model parameters

for each hyperelastic constitutive model are shown in Table 3-2. The values of the

shorter relaxation time-constants (0.01 and 0.1 s) emphasize fast rate viscoelastic effects

for blunt impacts at moderate and higher rates, while the longest relaxation time

constant (G_∞) represents the equilibrium relaxation. Four different types of

hyperelastic models were considered for modeling the instantaneous elastic function:

Neo-Hookean (Macosko 1994), Mooney-Rivlin (Treloar et al. 1976), and one-term and

two-term Ogden (Ogden 1972). Goodness of fit for each instantaneous elastic model

was determined using SSE metrics between the model prediction and experimental step-

hold stress response. Figure 3-4 shows the typical model fit of the final 2-term Ogden

model to a 10%, 20% and 30% step-hold test. Only the 2-term Ogden model was able to

capture the peak force behavior at all three levels in addition to the relaxation behavior

of the material.
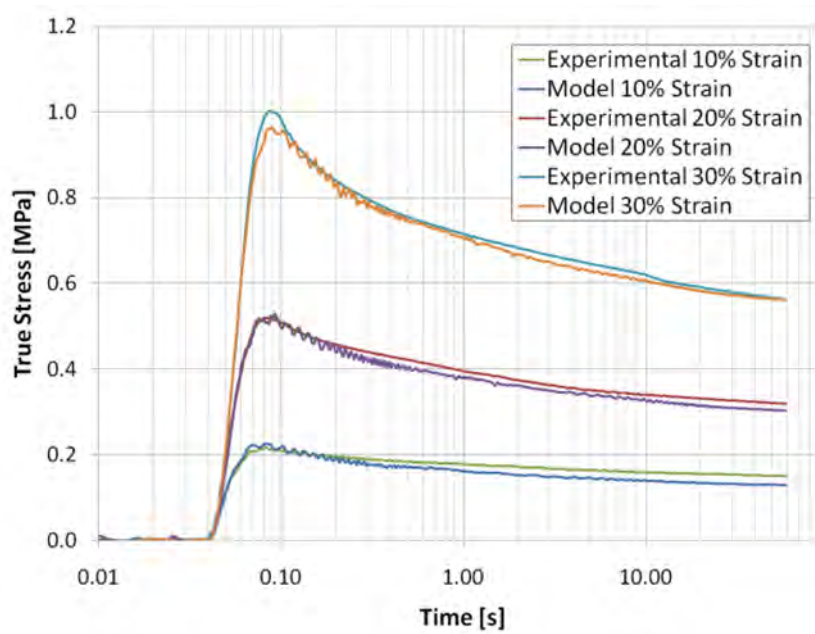
Figure 3-4: Typical model fit of the final 2-term Ogden model to a 10%, 20%, and 30% strain step-hold test shows good model agreement.

Table 3-2: Separable viscoelastic model parameters and goodness of fit.

	Reduced Relaxation Function Parameters						Instantaneous Elastic Parameters				
	G_1 τ_1=0.01s	G_2 τ_2=0.1s	G_3 τ_3=1.0s	G_4 τ_4=10s	G_5 τ_5=100s	G_∞ τ_∞=∞	μ_1	α_1	μ_2	α_2	SSE
Neo-Hookean	<0.001	0.235	0.115	0.082	0.039	0.530	1.020	----	----	----	44.157
Mooney-Rivlin	0.170	0.193	0.093	0.069	0.032	0.443	0.000	----	-0.899	----	10.575
1-Term Ogden	<0.001	0.250	0.103	0.097	<0.001	0.551	69.30	0.027	----	----	29.407
2-Term Ogden	0.235	0.172	0.087	0.065	0.028	0.414	0.318	1.492	-0.401	-3.316	8.423

Both the Neo-Hookean and one-term Ogden models were unable to adequately capture the nonlinear compression response. The inability to properly model the instantaneous elastic function forced the Neo-Hookean and one-term Ogden models to remove the influence of the 10 ms time-constant response. The Mooney-Rivlin model greatly decreased the SSE of the fit, and the two-term Ogden model provided the best fit of the data, having the lowest SSE value. Considering the results of the fits, the two-term Ogden hyperelastic model was chosen as the instantaneous elastic function.

The model was then validated using the constant strain rate experimental data. Figure 3-5 shows the average ± 1 SD response of the constant rate tests along with the predicted response of the model. The model agrees well with the experimental data up to 30% compressive strain (0.70 stretch), falling within 1 SD of the experimental average, for strain rates up to 10% 1/s. Some deviation from the experimental response exists beyond 10% 1/s compressive strain rate; however, the model behavior still falls within 1 SD of the experimental average for a majority of the response.
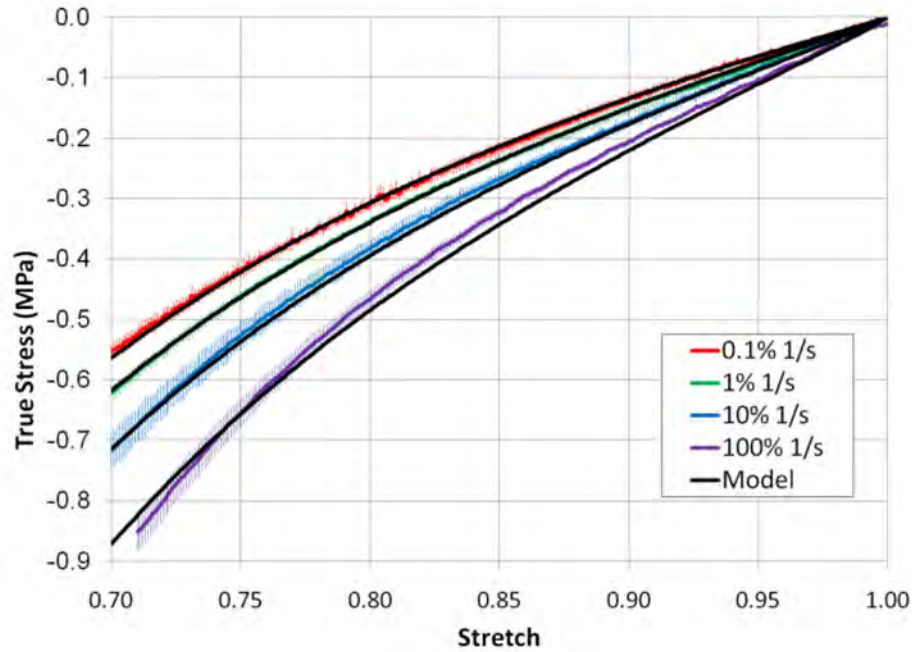
Figure 3-5: Viscoelastic model comparison to constant strain rate experimental data. Loading phase of tests is shown as average true stress response with ± 1 SD bars.

Material samples were taken from different sides of the head skin to compare the behavior according to location. Although there was no statistical difference found in the material behavior based on the side of the head where the sample was taken, there was a difference in the sample thickness. The average ± standard deviation of sample thickness from the left and right side were 9.97 ± 0.35 and 11.02 ± 0.25, respectively. This may cause a variation in lateral impact response for Hybrid III head.

3.4 Discussion

Model validation was considered successful since the predicted response fell within one standard deviation of the experimental constant strain rate data up to 30% compressive strain and 10% 1/s strain rate. Beyond 20% compression, the temporal

response of the material was no longer strain-independent, and the assumed

separability of temporal and spatial dependence was not valid The results in Figure 3-3

show that the transient response at 30% was statistically different than the response at

10% and 20% strain. However, Figure 3-5 shows that the deviation of the model from

the experimental results was only noticeable at the highest strain rate (100% 1/s), falling

outside of the one standard deviation corridor at a few levels of stretch. However, since

the model was completely within two standard deviations of the 100% 1/s experimental

results, the model was considered valid for the entire range of strain rates in this study.

A nonlinear viscoelastic model with dependent temporal and strain behavior (e.g.

Green-Rivlin Model (Findley et al. 1989)) may be required for larger strains and higher

strain rates to accurately characterize the behavior.

The reduced relaxation function for the step-hold test data had larger coefficients

for the 10 and 100 ms time-constants, suggesting that these short time-constants are

important for modeling the Hybrid III head skin in blunt impact. The instantaneous

elastic function represents the nonlinear elastic behavior of the material, and a

hyperelastic constitutive model was an ideal method for representing this behavior. Use

of these hyperelastic models carries the assumption that the material is isotropic and

incompressible, which rubbers are generally considered (Ogden 1972). Note that both

the Neo-Hookean and Mooney-Rivlin hyperelastic models are a subset of the Ogden

84

model, so it was expected that the increase in model generalization would result in an improved fit to the data.

Additionally, this model can only be considered validated for unconfined compression. Shear and tension tests were not done on this material, so the model could not be evaluated under these types of load. However, the general mode of loading on the Hybrid III head skin material during blunt impact would be compression, so characterizing the shear and tensile behavior of the material may not be necessary for many blunt impact scenarios.

Other factors to consider when testing rubber materials include testing temperature and material age. The temperature of the material during this study was not monitored, but all testing was carried out in a temperature controlled lab at room temperature. Previous work has shown that material behavior can change significantly over varied temperature (Lion , Plazek 1965). However, this behavior change occurs over a much larger temperature interval, approximately 50ºC, than the temperature range of this study. Experimental work has also shown that there are significant changes in the material behavior of rubber with age (Mott et al. 2001, Wei et al. 2004). The Hybrid III head skin used in this study was less than 1 year old, but many Hybrid III dummies in use today have skins that are much older. It may be necessary in the future to study the effect of age on the material properties of Hybrid III skins.

3.5 Conclusions

The Hybrid III crash test dummy is commonly used as a human surrogate for predicting injury in many different scenarios. Finite element models of the Hybrid III are also frequently used as a complement to experimental testing. The implementation of an accurate material model of the dummy into the current computational models will serve to improve their accuracy. This study presents a separable nonlinear viscoelastic model of the Hybrid III dummy head skin validated for strains up to 30% and strain rates varying from 0.1 to 100% 1/s. It was found that the coefficients associated with the shortest time constants, 0.1 and 0.01 s, were large when compared to the other relaxation coefficients. Results showed some strain dependent relaxation at compressive strains greater than 20%. The resulting validation shows that within the strain rate and level constraints of the model, Hybrid III head skin can be accurately characterized using linear viscoelasticity with a nonlinear instantaneous elastic function, Ogden hyperelasticity.

Chapter 4 - Behind Armor Blast Pressure Attenuation

Of great interest in recent military conflicts in Iraq and Afghanistan has been the observed increase in closed-head traumatic brain injury and corresponding decrease in pulmonary trauma thought to be caused from blast exposure. One of the leading hypotheses as to why this fundamental shift in injury has occurred is that increased usage of thoracic body armor provides protection to the pulmonary system while leaving the head vulnerable to blast. This chapter investigates the ability of modern ballistic body to attenuate blast pressure seen by the thorax. This chapter was previously published as a manuscript (Wood et al. 2012. Attenuation of blast pressure behind ballistic protective vests. Injury Prevention. 19:19-25.) and is adapted for this dissertation with permission from the publisher.

4.1 Introduction

Primary blast injuries, those injuries associated with the overpressure wave of a blast, have long been observed on the battlefield and are known to principally damage the air-containing organs, particularly the lungs (Hooker 1924). Animal studies performed between 1920 and 1945 resulted in quantitative assessments of human pulmonary injury risk (Bowen et al. 1968). These risks were published as injury tolerance and survivability risk curves and were determined by the peak overpressure and the overpressure duration of the pressure (Bowen and Fletcher 1968). The curves were later improved by inclusion of a much larger set of experimental data for short and

long overpressure duration blasts, and also by considering the problem of repeated

blasts (Bass et al. 2008, Rafaels et al. 2010, Panzer et al. 2012c). Throughout this period,

the air-containing organs, especially the lungs, were considered the most vulnerable to

injury and accordingly, the injury risk to other organs from blast overpressure was not

considered clinically meaningful. Most recently however, well documented cases of

blast injuries treated at military medical facilities in Iraq and Afghanistan have

presented with brain injury and not pulmonary injury (Martin et al. 2008, Ramasamy et

al. 2008). These findings conflict with historical research that shows the pulmonary

system being far more vulnerable to primary blast injury than the central nervous

system (Zuckerman 1941, Draeger et al. 1946, Rafaels et al. 2011).

One hypothesis to explain the relative lack of blast-related pulmonary injuries

and the emergence of blast-related head injuries is the widespread use of personal

protective equipment such as ballistic protective vests. Soft vests worn by law

enforcement (Montanarelli et al. 1975) and military (Raftenberg et al. 2004) personnel

provide protection from fragment and ballistic threats. Ballistic protection is further

increased through the use of hard armor inserts, commonly made of ceramic materials

(Rupert et al. 2001). Specialized protective equipment, namely explosive ordnance

disposal suits, are also effective in protecting against blast fragments and ballistic threats

(Bass et al. 2005, Hennessy et al. 2006); however, limited research has evaluated the

effectiveness of ballistic protective vests for protection from primary blast. Early work

suggested that protective vests were ineffective at reducing blast overpressure effects and increased pulmonary injury risk by acting as pressure amplifiers; a result inconsistent with contemporary reports of battlefield blast injury (Phillips et al. 1988, Cripps et al. 1996). These apparently conflicting results may be understood by other studies demonstrating the success of protective vests against blast overpressure waves could be increased with low-density decouplers (Cooper 1996). However, this previous work primarily examined fabrics with low areal densities, and did not consider the combination of ballistic vests with hard ceramic plate armor inserts. Recently a human torso surrogate model for blast has been developed (Merkle et al. 2010). Results of both free field and closed field testing with this surrogate have shown small effects of soft and hard body armor on pressure measured at different organ surrogate locations.

To reconcile the existing reports on ballistic vests and pulmonary protection, we hypothesized that both soft vests would attenuate the overpressure wave from primary blast exposure. We further hypothesized that this reduction in overpressure would protect the pulmonary system. Moreover, this pulmonary protection may be sufficiently effective so that solid organs like brain may indeed be at risk for injury from blast overpressure. To this end, we evaluated the blast attenuation from soft ballistic protective vests – with and without hard armor inserts - and assessed the resulting risk for pulmonary trauma. A shock tube was used to generate standardized and reproducible overpressure blast waves. Overpressure measurements were obtained

89

both at the anterior and posterior surface of the ballistic protective vest to determine the change in overpressure as the blast wave passed through the vest. The resulting experimental blast measurements were then compared with existing injury curves for lung (Bass et al. 2008) and brain (Rafaels et al. 2011) to assess the relative risk of lung and brain injury.

4.2 Methods

An 8″ nominal diameter, helium-driven shock tube was used to generate repeatable Friedlander-type blast waves, characterized by sharp rising and exponentially decaying overpressure. Shock tubes are commonly used to generate overpressure waves in laboratory settings. Three pressure transducers (Endevco 8530B-1000; San Juan Capistrano, CA) were mounted at the end of the shock tube to measure incident (side-on) overpressure of the shock tube output. Incident overpressure recorded from the shock tube sensors were converted to reflected overpressure using the ideal gas Rankine-Hugoniot relations (Iremonger 1997). The Rankine-Hugoniot relations are a function of atmospheric pressure (PA), incident overpressure (PI), and reflected overpressure (PR) as shown in Equation 4-1.

$$P_R = 2P_I\left(\frac{7P_A+4P_I}{7P_A+P_I}\right) \qquad \textbf{Equation 4-1}$$

Overpressure and overpressure duration measured at the end of the shock tube were adjusted to the desired levels by varying the rupture diaphragm thickness and driver section length. The diaphragm was constructed using up to 11 sheets of 0.01″

nominal thick polyethylene (Mylar, DuPont) film. The 'short driver' condition used a

driver section 5.1 cm in length, while the 'long driver' condition used a section 20.3 cm

in length. Adjustment of diaphragm thickness and driver length resulted in peak

reflected overpressures ranging from 210 to 3140 kPa, and positive-phase durations

ranging from 0.5 to 2.0 ms.

Shock tube tests were performed to assess the overpressure attenuation

capabilities of two types of representative police-force issue ballistic protective vests

(Protective Apparel Corporation of America [PACA], Jacksboro, TN). The soft vest was a

National Institute of Justice (NIJ) Level-2 vest made of woven Kevlar and the hard vest

was NIJ Level-4 armor vest consisting of the NIJ Level-2 soft vest with a ceramic insert.

The ceramic insert was designed to protect the mid-thoracic region over the heart,

greater vessels, and most of the anterior lung surface. The hard plate measures 25.4 cm

x 20.3 cm with a thickness of 25 mm and weighing 2.76 kg.

The vests were mounted tightly on a simplified, non-compliant human torso

surrogate consisting of a 10" nominal diameter steel pipe weighted down with sand

bags to restrict motion. Reflected (face-on) overpressure was recorded behind the vest

using three pressure transducers (Endevco 8530B-200) mounted in the torso surrogate

wall. These pressure transducers were spaced 64 mm apart along the vertical centerline

of the protective vest. The center pressure transducer was located at a position roughly

equivalent to the position of the human mediastinum (approximately the T-4/T-5

vertebral level) and positioned at the mouth of the shock tube in line with the center of

the open shock tube face according to the photograph and schematic in Figure 4-1. The

standoff between the end of the shock tube and torso surrogate was kept constant

throughout the tests resulting in standoffs to the anterior surface of the soft and hard

vests being 50 and 30 mm respectively.
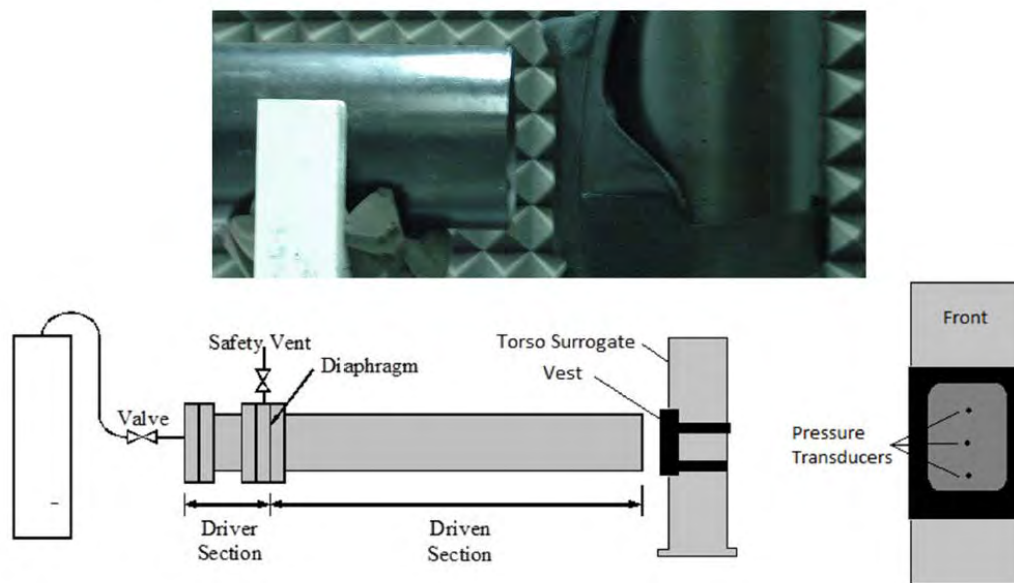
Figure 4-1: Photograph and schematic of shock tube and torso surrogate test setup.

A general linear model was used to identify correlations between measured

response behind the vest (peak overpressure and overpressure duration) and the input

blast conditions (peak reflected shock tube overpressure and shock tube overpressure

duration). Overpressure attenuation ratio, defined as the ratio between the peak

reflected tube overpressure and the peak behind vest overpressure, was also included in

the analysis. Variables found not statistically significant (α=0.05, p<0.05) were removed from the model to reduce model dimension.

Data was collected at a sampling rate of 1 MHz with a hardware anti-aliasing filter at 200 kHz, and post-processed with a 40 kHz 8-pole Butterworth filter (Bass et al. 2005). MATLAB (MathWorks), DADISP (DSP Development Corp.), and JMP (SAS Institute Inc) were utilized for analysis.

To understand the clinical significance of the overpressure exposures, pressure-time histories were compared to published overpressure risk curves. Unprotected pulmonary risk was compared with the existing pulmonary tolerance curves of Bass et al. (Bass et al. 2008). To determine the protected pulmonary blast injury curves, the ratio of peak overpressure measurements taken at the shock tube exit to those taken behind the vest were used to scale the unprotected pulmonary tolerance curves. The attenuation ratio for pressures beyond those tested was assumed constant at the level of the highest overpressure tested in this study.

To determine the risk of brain injury, the primary blast overpressure head injury tolerance curves of Rafaels et al., (Rafaels et al. 2011) were used. The comparative height of the pulmonary and brain pressures at each blast overpressure duration was used to assess the relative risk for injury to the two organs, with lower overpressure curves indicating greater risk for injury (i.e. lower overpressures are required to cause injury).

4.3 Results

Overpressure amplitude and wave shape were altered by the protective vests. Overpressure response behind the protective vests were typically a slower-rising wave with lower peak overpressure and longer positive-phase duration when compared to the incident overpressure wave, suggesting that the vests provide substantial overpressure wave attenuation (Figure 4-2). Behind vest overpressure for lower blast conditions were generally characterized by an immediate spike in overpressure following by a secondary rise of overpressure, most noticeably in the soft vest (Figure 4-2A). At larger blast conditions, the initial overpressure spike was less prominent or un-detectable (Figure 4-2B).
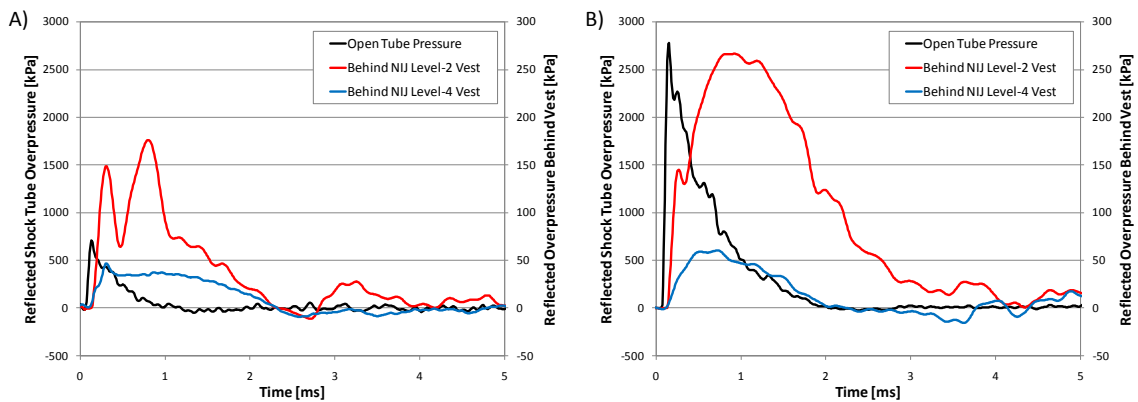
Figure 4-2: Typical behind vest responses for A) low and B) high blast severity show alteration of peak overpressure, rise time, and overpressure duration. NIJ, National Institute of Justice.

The top and bottom pressure sensors were in close approximation to various features on the vest such as flaps, heavy seams, and the edges of the armor insert and accordingly showed inconsistent results across trials with poor repeatability, especially

in the soft armor. For the top and bottom pressure sensors standard deviations ranged to

values as high as 50% of the peak overpressure. Therefore, these measurements were

not included in the model. However, the center pressure transducer produced highly

consistent measurements across the entire test matrix, with standard deviation of the

peak overpressure less than 11% of the average peak at each blast level, and the

standard deviation of the overpressure duration measurements less than 4% at each

blast level.

While both vests showed statistically meaningful reductions in overpressure that

increased with more severe blast exposures, the hard vest provided significantly greater

reductions, with correlations shown (Table 4-1). Overpressure wave duration for the

soft vest was strongly correlated with only input duration ($R^2 = 0.92$), and reached a

maximum at 5.3 ms. Overpressure wave duration behind the soft vest was 2.57±0.42

(mean±SD) times greater than the input duration (paired t-test, $p < 0.0001$). Peak

overpressure behind the soft vest was weakly correlated with input overpressure ($R^2 =$

0.12), but the overpressure attenuation ratio was strongly correlated with peak input

overpressure ($R^2 = 0.74$).

For the hard vest, both behind vest duration and peak overpressure were

correlated with input overpressure and duration ($R^2 = 0.76$ and $R^2 = 0.50$ respectively).

Duration behind the hard vest was 1.70 (±0.71) times greater than the input duration ($p <$

0.0001). The hard vest overpressure attenuation ratio was correlated with both input

overpressure and input duration ($R^2 = 0.97$), but a strong correlation with input

overpressure alone ($R^2 = 0.96$) was found. Estimates the coefficients for the linear

models (Equation 4-2) can be found in Table 4-1, coefficients that failed to reach

statistical significance are not shown.

$$Y = c_1 P_{Input} + c_2 \Delta t + Intercept$$
<div align="right">Equation 4-2</div>

Table 4-1: General linear model coefficients for alteration of overpressure seen by the chest due to body armor usage.

	Y	Peak Input Pressure Coefficient (x 1000)[*]	Input Duration Coefficient[*]	Intercept[*]	R^2
Behind Level-2 Vest	Peak Pressure	53.38 (25.93) p = 0.0483	---	162.1 (40.32) p = 0.0003	0.120
	Duration	---	3.391 (0.178) p < 0.0001	-0.883 (0.228) p = 0.0005	0.922
	Pressure Attenuation	3.809 (0.411) p < 0.0001	---	0.923 (0.639) p = 0.159	0.735
Behind Level-4 Vest	Peak Pressure	5.788 (2.611) p = 0.0339	12.95 (5.254) p = 0.0191	22.70 (3.711) p < 0.0001	0.759
	Duration	-0.399 (0.064) p < 0.0001	0.737 (0.140) p < 0.0001	1.466 (0.099) p < 0.0001	0.501
	Pressure Attenuation	16.06 (1.018) p < 0.0001	-4.604 (2.049) p = 0.0314	10.51 (1.447) p < 0.0001	0.967

* Estimate (standard error)

Blast overpressure-duration exposures in this study spanned the spectrum of

potentially injurious and non-injurious pulmonary exposures for the unprotected chest

(Figure 4-3). Comparing the results from both hard and soft vests demonstrated that the

hard vests provide increased protection by reducing both overpressure and duration when compared to the soft vest (Figure 4-4). Specifically, the soft vest had a 1.82 (±0.91) times greater behind-vest duration than the hard vest (p = 0.009). Peak overpressure levels behind the soft vest were larger than those behind the hard vest by a factor of 5.17 (±0.42) for the same blast conditions (p = 0.0002). Both soft and hard vests demonstrated increasing overpressure attenuation ratios as the blast overpressure increased, indicating that the blast attenuation capabilities of both types of vests improve with increasing blast severity.
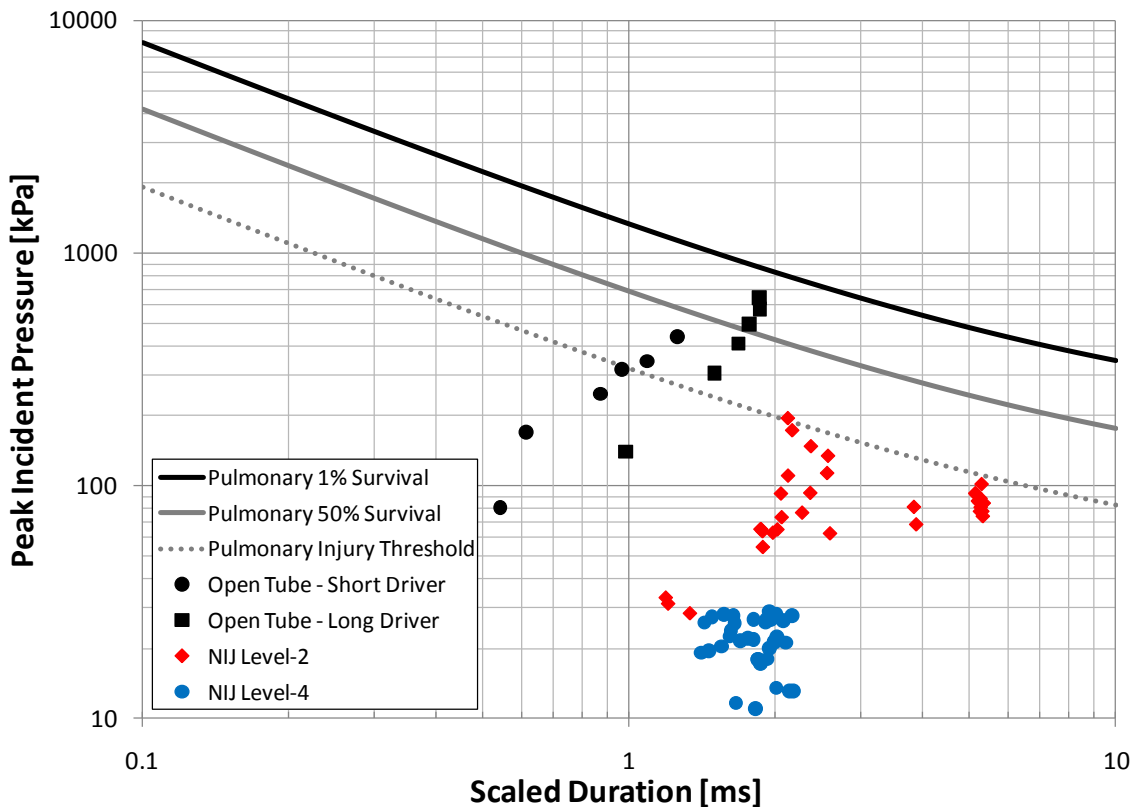
Figure 4-3: Unprotected and protected blast response compared with pulmonary injury reference curves for all study conditions.

97
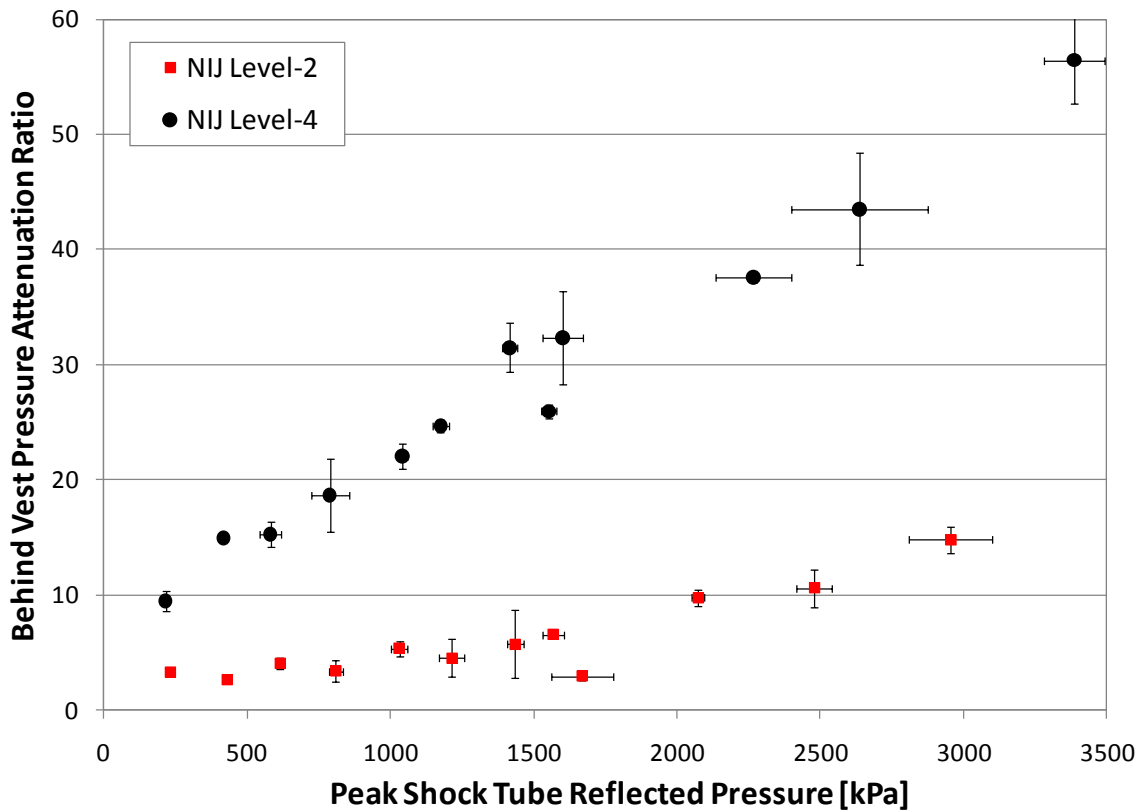
Figure 4-4: Behind vest attenuation ratios for soft and hard vests as a function of peak input pressure.

The resulting effect on overpressure exposure seen by the chest greatly increases

the pulmonary injury tolerance levels to blast overpressure scenarios. The addition of

body armor provides sufficient protection to the chest (i.e. increases the overpressure of

the injurious exposure for each duration) such that there are exposures in which there is

risk for injury to the brain and not the chest for both armor types (Figure 4-5, A and B).

This result is shown as the protective abilities of the hard and soft vests lower the peak

overpressure transmitted to the chest wall, but without any attenuation at the head,

there is a risk of fatality from brain exposure occurring at less severe exposures than

fatality from pulmonary injury.
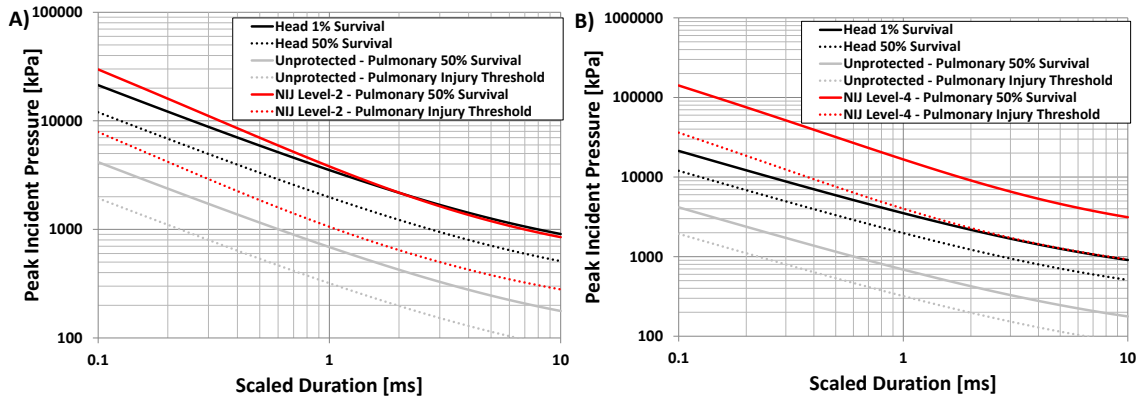
Figure 4-5: Pulmonary blast tolerance curves for A) soft vest and B) hard vest protected thorax.

A frequency power analysis was conducted to determine the filtering capabilities

of both the soft and hard armor vests. Figure 4-6 shows frequency power results for the

soft and hard vests at the highest pressure level tested. Although neither vest

demonstrated an ability to isolate and filter specific frequencies, both vests provided an

overall attenuation of power across the spectrum.
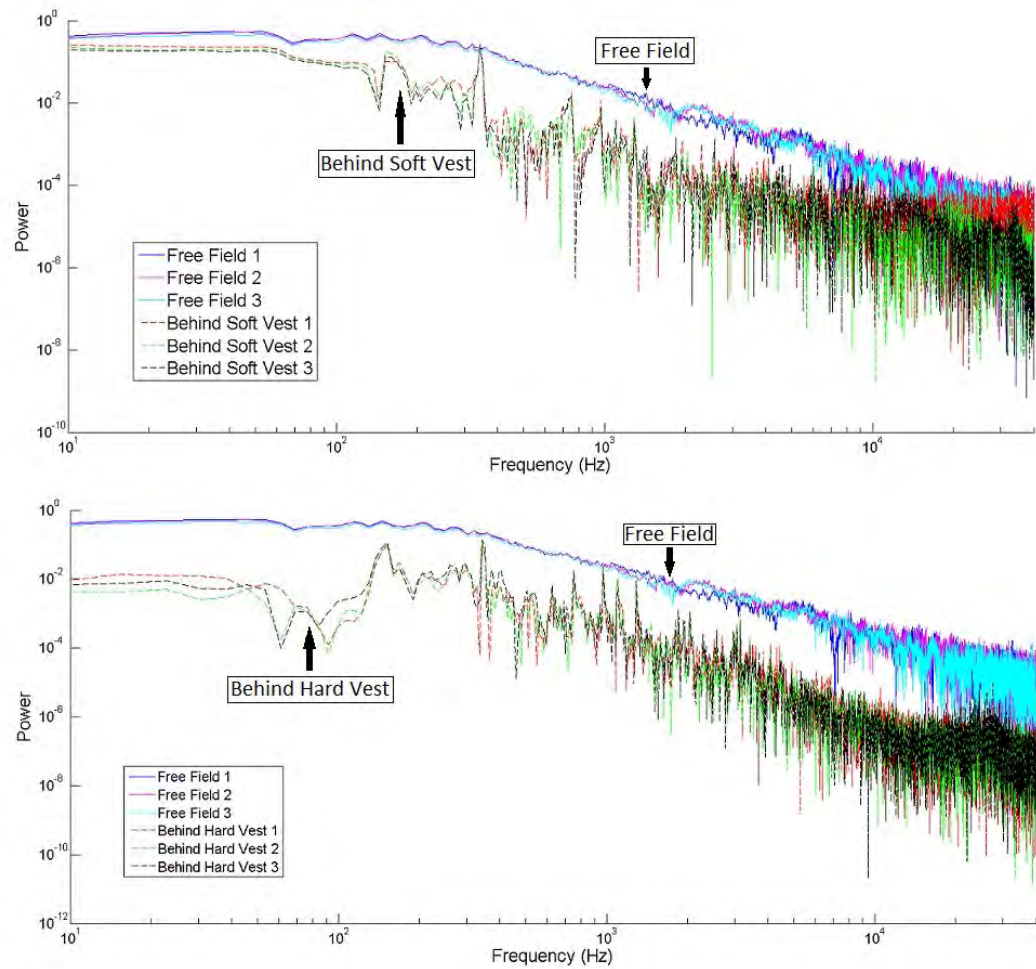
Figure 4-6: Frequency power spectrum at highest test level for soft and hard protective vests.

4.4 Discussion

This study is the first to characterize human injury tolerance to primary blast waves when ballistic protection is worn. These results address the hypothesis that an increase in thoracic protection and survivability to blast exposure may be the reason why wartime blast-related head injuries have become more prevalent. Specifically,

these results showed that for a wide range of exposures, chest protected subjects using similar protective equipment are likely at greater risk of brain injury than of chest injury.

Results of this study show that soft and hard police-issue ballistic vests substantially reduce the peak overpressure of primary blast waves measured on the thoracic surface behind the body armor. Peak overpressure attenuation ratios are observed to increase with increased input overpressure. The soft vest shows overpressure attenuation ratios ranging from 3.4 at low input overpressure levels to 14.2 at maximum input overpressure levels of this study. Similarly, the hard vest shows an ability to attenuate the peak reflected overpressure seen behind the protective vest from 9.5 at low blast levels to 56.8 at the highest blast input used in this study. The attenuation is not dependent upon frequency as the analysis (Figure 4-6) shows attenuation across the entire spectrum.

The scaled pulmonary injury curves presented in Figure 4-5a and Figure 4-5b demonstrate the strong protective effect of the ballistic vests on the primary blast exposure levels necessary to cause injury. Using the pressure scaling from this study, the soft ballistic protective vest pulmonary 50% survival curve was well above the 50% survival curve for primary blast to the head, indicating that fatality from brain injury will occur before fatal levels of pulmonary injury. The hard vest showed even greater protective ability against primary blast as the pulmonary injury threshold curve was at a higher level than the unprotected head 1% survival curve, indicating a 99% likelihood of

fatal brain injury prior to any resulting pulmonary injury. The ballistic vests tested

appeared to be especially protective at short overpressure duration levels, which

correspond to the moderate explosive charges today's military personnel are most

frequently subjected (Gondusky et al. 2005). Thus, both ballistic protective vests tested

in this study, especially the vests with hard plate armor, appear to protect the thorax

sufficiently that mild/moderate brain injuries may occur before pulmonary injuries.

Limited previous research on the effectiveness of soft ballistic protective vests

against blast had found little evidence of protective benefits of these vests in a blast

loading scenario (Young et al. 1985, Mellor et al. 1989). The strong attenuation found in

this study was likely due to substantially higher areal density ballistic protective vests,

especially with the hard armor plate, compared with the vests previously tested.

Further, established injury tolerance curves for primary blast show that as overpressure

pulse duration increases, the peak overpressure necessary to result in injury decreases

(Bass et al. 2008). However, the ballistic vest alters the sharp rising nature of the

overpressure wave. The injury tolerance curves presented in this study were based

upon an assumption of a sharp rising overpressure waveform; slower rising waveforms,

as seen in this study, are known to be less injurious to the pulmonary system (Richmond

et al. 1962c). Recent testing with a compliant human torso surrogate containing

modeled organs shows variable pressure attenuation capabilities of both soft and hard

armor depending upon free or closed field scenarios and also organ location. Pressure

102

measurements for determination of armor effectiveness in this study are taken within the torso at locations of simulated organs. Interpretation of these results proves difficult as there are no existing injury criteria for pressure measured at the organ surface. The results are further complicated due to the use of solid organ models for the heart, lungs, liver and stomach which may lead to unrealistic behavior, especially at the surface of the air-filled lungs.

The implications of these results are significant for military and law enforcement personnel. First, military ballistic personal protective equipment used in current conflicts likely provides protection to the thorax that greatly diminishes the occurrence of primary blast pulmonary injury. This increased tolerance of the pulmonary system to blast may be responsible for the limited observation of pulmonary injury despite the increased frequency of blast exposure. Second, the scaled injury tolerance curves found in this study demonstrate the possibility that ballistic protective equipment may protect the lungs from very high blast overpressure levels such that brain injury, possibly to severe or even lethal levels, may occur from primary blast exposure while no pulmonary injury is observed. This supports the anecdotal evidence and observations from recent military conflicts (Martin et al. 2008). As protection of the pulmonary system from blast improves, increasing clinical attention for mild to severe brain injury is warranted in the acute and long term clinical settings.

Limitations of this work include the inability to test to the highest levels of overpressure or longest levels of duration given by the pulmonary injury assessments of Bass et al (Bass et al. 2008). The behavior of the functional dependence of the shock attenuation is unknown beyond the highest overpressures tested. As the current variation of attenuation with overpressure is strongly linear, the assumption that attenuation ratios beyond this value are constant is likely strongly conservative. Further, the non-compliant surrogate used in this study may affect the attenuated overpressure seen behind a protective vest. Due to differences in viscoelastic behavior, there may be effects on blast wave propagation through the vests with a compliant chest wall. Future work should include a biofidelic blast testing surrogate. It should be noted that the head injury curves discussed in this study are based upon an unprotected head condition. The protective effects of modern ballistic helmets from blast are largely unknown but numerical work has shown them to have little influence (Nyein et al. 2010).

Finally, this study does not assess effects that likely arise from strong conversion of overpressure impulse into ballistic vest motion. Though these effects have not been shown to produce life threatening injuries, vest motion with hard armor plates has generated rib fractures in animal test specimens (Hennessy et al. 2006) and is likely important only for greater input overpressure durations, as the risk and severity of rib fracture was exacerbated with increasing blast duration. The effect of overpressure

104

onset time for primary blast injuries and blunt trauma owing to impulsive motion of the vests and hard armor plates should be further investigated.

The ability of modern ballistic protective equipment to limit injurious effects from primary blast has immediate importance for mitigating the occupational hazard of blast injury and providing appropriate clinical care after blast exposure. The present study confirms the capability of both "soft", the NIJ-2 ballistic vest, and "hard", the NIJ-4 ballistic vest with ceramic plates, to reduce peak blast overpressure. Military and law enforcement personnel likely to encounter blast injury should wear ballistic body armor to reduce the risk of pulmonary injury.

The first responder, emergency physician, or trauma surgeon can improve blast victim care with knowledge about the possible presence and type of ballistic protective vest worn by the victim. When it is known that no ballistic protective vest was in use during blast exposure, the appropriate initial focus should be evaluation for blast pulmonary injury (Lavery et al. 2004, Sasser et al. 2006). In the case where ballistic protective vests were in use during blast exposure, an initial focus on pulmonary injury may not be necessary. This study shows that the presence of ballistic protective vests protect the lungs such that the risk of primary brain blast injury will occur at blast overpressure and duration levels before the onset of pulmonary injury.

Chapter 5 - Brain Tissue Characterization and Modeling

Finite element modeling techniques are extensively used for the simulation of mechanical behavior of tissues for circumstances in which the details of mechanical response cannot be easily experimentally measured. Validated FE simulations allow us to simulate a wide variety of injurious inputs and measure the mechanical response of structures and tissues. These models rely on accurate and biofidelic constitutive models for tissues of interest. Brain tissue has been characterized in a variety of ways, but there are no studies that investigate a wide range of species with consistent methodology. To address this deficit, this study experimentally investigates the viscoelastic behavior of brain tissue in three common in vivo animal model species for neurotrauma and develops constitutive models for implementation in FE models. This chapter is currently being developed for journal publication.

5.1 Introduction

The prevalence of traumatic brain injury (TBI) constitutes a significant healthcare concern. Approximately 1.7 million people annually in the U.S. require a hospital visit due to TBI (Faul, Xu et al. 2010). In the U.S., TBI is the highest cause of long-term disability and most common cause of death in adults under the age of 45 (Coronado, Xu et al. 2011, Wright, Kellerman et al. 2013). In the civilian population, TBI is most often associated with motor vehicle accidents and falls. However, TBI is also a major concern for the military population. An estimated 320,000 of 1.6 million (19%) of Operation Iraqi

Freedom and Operation Enduring Freedom (OIF/OEF) veterans have some form of TBI as of 2008 (Tanielian and Jaycox 2008). A large portion of these military injuries occur via mechanisms that are similar to those common in civilian populations such as vehicle collisions and blunt impact due to falls. Additionally, exposure to blast and resulting blast-related TBI is a major concern due to the increased numbers of IEDs in current conflicts (Taber, Warden et al. 2006). For the accurate modeling and prediction of TBI thresholds, an understanding of the mechanics of brain tissue interaction with blunt impact and primary blast is required. Different resulting strain rates and strain magnitudes like lead to different underlying injury mechanisms (Panzer 2012).

In vivo animal models are essential to understanding the physiological response to injury. While, anthropometric test devices can replicate the kinematics and mechanical response to an external insult, they cannot replicate living processes like cell death, functional physiological deficits, and physiological cascades, which are especially important when studying TBI. A large range of in vivo animal model size and morphology have been used to study TBI; including mouse (Richmond, Goldizen et al. 1962, Goldstein, Fisher et al. 2012, Yu, Wang et al. 2012), rat (Long, Bentley et al. 2009, Svetlov, Prima et al. 2010, Garman, Jenkins et al. 2011), rabbit (Krohn, Whitteridge et al. 1941, Wang, Ye et al. 2010, Rafaels, Bass et al. 2011), ferret (Rafaels, Cameron et al. 2012), and pig (Saljo, Arrhen et al. 2008, de Lanerolle, Bandak et al. 2011, Shridharani, Wood et

al. 2012). Differences in brain mass alone in these models range over nearly four orders of magnitude from the mouse (0.3g) to humans (1350g).

While the morphological and size differences in neuroanatomy are clear, differences between tissue mechanics across species are not well defined. Some studies have reported interspecies differences in brain stiffness between humans and monkeys (Galford and McElhaney 1970) or pigs (Prange, Meaney et al. 2000). Alternatively, other published results indicate no difference between human and pigs (Nicolle, Lounis et al. 2004), and between mice and rats (Vappou, Breton et al. 2008). To account for differences between animal models and humans, interspecies scaling models calculate the necessary dose to match biomechanical or injury response across models. Such interspecies scaling models have been developed for blast injury (Bowen, Holladay et al. 1965)(Chapter 6-8) and for blunt trauma (Eppinger 1976, Panzer et al. 2014).

To develop biofidelic injury models, understanding the mechanical behavior of brain tissue and possible interspecies differences is crucial. Most brain tissue characterization research has focused on rates that are typical of automobile impact, or those associated with common daily living, 100Hz or lower. Brain tissue is soft, recent research shows complex shear moduli ranging from 0.3 to 2kPa (Cheng, Clarke et al. 2008, Chatelin, Constantinesco et al. 2010). Some older research indicating a significantly stiffer response with complex shear moduli up to 20kPa (Galford and McElhaney 1970, Metz, McElhaney et al. 1970). Brain tissue is often considered to

exhibit nonlinear viscoelastic (VE) behavior at large strain, but can be satisfactorily modeled by linear VE or quasi-linear VE (QLV) at sufficiently low strains. One study (Takhounts et al. 2003) determined that a linear VE model was satisfactory up to 0.2 and QLV was acceptable up to 0.4 lagrangian shear strains, with a fully nonlinear modeled required at higher strain levels.

When modeling brain tissue for research purposes there are other characteristics to consider. The brain has been shown have regional differences in behavior between the brainstem and cortex ((Arbogast and Margulies 1997), between hippocampal substructures (Elkin, Azeloglu et al. 2007), and between white and gray matter areas (Prange, Meaney et al. 2000, Nicolle, Lounis et al. 2004, Johnson, McGarry et al. 2013). Regional and local anisotropy has also been observed in brain tissue (Elkin, Ilankovan et al. 2011, Finan, Elkin et al. 2012, Feng, Clayton et al. 2013). Further, age-related differences in viscoelastic behavior have been measured in the rat hippocampus (Elkin, Ilankovan et al. 2009), rat cortex (Gefen, Gefen et al. 2003, Shulyakov, Cenkowski et al. 2011), and in the cortex of pigs (Thibault and Margulies 1998).

Many different methods have been used for material characterization of brain tissue. The decision to test brain tissue while still within the skull (in vivo or in situ) versus removed from the skull (in vitro) may be important for material modeling. In vivo (Fallenstein, Hulce et al. 1969, Gefen and Margulies 2004, Urbanczyk et al. 2015) and in situ (Elias and Spector 2012) models have the advantage of conserving boundary

109

conditions and constraints that are normally seen by the brain. In vitro testing often involves processing of the tissue into experimentally tractible shapes such as cubes (Coats and Margulies 2006) and cylinders (Arbogast and Margulies 1997, Bilston et al. 1997, Darvish and Crandall 2001). The soft brain tissue often creeps over long periods if tested in vitro, but in vitro testing enables the investigation of regions and locations that are not accessible in in vivo/in situ models. Research has shown that in vivo and in situ models result in very similar material models while in vitro models have an effect on the long term relaxation behavior of the tissue (Gefen and Margulies 2004).

Dynamic shear is the most common form of brain testing and it enables the measurement of energy storage and loss behavior over a range of input frequencies (Fallenstein et al. 1969, Shuck and Advani 1972, Arbogast and Margulies 1997). Compression was a popular experimental technique, especially in earlier research, as it provides a relatively simple analytical solution of material behavior (Estes and McElhaney 1970, Galford and McElhaney 1970, Miller and Chinzei 1997). One recent method of soft tissue characterization is magnetic resonance elastography (MRE). MRE allows for convenient measurement of brain stiffness clinically in living humans at low strain levels. In vivo MRE experiments compare well with other in vivo and in situ studies (Feng, Clayton et al. 2013, Johnson, McGarry et al. 2013). Indentation has become a popular nondestructive testing technique since it can be performed in vivo/in

situ and in vitro (Wang and Wineman 1972, Gefen and Margulies 2004, Elias and Spector 2012).

There are many challenges associated with the testing of brain tissue. Owing to the high metabolic activity of brain tissue, significant mechanical breakdown of the tissue begins to occur approximately six hours post-mortem (Gefen and Margulies 2004, Garo, Hrapko et al. 2007). This makes acquiring and testing tissue in sufficient time, especially for human tissue, difficult. Complicating the use of existing literature models for brain mechanics is the wide range of material properties reported. Published values of complex shear modulus and loss tangent vary over orders of magnitude, likely due to significant difference in testing methodology. Owing to the nature of brain tissue (very soft, nearly incompressible, highly viscoelastic, anisotropic), it is difficult to experimentally test and to implement complex material models into tools such as FE models of the head (Chatelin, Constantinesco et al. 2010, Panzer, Myers et al. 2012, Panzer, Myers et al. 2013).

FE models are valuable tools since they can predict biomechanical response of tissues and structures at a level of detail that is not possible through in vivo animal model testing. Response such as strain and strain rate, thought to be important for injury results, can be modeled and compared to physiological results from living models. FE models of the head have been developed for blunt impact (Yang, Hu et al. 2006, Ji, Zhao et al. 2014) and for blast exposure (Moss, King et al. 2009, Taylor and Ford

2009, Panzer, Myers et al. 2012). These models rely on accurate material properties for tissue mechanical response. The biofidelity of such models are often limited by a lack of mechanical data and constitutive models for biological tissues at relevant strain rates (Yang, Hu et al. 2006, Panzer, Myers et al. 2012).

The sensitivity of FE models to material properties at blast rates has been explored using a linear VE model for brain tissue (Panzer 2012). This study assessed sentivity to variations in both deviatoric (VE) and volumetric (density, sound speed) properties. While small changes in brain pressure response were observed relative to the size of change in brain properties, the VE properties were found to be important for strain response (Panzer 2012). When comparing material models used in some published FE brain models (Zhang, Yang et al. 2001, Moss, King et al. 2009, Panzer, Myers et al. 2012) an order of magnitude difference in peak Von Mises stress was observed at the same blast input levels for the different material models.

Though understanding of the injury mechanism and biomechanical thresholds for blast is limited. Investigations at lower rates have shown electrophysiological impairment in optic nerve axons at 18% strain (Bain and Meaney 2000) and cortical cell death between 10 and 20% strain in organotypic slice cultures (Elkin and Morrison III 2007). Neurological tissue injury thresholds have been shown to be strain rate dependent at rates seen in automobile injuries (Elkin and Morrison III 2007). TBI risk from blast is likely strain and strain rate dependent. FE simulations may allow us to

discover injury mechanisms by comparing biomechanical response to measured

physiological or injury response from in vivo models.

The goal of this study is to investigate brain material properties over a range of

species, including those with gyrencephalic and lissencephalic brains. The use of

consistent methodology will allow for the direct comparison of experimental results

across species. Viscoelastic constitutive models will be developed for each of the three

species. The development of more biofidelic constitutive models for brain tissue will

serve to improve FE simulation and modeling of brain response for TBI research.

5.2 Methods

5.2.1 Experimental

Three common in vivo animal model species used in TBI studies, mice, ferrets,

and pigs, were chosen for this study. These species cover a wide range of brain size and

include lissencephalic (mouse) and gyrencephalic (ferret, pig) species. Animals with

intact skulls were collected immediately post-mortem. All testing was completed within

5 hours to minimize mechanical changes due to tissue degradation (Gefen and

Margulies 2004, Garo, Hrapko et al. 2007). Testing was conducted on a total of 12 mice,

3 ferrets, and 8 pigs. Owing to experimental complications or damage to the specimen

during testing some animals were excluded from analysis. The total number of

specimens along with body mass and brain mass descriptions are presented in Table 5-1.

Table 5-1: Brain indentation test specimens with average body and brain mass.

	# of Specimens	Body Mass [kg±SD]	Brain Mass [g±SD]
Mouse	5	0.027±0.004	0.46±0.02
Ferret	5	1.39±0.25	8.3±1.1
Pig	3	36.4±3.0	75.9±5.8

After collection of the test specimen, the head was fixed to a large mass to prevent bulk specimen movement during preparation and testing. Skin and flesh was removed to expose a section lateral to the midsagittal plane and superior to the cerebral cortex of the brain. The surface of the brain tissue was accessed by drilling a small burr hole at the desired indentation location. The circular burr hole was 7mm in diameter for the pig and ferret specimens, and 3mm in diameter for the mouse specimens. The dura mater was removed from the indentation location. The brain tissue surface was kept moist with saline solution during the remainder of the test preparation. A schematic of burr hole and indentation location is presented in Figure 5-1.
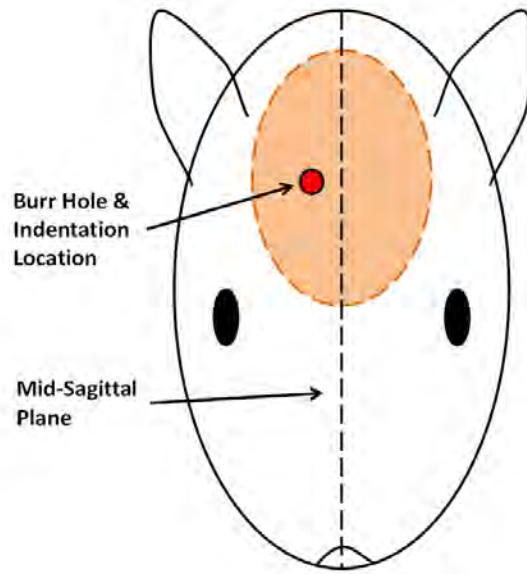
Figure 5-1: Schematic of indentation specimen preparation with burr hole and indentation location.

All tests were conducted on a BOSE Electroforce test machine (Eden Prairie, MN) capable of tension and compression testing. Load cells ranging from 0.5 (Model 31-50g, Honeywell, Columbus, OH) to 10N (LCFD-1kg, OMEGA Engineering, INC., Stamford, CT) were mounted above the indenter and used to measure indentation force. Displacement was measured by the internal LVDT of the test machine. An accelerometer (Endevco 7264C, Irvine, CA) was used to measure acceleration of the indentation for assessing inertial contributions to the applied force. A schematic of the test apparatus including location of the test specimen is presented in Figure 5-2.
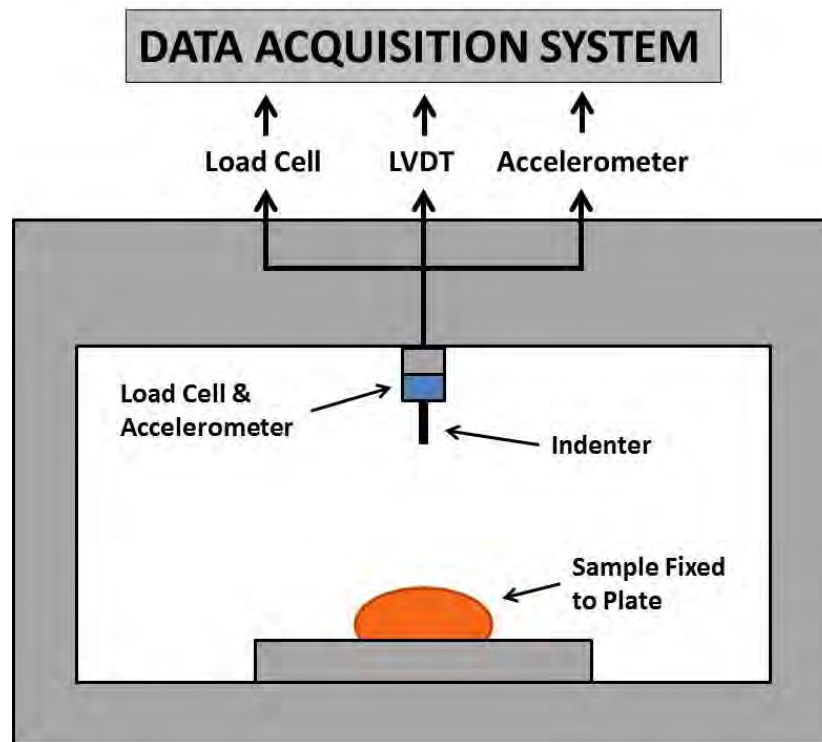
Figure 5-2: Schematic of indentation test apparatus and specimen location.

Viscoelastic material properties have been shown to be sensitive to environment, especially temperature (Bass, Planchak et al. 2007, Hrapko, van Dommelen et al. 2008). Accordingly, testing was conducted within an environmental chamber. Conditions were held to approximately 100% relative humidity and 37°C. Temperature was monitored in the air within the chamber and on the surface of the brain tissue using "K" type thermocouples (OMEGA Engineering, INC., Stamford, CT).

Characterization of material was conducted through displacement controlled indentation with cylindrical, flat-tip indenter shapes. For the two large species (pig, ferret) a 3.95mm indenter was used and for mice a 1.7mm diameter indenter was used.

Indenter tip edges were rounded to limit high stress concentrations at the edges that may result in tearing or cutting of the tissue. A viscoelastic test battery was conducted to assess both the displacement and time dependent behavior of the tissue.

One complication with indentation is determining a zero position where the indenter tip is in full contact, normal to the tissue surface, especially in very soft materials like brain tissue. To ensure a consistent staring load, a quasi-static indentation was performed and local zero position was defined at a location where a baseline stress was measured. This threshold was set according to a pressure underneath the indenter tip corresponding to baseline intracranial pressure values of 12mmHg in pig and ferret and 7mmHg in the mouse. All following indentation depth were relative to this zero position.

The viscoelastic test battery consisted of step-hold displacement and sinusoidal displacement tests. Tests were conducted at three different displacement levels for each specimen. Displacement levels of 1, 2, and 3mm were used for pig and ferret. Displacement levels of 0.085, 0.17, and 0.255 were used for mice. These will be referred to as L1, L2, and L3. The battery at each displacement level consistent of a step and hold for 10s, 1Hz sinusoidal for 20 cycles, and an additional step and hold for 10s. Following L2 and L3 tests a repeat of L1 step and hold test was conducted to assess a change in material behavior through damage or softening. The maximum achievable ramp speed for the step and hold tests was approximately 60mm/s. This results in approximate

117

strain rates of 8.1 1/s, 3.75 1/s, and 1.7 1/s for mice, ferrets, and pigs, respectively. The

step and hold tests will be used for development of a constitutive model of the brain

tissue. Sinusoidal tests will be used to validate model response at a different rate and

shape of input.

Force, displacement, and acceleration data were recorded at 10,000Hz through

the same data acquisition system (MEDAQ, Hi-Techniques, Madison, WI). All data was

filtered via an 8-pole Butterworth low-pass filter with a cutoff frequency of 250Hz.

Significant signal content occurs below 200Hz with large magnitudes of signal noise

occurring at 360 and 1050Hz. The large magnitude of noise is a result of significant

mechanical vibration within the test machine and electrical noise. A frequency power

spectrum is presented in Figure 5-3.
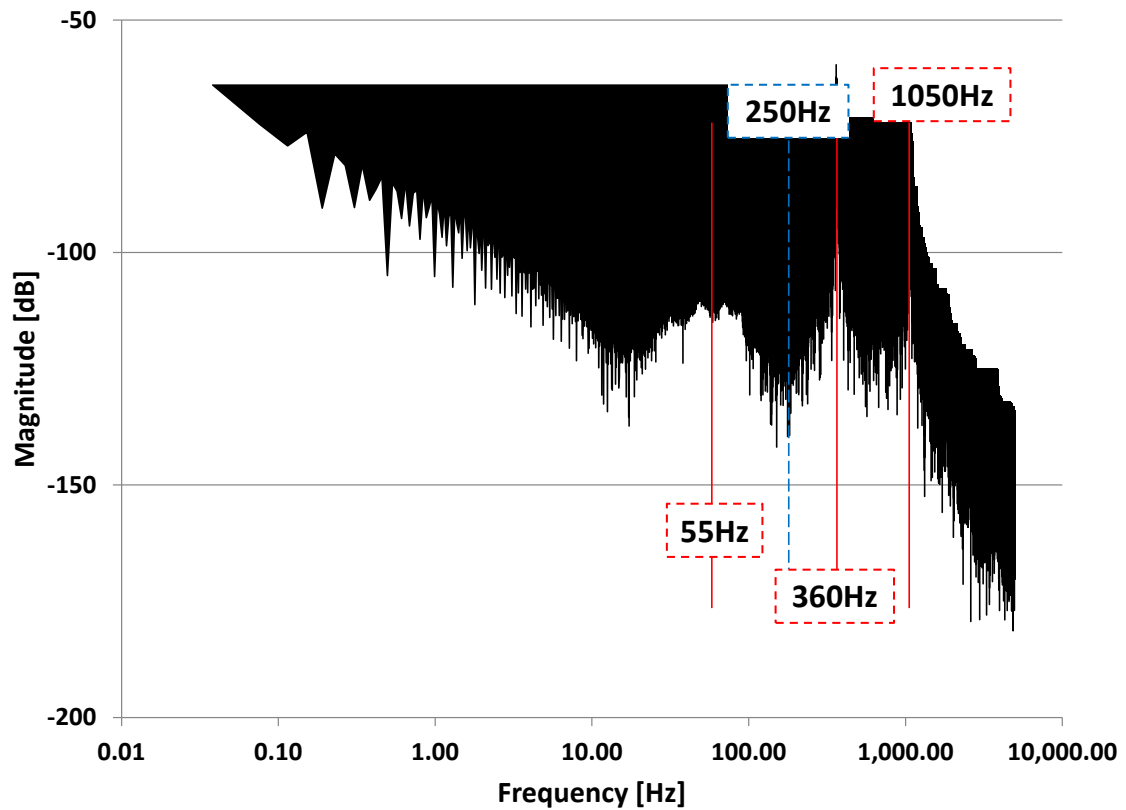
Figure 5-3: Typical frequency power spectrum for indentation test shows large noise components occurring at 360Hz and 1050Hz with signal content occurring at approximately 55Hz.

Due to the low loads associated with the testing of very soft tissues like brain, the inertial contribution of the indenter on measured load is substantial. To compensate for the effect, the measured indenter acceleration is used to calculate the inertial force contribution. Through testing of an unloading indentation step the effective mass of the two indenters was determined to be 35.7g and 4.7g for the large and small indenters, respectively. Finally, to minimize computational time for inverse FEA optimization the

119

data was downsampled. All data was retained during the high rate step and initial

relaxation but downsampling of the intermediate and long term relaxation behavior was

implemented by factors of 100 and 1000, respectively.

5.2.2 Material Modeling

Force response, F(x,t), was analyzed for each step test using a convolution

integral of the form in Equation 5-1.

$$F(x,t) = \int_0^t G_{red}(t-\tau)\frac{dF^e}{dx}\frac{dx}{d\tau}d\tau \qquad \text{Equation 5-1}$$

G_{red} is the reduced relaxation function, F^e is the instantaneous elastic function, x is the

indentation depth, t is time, and τ is a dummy variable for integration.

The reduced relaxation function is based on a series of Maxwell elements and is

expressed as a Prony series according to Equation 5-2.

$$G_{red}(t) = G_\infty + \sum_{n=1}^4 G_n e^{-t/\tau_n} \qquad \sum G_i = 1 \qquad \text{Equation 5-2}$$

G_∞ is the steady state relaxation coefficient and τ_n are the time constants corresponding

to each relaxation coefficient, G_n. For this study a four-term Prony series was used, with

decade time constants (10s, 1s, 0.1s, 0.01s) (Lucas et al. 2008).

An exponential instantaneous elastic function was assumed according to

Equation 5-3 (Fung 1981), where A and B are instantaneous elastic parameters.

$$F^e(x) = A(e^{Bx} - 1) \qquad \text{Equation 5-3}$$

The convolution integral (Equation 5-1) was numerically integrated in terms of

the instantaneous elastic parameters and relaxation coefficients. This technique allows

120

for the use of an exact displacement-time history for model calculations and avoids the

need for an idealized step-hold displacement form (Darvish et al. 1999). Reduced

relaxation coefficients and instantaneous elastic parameters were optimized using a

generalized reduced gradient technique (Excel Solver, Microsoft).

Instantaneous elastic parameters and reduced relaxation coefficients were

simultaneously optimized by minimizing the sum of the squared errors between

experimental and model response. Each step test was modeled individually to ensure

correct model response. Additionally, individual species models were derived by

optimizing model coefficients and parameters for all tests for a given species,

simultaneously. The quality of VE model fit was assessed using sum of the squared

errors (SSE) and R^2.

For evaluation of model fit, experimental results are presented with corridors

generated by calculating mean ± standard deviation response for all comparable tests.

Validity of species tissue models was verified by assessing model prediction of force

response to 1Hz sinusoidal indentation tests for each species.

5.3 Results

5.3.1 Experimental

Representative relaxation and sinusoidal tests show VE behavior in Figure 5-4.

Relaxation tests are shown in log time to better visualize short term elastic and long-

term relaxation behavior. A typical relaxation test (Figure 5-4a) is characterized by a

sharp rise in force from the indentation displacement. The force magnitude decreases

with time during a constant applied indentation depth. By 10s the force is approaching

an asymptotic value of long-term relaxation indicative of VE behavior. For sinusoidal

displacement inputs (Figure 5-4b) the force is sinusoidal in shape as expected. The peak

measured force decreases with an increasing number of cycles due to tissue relaxation.

A slight negative force region occurs due to surface tension between the indenter and

tissue surface. The tissue has not fully relaxed upon return to zero displacement

resulting in a small tension force.
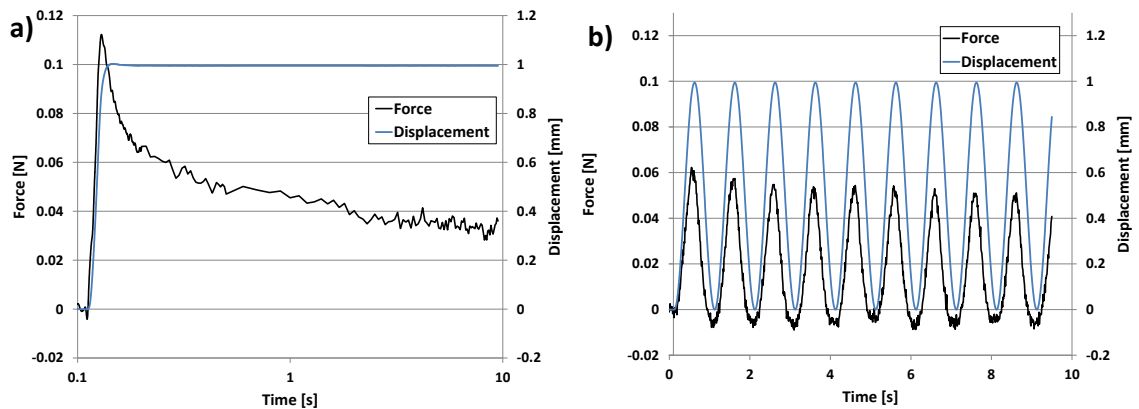
Figure 5-4: Representative displacement and force behavior for a) relaxation and b) sinusoidal indentation tests on brain tissue.

Example force behavior for increasing indentation depths for relaxation tests is

shown for a single specimen in Figure 5-5. The same instantaneous force response exists

with decay to a long-term relaxed state. The peak measured force increases with

increasing indentation depth and a similar path to peak force is followed for all three

indentation levels. A similar relaxation curve shape exists across all levels with the

long-term relaxation force increasing with indentation depth.
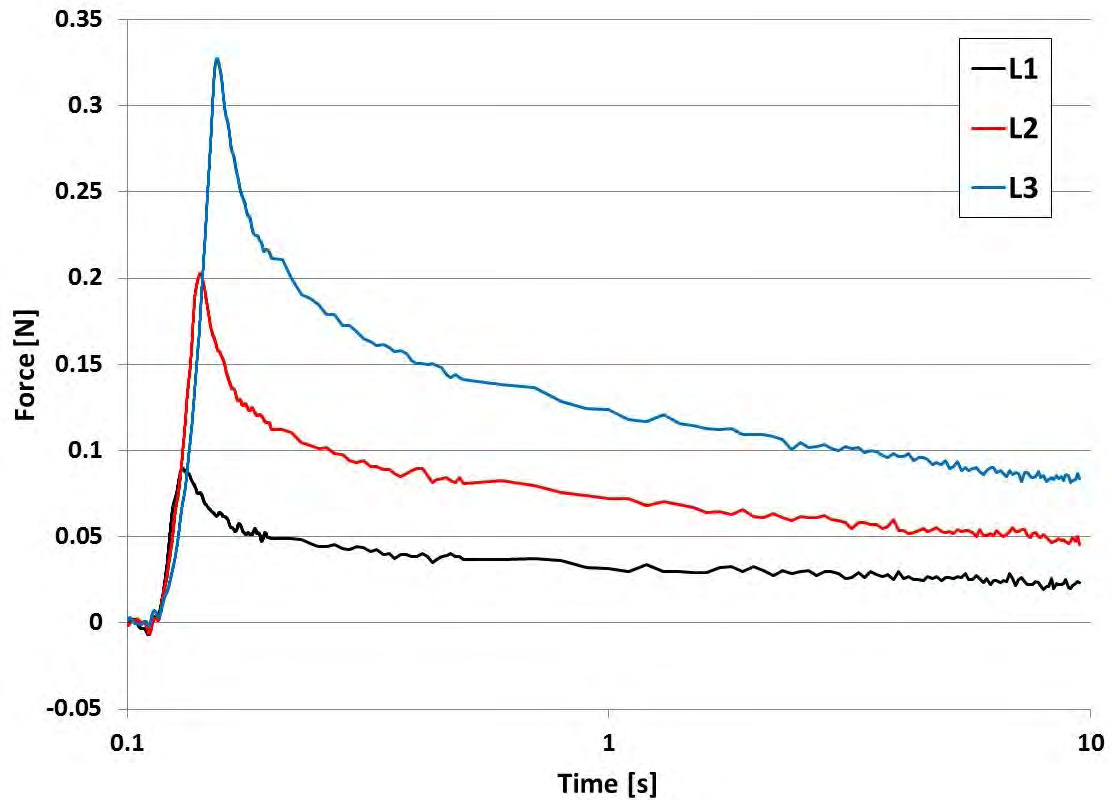
Figure 5-5: Representative relaxation force for a single specimen at three indentation levels shows increased force magnitude with similar relaxation form.

To assess changes in tissue behavior through damage or softening, L1 relaxation

tests were compared to additional L1 indentation depth tests which followed the L2 and

L3 indentation batteries. L1, Post L2, and Post L3 tests are presented in Figure 5-6.

Force behavior is presented as an average response ± 1 standard deviation (SD) for the

complete set of tests within each species. If no change in tissue mechanics through

damage or softening exists, all L1 relaxation tests should exhibit the same instantaneous

elastic and relaxation behavior.
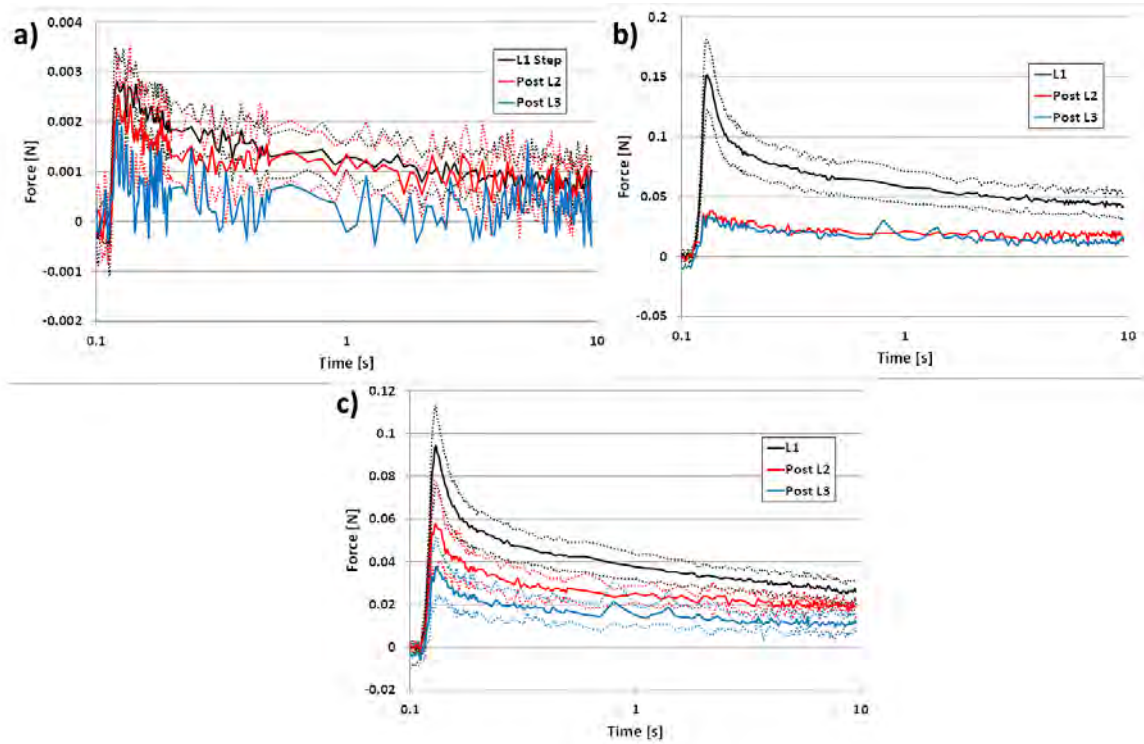
Figure 5-6: Relaxation test behavior for L1, Post L2, and Post L3 tests to assess progressive changes in material behavior for a) Mouse, b) Ferret, and c) Pig show changes in tissue behavior after higher level indentation tests (presented at average force ±SD).

The resulting force from all mouse L1 relaxation tests is shown in Figure 5-6a.

The mouse data exhibits the largest inter-test variation, resulting in the largest SD

corridors. This variability can be attributed to the very small displacements and loads.

Small differences in indenter contact or mechanical vibration of the test apparatus result

in a relatively larger effect on the measured force when compared to the other species

tests. The post L2 relaxation tests fall well within the corridor of the initial L1 tests. The post L3 behavior does fall outside of the corridors for L1 and post L2 for most of the 10s test duration. Post L3 data is presented as average response only, due to the limited number of available data sets. This suggests that there is a change in material behavior due to the L3 test battery.

In Figure 5-6b the L1 force data for ferret tests show a change in behavior after L2 indentation. Post L2 and post L3 behavior is presented as an average curve only due to the limited available data. The large decrease in force behavior suggests that L2 and L3 indentations alter the mechanics of the tissue. The large decrease in force response (~75% decrease in peak) suggests a change in material behavior after L2 tests.

Relaxation data from pig tests show a progressive decrease in peak force and long-term relaxation level (Figure 5-6c). The peak force decreases by 39% and 60% after L2 and L3 batteries, respectively. This in addition to the post L2 and post L3 average response falling outside of the corridor for L1 tests suggests there is a change in behavior above L1 indentation.

To assess the separability of time-dependent and displacement-dependent necessary for the use of a QLV model, the reduced relaxation response was compared across different indentation levels within each species. For QLV to be valid, the reduced relaxation curve should be the same for a given material at all indentation depths within

125

the valid range of the model. The average reduced relaxation response is shown by the force curve normalized by peak force (Figure 5-7).
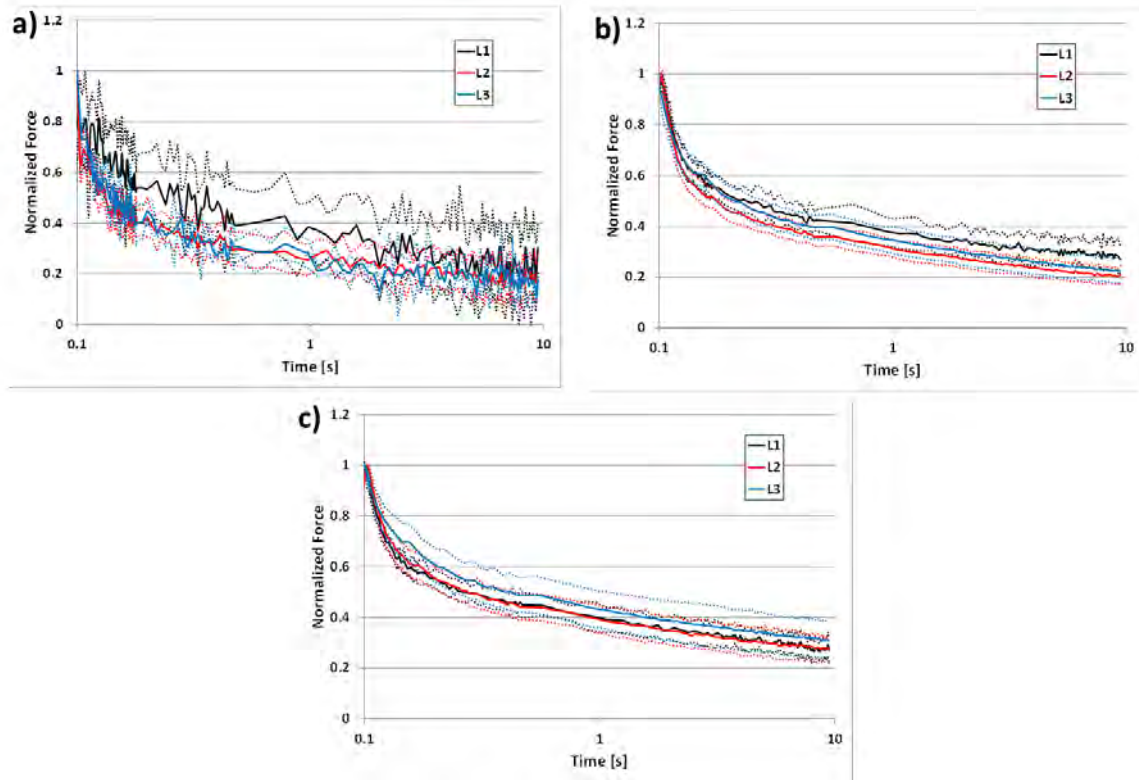
Figure 5-7: Reduced relaxation curves across all indentation levels for a) Mouse, b) Ferret, and c) Pig show differences in long term relaxation behavior (average ±SD corridors).

For mouse tests (Figure 5-7a) the relaxation curves fall within the SD corridors of the L1 tests. However, the corridors are large due to large variation across tests, making a visual interpretation of differences difficult. For ferret relaxation tests (Figure 5-7b) the corridors overlap for all three indentation levels. There is a difference in long-term relaxation behavior with a decrease of 17.3% and 16.8% from L1 to L2 and L3,

126

respectively. The ferret relaxation tests do not exhibit a progressive decrease in

relaxation behavior with increasing depth. For pig tissue characterization (Figure 5-7c)

the corridors overlap for all three indentation levels. Reduced relaxation behavior is

very similar between L1 and L2 tests with a decrease in long-term relaxation of

approximately 12.7% in L3 tests.

To statistically assess differences in reduced relaxation behavior between

indentation levels a paired two-sample t-test was used to compare relaxation values at

10s. Tests were performed with $\alpha = 0.05$, with $p < 0.05$ signifying a statistical difference

between the average values. For the mouse tests there was a significant difference

between L1 and L2 ($p < 0.001$). This difference in relaxation behavior lies primarily with

the early relaxation behavior. The shape and amount of tissue relaxation remains

consistent between all three levels after this short-term relaxation. For ferrets there is a

significant difference between relaxation level at 10s between L1 and L2 tests ($p = 0.022$).

In pigs the long-term relaxation behavior is significantly different between L2 and L3 (p

$= 0.002$). All other comparisons failed to achieve significant differences between mean

responses.

To make a general comparison between relaxation behaviors of the three species

the average reduced relaxation responses are presented in Figure 5-8. The ferret and pig

exhibit very similar relaxation behavior with mouse showing differences in shape and

relaxation level. Differences in the mouse response lies primarily in the short time

127

relaxation response where it is characterized by a much larger relaxation immediately
following peak force. Relaxation behavior after this initial period was similar in shape
and magnitude across the three species.
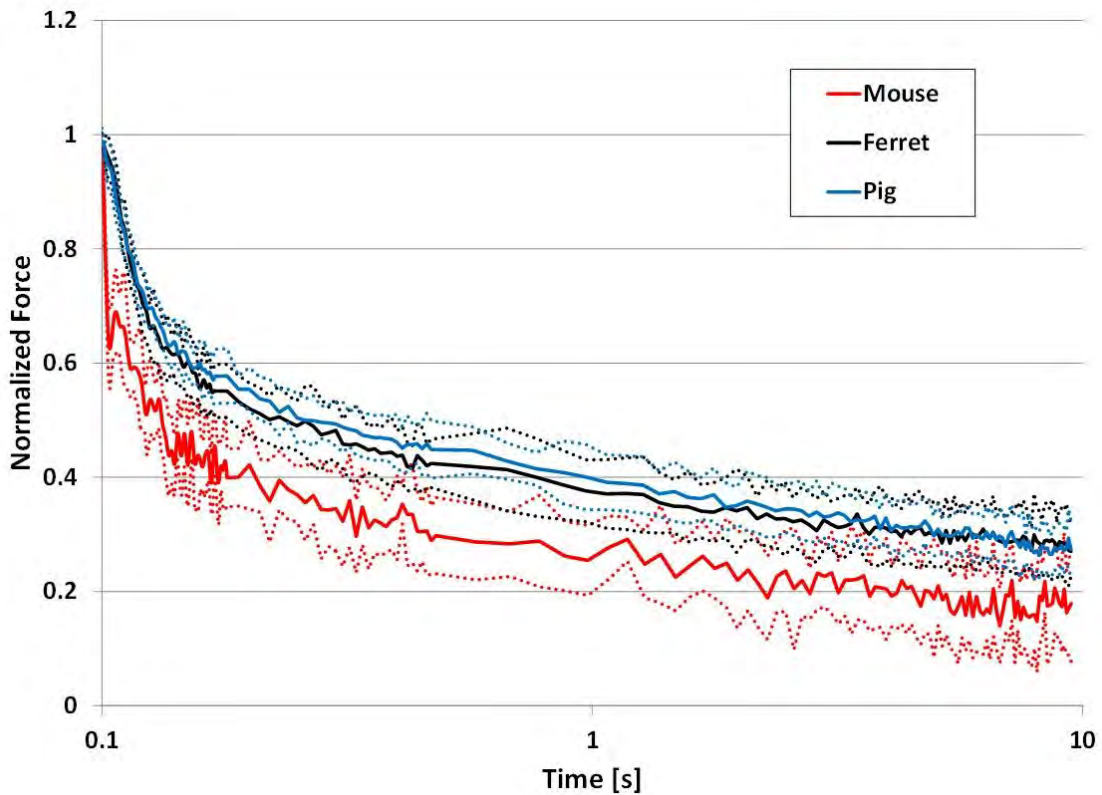
**Figure 5-8: Reduced relaxation response for all three species shows similar behavior
between ferret and pig with a greater short time relaxation in mice (average ±SD
corridors).**

However, it is important to note that this relaxation behavior cannot be
realistically compared across species due to large differences in brain geometry and
confinement effects due to skull interaction. There is large variation between species in
the relative size of the indenter to brain size, and displaced volume relative to the total

128

brain volume. Additional contributions to the difference in relaxation behavior seen by the mouse can likely be attributed to the much more compliant skull compared to the ferret and pig skull. This may necessitate the use of a more complex analysis technique than a traditional analytical model of VE behavior. Inverse FEA incorporates some of these geometric and mechanical differences to more accurately derive a constitutive model.

The investigation of changes in material behavior suggests that analysis and constitutive modeling should focus on L1 in pigs and ferrets and L2 for mice. It is desirable to use the largest acceptable indentation magnitude to maximize signal to noise ratio and signal clarity. Therefore, material modeling will utilize these indentation levels for constitutive model optimization.

5.3.2 Material Modeling

Instantaneous elastic and reduced relaxation functions were fit for each of the step-hold indentation tests for this study. Model fits were satisfactory for each tests, though ferret and pig models exhibiting better agreement with experimental data. This is primarily due to the lower relative signal to noise ratio in the mouse tests. Portion of experimental response accounted for by the model behavior was excellent with R^2 values of at least 0.992 and 0.990 for all pig and ferret tests, respectively. The experimental data for mice contained a much higher noise magnitude relative to force magnitude but the instantaneous elastic and relaxation behavior were well captured by

the model. In some cases, the model did not fully capture the immediate relaxation seen for mice but loading and long-term relaxation were accurately modeled, as indicated by R^2 values of at least 0.882. Representative model fits for each of the species show this behavior (Figure 5-9). For all individual step-hold tests modeled, the coefficients and parameters and graphical representations are included in Appendix A.
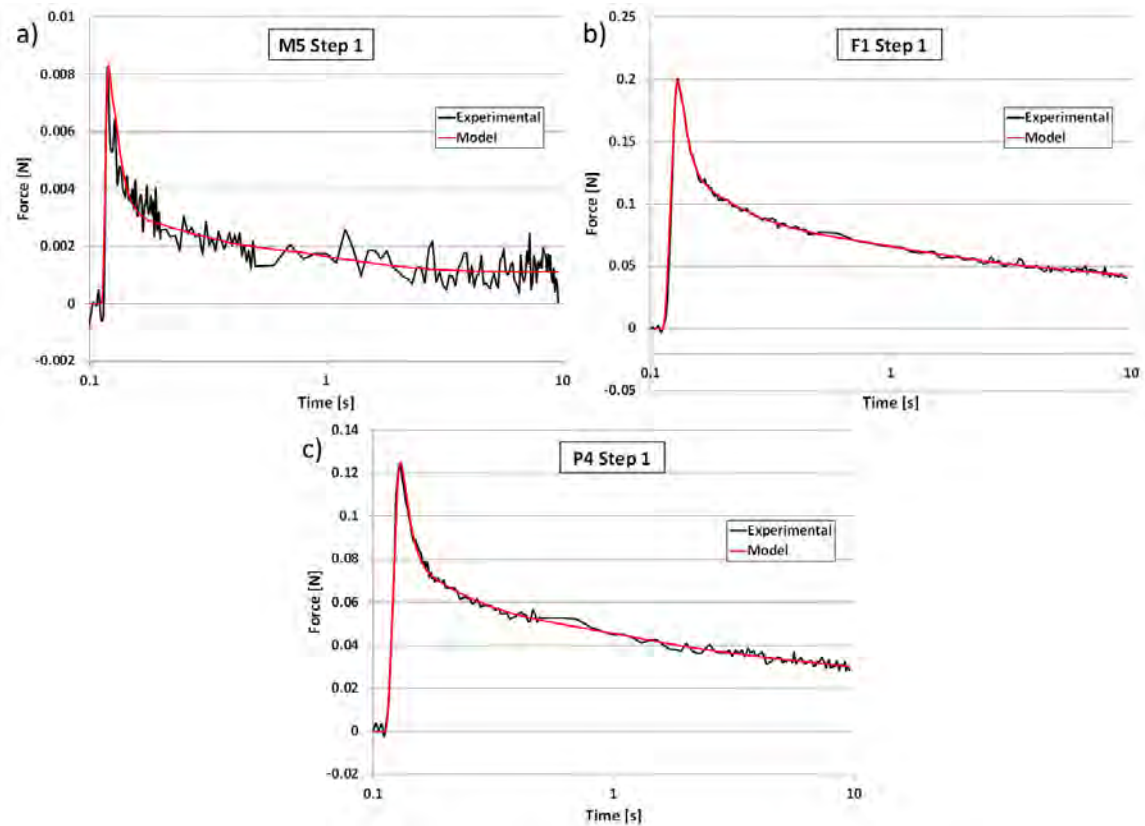
Figure 5-9: Typical model fits show good agreement between exeperimental step-hold data and model prediction for a) mouse, b) ferret, and c) pig.

Individual species models were created by simultaneously optimizing the model coefficients and parameters for all tests within a given species. The pig and ferret

models predict the average response well with the entire force-time history within the corridor. The mouse brain tissue model accurately predicts the initial loading and long-term relaxation, but fails to model the large magnitude immediate relaxation. The species material model falls outside of the corridor for this short-time relaxation response. The excellent ability of the model to describe variation in the experimental data is characterized by R^2 values of 0.946 and 0.943 for pig and ferret, respectively, with the mouse model slightly lower at 0.885.
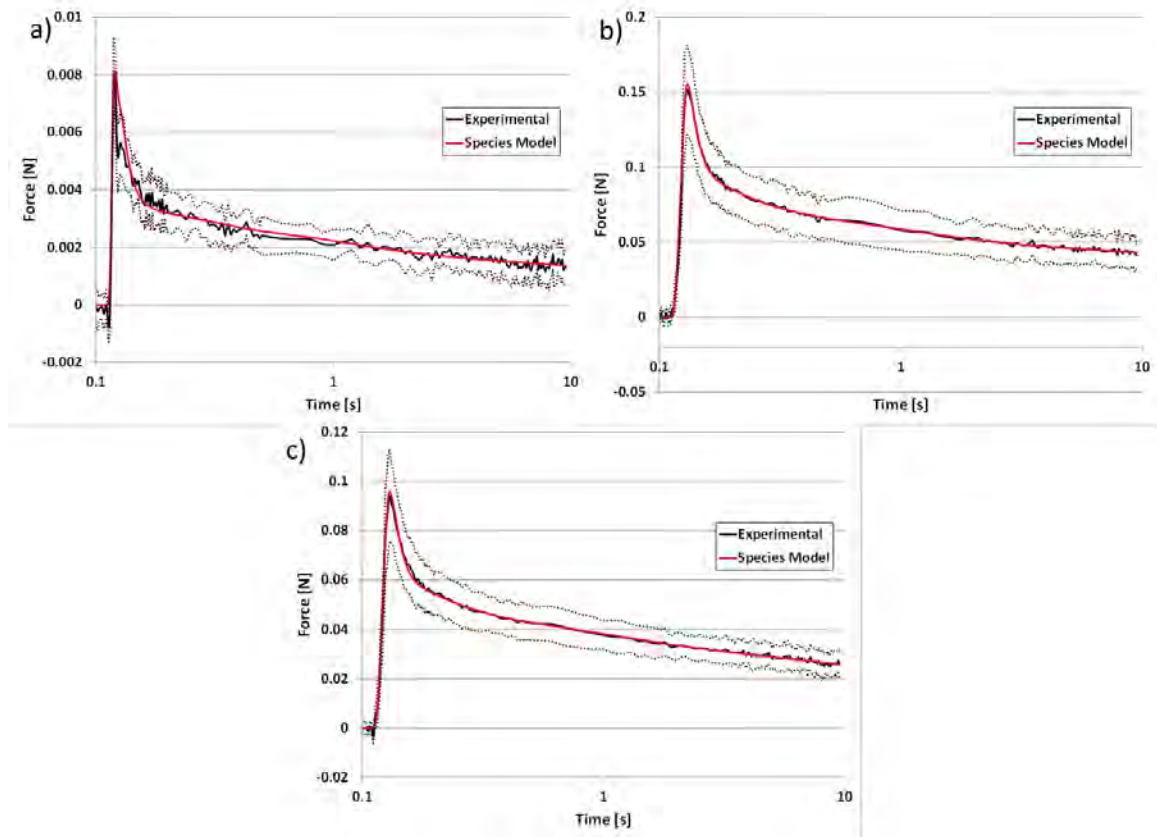
Figure 5-10: Species models compare well to experimental response with model prediction within the experimental response corridor (μ±SD) for a) mouse, b) ferret, and c) pig.

131

The relaxation response is dominated by the shortest time constant ($\tau = 0.01$s) for all three species and especially in mice (Table 5-2). The force response behavior in mice is characterized by an immediate large relaxation followed by a much lower magnitude relaxation. This is modeled by the relatively small reduced relaxation function coefficients for time constants greater than $\tau = 0.01$s. The immediate relaxation is smaller in ferrets and is modeled by a relatively smaller 0.01s time constant and relatively larger coefficient for $\tau = 0.1$s.

Table 5-2: Species brain constitutive model parameters and fit statistics. Relaxation behavior is dominated by short time constants.

	Instantaneous Elastic Parameters		Reduced Relaxation Function Parameters					Model Fit Statistics	
	A	**B**	**G_1** $\tau_1=0.01$s	**G_2** $\tau_2=0.1$s	**G_3** $\tau_3=1.0$s	**G_4** $\tau_4=10$s	**G_∞**	**SSE**	**R^2**
Mouse	4.175	0.018	0.722	0.047	0.092	0.053	0.086	0.028	0.885
Ferret	0.507	0.395	0.578	0.127	0.088	0.052	0.156	5.821	0.943
Pig	5.700	0.026	0.570	0.119	0.087	0.087	0.137	3.285	0.946

To assess model prediction for a different indentation rate and input form, model force was compared to experimental force measurements for 1Hz sinusoidal indenation tests (Figure 5-11). For the three species, the tissue material model derived for this study accurately predicted force response, with the model response falling within the experimental corridor for most of the time-history. Model and experimental response varied at low displacement magnitudes after the first indentation cycle. The models consistently predicted a more negative force magnitude.
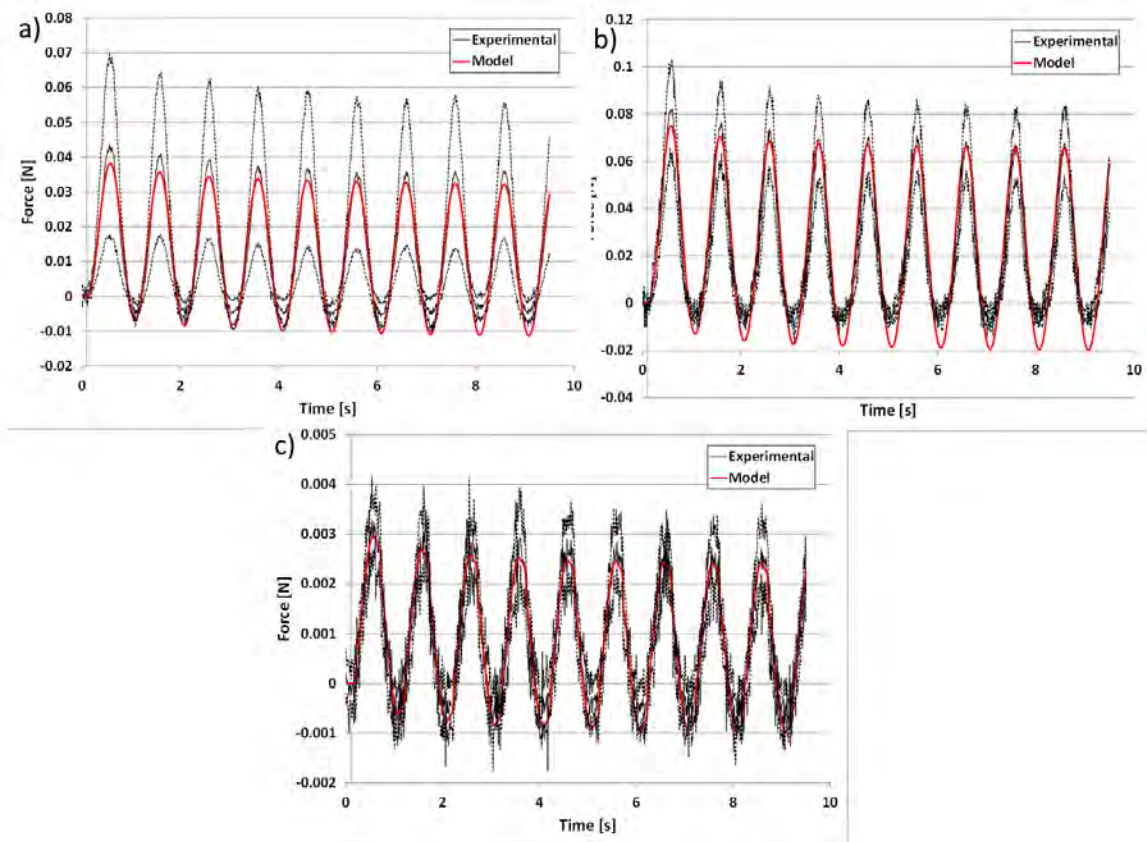
Figure 5-11: The VE model for a) mouse, b) ferret, and c) pig predicts tissue response to a sinusoidal input well with most of the response falling within the experimental corridor (μ±SD). Model prediction varies from experimental response during the low displacement portion of the sinusoidal input.

To make an interspecies comparison of tissue models, the three species models were subjected to an ideal 1mm magnitude step-hold displacement and the predicted force was compared (Figure 5-12). Large differences in magnitude of predicted force are seen. The peak force predicted for ferrets is nearly four times that for mice and and that predicted for pigs is nearly twice that for mice. This difference can be explained in part by the strain magnitude in the ferret tests being nearly three times that of the mouse and

133

pig. Qualitatively, the relaxation in the pig and ferret model are similar with the

majority of relaxation in mice occurring over a shorter time, as previously discussed.
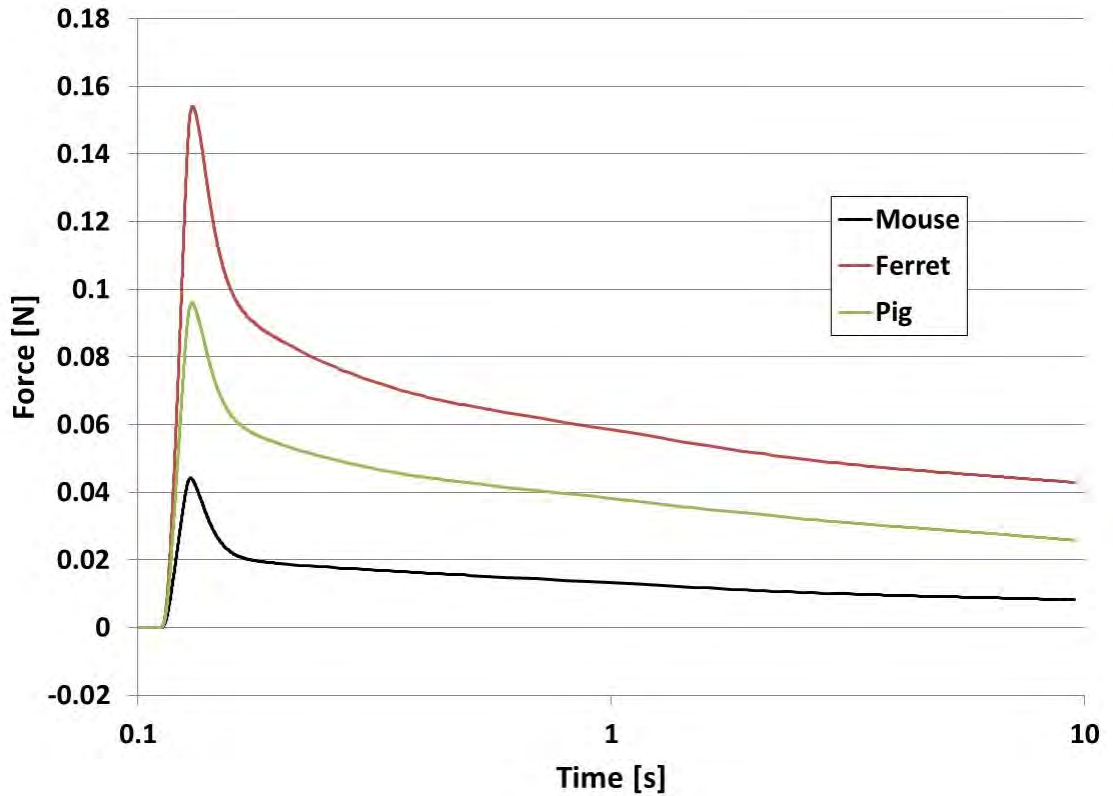
Figure 5-12: When the three species model responses to an idealized 1mm step tests are compared a large difference in force magnitude is observed, likely due to larger skull interaction effects in the ferret and pig tests and different indenter geometries.

5.4 Discussion

Brain tissue from three different common neurotrauma animal models was

characterized using controlled indentation methods. The tissue exhibited clear,

qualitatively similar, viscoelastic behavior, with a response to a fast ramp displacement

including an instantaneous elastic response followed by decay in force due to viscous

relaxation of the tissue. Increasing indentation magnitudes were assessed for changes in

tissue mechanics and also for separability of time-dependent behavior necessary for QLV modeling. The maximum indentation levels which did not result in tissue softening and fulfilled QLV assumptions were chosen to model. In the pig and ferret experiments changes in relaxation response were observed above L1 indentation. A decrease in measured force for L1 indentations was also measured after L2 indentation, suggesting damage or strain softening due to L2. Therefore, L1 was chosen for pig and ferret to develop constitutive models through FE analysis. For mice, small differences in relaxation behavior were measured between L1 and L2 indentation. However, due to large variation in L1 response across test animals, L1 could not be used for further analysis. Complications in the measurement of L1 force levels in mice was likely due to a combination of factors including consistent normal contact of the indenter and limited resolution of the test apparatus and data acquisition. Considering these effects, L2 was utilized for the development of material constitutive models through FE techniques.

Model validation by sinusoidal indentation tests was deemed successful. The brain tissue models showed good overall performance with the majority of the the force-time history falling within the experimental corridor. There was variation from the experimental response for low displacement magnitudes. This may be attributed to incomplete recovery of the brain tissue on the time-scale of the indentation waveform. Additionally, non-ideal surface interactions close to zero magnitude displacement, such as incomplete indenter contact and surface tension due to moisture, may contribute.

The reduced relaxation response was dominated by the shortest time constant for the three species (Table 5-2). Thre largest reduced relaxation coefficient was for τ = 0.01s. This indicates that rate dependent modeling is vital for brain tissue, especially with high-rate impacts and blast exposure that occur on a millisecond scale. An even shorter time constant may be beneficial to improve the model, especially for mice that showed a large magnitude immediate relaxation. It is uncertain whether there are differences between short term relaxation response between mice and the larger gyrencephalic species.

There are large differences in reported dynamic VE properties across literature. Reported values of complex shear modulus and loss tangent vary over orders of magnitude for brain tissue. Differences in constitutive model have been shown to significantly affect FE model response, especially for the high rate mechanics associated with primary blast exposure (Panzer 2012). Therefore, as the results of this study suggest, it may be necessary to implement species specific brain properties in FE models of brain tissue.

The species brain tissue models derived in this study suggest that there may be large interspecies differences in stiffness. However, this modeling technique does not take into account the geometry and morphology of the brain, skull, and indenter. The smaller displacements coupled with the compliant skull in mouse tests avoid large effects of brain tissue confinement within the skull. Alternatively, the larger

displacement magnitudes in the ferret and pig tests result in significant effects of interaction between the brain and skull. There is a larger relative volume displaced in the ferret compared to the pigs tests. As expected this result in larger confinement contributions and higher measured forces. In addition, there is no adjustment for the smaller indenter surface for the mouse tests. The much larger surface area of the indenter used for ferret and pig testing results in higher total force magnitudes and greater signal to noise ratio. These factors highlight the importance of a more complex analysis such as inverse FE simulation, which can account for some of these effects and would likely result in more similar force response across the species for a given displacement input.

Ideally brain tissue characterization would occur in vivo to ensure the measurement of material behavior that occurs in a living subject. However, in vivo testing is not without its own challenges such as tissue displacement due to blood flow and other active physiological processes. A study observed no measureable differences in tissue behavior between in vivo indentation and that occurring in situ immediately postmortem (Gefen and Margulies 2004). In situ testing maintains the mechanical environment well with only a small hole through the skull to access the brain surface. The study presented here includes both gyrencephalic and lissencephalic species that are commonly used for in vivo testing. This is important for the understanding of any

137

resulting differences in tissue mechanics and may help to improve not only modeling but our understanding of interspecies scaling for neurotrauma.

The experimental results of this study showed large variability in mechanical response, especially in the mouse model. There are many potential contributing factors including incomplete indenter contact and effects of proximity to sulci in the gyrencephalic species tested. Due to the low displacement amplitudes and measured indenter forces, the resolution of the test apparatus was challenges, especially in mouse tests. It may be possible to lessen data variability through the use of higher resolution equipment and sensors.

To improve the constitutive modeling of brain it may be valuable to include more intermediate indentation levels in the experimental procedure. The measurement of brain tissue mechanics is difficult due to the low stiffness and nearly incompressible behavior. A technique such as MR elastography may help to resolve the low strain and high strain-rate behavior of interest for blast modeling. A further advantage to MR elastography is the ability to perform testing in vivo without tissue damage, allowing clinical in vivo testing in humans.

After failure, constitutive model fidelity can be improved with the inclusion of damage or strain softening effects, which may be very important for TBI modeling, especially in blunt impact due to the higher tissue strain levels. From this study and extensive published experimental work is appears that irreversible changes in tissue

mechanical behavior occur at low strain levels for high rate events. The inclusion of

failure modeling will help to account for these changes that occur in the majority of

experimental characterizations of brain tissue. Many studies likely test beyond this

threshold for mechanical changes. Preconditioning is commonly used for brain tissue to

improve the consistency of subsequent mechanical test responses. However, the validity

of preconditioning with brain tissue is not clear. Physiological preconditioning inside

the skull is likely small. So it is difficult to determine appropriate strain magnitudes for

preconditioning. Due to the soft nature and microstructure of brain tissue, it does not

exhibit clear failure necessary for determination of preconditioning levels in boney or

connective tissues.

This study is the first to look at brain tissue VE behavior across a wide range of

brain sizes with consistent methodology. The brain tissue from the three common in

vivo animal model species tested exhibits clear VE behavior and shows damage or strain

softening at higher strain levels. The relaxation behavior for the three species is

dominated by short time ($\tau = 0.01s$) highlighting the need for high rate characterization

for constitutive modeling to be used for impact and blast biomechanics. Results from

this material characterization can be used to improve FE models for injury biomechanics

research. With high resolution biofidelic FE models of the brain and head for different

in vivo animal model species, it may be possible to elucidate interspecies mechanical

behavior and develop more appropriate scaling procedures for blunt and blast

neurotrauma research.

Chapter 6 - Blast Pulmonary Scaling

Historically, blast injury research has focused on the air-containing organs, especially the lungs, due to their susceptibility to injury. Extensive animal model research has been conducted to study injury threshold and fatality risk from primary blast exposure to the pulmonary system. Scaling for pulmonary fatality risk has been previously developed. This chapter incorporates a larger dataset from both small and large animal species than has been used before to update scaling and fatality risk models. This work was previously presented at Personal Armour Systems Symposium 2014 in Cambridge, England.

6.1 Introduction

The increased risk of exposure to blast in both military and civilian settings emphasizes the importance of blast trauma research. Use of improvised explosive devices (IEDs) has made blast the most common source of injury for American military personnel in Iraq and Afghanistan (Warden 2006). An apparent decrease in the occurrence of blast pulmonary trauma (Champion et al. 2009) has largely shifted the focus of blast injury research, historically dominated by pulmonary studies, to traumatic brain injury. This shift in injury pattern is thought to be the result of widespread thoracic body armor usage (Wood et al. 2012), and a previously unappreciated vulnerability to mild blast TBI (Rafaels et al. 2012). However, pulmonary blast trauma is

still of interest, and is of special importance in unprotected military personnel or civilian exposure to blast from terrorist or occupational explosive events.

Incidence and severity of pulmonary blast trauma is driven by blast physics. A shock is characterized by an approximately discontinuous increase in pressure, temperature, and density. The shock of a free-field blast results in a pressure profile, when measured at a stationary location, with a very short rise time (<10µs) to a peak overpressure followed by a decay to a negative pressure phase before returning to ambient conditions. In the absence of reflective surfaces or confinement of the shock, this pressure profile can by described as a Friedlander profile characterized by a peak overpressure, overpressure duration, and pressure impulse. This type of wave is ideal for research as it is a free-field representation of blast exposure and is dependent upon the size/type of charge and standoff distance. Wave complexity can be introduced through reflecting surfaces, and such complex blast waves are difficult to characterize and reproduce for injury research. Complex waves often contain more pressure impulse and are more injurious than simple waves with similar peak pressures (Richmond et al. 1985, Panzer et al. 2012c).

A large source of inconsistency and confusion within blast injury literature is the methodology for measuring pressure and the differences between incident and reflected pressure. A simple overpressure pulse may be measured in an incident orientation, perpendicular to the wave propagation (side-on), or reflected orientation, parallel to the

wave propagation (face-on), to receive different magnitudes of pressure (Bass et al. 2012). Depending on the shock strength, a reflected measurement will result in values 2 to 8 times greater in magnitude than incident measurements (Iremonger 1997). For ideal blasts the Rankine-Hugoniot relations may be used to reliably convert reflected to incident magnitudes and vice versa (Iremonger 1997). Therefore, it is vital to distinguish between these two types of measurement when reporting blast injury results.

Overpressure duration is overlooked or not reported in many blast injury studies, despite the importance of this parameter on the severity of blast trauma. Injury tolerance in animal models is dependent on peak pressure and overpressure duration, at least for short duration blast (<30ms scaled) (Bass et al. 2008). These short duration blasts are typical of the explosive exposures caused by the detonation of IEDs, artillery, and mortar fire (Hyde 1991). Pulmonary injury from short overpressure duration blast is thought to occur due an impedance mismatch mechanism between lung tissue and the air contained within, leading to localized trauma from spalling (Cooper 1996). Long overpressure duration blasts (>30ms) are less frequent in current conflicts and are produced from very large conventional explosive charges (>1000kg), thermobaric, or nuclear weapons (Bass et al. 2012). Injury tolerance to long overpressure duration blasts is primarily dependent on peak pressure and is characterized by large momentum transfer to the chest leading to diffuse lung injury (Cooper 1996). It is important to note

that the transition from short to long overpressure duration trauma is not clearly defined and there is not likely a discrete transition between the two (Rafaels et al. 2010).

One of the goals of blast injury research is to establish injury thresholds and mechanisms from different types of exposures. To measure these experimental injuries it is necessary to employ living systems with active physiology and biophysical response, thus, animal models are required. Many species have been used to assess blast injury. Small species, particularly mice and rats, are commonly used due to easy handling and care, as well as established injury biomarkers, gene expression, and immune response (Celander et al. 1955, Saljo et al. 2000, Chavko et al. 2006). Large species such as pig and sheep are used as models with similar body size to humans but are studied less often since they have more extensive care requirements, are more expensive, and exhibit more variability between subjects (Young et al. 1985, Suneson et al. 2000).

Interpretation and comparison of injury results across species is complicated by large differences in size and morphology. Variation in physiology between common animal model species may further complicate comparison of injury endpoints. Differences in parameters such as heart rate, life span, and immune response may dictate time course and severity of injury response to blast exposure. Biomechanical and other scaling procedures are often necessary when comparing experimental results across different subjects and across different species. Allometric scaling laws have been

144

developed for many parameters across a very large range of mammalian species, mouse to elephant. Body size, organ size, metabolic rate, respiratory rate, and many other parameters have been measured and scaling models have been empirically derived (Stahl 1967, Lindstedt et al. 1981, Boxenbaum 1982).

In early pulmonary blast injury research, Bowen et al. (Bowen et al. 1965) recognized the need for interspecies scaling when combining different species to derive a human equivalent exposure. Bowen found injury tolerance and fatality risk to require scaling of overpressure duration while peak pressure scaling based upon animal size was found to be negligible. Bowen's interspecies scaling is a simple model using the cubed root of a body mass ratio producing an effective overpressure duration scaling by characteristic body length. The reference mass is a 70kg human body mass. In blast literature where interspecies scaling is considered, Bowen's scaling is commonly used (Rafaels et al. 2011, Panzer et al. 2012c). The validity of Bowen's scaling, especially outside of pulmonary injury for which it was derived, is unknown, and the biomechanical basis for Bowen's scaling is unknown. It is possible that interspecies scaling for blast traumatic brain injury or other injury endpoints do not follow this model.

Blast injury risk models have been derived from literature data on pulmonary trauma but have focused primarily on large animal species (Bass et al. 2008, Rafaels et al. 2010, Panzer et al. 2012c). Separate non-linear pulmonary risk models for short (Bass et

al. 2008) and long (Rafaels et al. 2010) overpressure duration exposures have been published. Recent work by Panzer (Panzer et al. 2012c) derived risk models across a large overpressure duration range by implementing a piecewise log-linear model and considering the effects of multiple blast exposures. These studies assume Bowen's scaling to account for interspecies differences.

The goal of this study is to develop a fatality risk model due to pulmonary injury from primary blast exposure based on a meta-analysis of a large database of animal model injury data. Additionally, an interspecies scaling model based upon this dataset will be empirically derived to optimize the model fit.

6.2 Methods

A database of blast animal model data was created which includes 14 different species and over 12,000 tests. This body of data was filtered for this study through the use of several exclusion criteria. Only studies reporting fatality data from a simple Friedlander type pressure wave were included. Studies with thoracic protection were excluded along with multiple blast exposure data, except in cases that resulted in no injury. Studies were excluded which did not provide sufficient methodological detail to recreate the blast dosage, mainly peak overpressure and overpressure duration. In some cases, especially with free-field explosives where only charge size and standoff distance was reported, blast data was calculated through the use of CONWEP to calculate exposure level (Hyde 1991). Orientation and the presence of a reflecting surface behind

the animal were not considered as their effects were previously found to be insignificant in large animals (Bass et al. 2008, Rafaels et al. 2010). Only species with sufficient data to fit a single species fatality risk model were included, resulting in a dataset of 4193 total tests with 5 different species which were used to develop pulmonary fatality risk in this study. A list of studies and number of tests per species are presented in Table 6-1 and Table 6-2, respectively. A more detailed description of in vivo tests used for this analysis are presented in Appendix B, and include blast exposure levels and fatality rates. Injuries reported varied from minor petechiae (Chavko et al. 2006) and hemorrhage (Celander et al. 1955) to rapid fatality resulting from major lung hemorrhage (Bowen et al. 1968).

Table 6-1: Published blast animal model work used for pulmonary interspecies scaling and injury model derivation.

Reference	Species Used	Reference	Species Used
Bowen 1968	Sheep	Richmond 1961	Mouse, Rabbit, Dog, Goat
Celander 1955	Mouse	Richmond 1962a	Mouse, Rabbit
Cernak 2011	Mouse	Richmond 1962b	Mouse, Rabbit
Clifford 1984	Sheep	Richmond 1966	Mouse, Rabbit, Dog, Goat
Damon 1964	Mouse	Richmond 1968	Dog, Goat, Sheep
Damon 1966	Dog, Goat	Richmond 1981	Sheep
Damon 1970	Dog, Sheep	Richmond 1982	Sheep
DASA1656 1965	Goat	Rubovitch 2011	Mouse
Dodd 1989	Sheep	Woods 2013	Mouse
Mundie 2000	Sheep	Yang 1996	Sheep
Phillips 1988	Sheep	Young 1985	Sheep

147

Ambient pressure scaling (Equation 6-1 and Equation 6-2) was employed for both peak pressure and overpressure duration for body mass scaled durations longer than 30ms as described by Bowen (Bowen et al. 1968) but was not used for scaled durations less than 30ms as discussed by Bass (Bass et al. 2008). This accounts for the effects of high altitude testing or the modification of ambient pressure during testing, and this scale factor approaches one at normal sea level ambient pressure.

$$P_{P,scaled} = P\left(\frac{P_{sea\ level}}{P_{ambient}}\right) \qquad\qquad \text{Equation 6-1}$$

$$\Delta t_{P,scaled} = \Delta t\left(\frac{P_{ambient}}{P_{sea\ level}}\right)^{1/2} \qquad\qquad \text{Equation 6-2}$$

A simple overpressure duration scaling model was used to account for interspecies body mass differences (Equation 6-3). This scaling uses a ratio of body masses between the test subject and a reference human body mass. This allows the blast dosage to be transformed to an equivalent human biomechanical input. The scale factor, α, was optimized to best fit the experimental data.

$$\Delta t_{scaled} = \Delta t\left(\frac{mass_{reference}}{mass}\right)^{\alpha} \qquad\qquad \text{Equation 6-3}$$

To describe the fatality risk a nonlinear logistic regression model was constructed (Equation 6-4) that was dependent upon peak incident pressure and scaled overpressure duration (Bowen and Fletcher 1968, Bass et al. 2008).

$$P = P^*\left(1 + a\Delta t^{-b}\right) \qquad\qquad \text{Equation 6-4}$$

where P*, a, and b are model parameters to be fit by the data. This form describes the

decreasing peak pressure tolerance as overpressure duration increases while at short

durations. As durations increase, the peak pressure tolerance approaches a constant, P*.

Fatality risk models were fit to the five individual species to determine the long

overpressure duration peak pressure threshold, P*, for each species. Values of P* fell

into two distinct groups, large and small species (Bowen and Fletcher 1968). As human

body size and pulmonary system anatomy suggest it would fall within the large animal

group, a mean P* value for the three large species was used as the human P*. To correct

for differences in peak pressure tolerance, the pressure values for each test were scaled

according to a ratio of the human P* value and that for the species (Equation 6-5).

$$P_{P^*,scaled} = P\left(\frac{P^*_{human}}{P^*}\right)$$ **Equation 6-5**

Regression was then performed on the complete set of data from five species to

simultaneously determine the fatality risk model and overpressure duration scaling

model. Nonlinear regression and statistical analyses were performed in Excel (Excel

2010, Microsoft, Redmond, Washington) and JMP (JMP Pro 10, SAS Institute Inc., Cary,

NC) for the logistic regression model in Equation 6-6.

$$\pi = \frac{e^F}{1+e^F} \qquad F = f\{ln[P^*(1+a\Delta t^{-b})] - ln(P)\}$$ **Equation 6-6**

where f, a, and b are fitted model parameters and π is the probability of fatality.

The area under the receiver operating characteristic curve (AUC) was used to assess model goodness-of-fit. AUC measures sensitivity versus (1-specificity) of the fit and values greater than 0.8 are considered good model discrimination.

Unscaled fatality and survival data is shown in Figure 6-1. It is important to note that when all of the injury data across different species is plotted against pressure and overpressure duration exposure without incorporating any interspecies scaling the data appears unorganized, and there is no clear delineation between injury and non-injury cases. Many injury points fall well below levels of non-injury nd likewise, non-injury points appear at high exposure levels for some species relative to others. Without interspecies scaling, model fit statistics in Table 6-2 show poor model parameter fits with large standard error values, additionally the AUC value of 0.78 indicates only fair specificity and sensitivity of the unscaled model.
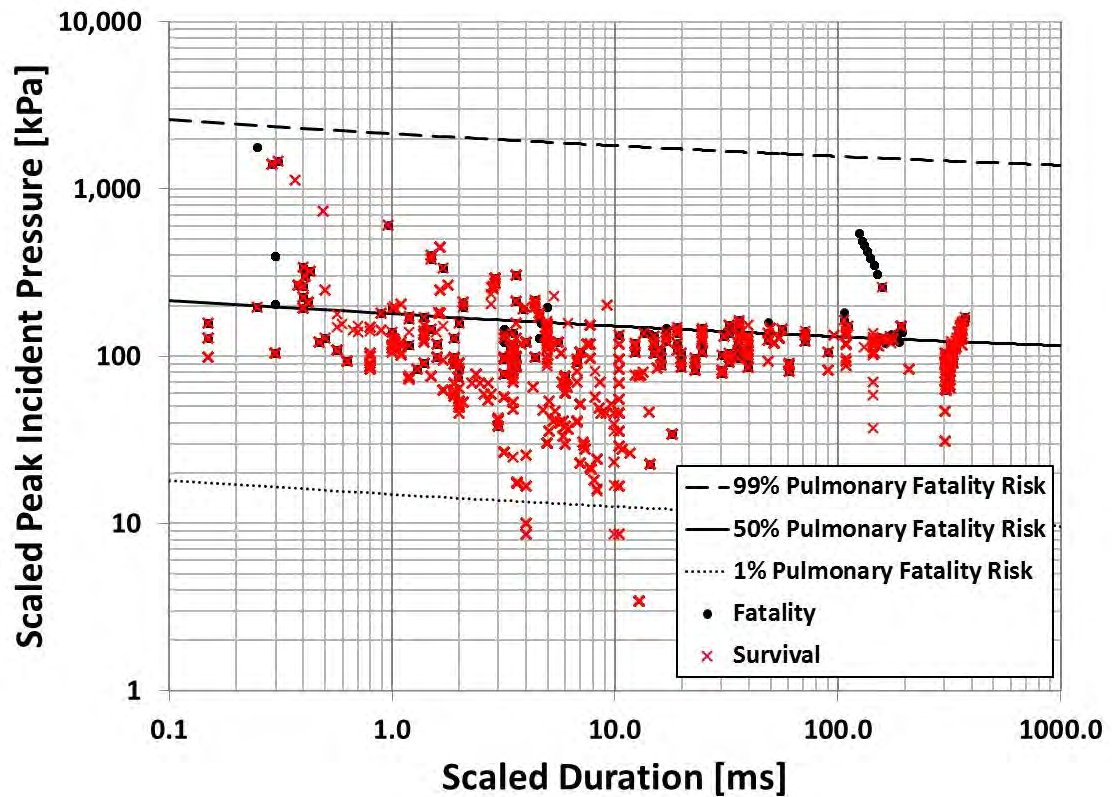
Figure 6-1: Unscaled pulmonary injury data across five species lacks separation between injury and non-injury cases.

6.3 Results

When each of the five species were fit with individual fatality models to

determine long term pressure tolerance (P*) values, there was a clear grouping of small

species (mouse, rabbit) and large species (dog, goat, sheep). Figure 6-2 shows the small

species grouped around a pressure value of 90kPa and the large species around

approximately 145kPa. Since human pulmonary anatomy most closely resembles that of

the large species (Crosfill et al. 1961) a mean of those P* values (143.4kPa) was used as

the human reference value. P* is equivalent to the lowest peak pressure capable of 50%

fatality from exposure. This means that, independent of overpressure duration, peak

pressure values less than P* will always produce less than 50% fatality, regardless of

blast duration. As the overpressure duration decreases, the risk will decrease.
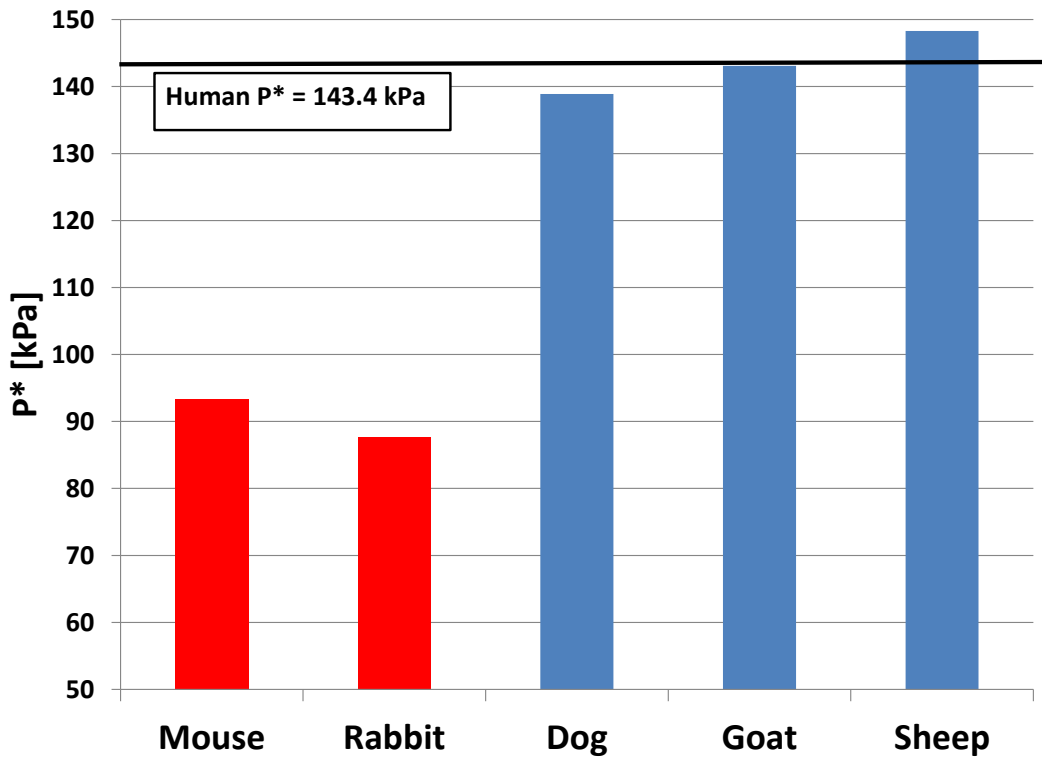
Figure 6-2: Long overpressure duration 50% fatality values, P*, for individual species shows a clear separation between small and large animal model species.

From five species 4193 data points were fit with an interspecies scaling and

fatality risk model. This dataset included 2866 survival and 1327 fatality cases. The

results of the nonlinear regression are presented in Table 6-2. The optimized

overpressure duration scaling according to Equation 3 resulted in an α of 0.351. The use

of interspecies scaling improved the model fit, supporting the need for interspecies

scaling to describe fatality risk. An AUC of 0.88 indicates good specificity and

sensitivity of the model. The fatality risk model is shown in Figure 6-3 along with the

fatality data. Not only does the interspecies scaling organize the injury data to see a

clear delineation between fatality and survival levels across all species, model

loglikelihood data shows that this holds true individually for large and small species.

Values in Table 6-2 for average loglikelihood show that contribution, per test, to the

overall loglikelihood is consistent across species. The model best fits the sheep data as

shown by the low average loglikelihood of 0.105. The other four species have similar

values indicating that the model does not fit either small or large species better than the

other.
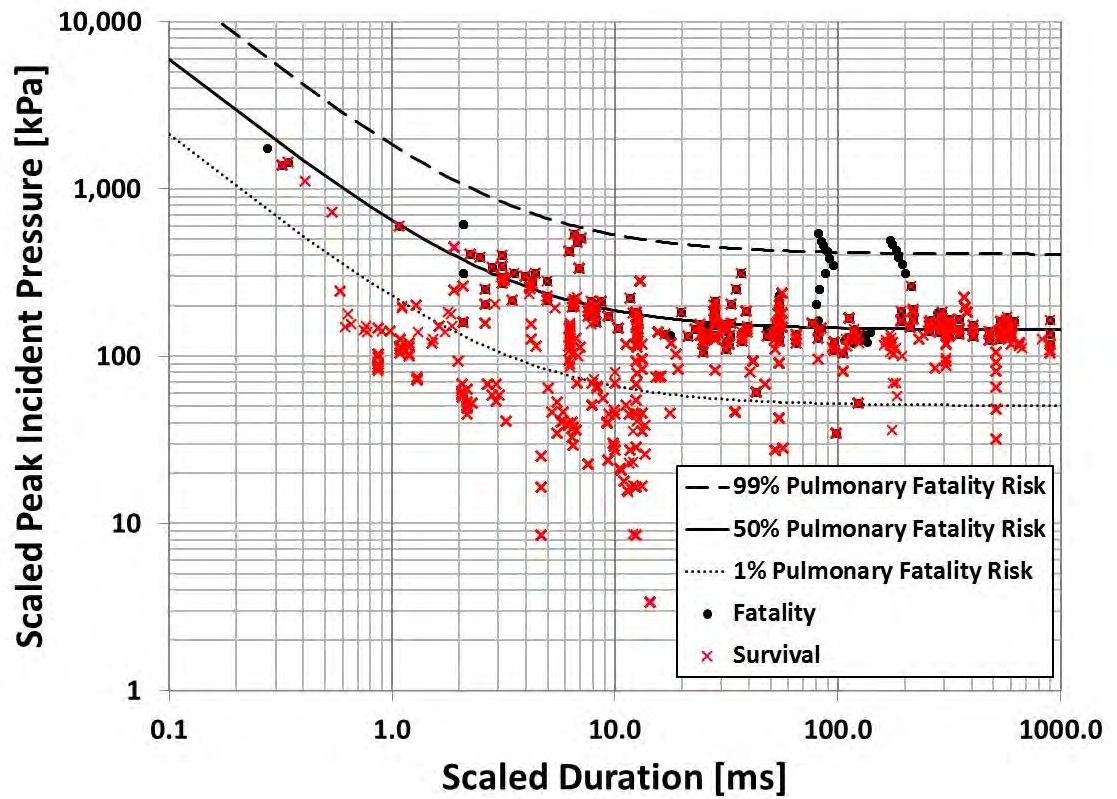
Figure 6-3: Opimized interspecies scaling results in a regression model for fatality due to pulmonary trauma that describe behavior well over five large and small species (α = 0.351).

Table 6-2: Species data with regression model coefficients and goodness of fit [coefficient ± SE].

		Mouse	Rabbit	Dog	Goat	Sheep	
	# of Tests	1828	392	409	255	1309	
	Reported Mass [kg±SD]	0.023±0.004	2.08±0.55	16.36±1.30	24.16±4.17	47.76±8.75	
	P* [kPa]	93.4	87.7	138.9	143.1	148.3	
	Avg. loglike	0.555	0.567	0.531	0.578	0.105	
	P*	a	-b	f	α	loglike	AUC
Unscaled	71.84±74.04	1.49±2.55	0.13±0.13	1.85±0.08	0	2202.6	0.78
Full Model	143.4	3.53±0.23	1.06±0.04	4.41±0.20	0.351	1737.3	0.88

6.4 Discussion

This study produced the first statistically based interspecies scaling for fatalities from pulmonary blast based on five model species of disparate sizes. The new scaled pulmonary fatality model (Figure 6-4) behaves similarly to previously published fatality risk curves (Bowen et al. 1968, Bass et al. 2008, Rafaels et al. 2010, Panzer et al. 2012c). The model from this study predicts a slightly higher peak pressure tolerance at very short durations, less than 0.5ms. At 0.1ms Panzer's model predicts 50% fatality at 3994kPa while the current model from this study predicts a 50% risk of fatality at approximately 6000kPa. The models behave similarly beyond 1ms with the exception of the long and short bounds of the Bass (Bass et al. 2008) and Rafaels (Rafaels et al. 2010) curves, respectively. However, if the model of Bass is considered to transition to Rafaels at approximately 15ms they create a single model which agrees well with the other models presented. Bass , Rafaels, and Panzer utilized only large animals in their risk models and the good agreement with the current model supports the use of pressure scaling to compare small and large animal results.
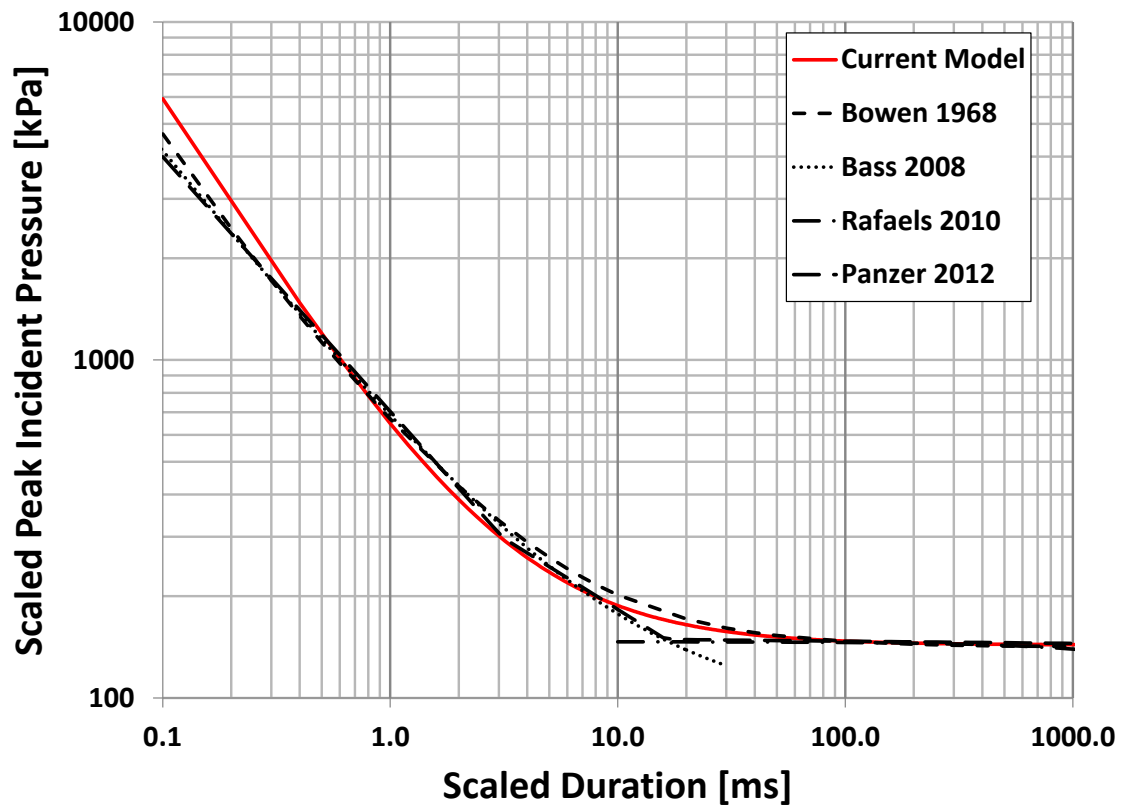
Figure 6-4: 50% pulmonary injury risk models compare well to existing models (Bowen et al. 1968, Bass et al. 2008, Rafaels et al. 2010, Panzer et al. 2012d).

If the pulmonary risk model derived here is intended to be used across all mammalian species and compared to humans it must fit other existing pulmonary blast fatality data. Other species can be used as essentially validation cases for this risk model. Four additional species have a substantial set of blast pulmonary fatality data but were not over a wide enough range to develop individual species models. Since long term pressure tolerance values, P*, for each of these species could not be derived, they were assumed to follow either small (rat) or large (cattle, monkey, pig) animal behavior. Average values of 90.6 and 143.4kPa were used for small and large species,

respectively. The peak pressure and overpressure duration scaling described in this study were then applied to the fatality data. Data from cattle, monkeys, pigs, and rats are compared to the pulmonary fatality risk models derived from this study in Figure 6-5. The fatality risk model described the behavior of this data well. There was a clear delineation, by the 50% fatality risk, between the survival and fatality cases. The average loglikelihood values for cattle (0.389), monkey (0.567), pig (0.276), and rat (0.761) data were comparable to those species used to fit the model. This suggests that this pulmonary risk model can be used for species beyond the five used to derive the model.
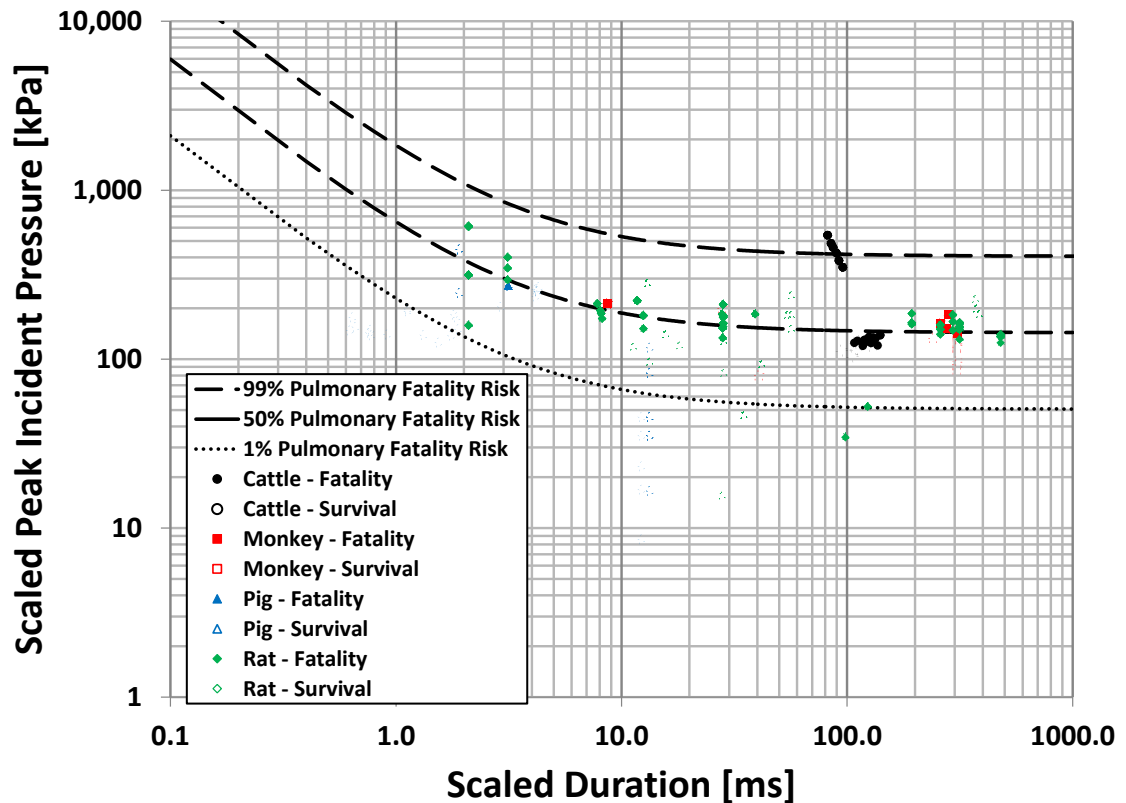
Figure 6-5: Experimental blast pulmonary fatality data from additional animal model species compares well to the pulmonary fatality risk models derived in this study.

Large differences in body size, morphology, and anatomy between large and small species have led to the idea that injury tolerance and perhaps scaling laws cannot apply to both groups without some additional compensation. For blast models, species have generally been categorized as large animal models if they exceed 15kg in body mass or are of high phylogenetic order (Bowen et al. 1968). The source of the influence of phylogeny is unclear, but the effects are clear. For example, squirrel monkeys (~ 1 kg body mass) have 'large animal' blast response while rabbits (~3 kg body mass) have 'small animal' response (White et al. 1971). It is thought that small animal species, especially rodents, are more susceptible to lung injury from blast because of lower normalized lung density (White et al. 1971). Other pulmonary variables such as average gaseous lung volume have been correlated to differences in long overpressure duration tolerance (Bowen and Fletcher 1968) but an interspecies scaling method has not been developed. This led to Bowen (Bowen and Fletcher 1968) to develop separate fatality risk models for large and small species. Large differences in physiology, especially rate-dependent processes such as metabolism, may also lead to different injury response in small animal model species.

Developing fatality risk models for small species is complicated by the lack of test data below 10ms when body mass scaling is used, therefore the current model is dominated by large animal data at short overpressure duration. The validity of the

model in this study is supported by its ability to fit data well over a size range of three orders of magnitude from mouse to sheep.

There are a number of important features of the pulmonary fatality risk models. First, the overall form of the model can inform as to the nature of injury dependence on different aspects of the blast exposure. For short durations, the slope of the model suggests a strong dependence upon overpressure duration on the peak pressure tolerance for injury. Alternatively, at long durations, the curve flattens and implies that injury tolerance is primarily dictated by the peak pressure alone. The transition to flat portion of the curve may approximately indicate a shift in injury mechanism leading to this change in dependence upon overpressure duration. This transition occurs at approximately 30ms duration, but a precise cutoff between "short" and "long" overpressure duration is not provided by this data.

The results of this study are important in the context of the recent focus on blast neurotrauma. There are some pervasive methodological practices in recent blast animal model testing which complicate interpretation and application of findings. Despite the susceptibility of the pulmonary system to blast injury, many studies focused on traumatic brain injury fail to protect the thorax from blast exposure. The effect of pulmonary injury in these studies is largely unknown but it would be expected to influence brain injury findings. The threshold for pulmonary injury has been shown to

be lower than some neurotrauma endpoints, including blast-induced apnea and moderate brain bleeding (Rafaels et al. 2012).

Perhaps more importantly, there is a large body of blast injury literature which ignores the effects of interspecies scaling and the dependence of injury upon overpressure duration. The inclusion of scaling principles when attempting to interpret any findings as they relate to human exposure is essential. The failure to consider interspecies differences has led to experimental exposure levels in animal model tests that directly mimic human exposure. When interspecies scaling is considered, especially in rodent species, it leads to scaled durations well outside the realm of exposures which would reasonably be expected to occur (Figure 6-6). The majority of data that falls within the realistic exposure range is that of large animal tests where scaling has a smaller effect. In addition, most of the small animal test conditions within the realistic range are that of rabbits with almost all of the rodent model test conditions having scaled durations much longer than conventional explosives weapon exposure. This realistic exposure range is bounded by a small 0.25kg charge and a very large 1000kg charge size, as determined by CONWEP (Hyde 1991). The test conditions are also compared to the exposure due a 155mm artillery round at varied standoff, which is representative of a common IED threat of approximately 7.5kg TNT charge equivalent. Many current studies test blast rodent models at scaled overpressure duration levels only achievable by large thermobaric devices or nuclear weapons. Though some early

animal model blast testing studied nuclear blast effects, these effects are qualitatively

different than effects of high explosives. This points to the importance of

standardization of blast methodology to ensure we maximize the useful information

gained from animal model studies.
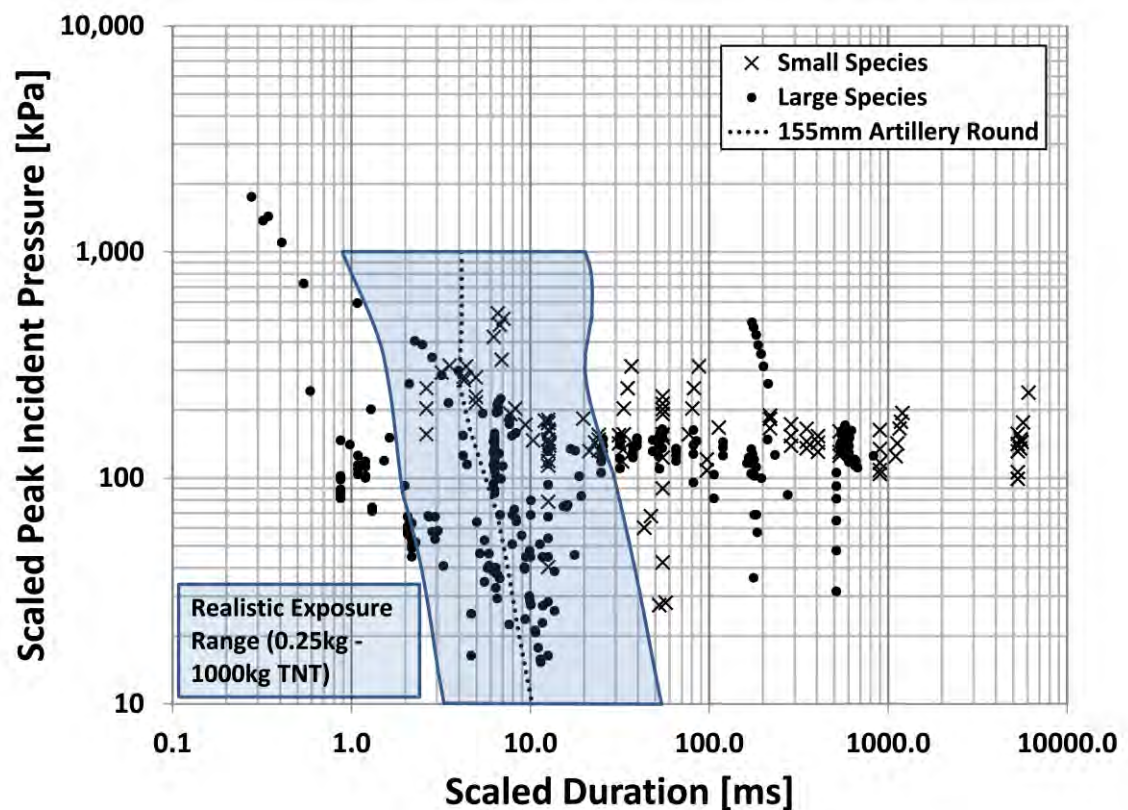
Figure 6-6: Many scaled pulmonary injury test conditions fall outside realm of realistic exposure, especially for small animals.

The scaling methodology of this study is limited by the consideration of only

body mass interspecies scaling. While this simple body mass scaling is commonly used

and describes injury well, there may be other anatomical parameters such as lung

density and physiological parameters which would improve the predictive capability of

the injury risk model and better account for interspecies differences. This study

considers only peak overpressure and overpressure duration for description of the blast

exposure. It is possible that other blast characteristics, including overpressure impulse

which accounts for pulse shape, may improve the exposure description for the model for

more arbitrary and non-ideal blast exposure.

In conclusion, this study utilized a large set of published experimental data to

optimize interspecies scaling for fatalities from exposure to blast using a overpressure

duration scaling model for 5 different animal model species. An interspecies scaling

exponent, α, of 0.351 compares well with previously published pulmonary injury scaling

by Bowen (Bowen et al. 1965). This suggests a characteristic length scaling based on

cube root of mass is appropriate for pulmonary injury. Pulmonary injury risk is largely

overpressure duration dependent for short scaled durations but is peak pressure

dictated as overpressure duration increases. The clinical implications of this study are

that without thoracic protection the pulmonary system is susceptible to blast injury and

should be a treatment focus in a trauma setting.

Chapter 7 - Blast Apnea Scaling

Little work has been done to establish interspecies scaling for blast-induced neurotrauma. One neurotrauma injury endpoint that has been reported epidemiologically is apnea, in the absence of pulmonary trauma. This chapter looks at the existing experimental data on neurotrauma induced apnea and develops a simple interspecies scaling relation. This work was previously presented at the International Research Council on the Biomechanics of Injury (IRCOBI) Conference 2013 in Gothenburg, Sweden.

7.1 Introduction

An increased incidence of blast exposures in military conflicts has spurred a focus on traumatic brain injury (TBI) in recent blast research. This effort contrasts with historical focus on pulmonary blast trauma since observed blast fatalities were clearly attributable to blast lung injury rather than blast brain injury (Hooker 1924, Clemedson 1953, Bass et al. 2008). However, recent research has shown that modern body armor, especially body armor with hard inserts, is strongly protective against blast. The use of body armor allows an individual to withstand blast dosages above unprotected fatal levels for pulmonary injury, potentially exceeding brain injury blast thresholds (Wood et al. 2012). Further, an unexpected risk of mild neurotrauma for isolated blast exposure to the head was recently established at blast intensity levels comparable to the unprotected pulmonary threshold risk (Rafaels et al. 2012).

Animal models are an important tool in injury research as they provide physiological and behavioral measurements not afforded by cadaveric or dummy surrogates. Animal models have been used extensively in blast research since much of blast trauma is dependent upon physiological response which is only accessible in a living model. These models include: mouse (Richmond et al. 1962, Goldstein et al. 2012, Yu et al. 2012), rat (Säljö et al. 2001, Svetlov et al. 2010, Garman et al. 2011, Leonardi et al. 2011), rabbit (Clemedson 1953, Richmond et al. 1966, Rafaels et al. 2011), ferret (Rafaels et al. 2012), pig (Saljo et al. 2008, Shridharani et al. 2012b). Large differences in size, structure, morphology and physiology between the injury models and humans necessitate the use of scaling procedures to relate the dynamic input and physical and physiological response from one species to another. Scaling methods are developed to match response of the animal model among species and to an equivalent human response. However, there are only a limited number of previous investigations available to support the development of cross-species scaling principles for blast neurotrauma owing to the presence of comorbid pulmonary trauma from blast exposure to unprotected animal pulmonary systems. Scaling models have been developed for blast pulmonary trauma (Bowen et al. 1968) and for blunt trauma (Eppinger 1976). However, blast neurotrauma scaling is unknown.

In earlier blast injury research, Bowen and colleagues recognized that some form of scaling procedure was needed to compare injury endpoints across different species

(Bowen et al. 1965). Scaling overpressure duration and peak overpressure was required

to match equivalent injury response between different species (Bowen and Fletcher

1968). Simple scaling models use a ratio of a reference mass (generally a human value)

to an animal mass, where Δt is the overpressure duration of the positive overpressure

phase (Equation 7-1). This form of scaling model increases the human equivalent value

for animal models that are smaller than humans.

$$\Delta t_{scaled} = \lambda \Delta t \quad \text{where} \quad \lambda = \left(\frac{\text{Reference Mass}}{\text{Mass}}\right)^{\alpha} \qquad \textbf{Equation 7-1}$$

The work of Bowen et al. covered many species of animals to investigate the

differences in injury response (Bowen and Fletcher 1968) Bowen developed a model for

interspecies scaling of pulmonary injury risk (Bowen et al. 1965). This model related the

animal body mass to a reference human body mass and was scaled by the cubed root,

meaning the blast overpressure duration was effectively proportional to an animal

model body length scale.

Panzer (Panzer et al. 2012a) recently developed a blast neurotrauma scaling

methodology based upon simple finite element (FE) models of the head and brain. For

this study, five scaled-replica spherical head models comprised of skull, cerebrospinal

fluid and brain were developed ranging in diameter from mouse to human head size.

Strain, acceleration and peak pressure were calculated within the brain tissue during

blast exposure. Both peak strain and peak acceleration were found to be larger in the

smaller heads at the same blast condition, but peak brain pressures were fairly

consistent between brain sizes. For instance, peak shear strain was observed to increase

by 50% when halving the head size. From these results, Panzer developed a scaling

model to relate the brain's relative biomechanical response (X) between two brain

masses (M) to the applied peak overpressure (P) and overpressure duration (Δt); where

α, β and γ are the scaling parameters (Equation 7-2).

$$\frac{X_2}{X_1} = \left(\frac{P_2}{P_1}\right)^{\alpha} \left(\frac{\Delta t_2}{\Delta t_1}\right)^{\beta} \left(\frac{M_2}{M_1}\right)^{\gamma} \qquad \textbf{Equation 7-2}$$

This model was fit to the 50th percentile peak brain strain and pressure results of

the FE simulations. By combining the models for brain pressure and brain strain for a

consistent injury outcome (X1 = X2), blast pressure and overpressure duration scaling

become separable and similar in form to Bowen's scaling model. The pressure and strain

scaling models were combined to isolate pressure and overpressure duration scaling.

From the isolated scaling models the peak pressure scaling factor was found to be 0.004,

with small effect over the possible interspecies pressure conditions, while the

overpressure duration scaling factor was found to be 0.248. This result is consistent with

the expectation that peak intracranial blast pressure is relatively insensitive to animal

model size while global strain response is sensitive to overpressure duration.

Other methods for scaling between species include simple empirical allometric

scaling methods covering orders of magnitude in body size (Stahl 1967, Lindstedt et al.

1981, Boxenbaum 1982). Many of these parameters (e.g. brain mass, metabolic rate,

respiratory rate, etc.) are scaled across a large range of species, even between mice and

elephants (Lindstedt and Calder 1981). These scaling laws were derived by optimizing

assumed scaling variables to fit large compilations of experimental data.

The goals of this study are to establish a clinical biomarker for central nervous

system (CNS) overpressure mediated trauma using simple scaling methods to determine

equivalent cross-species and human exposure in models of blast neurotrauma. The

injury outcome of interest is apnea as it is known to occur as a result of primary blast

exposure (Rafaels et al. 2012, Shridharani et al. 2012b, Yu et al. 2012) and may produce

secondary injury from hypoxia. It is important to note that scaling may be different for

different injury endpoints (e.g. apnea, death, axonal injury, etc.) and therefore injury

scaling must be considered specific to the injury response.

7.2 Methods

7.2.1 Animal Model Testing

Data were compiled for 266 live animal model tests with four species subjected to

primary blast, comprised of previously reported data for mice (n=166), rabbits (n=13),

ferrets (n=65) and pigs (n=18) (Rafaels et al. 2011, Rafaels et al. 2012, Shridharani et al.

2012, Yu et al. 2012) along with previously unreported data for ferrets (n=4). All

unpublished studies were performed in accordance to the guidelines and regulations of

the institutional animal care and use committee (IACUC) at Duke University. The blast

effects were associated only with the pressure wave applied using a compressed gas-

driven shock tube. The shock tube consisted of a driver section filled with high pressure

gas separated from an open-ended driven section by a diaphragm. By pressuring the

driver section, the diaphragm is caused to rupture, propagating a pressure shock wave

down the length of the shock tube. Peak overpressure and overpressure duration were

controlled by varying the driver gas used and the diaphragm thickness separating the

driver from the driven section of the shock tube. Incident pressure-time history was

recorded at the exit of the shock tube for each test to determine blast dosage and the

pressure wave characteristics of interest. All animals were anesthetized and were

provided with pulmonary protection to ensure isolation of injury to the head. Further

detail on each test animal, including blast dosage and anesthesia protocol is included in

Appendix C. Necropsy was performed to verify that no pulmonary injury existed. The

test animal was placed at the center of the shock tube exit face to maximize shock wave

planarity while limiting pressure reflections.

Animals were monitored for occurrence of apnea immediately post blast

exposure. Apnea in the studies of interest was defined as a complete cessation of

breathing immediately post-blast exposure for at least 10 seconds (Rafaels et al. 2011,

Rafaels et al. 2012, Yu et al. 2012) or at least 30 seconds (Shridharani et al. 2012b). It is

important to note that this is not blood-gas mediated apnea and is a result of direct

central nervous system exposure rather than systemic injury. Apnea intervention for the

rabbits and ferrets were identical with hand bagging of room air up to 1 minute,

ventilator support with supplemental oxygen up to 5 minutes and administration of

169

doxapram if apnea persisted greater than 5 minutes in duration (Rafaels et al. 2011, Rafaels et al. 2012). For the mouse study, upon observation of apnea post-blast animals were intubated and placed on a mechanical ventilator with supplemental oxygen until spontaneous breathing returned (Yu et al. 2012). Apneic pigs were hand bagged immediately, doxapram was administered if breathing did not return within 5 minutes and ventilator support was employed if the animal was non-responsive to chemical intervention. For this analysis 266 tests were used with 4 different species represented.

7.2.2 Scaling

Blast exposure data were scaled using four different methods. Each method scales the overpressure duration to account for differences between the animal model species and follows the form of Equation 1. The measured overpressure duration for each test was scaled to a human exposure equivalent according to each scaling method. The effects of optimized scaling of peak overpressure were found to be small relative to those for overpressure duration and were therefore excluded from this study.

The first method uses the traditional pulmonary blast scaling model developed by Bowen, using a body mass ratio and scaling exponent, α, equal to 0.333.(Bowen et al. 1968) The second method uses the blast brain scaling model derived by Panzer from computational models, using a brain mass ratio and α of 0.248.(Panzer et al. 2012a) The third method is an allometric scaling relation of physiological parameters (Stahl 1967, Boxenbaum 1982) based on physiological time relations between small and large

mammals that scales biometrics such as heart rate, breathing rate and life expectancy

scale with mass, which uses a brain mass ratio and α equal to 0.400. The fourth model is

based on optimizing the parameters in the standard brain mass scaling model to the

experimental apnea data. Brain masses were estimated for each species, 0.3g for mice,

11g for rabbits, 7g for ferrets, and 80g for pigs.

Following the application of each scaling method to the experimental data, apnea

risk functions were developed. A logistic regression was conducted fitting a log-linear

dose-response (Equation 3) to the scaled apnea outcome data by minimizing log

likelihood (JMP Pro 10, SAS Institute Inc, Cary, NC). A simple weighting scheme was

used to account for differences in total number of tests between species. Each species

was given an overall equal weight to the model fit. Two goodness-of-fit indicators were

used to assess each regression model. The generalized coefficient of determination (R2)

was used to assess the proportion of variability in the dataset accounted for by the

model. Additionally, the area under the receiver operating characteristic (ROC) curve

was used for measuring the sensitivity versus 1-specificity for the model fit. Apnea risk

curves (1, 50 and 99% risk) were generated for each scaling method. The optimized

scaling model was found by simultaneously optimizing for the scaling parameter, α, and

the dose-response model for apnea occurrence (Equation 3). This scaling model was

used by Panzer (Panzer et al. 2012c) for functional forms chosen in this study for scaling

and dose response and follows Equation 7-3.

171

$$\ln\left[\frac{\Pr(\text{apnea}|P_i)}{1-\Pr(\text{apnea}|P_i)}\right] = \beta_0 + \beta_1\log_{10}(\text{Peak Pressure}) + \beta_2\log_{10}(\Delta t) \quad \textbf{Equation 7-3}$$

7.3 Results

Unscaled and scaled apnea outcome data are shown for each of the four scaling methods below. Scaling results are presented with 1, 50 and 99% risk of apnea curves. Since each of the species investigated were smaller than humans, the result of scaling is a large shift of the experimental data to larger human equivalent durations. The unscaled data presented in Figure 7-1 is grouped together with no interspecies delineation between apnea and no apnea cases.
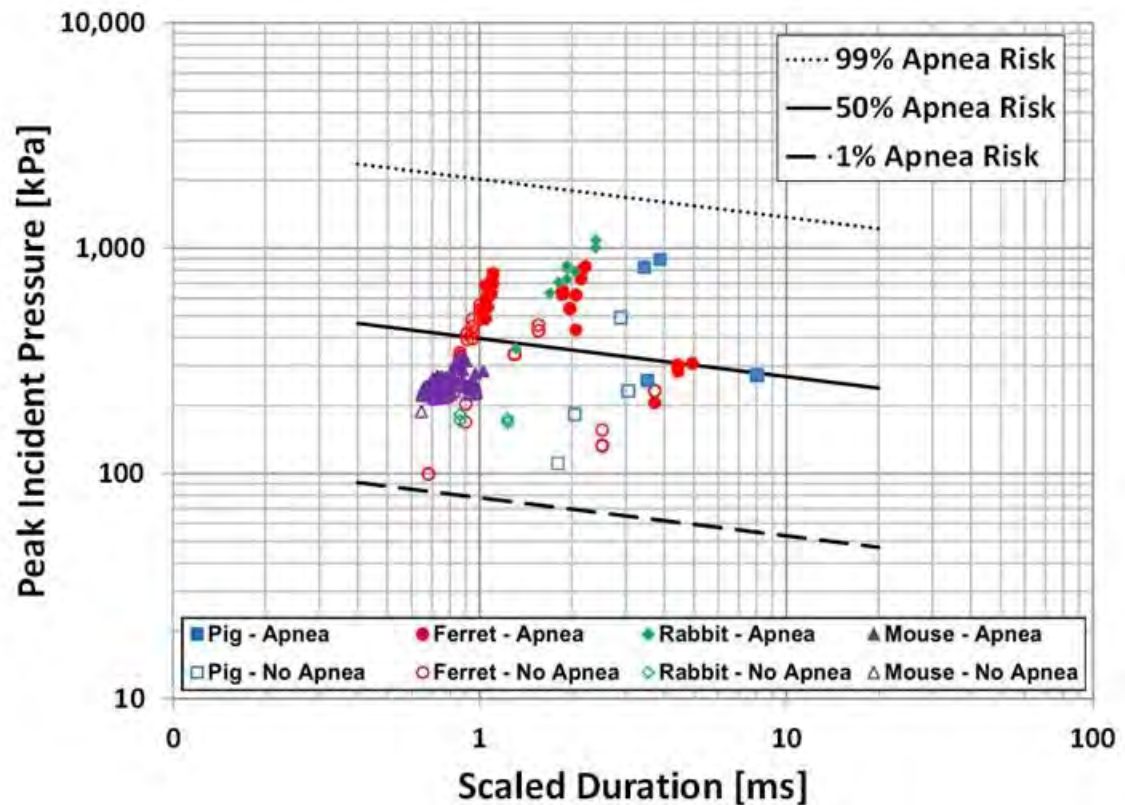
Figure 7-1: Unscaled experimental apnea data shows no clear interspecies delineation resulting in poor apnea risk models.

After scaling is employed for the different methods (Figure 7-2, Figure 7-3, Figure 7-4), the apnea outcome data become organized and overpressure duration dependence is seen in the injury risk models. The effect of scaling is to increase the human equivalent overpressure duration and the effects are greatest for the smallest animal models. The optimized scaling exponent was found to be 0.336 and is shown in Figure 7-5 which is comparable to the pulmonary scaling value.
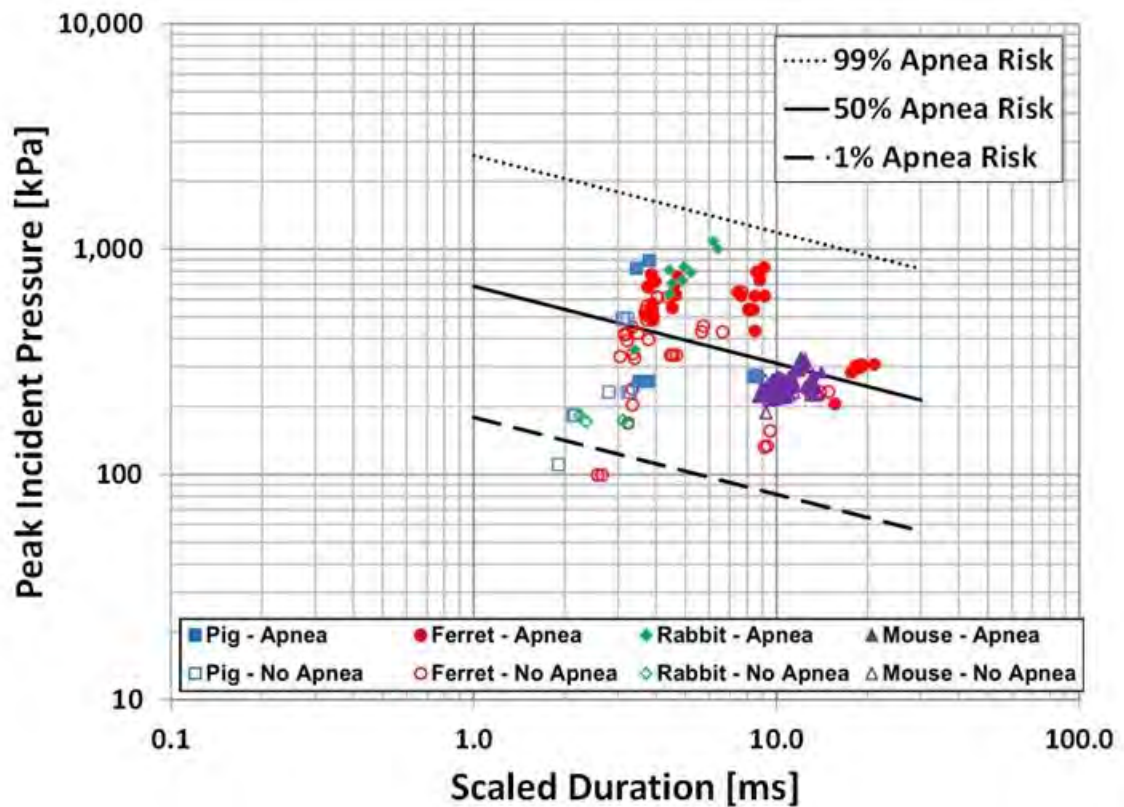
Figure 7-2: Scaling experimental apnea data according to blast pulmonary scaling model shifts the data to larger overpressure durations.
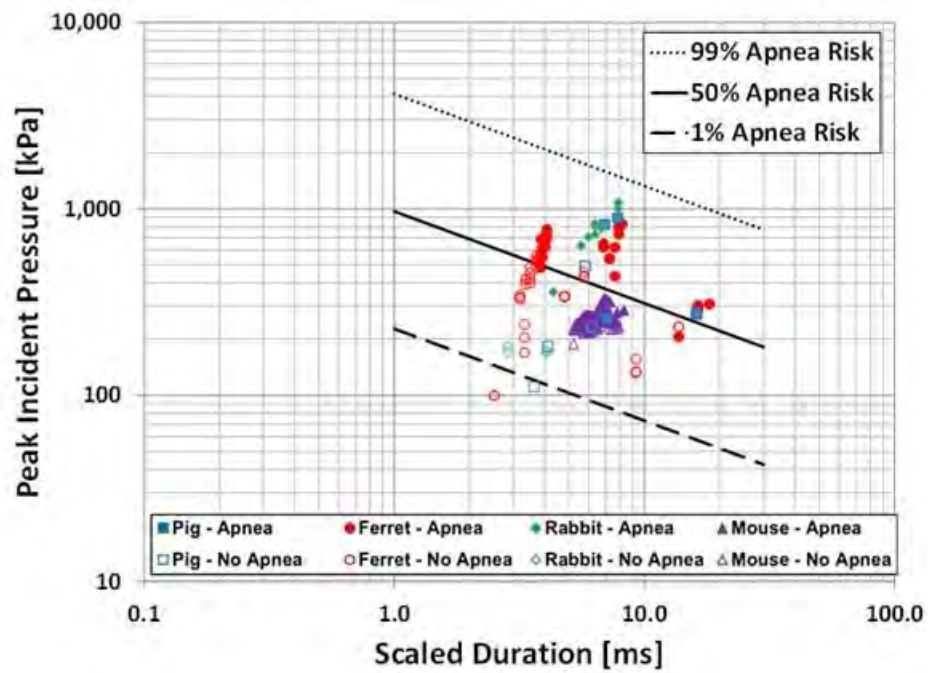
Figure 7-3: Computational scaled data with apnea injury risk models.
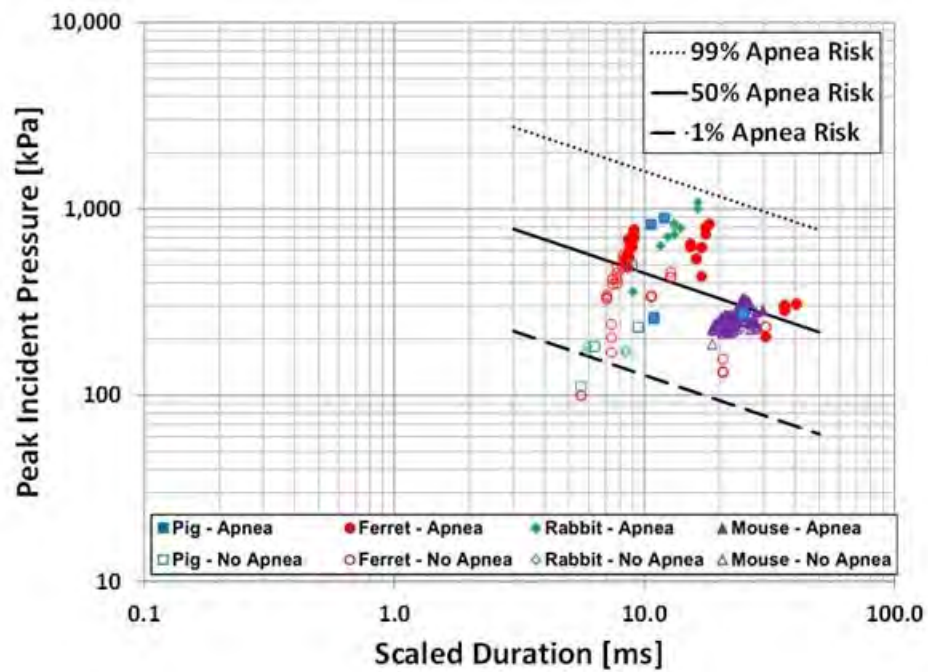
Figure 7-4: Physiological scaled data with apnea injury risk models.

174
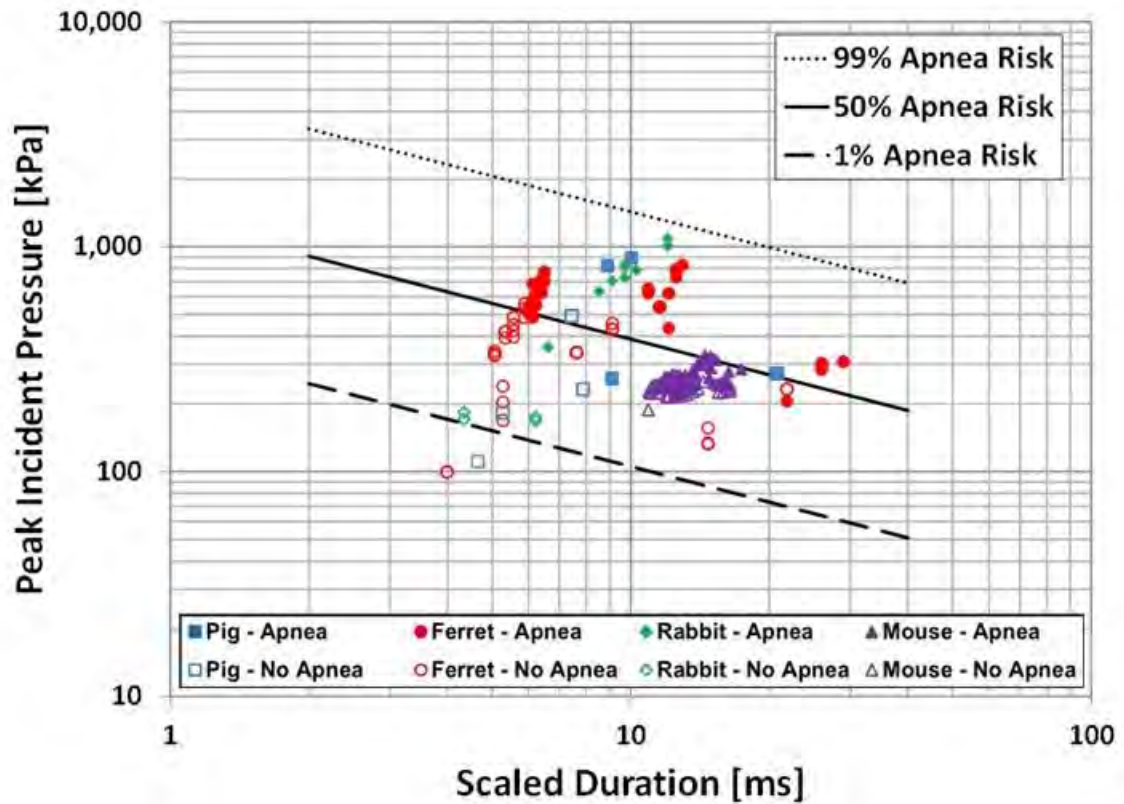
Figure 7-5: Scaling experimental apnea data according to an optimized scaling model (α = 0.336) shifts the data to larger overpressure durations and results in clearer delineation between apnea and no apnea occurrence.

The resulting apnea risk curves demonstrate that the choice of scaling procedure

can have large effects within the range of realistic exposure as seen in Figure 7-6. The

realistic exposure range was calculated using CONWEP (Hyde 1991) to calculate blast

exposure levels associated with charge sizes ranging from 0.25 to 1000kg of TNT at

various standoff distances. The most common IEDs are composed of one or more

artillery rounds, such as the M107 155mm projectile containing a 7.5kg TNT equivalent

charge. At a constant overpressure duration of 2ms the 50% apnea risk occurs at peak

overpressures of approximately 900kPa for the physiological and optimized scaling

models, 700kPa for the computational model and 550kPa for the pulmonary scaling

method. At a constant overpressure duration of 20ms the 50% apnea risk occurs at peak

overpressures of approximately 330kPa for the physiological scaling, 270kPa for

optimized, 260kPa for pulmonary and 220kPa for the computational scaling method.

Likewise, at a constant peak overpressure of 500kPa the overpressure duration resulting

in 50% apnea risk varies from 3ms for the pulmonary model to 8ms for the physiological

scaling. Comparing the scaling models using the 95% confidence intervals presented in

Figure 7-6, the physiological and optimized scaling models separate from the

computational and pulmonary models. At larger durations however, the models are

more tightly grouped with physiological scaling separate from the other three models

whose confidence intervals overlap.
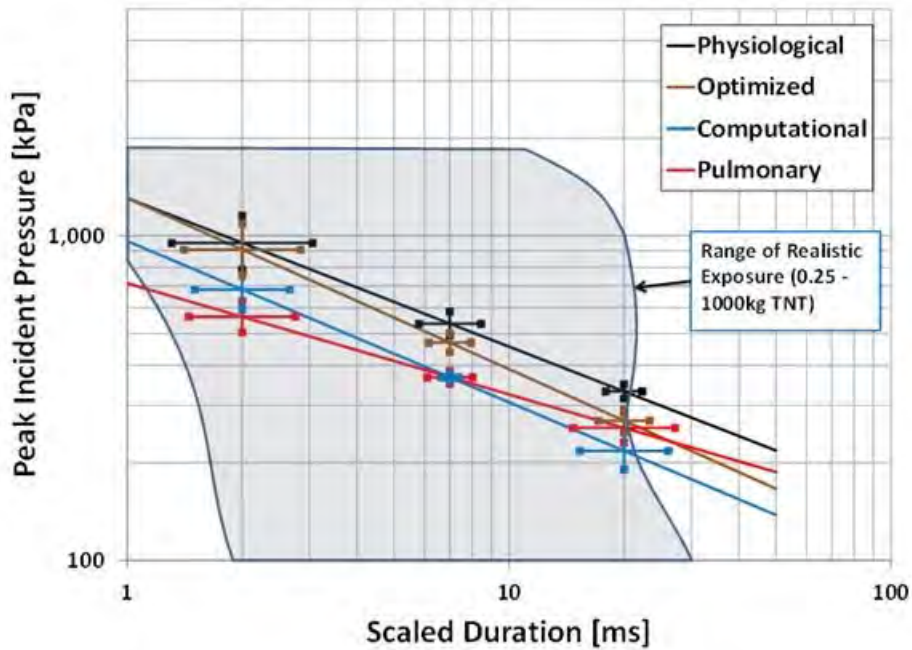
Figure 7-6: 50% apnea risk curves with 95% confidence intervals vary significantly within a realistic human exposure range.

Physiological scaling (Figure 7-4) shifted the experimental data furthest to the right of the plot as the higher scaling exponent results in higher scaled durations, especially for the small animal models. The result of using each scaling law for apnea risk is presented in Table 7-1.

Table 7-1: Apnea risk scaling model scale factors vary from approximately 1 for pulmonary scaling in pigs up to 29 for physiological scaling in mice.

	$\Delta t_{scaled} = \lambda \Delta t$			
Species	$\lambda_{Pulmonary}$	$\lambda_{Computational}$	$\lambda_{Physiological}$	$\lambda_{Optimized}$
Human	1	1	1	1
Pig	1.1	2.0	3.1	2.6
Rabbit	2.6	3.3	6.8	5.0
Ferret	3.9	3.7	8.2	5.9
Mouse	13.7	8.1	29	17

Apnea risk model coefficients and model fit statistics are presented in Table 7-2. All model coefficients were significant on a 0.01 level except for the overpressure duration coefficient for the unscaled data model fit, which was significant on a 0.05 level. The area under the ROC curve was similar for all scaling models. Values of area under the ROC curve greater than 0.8 indicate excellent discrimination by the model. Generalized R2 indicates that the optimized scaling model explains the greatest proportion of variability within the data.

Table 7-2: Apnea risk model coefficients and fit statistics.

Model	β_0	p	β_1	p	β_2	P	- Log- Likelihood	Area Under ROC Curve	Generalized R^2
	Regression Coefficients						**Model Fit Statistics**		
Unscaled	16.9	<0.01	-6.5	<0.01	-1.1	0.028	124.3	0.86	0.472
Pulmonary	22.4	<0.01	-7.9	<0.01	-2.7	0.001	119.6	0.85	0.502
Computational	21.8	<0.01	-7.3	<0.01	-3.6	<0.01	117.4	0.88	0.516
Physiological	26.1	<0.01	-8.4	<0.01	-3.8	<0.01	116.6	0.85	0.521
Optimized	25.2	<0.01	-8.1	<0.01	-4.3	<0.01	115.6	0.85	0.527

7.4 Discussion

This study is the first to empirically derive a blast neurotrauma scaling model for blast neurotrauma endpoint between common animal model species. These results show that the choice of scaling parameters influences the estimated human equivalent response. Scaling is needed to provide realistic input that replicates human biomechanical exposure and also to compare human and animal model endpoints. As expected, scaling effects were much larger for the smaller species due to the vast differences in body and brain mass between the animal model and humans. However, currently this model does not include species with brain size equivalent or larger than humans and therefore scaling to human levels is an extrapolation. As the use of blast neurotrauma models increases, the importance of employing proper scaling techniques during experimental design grows.

Comparing the 50% apnea risk functions between the different scaling exponents, a larger peak pressure is required for injury when using the physiological and optimized scaling factors compared to the pulmonary and computational scaling. At 2ms scaled overpressure duration the 50% apnea risk pressure value is 69% higher for the physiological scaling than the pulmonary scaling, 563 to 952kPa, respectively. At 20ms there is a similar increase of 52% from computational to physiological scaling, 218 to 332kPa, respectively. There is a potential that blast neurotrauma scaling is more

prominent than blast pulmonary scaling (Table 7-1), therefore making consideration of

scaling more important for blast TBI research.

There are many advantages which have made rodents the most popular animal

models in blast neurotrauma research (e.g. expense, size, genetic knockouts). The

majority of rodent blast models use shock tubes to introduce a primary blast with

durations between 4 and 10ms (Saljo et al. 2010, Bolander et al. 2011, Cernak et al. 2011,

Leonardi et al. 2011, Goldstein et al. 2012, VandeVord et al. 2012). Even longer durations

have been used in rodent models in excess of 10ms (Cernak et al. 2001, Pun et al. 2011).

When the optimized apnea scaling from this study is implemented, these rodent models

correspond to scaled durations close to and exceeding 100ms. Overpressure durations

of this magnitude are difficult to achieve without the use of nuclear weapons and are

therefore of little interest in current neurotrauma research. The apnea outcome data

used in this study are presented with scaled representative rodent neurotrauma

conditions from literature in Figure 7-7.
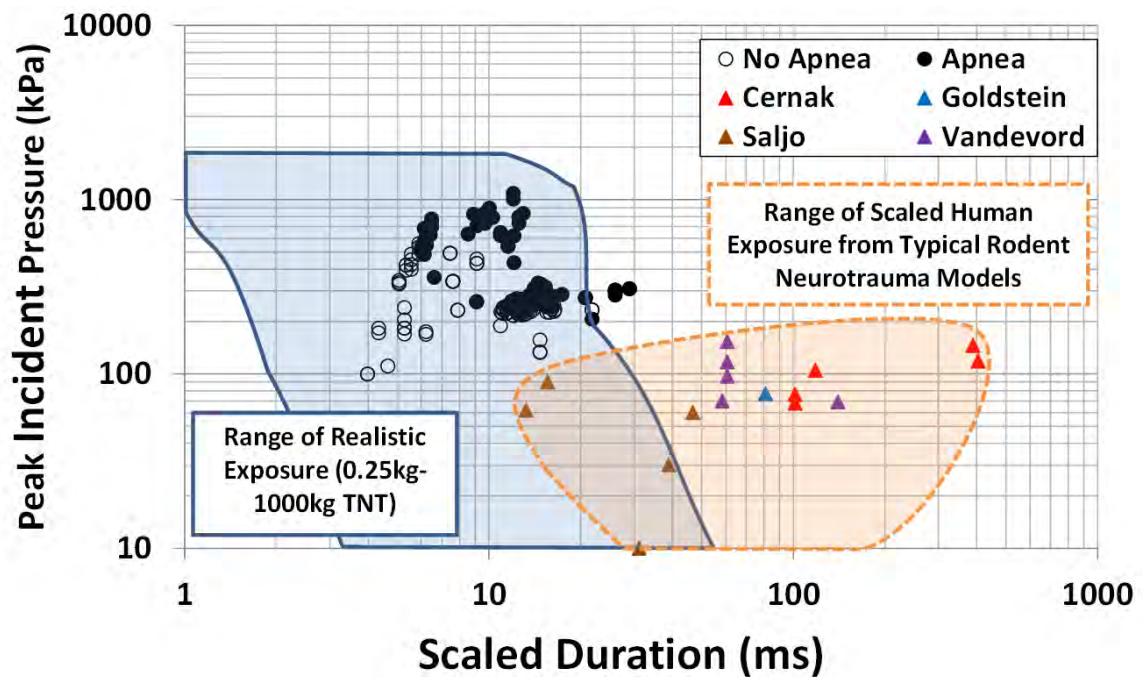
Figure 7-7: Most scaled rodent neurotrauma test conditions fall outside of a range of realistic exposure (Cernak et al. 2001, Cernak et al. 2011, Goldstein et al. 2012, Saljo et al. 2000, Saljo et al. 2010, Bolander et al. 2011, Leonardi et al. 2011, VandeVord et al. 2012).

The range of realistic exposure presented corresponds to charge sizes ranging

from 0.25 to 1000kg of TNT at varied standoff distances. As shown, the bulk of test

conditions in literature greatly exceed the maximum overpressure duration which have

been encountered in most combat casualties. Complicating the interpretation of injury

outcomes in these rodent models is the lack of pulmonary protection during blast

exposure, resulting in an uncertain contribution to injury or fatality endpoints. Some

studies mount the test animal within the shock tube on metal structures leading to

pressure reflections and likely resulting in a more severe exposure (Saljo et al. 2000,

Chavko et al. 2011). Also, some studies subject animals to pressure waves which

plateau, therefore having a larger impulse for a given peak pressure and overpressure

duration (Cernak et al. 2011)(28). It is also important to note that this range estimation is

likely conservative as a majority of improvised explosive device (IED) threats are made

up of artillery rounds equivalent to 7.5kg of TNT explosives or less (Hyde 1991).

The overall implication of large, scaled durations used in literature is that in

some cases researchers are likely testing well outside the realm of likely human

exposures. Scaled durations greater than 100ms are characteristic of nuclear rather than

conventional high explosives (Glasstone 1964) and are therefore of limited interest in

blast neurotrauma research. Compounding the problem is that for scaled durations that

are orders of magnitude higher than normal exposure, there is a risk of changing the

injury mechanism. For example, for pulmonary blast, injury mechanisms change from

short overpressure duration to long overpressure duration (Bass et al. 2008). For large

overpressure duration and impulse, injuries more likely stem from acceleration-based

mechanisms than primary blast injuries associated with the transmission of a blast wave

through the tissue (Panzer et al. 2012b). At extremely long durations, enough

momentum is transferred by the blast wave to cause large accelerations and

displacements of the head and skull which are not seen at short durations (<10ms

scaled), much like the change in injury mechanism seen with pulmonary blast injury.

Pulmonary injury from short durations is associated with localized, spalling-type injury

while long overpressure duration injury is associated with more diffuse crushing-type injuries (Bass et al. 2008).

This study is limited primarily by the range of species included. Ideally, more large animal species should be used, including species larger than human as scaling to human levels with the current model is an extrapolation. However, this is the largest range of scale to date for apnea risk assessment and additionally gyrencephalic (convoluted brain) and lissencephalic (smooth brain) species are included. Additional data are needed to validate the scaling model presented. Due to the large differences in structural anthropometry and pathophysiology between species, it is currently unknown if a unifying scaling procedure across all species is appropriate. For example, large differences in skull thickness and stiffness between model species may contribute to the variable injury tolerance to blast exposure by affecting brain strain levels close to the skull. The relatively thin and flexible rodent skull may account for some differences in blast neurotrauma threshold when compared to thick skulls in pigs. The apnea risk model is sensitive to the removal any of the four species represented, especially to mice. Determination of whether multiple scaling methods are necessary for a single injury endpoint like apnea requires a larger set of test species.

Ideally, histological examination of brain tissue post-euthanasia for indications of injury due to transient hypoxemia would be included to support apnea as a contributor to blast neurotrauma. However, this is not possible for the included studies due to

immediate mechanical and chemical intervention post-blast. While type and depth of anesthesia may have some effect on immediate blast apnea response, this is not known for the studies included in this analysis. However, protocol was consistent within species and comparable methods were used across studies to determine and maintain anesthesia depth.

Blast animal model work has provided strong evidence that blast traumatic brain injury tolerance is dependent upon differences in body and brain size (Rafaels et al. 2011, Rafaels et al. 2012, Shridharani et al. 2012b, Yu et al. 2012). This study presents a risk model for apnea as a surrogate for the clinical presentation of blast neurotrauma. It also has derived the first empirical scaling for primary blast brain injury across animal species commonly used for blast brain research. Implications of this study are that many current studies are investigating blast doses well outside the realm of clinical interest. According to the derived apnea scaling of this study, unscaled blast test durations should be limited to approximately 1ms for mice, 3ms for rabbits and ferrets, and 6ms for pigs. Scaling provides realistic model inputs and the ability to scale for different injury endpoints or experimental outcomes. These findings emphasize that the choice of scaling method matters in the blast domain of interest and care must be taken to consider scaling during experimental design.

Chapter 8 - Blast Neurotrauma Scaling

The focus of blast injury research has shifted to neurotrauma over the last 15 years (e.g. Rafaels et al. 2012). Motivated by the large increase in observation of closed-head trauma resulting from blast, extensive in vivo animal model research has been conducted. The effects of interspecies differences on blast neurotrauma tolerance are not well understood, but differences in interspecies responses have been confirmed through experimental work (e.g. Panzer et al. 2012b). This chapter investigates fatality risk from primary blast isolated the head in in vivo animal models. Also discussed are some of the significant challenges when comparing experimental results across studies.

8.1 Introduction

Prolonged low-intensity warfare in recent conflicts has led to a change in the types and numbers of casualties seen. In recent multinational military operations in Operation Enduring Freedom (OEF) and Operation Iraqi Freedom (OIF), injuries to military personnel have been dominated by those associated with blast, especially from improvised explosive devices (IEDs) (Taber et al. 2006). Estimates from clinical presentation and surveys suggest that approximately 320,000 of the 1.6 million (19%) U.S. OEF/OIF veterans have some form of traumatic brain injury (TBI) (Tanielian et al. 2008). However, TBI from explosive events is not solely a military concern. From 2001 to 2011 over 3,000 civlian blast-related fatalities and a much larger number of injuries were reported in Iraq and Afghanistan along with another 575 from a select few major

terrorist attacks across the world (Bass et al. 2012). This has motivated an intense

research effort to understand the effects of blast to the head, especially those associated

with the blast wave only, or primary blast. This is a change of focus from the more

extensive body of blast pulmonary trauma research (Bowen et al. 1968, Richmond et al.

1968) and has resulted in a range of methodologies.

8.1.1 Scaling

Extensive blast research has been conducted using human surrogates, such as

specially designed anthropomorphic testing devices (Shridharani et al. 2012a, Ganpule

et al. 2013) and computational models (e.g. Moss 2009, Panzer et al. 2012a, Panzer 2012).

The information that can be gained from these testing models is limited, and in vivo

models are necessary to measure physiological, cognitive, and other responses to injury.

This is especially important in blast neurotrauma which may have a dependence upon

injury and immune cascades occurring in a living model. A wide range of in vivo

animal model species have been used to study blast effects with the most common being

mouse (Richmond et al. 1962, Goldstein et al. 2012, Yu et al. 2012), Rat (Long et al. 2009,

Svetlov et al. 2010, Garman et al. 2011), Rabbit (Krohn et al. 1941, Rafaels et al. 2011),

Ferret (Rafaels et al. 2012), and Pig (Saljo et al. 2008, de Lanerolle et al. 2011, Shridharani

et al. 2012b). Substantial differences between these species include body size, brain size,

morphology, and physiological measures. These differences produce different

responses to blast trauma (e.g. White et al. 1971) across species. For example, for long

overpressure duration pulmonary blast 50% 24-hour fatality risk ranges from 26 to 55psi

in mice and pigs, respectively. Even more extreme differences have been measured for

50% 24-hour fatality risk at 1ms overpressure duration, varying from 39 to

approximately 400psi in mice and pigs, respectively (White et al. 1971). To account for

these large differences, scaling is necessary to compare animal model results to human

response on a similar biomechanical and physiological basis. Appropriate scaling will

determine the injury input necessary for the same biomechanical or injury response

between an in vivo model and human. Scaling models have been investigated and

developed for blunt TBI (Eppinger 1976) and for blast pulmonary trauma (Bowen et al.

1965) while limited work has been done to understand and develop methodologies for

interspecies blast neurotrauma scaling.

Interspecies scaling has long been recognized as necessary and accordingly work

has been done to develop simple but theoretically plausible and effective scaling rules.

Research areas that have investigated scaling include comparative anatomy (Lindstedt et

al. 1981), animal care (Kleiber et al. 1961, Hofman 1983), and pharmacokinetics research

(Boxenbaum 1982, Mordenti 1985). Some descriptive parameters, when assessed on a

log-log scale, form a linear relationship across a large range of animal size, and this is

referred to as allometry (Equation 1). One common form of allometric scaling is a power

law relationship between a response variable and in intrinsic property of a given

species, often mean body mass. For example, power law scaling relations may be used

to predict the parameter value, X, using body mass and a scaling exponent, α (Equation 8-1). The constant, b, is associated with a subset of species, often applying to a majority mammals. Many of these parameters fall into categories that scale similarly according to body mass; organ size, which scales isometrically ($\alpha = 1$) (Lindstedt and Calder 1981), volume-rate parameters like metabolic rate ($\alpha = 0.75$) (Hofman 1983), and cycle lengths and frequencies such as heartbeat time, respiratory time, and life span ($\alpha = 0.25$) (Lindstedt and Calder 1981, Boxenbaum 1982). This cycle length scaling is often referred to as physiological time since it describes a base unit of time for each species. The implication is that each heartbeat or breath is approximately the same percentage of lifetime for mammals (Boxenbaum 1982).

$$X = bMass_{body}^{\alpha}$$
<div align="right">Equation 8-1</div>

The need for interspecies scaling in blast research was recognized by Bowen and colleagues during their extensive research on pulmonary blast tolerance (Bowen et al. 1965). While conducting blast tests with a wide range of species they noticed a large difference in lung injury tolerance, loosely related to species mass. This motivated the development of a scaling model using dimensional analysis to relate lung pressure between difference animal model species using a lumped-mass thoracic model (Bowen et al. 1965). The resulting scaling model, shown in Equation 8-2, used a ratio of human reference body mass to the subject body mass and a scaling exponent.

$$\Delta t_{scaled} = \lambda \Delta t \quad where \quad \lambda = \left(\frac{Reference\ Mass}{Mass}\right)^{\alpha}$$
<div align="right">Equation 8-2</div>

This model scales the overpressure duration of the blast wave input, where the human reference mass is 70kg and the scaling exponent, α, is equal to 1/3. This scaling produces an increased value of scaled overpressure duration for species smaller than humans in body size. Essentially, the overpressure duration is scaled by a characteristic length of the animal assuming a spherical body shape. Interestingly, scaling later developed for blunt impact scaling in automotive injury research had the same form (Eppinger 1976).

Recently, severeal studies focused on blast neurotrauma scaling. Panzer (Panzer 2012) used finite element (FE) analysis to study differences in biomechanical response across species using simplified, spherical head models over a range of mouse to human sizes. These models were subjected to a range of peak pressure and overpressure duration while measuring the mechanical response of the brain. The resulting model response was used to develop a scaling model for the blast wave input to match biomechanical behavior across brain sizes. They found the peak intracranial pressure was relatively insensitive to model size and the global strain response was sensitive to overpressure duration and the size of the model head. This led to a scaling model of the same form as that developed by Bowen (Equation 2), but with a different power-law coefficient. Panzer's model used the ratio of a human reference brain mass to the brain mass of the test subject with a scaling exponent, α, of 0.248 (Panzer 2012). Scaling effects of peak pressure were found to be negligible in this study since the global peak pressure is not sensitive to the head size.

8.1.2 Blast Injury Risk Models

Early blast injury risk models were developed by Bowen and colleagues (Bowen et al. 1968). Bowen's scaling procedure was later validated using almost 2000 animal tests ranging from small rodents to cattle (Bowen et al. 1968). These pulmonary injury risk curves are commonly referred to as the "Bowen Curves" (Bowen et al. 1965) and have been used extensively for prediction of injury and fatality from blast. This risk model was of a nonlinear log-log form with a change in behavior from short to long durations. For short durations (<10ms) the risk of injury is dependent upon peak pressure and overpressure duration, with an increase in either metric resulting in increased risk of injury. For long durations (> 30ms) the injury risk is dependent only on the peak pressure. Bowen noticed a difference in pulmonary risk between two sets of species that he termed "small" and "large". Large animal species were those exceeding 15kg in body mass or those of high phylogenetic order (Bowen et al. 1968). This difference in injury risk behavior is thought to be due to the lower normalized lung density in small animal species making them more susceptible to blast pulmonary injury while the effects of phylogenetic order are unknown (White et al. 1971). This led to the development of separate small and large animal risk models.

Bowen's curves were later updated with a larger set of large animal data resulting in a similar pressure and overpressure duration dependence on injury risk. This analysis considered short (Bass et al. 2008) and long overpressure duration (Rafaels

191

et al. 2010) separately, with the same non-linear form. A cubed-root of body mass

scaling was assumed for interspecies differences in these studies. The combination of

these two injury risk curves results in a model comparable to that of Bowen, over the

total range of durations.

Recently, further work has investigated the risk of pulmonary injury to single

blast events and repeated blast in large animals (Panzer et al. 2012c). This study

combined long and short overpressure duration data into a piece-wise linear model.

The breakpoint in the model was found to be near 10ms and represents the transition

from a region of duration dependence to a long overpressure duration region where

injury risk is dependent only upon peak pressure. The injury risk model for single blast

exposure was similar to those previously published (Bowen et al. 1968, Bass et al. 2008,

Rafaels et al. 2010).

Existing data to develop scaling injury risk curves for isolated blast neurotrauma

are limited. In contrast with pulmonary blast, available test data across multiple test

conditions and species, necessary for development of injury risk curves, is lacking.

Single species neurotrauma models have been developed using in vivo ferret apnea and

brain bleeding endpoints (Rafaels et al. 2012). This study investigated graded bleeding

and found that moderate to severe brain bleeds were overpressure duration and peak

pressure dependent over the range tested. However, bleeding categorized as mild was

found to be dependent on peak pressure only and was seen at levels comparable to the

onset of pulmonary injury (Rafaels et al. 2012). Fatality results in ferrets (Rafaels et al. 2012) were combined with fatality data from rabbits (Rafaels et al. 2011) to develop risk curves for fatality from blast neurotrauma. Scaling was assumed to follow that of pulmonary injury risk.

The body of isolated blast neurotrauma literature is limited due to many challenges in using the in vivo results for direct comparison of injury endpoints. These challenges include inappropriate methodology (Wang et al. 2010, Koliatsos et al. 2011, Arun et al. 2012) or comorbid pulmonary and gut trauma in animals without sufficient protection of the thorax and abdomen (Kato et al. 2007, Cernak et al. 2011, Dalle Lucca et al. 2012). The limited number of existing in vivo isolated blast neurotrauma studies is also due in part to the relatively recent focus on blast neurotrauma.

8.2 Methods

Data was taken from an extensive database of blast animal model research. This database contains over 100 separate blast trauma studies with over 12,000 in vivo animal model tests representing 14 different species. This study aimed to investigate fatality risk and interspecies scaling for blast trauma isolated to the head. For inclusion in this analysis subjects were required to have received thoracic protection sufficient to prevent comorbid pulmonary and gut trauma. The blast dose must must be approximately a simple Friedlander type blast wave characterized by peak pressure and overpressure duration. Studies with complex blast wave dosage, most commonly from multiple wave

reflections, were excluded due to the increased impulse and difficulty in simply characterizing the input. Sufficient description of the blast wave input was required in the form of peak pressure and overpressure duration. Alternatively, for free-field explosives tests, studies were accepted where they had sufficient detail to estimate the blast input. Recreation of free-field explosives tests was conducted using the Conventional Weapons Database (CONWEP) (Hyde et al. 1991) to calculate peak overpressure and overpressure duration values at a known standoff distance from a specified explosive charge. Blast injury risk has been shown to be a multiparameter problem and cannot be sufficiently described using peak pressure alone.

Additionally, a description of pressure wave measurement technique was required to determine if reported pressure parameters were to be considered incident or reflected measures. Method of overpressure method can have a large effect on pressure magnitude reported, with reflected measurements up to 8 times larger than incident measurement for the same overpressure wave, when assuming ideal gas (Iremonger 1997, Chapter 2.1.1). Finally, data used for this study was limited to those studies using a single blast dose or cases where multiple blast doses at a single level did not result in an injury.

A subset of 189 in vivo tests from six different studies qualified for this analysis. These studies represent five different species; mouse (Goldstein et al. 2012, Yu et al. 2012), Rat (Garman et al. 2011), Rabbit (Rafaels et al. 2011), Ferret (Rafaels et al. 2012),

and pig (Shridharani et al. 2012). These tests were conducted using gas-driven shock

tubes with a pressurized driver section separated from a low pressure driven section by

a frangible membrane. In these tests, the anesthetized animal was placed immediately

outside of the shock tube exit or within the driven section of the shock tube with

sufficient room to avoid confinement effects or reflections from the tube walls. Thoracic

protection was used in testing to ensuring no observable injury in the pulmonary system

or gut. Test subjects were observed for several post blast injury endpoints including

neurotrauma induced apnea, brain bleeding, and histological findings. A description of

the animal characteristics and blast dosage for the studies are included in Table 8-1. A

more detailed presentation of in vivo animal model data used for this analysis is

included in Appendix D of this dissertation.

Table 8-1: Description of data used for neurotrauma fatality risk assessment.

	Mouse	Rat	Rabbit	Ferret	Pig
# of Tests	72	21	12	64	20
Peak Incident Pressure Range[kPa]	77.0-266.7	241.3	168.5-1084.6	97.5-818.5	107.0-741.0
Unscaled Duration Range [ms]	0.7-4.8	4	1.2-2.4	0.7-4.8	1.2-3.4
Body Mass (Ave ± SD)[kg]	0.026±0.004	0.388	4.2±0.6	1.2±0.2	60.7±8.2
Brain Mass [g]	0.3	3	11	7	80

Table 8-2: Interspecies blast neurotrauma scaling models.

$$\Delta t_{scaled} = \lambda \Delta t \qquad \lambda = \left(\frac{Reference\ Mass}{Mass}\right)^{a}$$

Model	Scaling Mass	α
Pulmonary	Body	0.333
Computational	Brain	0.248
Physiological	Body	0.25
Optimized	Brain	---

The blast dose was scaled using four different methods. The simple scaling method followed the form of that previously used for pulmonary injury involving a mass ratio and a scaling exponent, α (Equation 2). The first scaling method used was the traditional pulmonary scaling model developed by Bowen (Bowen et al. 1965), where overpressure duration is scaled by the cubed root of the body mass ratio between the animal and a human reference value. The scaling method developed by Panzer (Panzer 2012) was also used as previously described, and is referred to as computational scaling. This method also scaled the overpressure duration but is dependent upon the ratio of brain masses between the model species and a human reference. The third method of scaling uses differences in physiology between the animal model species and humans (cf. Lindstedt et al. 1981, Boxenbaum et al. 1982). This scaling is dependent upon a body mass ratio and assumes that injury risk is dependent upon the relationship between the time scale of the blast input and the time scale of physiological processes within the animal. Finally, a scaling model was optimized based on the dataset investigated in this study. This scaling assumed that injury risk can be described by a brain mass ratio. Scaling of both peak pressure and overpressure duration will be considered. Brain masses for individual test animals are rarely reported so a constant estimated brain mass was used for each species. Information on each of these scaling models is presented in Table 8-2.

Following the application of the scaling models to the data, fatality risk functions were fit using a logistic regression with a log-linear dose-response to fatality outcome. The log likelihood of the model was minimized to provide a cost function. The model is dependent upon peak pressure and overpressure duration of the blast input and follows Equation 8-3.

$$ln\left[\frac{Pr(fatality|P_i)}{1-Pr(fatality|P_i)}\right] = \beta_0 + \beta_1 log_{10}(Peak\ Pressure) + \beta_2 log_{10}(\Delta t)$$

Equation 8-3

This model predicts the probability of fatality using the peak pressure and overpressure duration input, where β_0, β_1, and β_2 are model constants. The optimized scaling risk model was fit by simultaneously optimizing for the scaling exponents, α, and the dose-response model coefficients. 1%, 50%, and 99% fatality risk lines were developed for each of the scaling models.

Model fits and statistics were conducted using JMP (JMP Pro 11, SAS Institute Inc., Cary, NC). Goodness-of-fit was assessed using two metrics. The area under the receiver operating characteristic curve (AUC) was used to measure sensitivity versus 1 – specificity of the model fit. The Hosmer-Lemeshow (H-L) statistic was used to test for exclusion of a model fit (α = 0.05).

Blast neurotrauma fatality risk models and common literature blast conditions were compared to a realistic exposure range. This realistic exposure range was created using CONWEP (Hyde 1991) to calculate the expected blast dosage levels at various standoff distances from a wide range of explosive charges. Charges ranging from 0.25 to

1000kg of TNT equivalent represent small IEDs up to vehicle borne weapons and aerial bombs. This range is intended to represent a conservative estimate of blast exposure levels seen in current combat scenarios.

8.3 Results

Figure 8-1 presents the unscaled fatality data for blast neurotrauma separated by species. It is clear from the graph that, without interspecies scaling, the unscaled data lacks organization that would provide a clear separation of survival and fatality cases across species. Within data from single species there is an increase in injury risk associated with increased peak overpressure and overpressure duration. Therefore, in combined datasets the same behavior is expected, if scaled properly. There is also a difference in fatality risk behavior across the species size, for example there are many survival data points associate with pigs that fall well above instances of fatality in the smaller species.
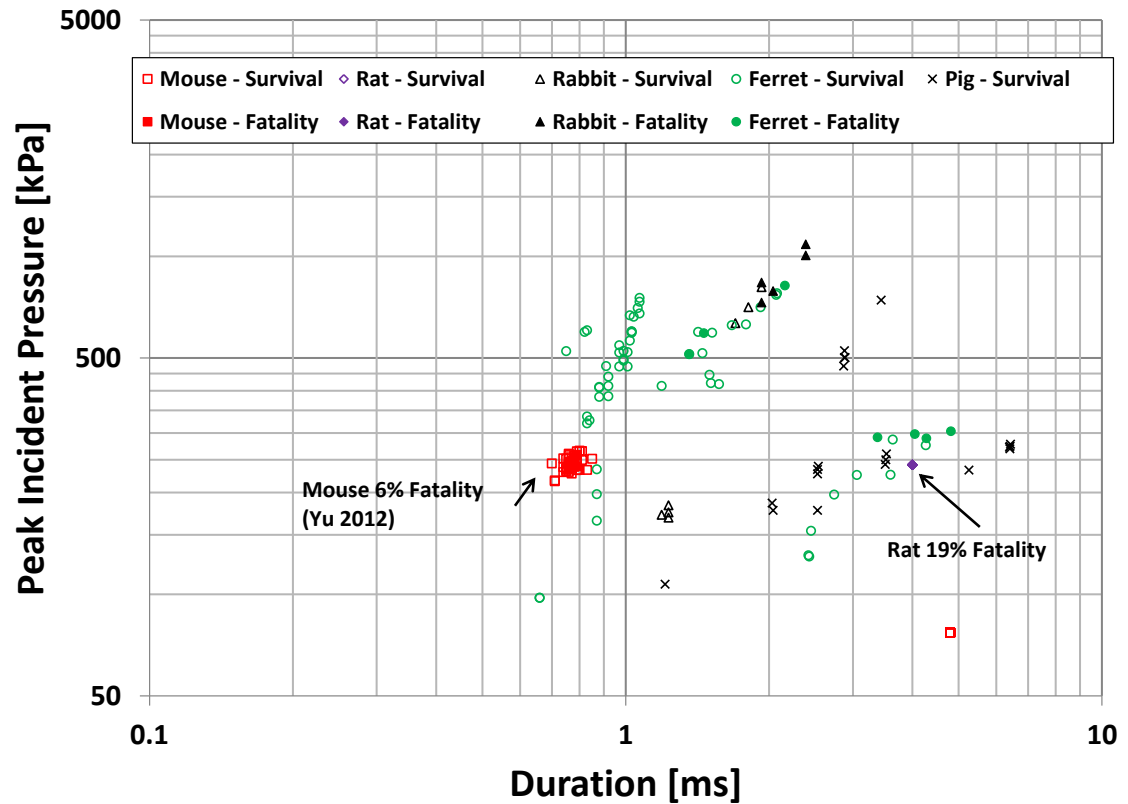
Figure 8-1: Isolated blast neurotruama fatality data does not follow a defined risk behavior dependent upon peak overpressure or overpressure duration.

The scaled fatality outcome data is shown below for each of the four scaling methods incorporated in this study. Each scaling method is presented with 1%, 50%, and 99% fatality risk lines. Since each species included in this study is smaller in body and brain mass than humans, the result of scaling is to shift the data to larger scaled overpressure duration and peak pressure human equivalent values. Pulmonary, computational, and physiological scaling data with resulting fatality risk lines are presented in Figure 8-2, Figure 8-3, and Figure 8-4, respectively.

Peak Incident Pressure [kPa]

10000

1000

100

10

- - - 99% Fatality Risk
— 50% Fatality Risk
······ 1% Fatality Risk

□ Mouse - Survival ◇ Rat - Survival   △ Rabbit - Survival ○ Ferret - Survival × Pig - Survival
■ Mouse - Fatality ◆ Rat - Fatality   ▲ Rabbit - Fatality ● Ferret - Fatality

1   10   100

Scaled Duration [ms]
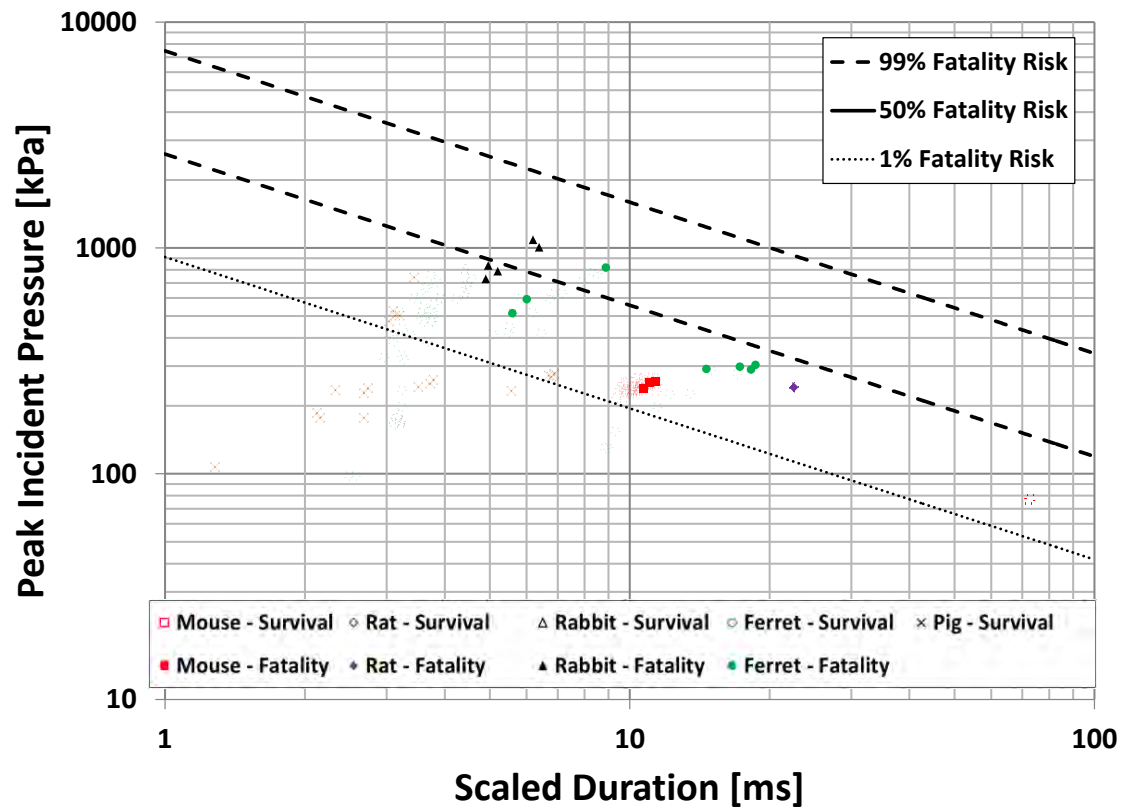
Figure 8-2: Neurotrauma fatality risk model using pulmonary scaling shows good delineation for all species.
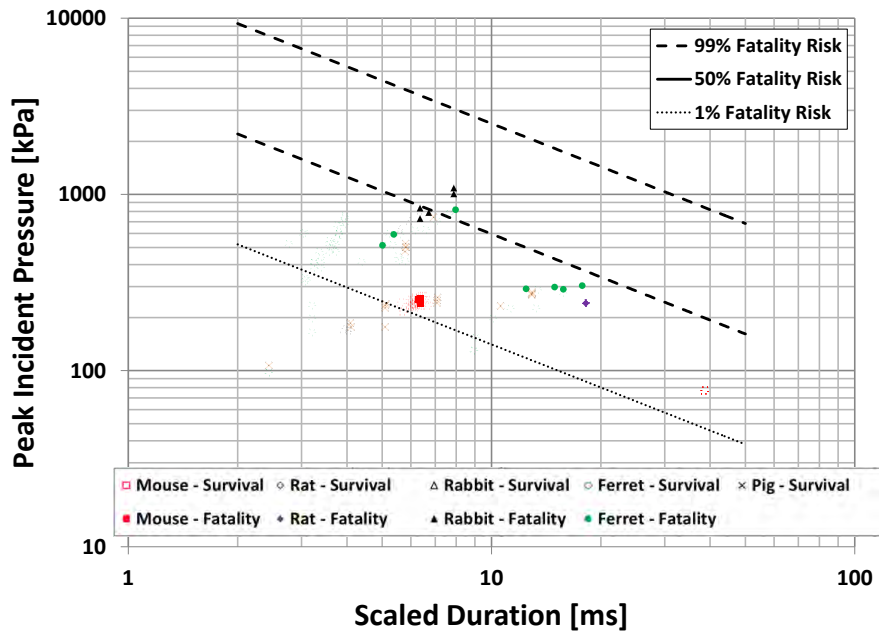
Figure 8-3: Computational scaling neurotrauma fatality risk models show fatality and survival delineation for all species.
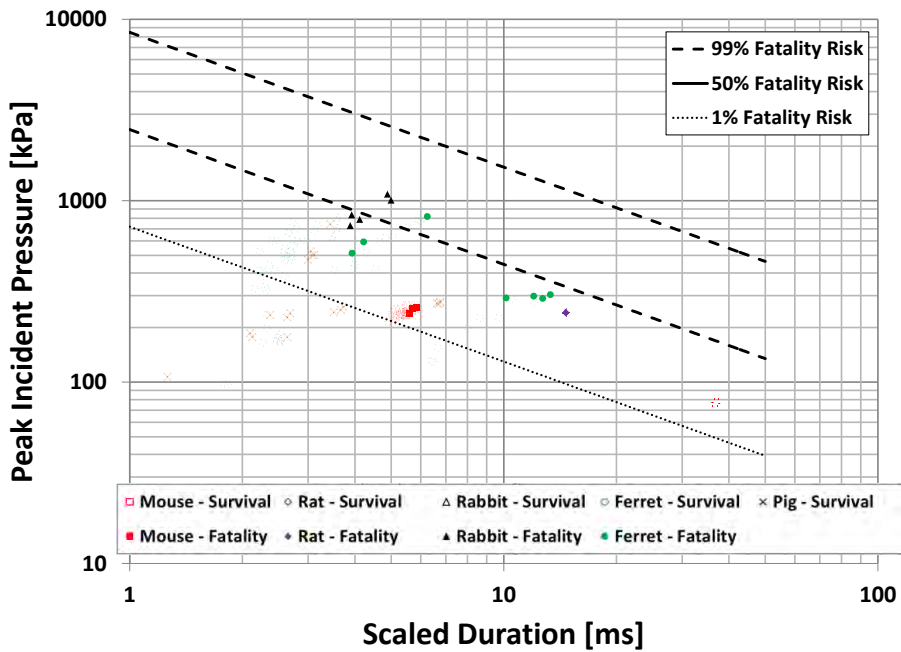
Figure 8-4: Physiological scaling neurotrauma fatality risk models show fatality and survival delineation for all species.

After the scaling relations are implemented, the data becomes more organized

and the overpressure duration and peak pressure dependence of fatality risk becomes

clearer. The overall effect of scaling is to increase the overpressure duration values and

the effect is strongest in the smaller species which differ the most from humans in body

size, brain size, and physiology. Each these three scaling models scale the overpressure

duration only, and to a different degree. This is seen by the range of durations that the

scaled data now covers and effects the range over which these fatality risk models may

be considered valid. The pulmonary scaling results in the largest spread of data over

approximately 1 to 100ms. The physiological data results in coverage of approximately

1 to 50ms, while the smallest range is covered by the computational model from 2 to

50ms.

For the optimized scaling model, peak pressure and overpressure duration

scaling were found to improve the fatality risk model fit. The overpressure duration

scaling was larger with an α of 0.316, while the peak pressure scaling resulted in an α of

0.080. While the peak pressure scaling was small relative to the overpressure duration

scaling, it still serves to shift the animal data to higher levels and therefore the resulting

fatality risk models are at higher peak pressure levels compared to the other three

scaling models. Optimized overpressure duration scaling was comparable to that

biomechanically derived for neurotrauma (Panzer 2012) and that developed for

pulmonary (Bowen et al. 1965). The optimized scaling fatality data and risk models are

presented in Figure 8-5.
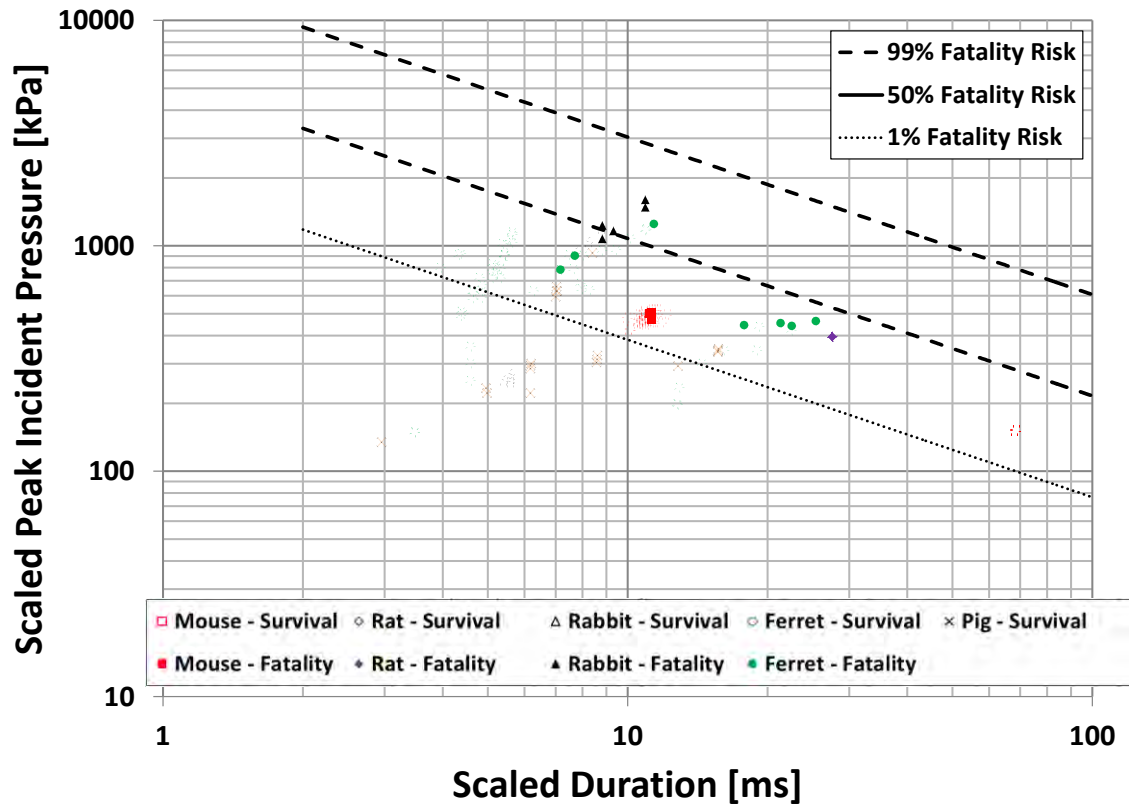
Figure 8-5: Optimized scaling neurotrauma fatality risk models shows fatality and survival delineation for all species.

The resulting fatality risk models show that the choice of scaling procedure can

have large effects on the predicted injury outcome within the range of realistic exposure

in current military settings. The most common IEDs are composed of one or more

artillery rounds such as M107 155mm projectiles which contain a 7.5kg TNT equivalent

charge. This range conservatively represents the realistic charge sizes seen in current

combat and is comparable to those previously reported (Nelson et al. 2008, Panzer et al. 2012a).
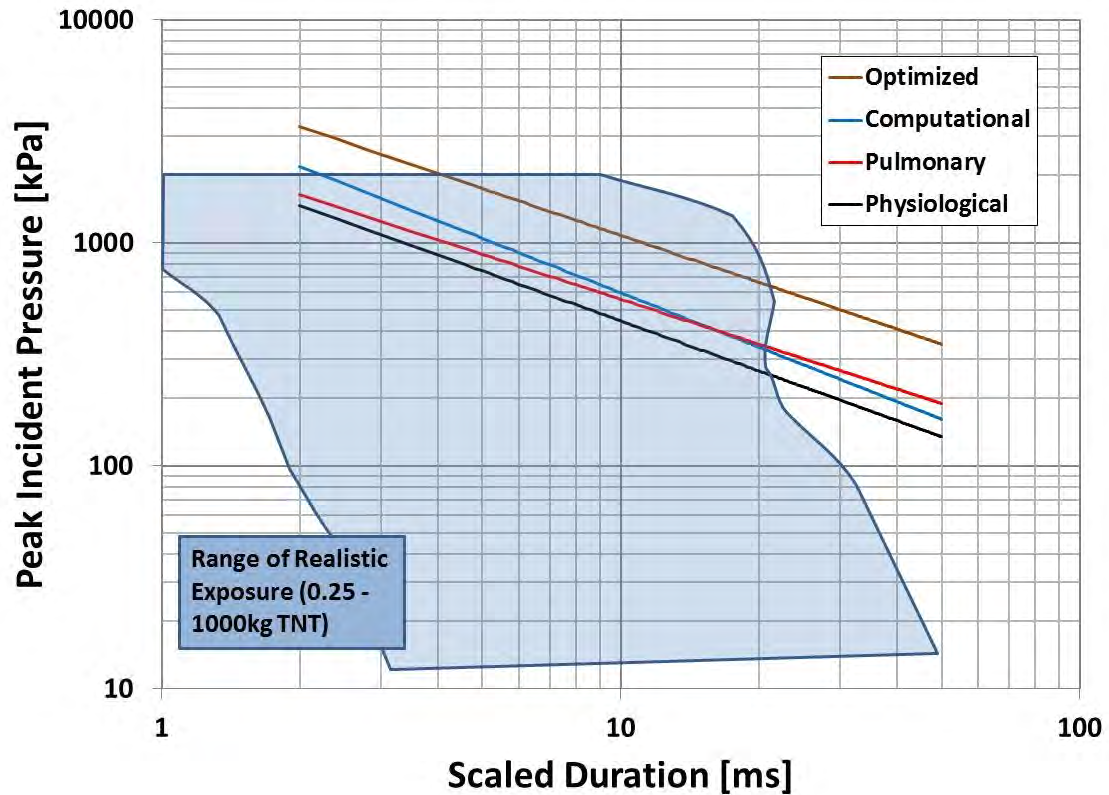
Figure 8-6: 50% fatality risk for four different scaling models vary within a realistic range of blast exposure.

Figure 8-6 shows the 50% fatality risk models for the three existing scaling methods. The optimized scaling model shifts the 50% fatality risk to a higher peak pressure value due to its inclusion of peak pressure scaling. This means that the blast dose necessary for fatality is predicted to be higher in the optimized model than the other three presented. In the range of our current dataset, the physiological scaling results in the lowest pressure threshold for injury while the optimized scaling results in

the highest. If the models are calculated at a constant scaled overpressure duration of

2ms, the 50% risk of fatality varies from 1475kPa in the physiological scaling model up

to 3320kPa in the optimized scaling model developed in this study. Likewise, at a

constant overpressure duration of 30ms, the 50% fatality risk varies from 200kPa to

500kPa in the physiological and optimized models, respectively. In terms of a constant

peak pressure of 500kPa, the scaled overpressure duration necessary for 50% fatality risk

varies from 8.5ms in the physiological model up to 30ms in the optimized model. These

results emphasize the importance of interspecies scaling considerations and

development of neurotrauma specific scaling.

  The computational and optimized scaling models resulted in the largest scaling

effect on the data due to the differences between animal model and human brain mass

being greater than the difference in body mass. The scaling factor, λ, is the factor by

which you would multiply the unscaled blast wave parameter to determine the scaled

human equivalent value. These scaling factors are presented in Table 8-3 for each of the

species and scaling models. These factors remain relatively small for large species like

the pig but can be large for small species like the rodents. For the TBI fatality risk

scaling derived in this study the scaling factors for overpressure duration range from 2.4

to 14.3 in the pig and mouse, respectively. The pressure scaling factors range from 1.3 to

2.0 in the pig and mouse, respectively. The scaling factors can likewise be used to

calculate what blast dosage level is appropriate when designing a test to match a desired

human equivalent exposure.

Table 8-3: Interspecies peak overpressure and overpressure duration scaling factors for human equivalent dose based upon a mass ratio to humans vary from 1.1 for pulmonary scaling in pigs up to 14.3 in optimized scaling for mice.

$X_{scaled} = \lambda X$					
Species	$\lambda_{Pulmonary}$	$\lambda_{Computational}$	$\lambda_{Physiological}$	$\lambda_{Optimized}$ (Δt,P)	
Human	1	1	1	1	1
Pig	1.1	2.0	1.0	2.4	1.3
Rabbit	2.6	3.3	2.0	4.6	1.5
Ferret	3.9	3.7	2.8	5.3	1.5
Rat	5.6	4.5	3.7	6.9	1.6
Mouse	14	8.1	7.2	14.3	2.0

Table 8-4: Blast neurotrauma fatality risk model coefficients and fit statistics.

	Regression Coefficients						Model Fit Statistics		
Model	β_0(SE)	p	β_1(SE)	p	β_2(SE)	P	Area Under ROC Curve	Hosmer-Lemeshow	P
Unscaled	13.4(3.1)	<0.001	-4.1(1.1)	<0.001	-3.0(1.0)	<0.001	0.79	13.2	0.10
Pulmonary	34.4(7.4)	<0.001	-10.1(2.2)	<0.001	-6.7(1.8)	<0.001	0.86	3.4	0.91
Computational	26.2(5.5)	<0.001	-7.3(1.6)	<0.001	-5.9(1.6)	<0.001	0.83	11.1	0.20
Physiological	29.1(6.1)	<0.001	-8.6(1.9)	<0.001	-6.4(1.6)	<0.001	0.85	9.1	0.33
Optimized	38.1(8.1)	<0.001	-10.2(2.2)	<0.001	-7.1(1.8)	<0.001	0.85	11.1	0.20

The blast neurotrauma fatality risk model coefficients and model fit statistics are shown in Table 8-4. All model coefficients were significant on the $\alpha = 0.01$ level. The area under the ROC curve was similar for each of the risk model fits. An AUC > 0.8 indicates excellent discrimination by the model. The H-L goodness-of-fit statistic does not exclude a fit for any of the fatality risk models with all models using interspecies scaling resulting in p > 0.2.

8.4 Discussion

This work is the first study to empirically derive a blast neurotrauma fatality model across a wide range of species size. We know that scaling is important based on differences in fatality risk determined experimentally between mouse (Yu et al. 2012), rabbit (Rafaels et al. 2011), ferret (Rafaels et al. 2012), and pig (Shridharani et al. 2012) models. The peak overpressure and overpressure duration levels at which fatality has been shown to occur in mice, fall well below observed levels at which fatality can occur in ferrets and rabbits. Similarly peak overpressure and overpressure duration levels which are fatal in mice have been observed to fall below the injury threshold for pigs. This study reinforces previous research in showing that interspecies scaling is required to directly compare results from different animal models and draw any resulting conclusions. This scaling has been shown to be especially important in the small rodents which are most commonly used in blast research. With increased blast neurotrauma

research, and the resulting increase in animal model usage, our understanding of interspecies scaling for blast only becomes more important.

Due to the limited range of scaled durations over which the data for this study falls, the resulting fatality risk models are essentially short overpressure duration risk models (<30ms). This is the region that has been shown to be highly dependent upon peak pressure and overpressure duration for both pulmonary and neurotrauma. The scaling exponent for overpressure duration is close to the 1/3 derived previously for pulmonary injury. This 1/3 power of mass is essentially a scaling by length, as mass is assumed to be a measure of volume with constant density. Similar to pulmonary scaling, where the length scaling depends on a characteristic body length of animals of similar body shape, the neurotrauma scaling here depends on a characteristic length of animals of similar brain shape.

Two studies included in this analysis consist of sets of animals tested at approximately the same blast dose level (Garman et al. 2011, Yu et al. 2012). This allows us to look at these specific sets of animals and determine how well the fatality risk model predicts the results of the experiments. For the set of 21 rats tested at 394kPa and 27.6ms scaled the risk model predicts approximately 21% fatality. The actual rate of 19% fatality (Garman et al. 2011) compares well with the model. For the set of 50 mice tested at approximately 478kPa and 11.0ms scaled the model predicts a 5.6% fatality rate. The

tests at this level for mice resulted in an actual fatality rate of 6% (Yu et al. 2012) which

agrees very well with the risk model.

An important consideration for the results of this analysis is how the resulting

fatality risk compares to other blast neurotrauma risk models. In Figure 8-7 the 50%

fatality risk line from this study is compared to previously derived apnea risk

representing four different species (Chapter 7) and graded bleeding lines from in vivo

blast tests on ferrets (Rafaels et al. 2012). As expected, the 50% fatality risk occurs at

higher pressure and overpressure duration values than the survivable injury metrics.

The apnea and moderate/severe bleeding risk show similar peak pressure and

overpressure duration dependence to the fatality risk, occurring at a lower peak

pressure level. The 50% risk of apnea and moderate/severe bleeding risk occur at very

similar levels suggesting that that they could be related outcomes. The mild bleeding

risk line occurs well below the other injury outcomes and is approximately equal to the

pulmonary injury threshold.
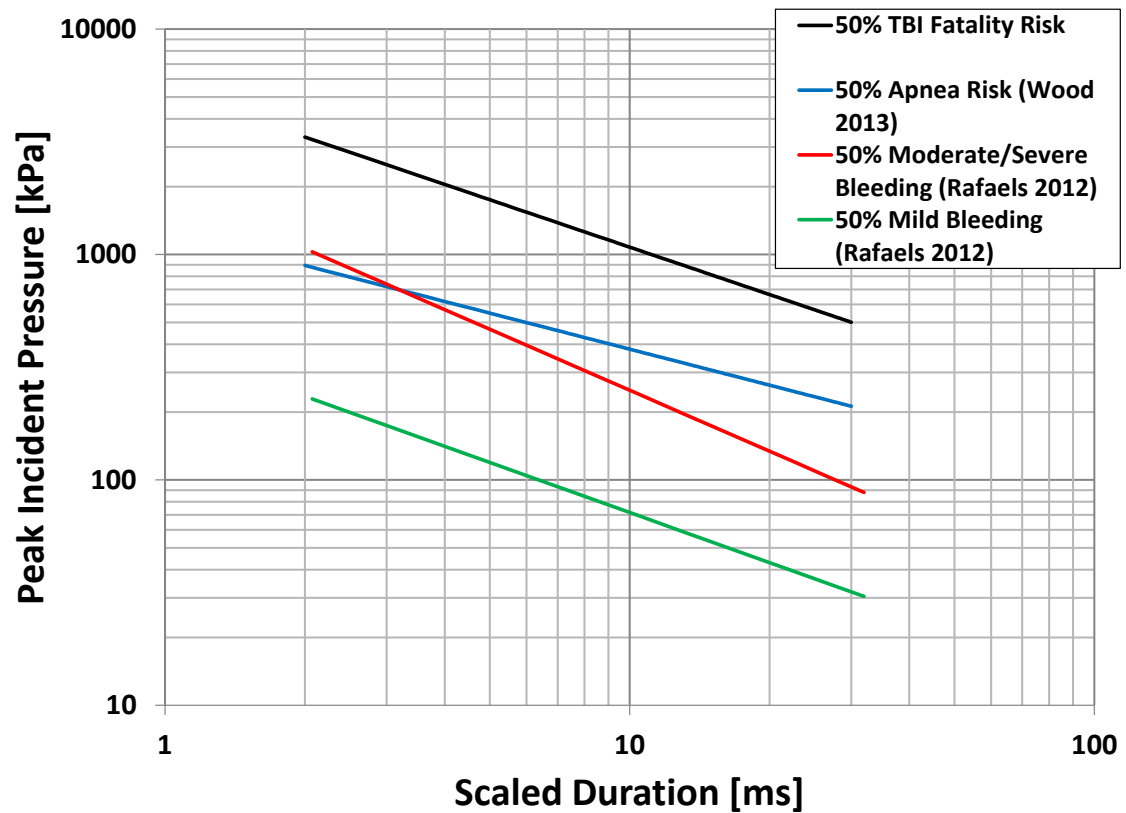
Figure 8-7: 50% TBI fatality risk occurs at higher levels than apnea risk. 50% moderate/severe bleeding and 50% apnea risk occur at similar levels for short durations.

There are many advantages to using smaller animal model species in blast research such as expense, ease of handling, and availability of genetic knockouts. However, these are also the species that have the largest differences both anatomically and physiologically from humans. One major and possibly important difference is cortical folding. In general, mammals of increasing body mass have increasing folding of the cortical surface, referred to as gyrencephaly. Most small mammal species (i.e. mouse, rat, rabbit) have smooth cortical surfaces and are referred to as lissencephalic.

212

The degree of folding is often referred to as a folding index, usually calculated by the ratio of brain surface area compared to surface area assuming a completely smooth contour (Van Dongen 1998). Therefore, lissencephalic animals have a folding index close to 1 while highly gyrencephalic species may have folding indices in excess of 5. Humans have a folding index of approximately 2.8 (Van Dongen 1998). Finite element simulations of head impact have shown brain folding to reduce the measured strain in some regions of the brain (Ho et al. 2009). However, the effect is unknown for primary blast interaction. Perhaps brain folding is analogous to the large vs small animal pulmonary risk differences. The differences in two groups of animal model species in normalized lung volume and density help to describe categorical tolerance differences to blast pulmonary trauma. If a similar case is to be made for blast neurotrauma and cortical surface differences, a much larger set of data is needed to empirically determine these effects. This may be one explanation for the peak overpressure scaling found in this study.

Another source of wide variation across the typical blast animal model species is in skull thickness and morphology. The differences in skull thickness vary to a large degree, from mice with thickness of less than 1mm in some locations up to pigs with frontal and parietal skulls in excess of 12mm thick. This may be a significant contributor to attenuation of primary blast energy before it reaches the brain tissue. Thicker skulls also likely mean less bulk displacement when compared to the very thin skulls in mice.

Differences in the shape and size of the skull will also have an effect on the resonant frequency response as shown to vary from 41 kHz down to 2 kHz in simplified FE head models of mice and humans, respectively (Panzer 2012). The difference in mechanical behavior of the skull may have a significant effect on brain mechanical response near the brain surface, especially in strain magnitude. In fact, skull flexure has been proposed as a possible injury mechanism from primary blast in rodents, but likely at scaled blast levels outside the realm of realistic human exposure (Bolander et al. 2011).

8.4.3 Implications

Assuming the scaling model derived in this study, there are concerns about the blast levels which are most commonly used in the blast neurotrauma field. As evident from the scaling factors presented here, the human equivalent durations are very long, especially in rodent models which constitute the bulk of tests. Currently, a majority of rodent blast neurotrauma tests use unscaled durations between 4 and 10ms (Saljo et al. 2010, Bolander et al. 2011, Cernak et al. 2011, Leonardi et al. 2011, Goldstein et al. 2012). There are even studies which test at unscaled durations in excess of 10ms in rodents (Cernak et al. 2001, Pun et al. 2011), often with non-ideal overpressure time histories with large impulse compared with Friedlander blasts. With the current neurotrauma scaling model, these blast levels result in scaled overpressure durations close to or exceeding 100ms. These large overpressure duration blasts can generally only be

214

achieved through thermobaric or nuclear devices (Glasstone 1964) which are not typical of exposure of current concern.
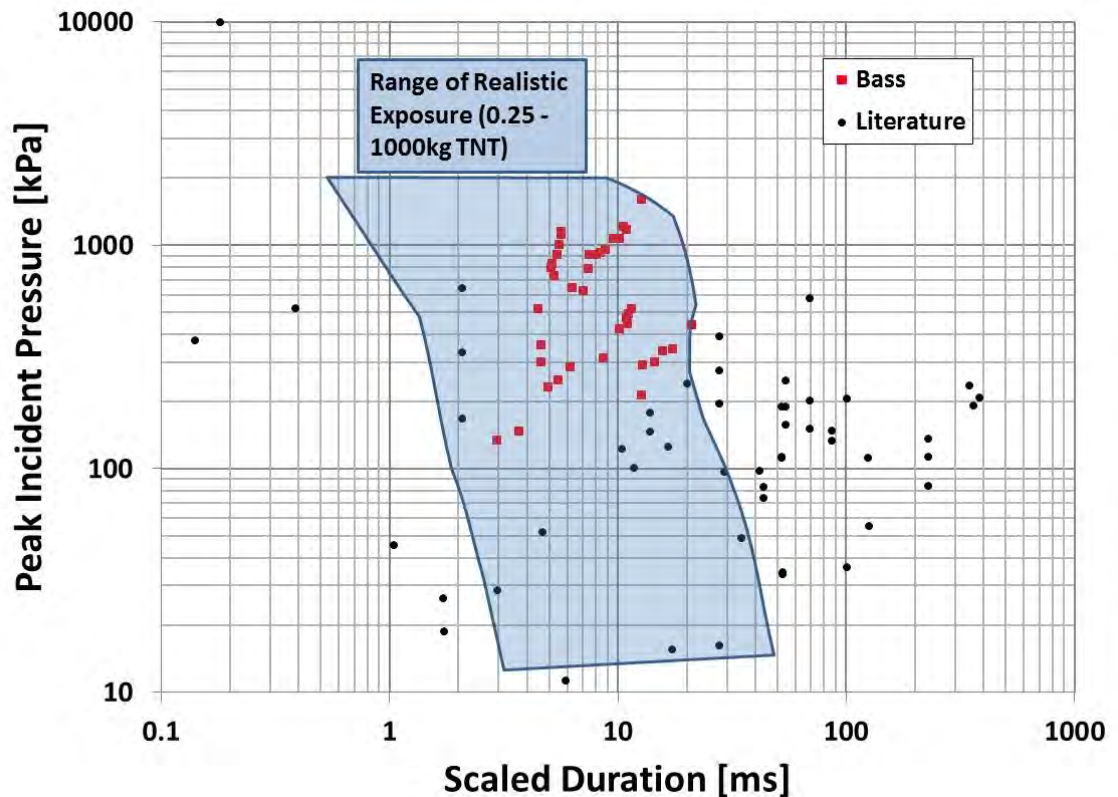
Figure 8-8: Many literature blast test conditions scaled by the TBI fatality model from this study fall outside of a range of realistic exposure.

When interspecies scaling is applied to blast conditions used on current blast neurotrauma models there is a wide range of human equivalent exposures (Figure 8-8). Much of the literature conditions fall outside of the conservative range of realistic exposure. Further, the bulk of test conditions within this realistic range are the work of Bass and colleagues (Rafaels et al. 2011, Rafaels et al. 2012, Shridharani et al. 2012b, Yu et al. 2012). Others have limited this range of exposures even further to approximately 50

to 1000kPa and 1 to 10ms (Nelson et al. 2008, Panzer et al. 2012a). The results of this study emphasize that researchers should carefully assess the desired conditions relative to human exposures. For scaled durations that are orders of magnitude greater than the normal human exposure range there is a risk of changing the injury mechanism in our models. This has been thoroughly discussed for pulmonary injury and there is a clear difference in injury risk behavior from short to long durations (Bass et al. 2008). Short overpressure duration primary blast exposure can be characterized by small displacement and high strain-rate response that is highly dependent upon both peak pressure and overpressure duration. Injury from short overpressure duration exposure is a result of transmission of the blast wave through tissue (Panzer et al. 2012b). Long overpressure duration exposure leads to a high impulse load that more likely results in acceleration based injury mechanisms such as compression of the tissue (Bass et al. 2008). At extremely long durations (> 100ms), which are representative of nuclear devices, enough momentum can be transferred to result in large accelerations and bulk displacement of the head and skull transmitted to the brain tissue. The results of interspecies scaling of test conditions suggests that in some animal models, especially rodents, we are essentially modeling blunt impact as opposed to the low momentum transfer normally associated with primary blast.

Due to the challenges discussed, there are limitations on this study on fatality risk in blast neurotrauma. Ideally we would directly measure biomechanics or

physiological response to develop analytical scaling models. However, this is difficult to achieve and empirically derived scaling and injury risk models are sufficient and made possible with comprehensive sets of model input (blast dose) and output (i.e. fatality, apnea, and behavioral deficit). The current study is limited by the fact that there are no existing animal model experiments in primary blast neurotrauma using a species with brain size equivalent to or larger than humans. This makes the scaling model an extrapolation, though a small extrapolation in pigs. Ideally the scaling and risk model would include a range of brain size to encompass humans. Further, the largest brain size in this study with fatality points is the rabbit, which at a brain mass of 11g is much smaller than the human brain. Additional data with larger animal brain sizes, such as pig, would better serve ensure the validity of the scaling model up to human response. It is however important to understand that blast neurotrauma research in large animals is limited, especially investigating fatality. Large animal, neurotrauma fatality research is made challenging by the magnitude of blast wave required to observe positive endpoints, and is outside the operating range of many existing shock tubes.

As a research field we are responsible for maximizing the information gained from animal model research conducted and this means considering the challenges outlined here. There are clinical and real-world implications to the results of this research as it will be used to aid in diagnosis and prediction of neurotrauma from blast, as well as for the design of personal protective equipment and policy decisions on

217

acceptable blast exposure. Based on the scaling model for blast neurotrauma fatality developed here it is suggested that testing with common animal model species be limited to a maximum unscaled blast dose; approximately 500kPa and 1ms in mice, 600kPa and 1.5ms in rats, 700kPa and 2ms in rabbits and ferrets, and 800kPa and 4ms in pigs. Interspecies scaling is absolutely necessary if we desire to compare injury results across different animal models and predict physiological and active response to blast input in humans.

Chapter 9 – Current Literature and Recommendations

There are a number of significant problems in the current blast neurotrauma literature that limit the value of many animal model studies. To help maximize the information gained from in vivo animal model studies methodological consideration must be made. This chapter discusses some of the weaknesses in current blast neurotrauma literature and makes recommendations for improving the utility of experimental results.

9.1 Limitations of Current Literature

Limitations in current blast neurotrauma literature make application of experimental results challenging. Many of these considerations prevent the direct comparison of study results, such as is presented in this fatality analysis. A common limitation is insufficient reporting or measurement of methodological details. To compare in vivo results across studies, or determine important factors like injury risk, we must have sufficient description of the blast wave dosage to model or recreate the event. Unfortunately, it is common to report a blast wave using only peak pressure or impulse alone. Without a measurement of overpressure duration we cannot assess the appropriate blast dose for a problem that is multiparameter at the short durations we are interested in. While some assumptions can be made as to the shape of the blast waveform it is desired for studies to report the shape of their input either graphically or through impulse measurement, in addition to the peak pressure and overpressure

duration. Two studies subjecting animals to identical peak pressure and overpressure

duration may have very different outcomes depending upon the impulse contained

within the blast wave. It is especially common for air-driven shock tubes to result in

larger impulse waves indicated by a plateauing of the measured pressure wave (Cernak

et al. 2011).

Another common problem in the reporting of blast methodology is the confusion

or neglect to properly distinguish incident versus reflected pressure measurements.

Incident pressure measurements are ideal as they do not rely on the interaction of the

blast wave with an object that may vary from study to study. The failure to report

sensor orientation may lead to large errors in the estimated peak pressure of the test, as

the reflected pressure measurement varies from 2 to 8 times higher than the incident

measurement when assuming ideal gas and may increase up to 20 times higher or more

when deviations from ideal gas occur (Iremonger 1997).

Consideration of animal placement when using gas-driven shock tubes, which

are the most common tools in blast research today, is important to limit unintended blast

doses and comorbid injuries due to other mechanisms. Something as simple as

appropriate head restraint is important when attempting to study primary blast,

especially in rodent models where large head displacements and accelerations are

possible. Rodent tests with heads free to translate have been shown to provide different

injury outcomes from tests in which the animal head is fixed (Goldstein et al. 2012).

Animal placement within or outside the exit of a shock tube has been a highly debated topic. Without careful consideration, placement of the animal within the driven section of the shock tube can result in confinement effects or large pressure reflections of the tube walls which increase impulse and more closely mimic a complex blast wave (Saljo et al. 2000, Chavko et al. 2011). Likewise, inappropriate placement of animals too far away or offset from the tube exit leads to expansion wave interactions which result in a large negative pressure pulse and a lack of wave planarity (Svetlov et al. 2010). This exterior placement can also lead to a momentum dominated exposure often referred to as "blast wind". The effects of specimen placement in shock tube tests have been experimentally measured and caveats for the implementation of different methodologies have been provided (Yu et al. 2014).

The choice of injury endpoint and the method of measuring these endpoints can also complicate the interpretation and implementation of research results in further analysis. A common and useful technique in studying neurotrauma is through the use of histopathology. Histological analysis has been used to look at cellular injuries in different areas of the brain; cortex (Goldstein et al. 2012), cerebrum (Koliatsos et al. 2011), hippocampus (Cernak et al. 2011, Dalle Lucca et al. 2012), and brain stem (Cernak et al. 2011). These different brain substructures mean different manifestation of injury on an organism level. Due to differences in size, shape, mechanical properties, and proximity to the ventricles these substructures may exhibit different injury tolerances.

Because of this, care should be taken when directly comparing cellular injury results from different areas of the brain. Many different histological stains have been used to assess injury in blast neurotrauma models and each stain represents a different cellular injury outcome; neuronal loss (NeuN) (Kato et al. 2007, Lu et al. 2012), shrunken and thinning nuclei (H&E) (de Lanerolle et al. 2011), degenerating axons (Silver) (Long et al. 2009, Svetlov et al. 2010), degenerating neurons (Fluoro-Jade b) (de Lanerolle et al. 2011), blood brain barrier breakdown (IgG) (Readnower et al. 2010, Yeoh et al. 2013), astrocytosis (GFAP) (Svetlov et al. 2010, Cernak et al. 2011), and axonal immunoreactivity (Beta-APP) (de Lanerolle et al. 2011, Risling et al. 2011). While there is value at considering the results of each of these studies individually it is impossible to make interstudy comparisons due to differences in methodology. Commonly, these studies use injury timepoints which vary widely. It is inappropriate to directly compare the result of histological staining from an animal sacrificed at 12 hours to one survived 12 days prior to staining. The timecourse of different types of cellular injuries from blast are likely different, for instance cellular manifestation of mild blast neurotrauma may occur over an entirely different timeframe then moderate or severe injuries. Differences in methodology may mean that we two animals treated in exactly the same manner but classify the injury outcome differently depending on the timepoint of measurement. To fully utilize histological injury endpoints in blast neurotrauma it is necessary to conduct tests over a broad timescale with similar methodologies.

Measurements of cognitive injury through behavioral tests are also a valuable tool afforded by in vivo animal models. A common test to measure motor and coordination deficits is the rotarod test used widely in rodents (Cernak et al. 2011, Wang et al. 2011). Another popular tests using in blast neurotrauma in the Barnes water maze which measures for spatial learning and memory deficits post-injury (Kovesdi et al. 2012). These tests can provide valuable insight for the manifestation of injuries on the cellular or tissue level within the nervous system. The results of these tests face some of the same challenges as histological analysis, as injuries may not manifest immediately and may be transient (Bogo et al. 1971). This makes the timeline for testing extremely important to determine the time course of injury.

9.2 Thoracic Protection

The current blast neurotrauma body of literature is severely limited by the oversight or neglect of the effects of comorbid injuries to other organ systems. It has been shown that the air-containing organs, and the pulmonary system especially, are more susceptible to fatal blast injury than the head. This is shown in Figure 9-1 where there is a large region of blast dose where the risk of pulmonary injury is significant before neurotrauma is. This has large implications when attempting to test animals for blast neurotrauma without preventing injury to the pulmonary system and gut. It is likely that these comorbid injuries initiate immune and physiological response that limit what can be learned from an in vivo model focused on neurotrauma only.

223
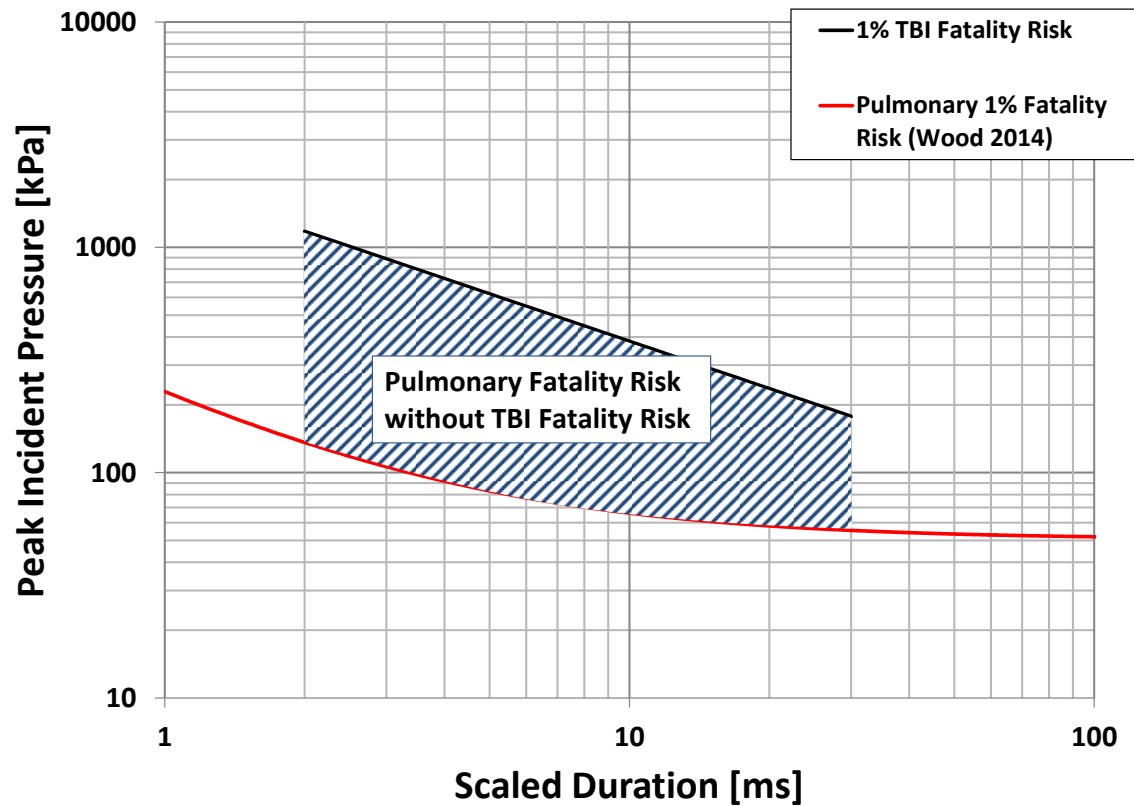
Figure 9-1: A large range of pulmonary injury risk occurs below that of TBI risk. Pulmonary 1% fatality risk from Chapter 6 compared to 1% TBI fatality risk developed in Chapter 8.

Despite the widespread acceptance that blast pulmonary injury comes before neurotrauma, there is a lack of effort to protect the pulmonary system during neurotrauma focused tests. The blast animal model database used for this study contains 2638 animals from 49 studies whose goal was to study blast neurotrauma. Of those, only 17 studies provided some form of thoracic protection for a total of 612 animals, or approximately 23% of the total neurotrauma tests. The study of blast isolated to the head is especially important due to the blast loads that current military

personnel are subjected to. It has been shown that modern thoracic body armor is

protective against blast and provides pressure attenuation for the thorax (Wood et al.

2012). The effect of widespread body armor usage is shown in Figure 9-2. Figure 9-2a

shows that the use of soft ballistic protective vests provides enough thoracic protection

that 1% fatality risk from pulmonary and TBI are now comparable. Further, the use of

hard body armor inserts, in conjunction with the soft vest, results in the 1% fatality risk

from blast TBI occurring below the level of 1% pulmonary fatality risk (Figure 9-2b).

The end result of body armor usage is that significant neurotrauma can now occur at

levels which pulmonary trauma will not be observed. Therefore, in vivo blast

neurotrauma research should seek to model this effect.
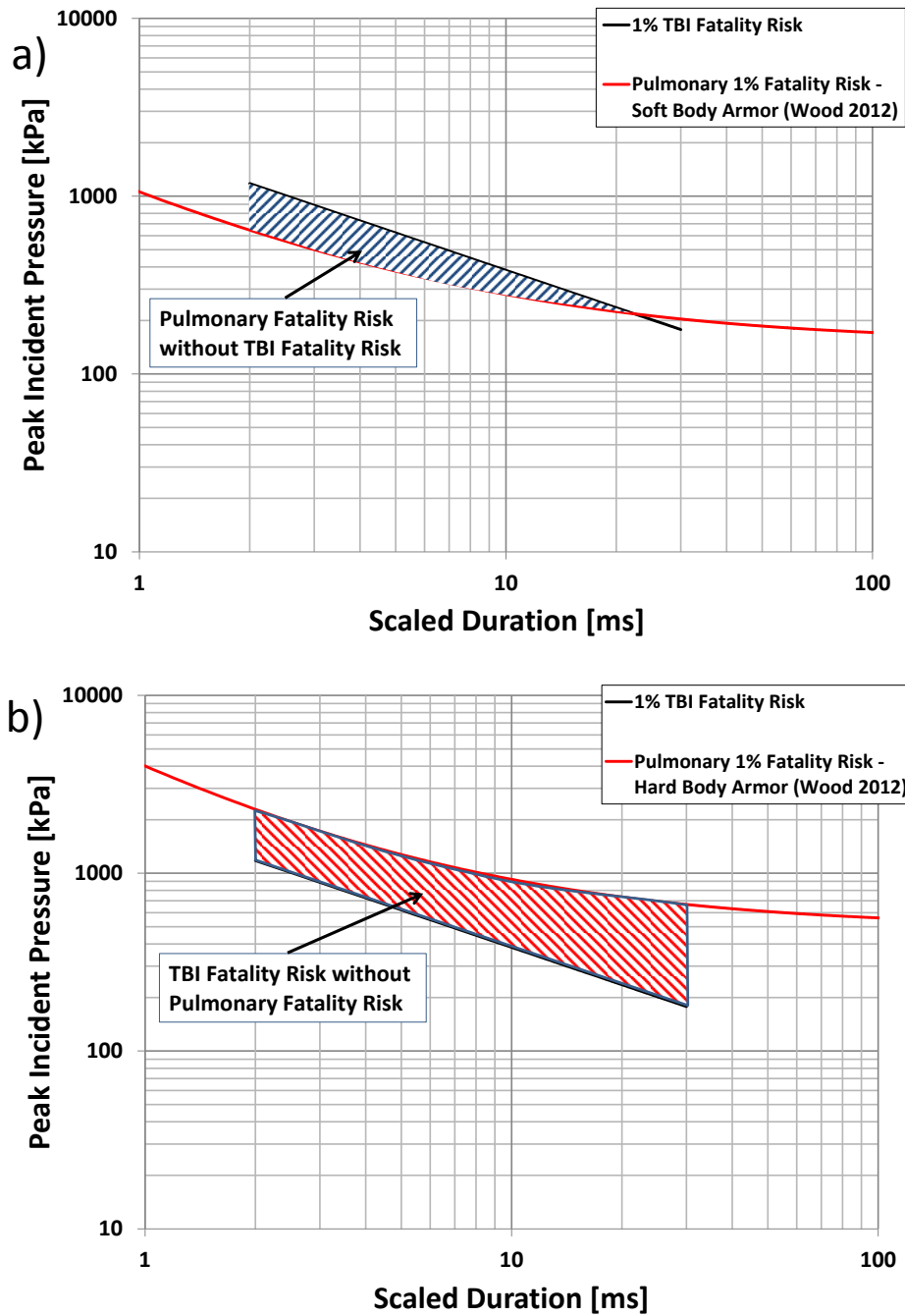
Figure 9-2: Thoracic body armor usage effects the relative risk of pulmonary and neurotrauma with a) NIJ Level-2 soft armor risk (Chapter 4) occurring at similar levels to 1% TBI fatality (Chapter 8) and b) NIJ Level-4 hard armor risk (Chapter 4) occurring at levels above 1% TBI fatality risk (Chapter 8).

9.3 Implications

The major implication of the many challenges in methodology across blast neurotrauma research is that a large percentage of the existing literature cannot be used for synthesized analysis of injury risk. Of the 2638 animal model tests for blast neurotrauma compiled, only 189 (~7%) met our criteria to include in a fatality risk analysis. This makes it challenging to derive injury risk models for blast neurotrauma across species and develop appropriate scaling to relate the results to human response.

Efforts to synthesize the current body of blast neurotrauma work are made difficult due to many common methodological characteristics including incomplete reporting of blast dose, unclear measurement and reporting of injury endpoints, and comorbid acceleration injuries to the head from bulk movement or blast injuries to the thorax and gut in unprotected animals. Even if many of these methodological issues are resolved, interspecies scaling suggests that a majority of blast neurotrauma research is using blast levels which fall well outside the realm of interest for human exposure levels.

As a research field we are responsible for maximizing the information gained from animal model research conducted and this means considering the challenges outlined here. There are clinical and real-world implications to the results of this research as it will be used to aid in diagnosis and prediction of neurotrauma from blast, as well as for the design of personal protective equipment and policy decisions on

acceptable blast exposure. Therefore, it is a problem if we are not modeling the exposures that what we think we are. Changes in injury mechanism due to inappropriate blast conditions may suggest incorrect injury risk or injury manifestation. The solution is to use animal models which allow us to most closely model human response, which likely includes the use of gyrencephalic species as they are generally closer in body and brain size and offer a closer morphological match to humans. Based on the scaling models for blast neurotrauma fatality developed in this dissertation it is suggested that testing with common animal model species be limited to a maximum unscaled blast dose; approximately 500kPa and 1ms in mice, 600kPa and 1.5ms in rats, 700kPa and 2ms in rabbits and ferrets, and 800kPa and 4ms in pigs. These recommended ranges result in scaled peak overpressure and overpressure duration that fall within a realistic range of human exposure (Figure 9-3). Interspecies scaling is absolutely necessary if we desire to compare injury results across different animal models and predict physiological and active response to blast input in humans.
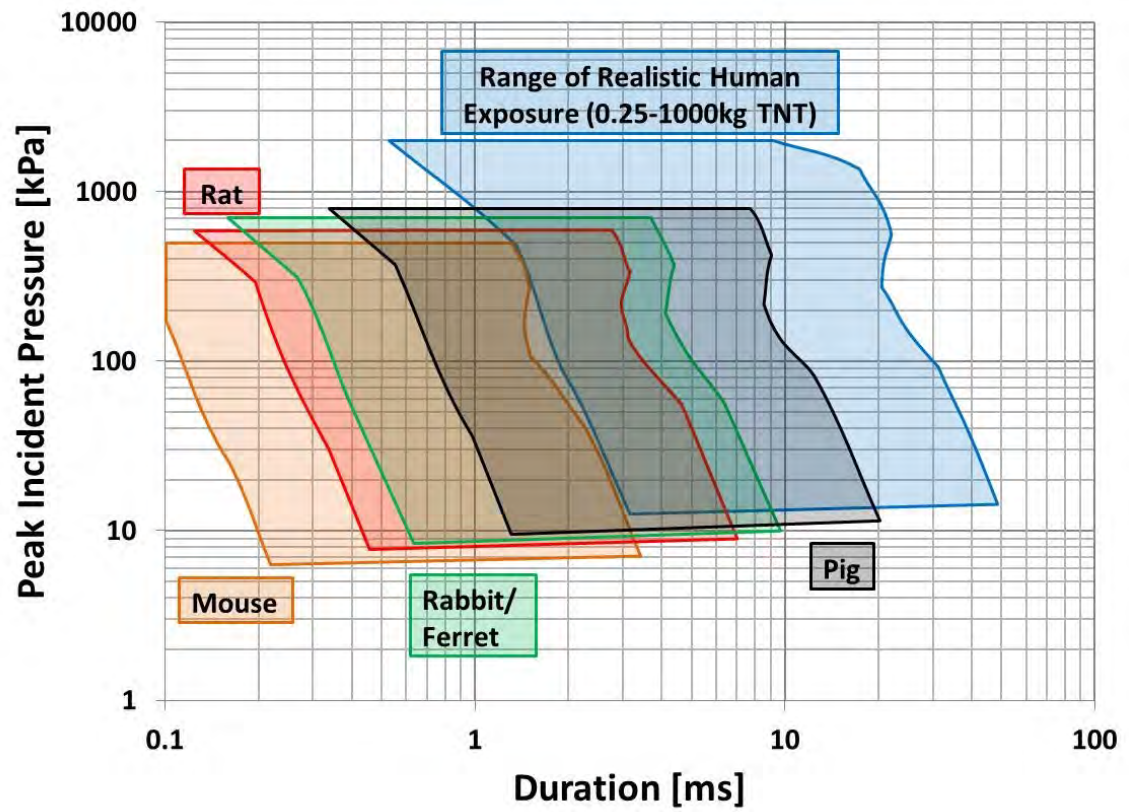
Figure 9-3: Recommended unscaled testing ranges for common animal model species are smaller in peak pressure magnitude and overpressure duration.

Chapter 10 - Conclusions

Blast is a common source of injury in recent military conflicts. As of 2008 nearly

81% of all OIF/OEF veterans had sustained some injury from a blast event (Owens et al.

2008). Nearly 90% of blast-related injuries treated at Walter Reed Army Medical Center

included closed-head injury (Warden et al. 2006). In 2011 alone a total of over 32,000

TBIs were reported among U.S. military personnel (Bagalman 2013). Diagnosis and

treatment of TBI is often very difficult due to comorbid injuries and conditions like

PTSD (Capehart et al. 2012).

The occurrence and importance of blast TBI was widely neglected prior to the

late 1990's due to research that showed that fatalities occurred from pulmonary injury at

blast intensities that were lower than for isolated brain injury (Bogo et al. 1971, Hooker

1924, Krohn et al. 1941). With a large increase in TBI occurring after blast exposure with

the apparent lack of blunt impact, research focus has shifted to blast neurotrauma. Over

the last 20 years, the occurrence and likelihood of primary blast TBI has been shown in

many in vivo studies. Injury endpoints measured range from the cellular level (Saljo et

al. 2000, Moochala et al. 2004, Cernak et al. 1996) up to the behavioral level (Cernak et al.

2001, Risling et al. 2002).

However, large important questions remain that would help us to understand

blast TBI. The mechanism by which blast neurotrauma occurs remains unclear. Some

work has suggested it to be highly dependent upon strain and strain rate level (Panzer

2012). It is generally accepted that the mechanism for injury is different in low energy

and moment transfer blast events from that of blunt impact. Interspecies scaling for in

vivo animal model research is vital to our understanding of research outcomes but is

commonly neglected in experimental analyses. Extensive research has shown the need

for scaling relations between different animal model species to derive an equivalent

human exposure level. A better understanding of these questions will directly lead to

better treatment and injury prevention for primary blast exposure. This dissertation

used experimental analysis to determine the protective effects of modern thoracic body

armor against blast overpressure. The viscoelastic behavior of brain tissue in multiple

common blast animal model species was also experimentally investigated to help

improve our understanding of interspecies differences and improve the biofidelity of

computation models for blast. Additionally, published in vivo blast trauma data was

used to update and develop interspecies scaling relations and injury risk models for

both blast pulmonary trauma and neurotrauma. In vivo models are one of the only tools

available to researchers to stud physiology and this dissertation stands to improve our

usage of existing data and to improve the experimental design of future in vivo studies.

10.1 Major Contributions

This dissertation provides three major contributions to the field of injury

biomechanics and the study of blast TBI. The contributions fill a gap in our

understanding of blast biomechanics and improve future research.

Research in this dissertation determined that modern thoracic body armor has the ability to substantially reduce blast overpressure to the torso and therefore protect the pulmonary system from blast exposure relative to the head. This work helps to explain the shift in types of blast injury observed clinically from pulmonary pathology to TBI.

The study presented in Chapter 4 shows that the use of body armor significantly decreases the risk of injury from a given exposure level. Modern body armor is protective in two primary ways. Usage of armor significantly decreases the peak overpressure delivered to the chest relative to overpressure in the incoming waves, while increasing the rise time of the pressure input which is also known to decrease pulmonary injury risk. The use of soft NIJ Level-2 armor results in similar exposure thresholds for pulmonary and blast neurotrauma. The addition of hard plates in a NIJ Level-4 vest results in TBI injury risk occurring at lower levels than that of adjusted pulmonary injury risk. These findings are important as they not only help to explain current trends in battlefield injury but also highlight the importance of using armor to lower injury risk not only from ballistic threats but from blast as well.

This study is the first to provide brain tissue viscoelastic characterization data across three common in vivo blast animal model species using a consistent test methodology.

The experimental study presented in Chapter 5 investigated brain tissue behavior in three common animal model species used for blast TBI research that cover two orders of magnitude in brain size. Further, gyrencephalic and lissencephalic species

232

are represented. This study is one of few that look at brain tissue mechanics either in vivo or in situ to assess the effect of confinement within the skull. Inverse finite element techniques were used to incorporate the non-ideal effects of confinement and unique geometry that make analytical constitutive modeling difficult.

This is the first study to develop interspecies scaling for blast neurotrauma based on experimental data across a wide range of common in vivo animal model species. This investigation shows a clear injury risk dependence upon species size.

The work presented in Chapters 7 and 8 assess the body of blast TBI literature and show the need for interspecies scaling in experimental analysis. Injury risk shows a clear peak pressure and overpressure duration dependence like that of much more extensively studied pulmonary injury. Two common and easily measured neurotrauma injury endpoints were investigated, apnea and fatality. Optimized scaling models were similar between the two TBI endpoints. Further, scaling for neurotrauma was similar to the characteristic length type scaling previously derived for pulmonary injury (Bowen et al. 1965, Chapter 6) is brain size is instead considered. Neurotrauma scaling was found to be approximately equal to a characteristic length scaling of the brain if geometry is considered to be similar across species of interest. A more extensive set of data for primary blast isolated to the head is needed to investigate other injury endpoints for scaling and risk models such as bleeding and cellular injury through histology. This scaling procedure is important because it allows researchers to match appropriate

human equivalent dose levels and develop human injury risk models from in vivo animal experimentation.

The work in this dissertation included an in depth assessment of the current blast neurotrauma literature and the state of the field for blast TBI research. This provided important recommendations for future research to maximize the value of in vivo animal model experimentation for blast injury research.

There are major concerns about the bulk of blast TBI literature that either limit or prevent its use for furthering our understanding of injury mechanisms and thresholds. These concerns are outlined and discussed in Chapter 8 of this dissertation. To use experimental results to determine injury mechanisms and thresholds and therefore improve prevention, diagnosis, and treatment, we must be able to recreate results and compare across studies. In order for this to be possible, a better understanding is needed of blast physics and experimental design to recreate blast exposures. A better understanding by researchers of the physics and biomechanics involved will improve the reporting of selection of blast exposure levels so that results across studies can be compared.

The effects of interspecies scaling, which are largely ignored, have a significant effect on the applicability of research results. The total neglect of scaling principles, especially in rodent models, often results in test conditions with human equivalent exposures well outside of a realistic range of exposure. The exposure of small animals to

common blast levels seen in the literature is representative of nuclear blast levels which are not of current interest. With these human equivalent exposure levels there is likely a change in injury mechanism due to the large energy deposition relative to short overpressure duration events, and therefore we are likely not even studying what we aim to. Recommended unscaled exposure ranges for common in vivo neurotrauma animal model species were developed as part of this dissertation. It is recommended that unscaled blast peak overpressure and overpressure duration exposure be limited to less than 500kPa and 1ms in mice, 600kPa and 1.5ms in rats, 700kPa and 2ms in rabbits and ferrets, and 800kPa and 4ms in pigs.

10.2 Other Contributions

In addition to the major contributions outline above, this dissertation provides other important contributions to further the field of blast biomechanics and blast TBI research. These contributions either build upon existing research or lay the groundwork for future research studies in blast trauma.

This dissertation updated existing pulmonary injury risk models for primary blast and empirically validated the blast pulmonary interspecies scaling model commonly used.

In Chapter 6 of this dissertation the most extensive set of experimental data used to date was utilized to empirically optimize appropriate interspecies scaling across a large range of species body size. The scaling model presented is similar to the previously published (Bowen et al. 1965) and commonly used for blast injury modeling.

The resulting injury risk models for pulmonary blast exposure agree well with existing model but incorporate data from both small and large animals as opposed to some recent models which look at large animal species only (Bass et al. 2008, Rafaels et al. 2010). This work highlights the importance of interspecies scaling considerations for in vivo blast pulmonary testing.

This dissertation developed blast neurotrauma risk models using the widest range of in vivo animal model species to date. Species ranged in brain size over two orders of magnitude, from mouse to pig.

This dissertation included the development of apnea (Chapter 7) and fatality (Chapter 8) risk models for primary blast exposure isolated to the head. Injury risk models were developed for short durations only, where injury response is heavily dependent upon both peak pressure and overpressure duration. The results affirm previous findings that the unprotected thorax (Chapter 6) is more susceptible to blast injury than the unprotected head. More qualifying data is needed at long scaled overpressure duration levels to further expand the model validation region. Injury risk models and interspecies scaling models for blast neurotrauma can be improved with more data from a wider range of species.

10.3 Future Work

For much of the research presented in this dissertation, there are logical steps to expand the research studies and improve the experimental and computational results presented. Some of these future directions are outlined below.

The expansion of viscoelastic brain tissue characterization study will improve our understanding of interspecies differences and improve out computational models.

To improve the utility of the brain tissue property data presented in this dissertation an expansion of the indentation study is desired. The inclusion of species across a wider range of brain sizes including humans and species with larger brains than humans would help to inform on interspecies differences in brain tissue material behavior. With additional species it may be possible to determine if there are differences in cortical tissue behavior between gyrencephalic and lissencephalic species. Beyond the addition of species, the inclusion of indentation testing of brain substructures can provide valuable information when applying species specific models to FE analysis. To improve our understanding of brain tissue viscoelastic behavior in blast applications, higher rate properties may be acquired through methods such as magnetic resonance elastography. Finally, better constitutive models for inclusion in FE models are desired for blast simulations and biomechanical measurements. The inclusion of constitutive models that account for strain softening and damage of brain tissue will greatly improve modeling capability and the prediction of tissue injury from simulations.

The implementation of brain viscoelastic constitutive models into improved FE models will improve predictive capabilities and our ability to match biomechanical measures from computational models to experimentally measured injury endpoints.

The development of high resolution FE models of common blast animal model species, like that previously done for the ferret (Panzer 2012), will allow us to directly compare simulated biomechanical measurements with experimental results. This would allow for the discovery of injury mechanisms and thresholds for primary blast neurotrauma. A high resolution blast FE model of the mouse head is currently being developed and should be augmented by additional species models in the future. In vivo animal models in conjunction with high resolution, blast validated FE models will maximize our understanding of blast neurotrauma.

Additional experimental data from in vivo blast neurotrauma models with properly designed experiments is necessary for further development of interspecies scaling and injury risk models.

Experimental data is needed with repeatable, simple Friedlander-type pressure waveform exposures. Studies with complete reporting of blast exposure methodology are needed for direct comparison of injury endpoint measurements. To prevent comorbid injuries, especially to the pulmonary system, studies with sufficient thoracic protection are needed. To develop neurotrauma models like those presented for pulmonary trauma (Chapter 6) a much larger set of data is needed over short and long

238

scaled overpressure duration ranges. Finally, a wider range of species, especially in brain size, is needed improve the reliability and significance of both interspecies scaling models and neurotrauma risk models for additional injury endpoints.

The consideration of more scaling factors which vary between species may improve the validity of interspecies scaling relations for blast neurotrauma.

A more extensive set of experimental data will allow for the comparison of blast neurotrauma response dependent upon interspecies variation such as cortical surface morphology. In pulmonary blast injury response there is a clear delineation between large and small animal model species according to differences in pulmonary anatomy. It is possible that similar groupings exist for blast neurotrauma, perhaps with gyrencephalic and lissencephalic model species. Head and brain morphology differences, for example in skull thickness, likely effect injury risk from blast exposure but insufficient data currently exists to investigate these effects. An investigation into some of these more complicated interspecies differences may be made possible with an increased amount of experimental data and through improved FE model simulations to measure the underlying tissue biomechanics. Ideally, the injury mechanism for blast neurotrauma will be discovered by combining extensive experimental data with FE model results to develop biomechanical scaling of the mechanical parameter of interest (i.e. strain, strain rate).

Appendix A – Brain Tissue Model Parameters and Fits

Table A-1: Optimized QLV model parameters for each step test investigated

	Instantaneous Elastic Parameters		Reduced Relaxation Function Parameters					Model Fit Statistics	
	A	**B**	**G$_1$** τ_1=0.01s	**G$_2$** τ_2=0.1s	**G$_3$** τ_3=1.0s	**G$_4$** τ_4=10s	**G$_\infty$**	**SSE**	**R^2**
P1 L1-1	0.242	0.455	0.539	0.174	0.058	0.114	0.115	0.016	0.996
P1 L1-2	0.190	0.473	0.537	0.144	0.093	0.103	0.122	0.012	0.997
P2 L1-1	0.541	0.277	0.549	0.144	0.090	0.084	0.132	0.022	0.995
P2 L1-2	0.676	0.234	0.547	0.143	0.090	0.060	0.160	0.035	0.993
P3 L1-1	0.437	0.278	0.516	0.140	0.059	0.113	0.172	0.028	0.993
P3 L1-2	0.274	0.331	0.485	0.133	0.075	0.134	0.173	0.021	0.992
P4 L1-1	10.000	0.020	0.582	0.131	0.091	0.075	0.122	0.018	0.997
P4 L1-2	0.387	0.376	0.584	0.119	0.086	0.081	0.129	0.016	0.997
P5 L1-1	0.304	0.359	0.582	0.094	0.123	0.059	0.143	0.018	0.995
P5 L1-2	0.341	0.322	0.550	0.157	0.041	0.141	0.112	0.018	0.996
F1 L1-1	8.976	0.034	0.576	0.154	0.091	0.071	0.108	0.042	0.997
F1 L1-2	6.909	0.035	0.577	0.156	0.067	0.078	0.122	0.036	0.995
F2 L1-1	6.603	0.029	0.553	0.164	0.062	0.060	0.160	0.049	0.991
F2 L1-2	6.085	0.030	0.537	0.169	0.104	0.023	0.167	0.054	0.990
F3 L1-1	7.619	0.033	0.527	0.133	0.096	0.037	0.207	0.104	0.991
F3 L1-2	6.583	0.034	0.490	0.167	0.066	0.083	0.194	0.116	0.989
M1 L2-1	4.369	0.017	0.759	0.000	0.060	0.181	0.000	0.001	0.938
M1 L2-2	4.120	0.016	0.755	0.004	0.059	0.182	0.000	0.001	0.916

	Instantaneous Elastic Parameters		Reduced Relaxation Function Parameters					Model Fit Statistics	
	A	**B**	**G₁** $\tau_1=0.01s$	**G₂** $\tau_2=0.1s$	**G₃** $\tau_3=1.0s$	**G₄** $\tau_4=10s$	**G∞**	**SSE**	**R²**
M2 L2-1	4.301	0.018	0.755	0.011	0.057	0.177	0.000	0.002	0.924
M2 L2-2	4.026	0.017	0.717	0.012	0.000	0.271	0.000	0.003	0.882
M3 L2-1	5.267	0.020	0.707	0.092	0.071	0.130	0.000	0.002	0.959
M3 L2-2	4.378	0.022	0.725	0.063	0.031	0.181	0.000	0.002	0.947
M4 L2-1	4.277	0.016	0.672	0.137	0.013	0.174	0.004	0.001	0.928
M4 L2-2	4.360	0.016	0.673	0.083	0.106	0.050	0.088	0.001	0.931
M5 L2-1	2.505	0.032	0.749	0.070	0.097	0.000	0.084	0.001	0.923
M5 L2-2	0.316	0.216	0.704	0.059	0.038	0.066	0.133	0.002	0.913
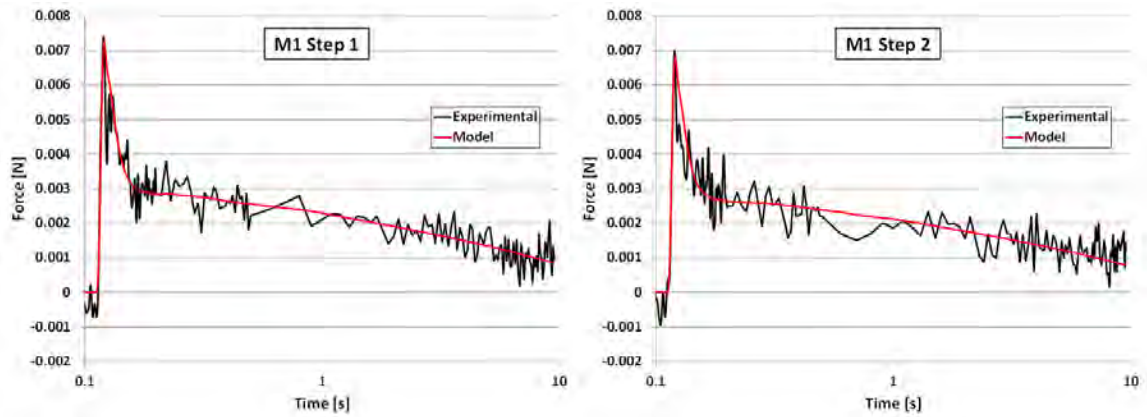
Figure A-1: Experimental data with model fit for M1 step tests.
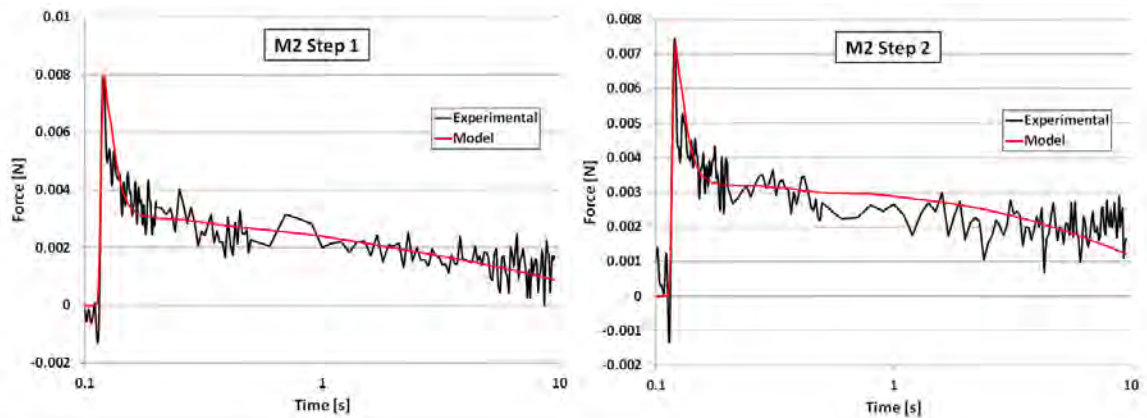
Figure A-2: Experimental data with model fit for M2 step tests.
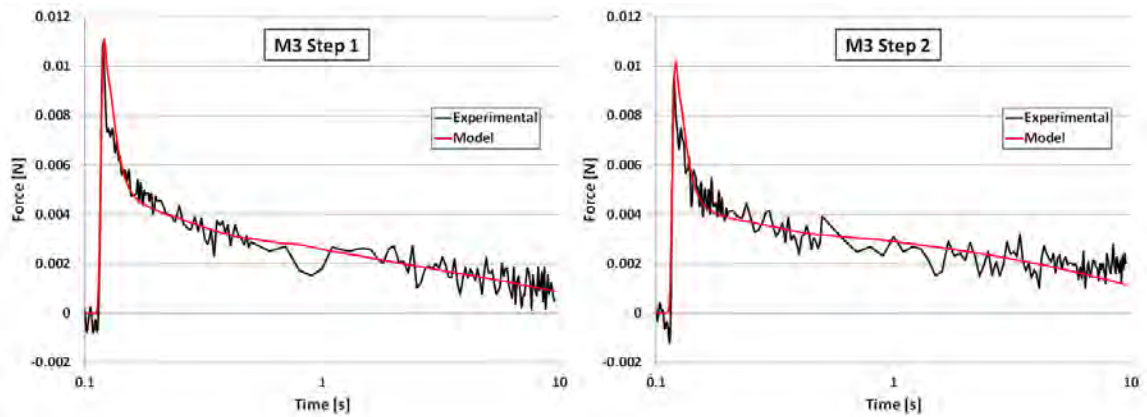
Figure A-3: Experimental data with model fit for M3 step tests.

242
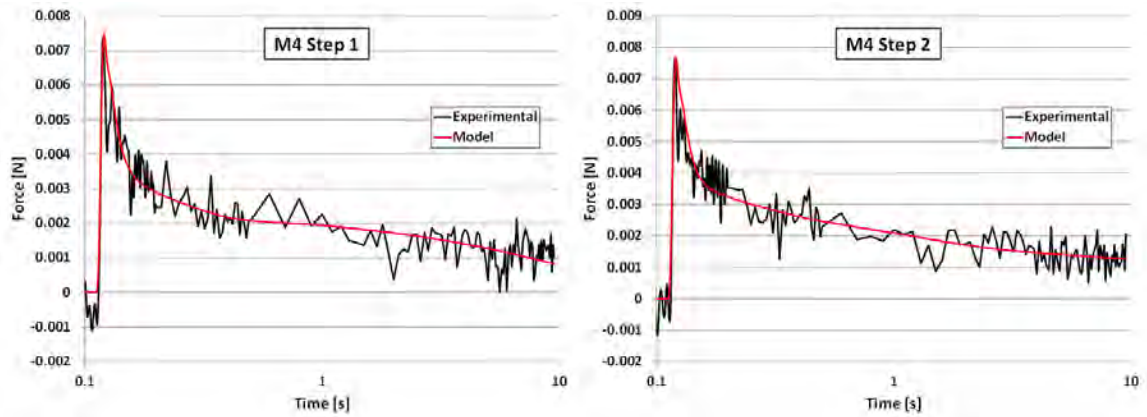
Figure A-4: Experimental data with model fit for M4 step tests.
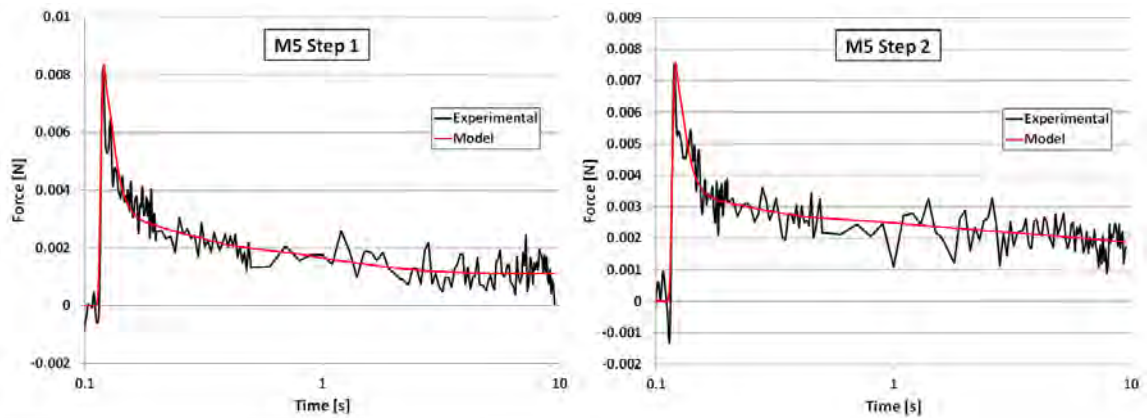
Figure A-5: Experimental data with model fit for M5 step tests.
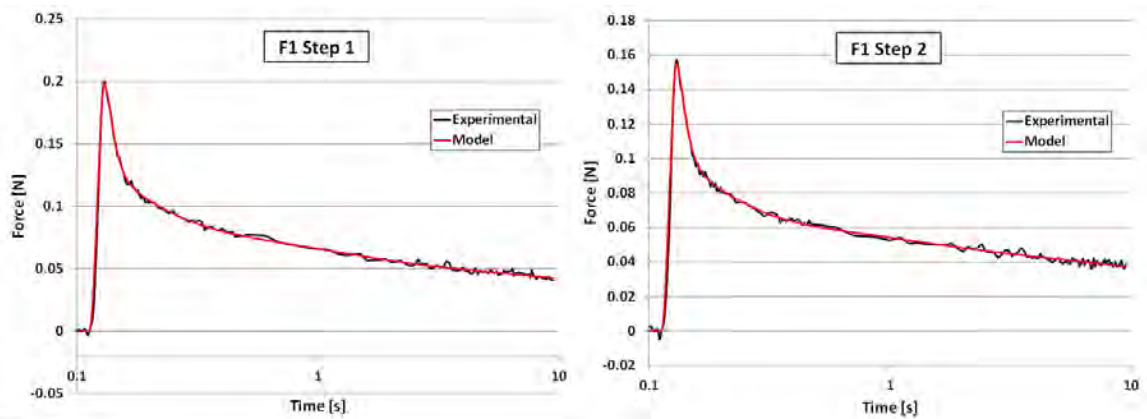
Figure A-6: Experimental data with model fit for F1 step tests.

243
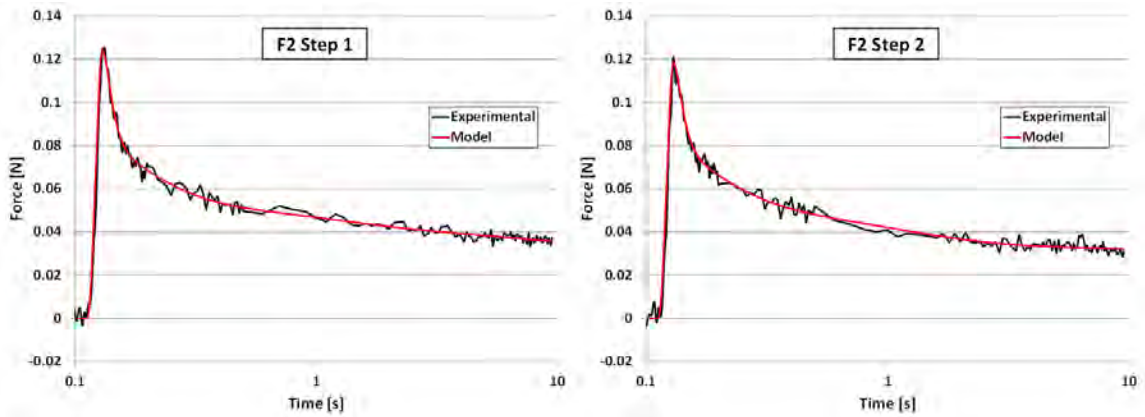
Figure A-7: Experimental data with model fit for F2 step tests.
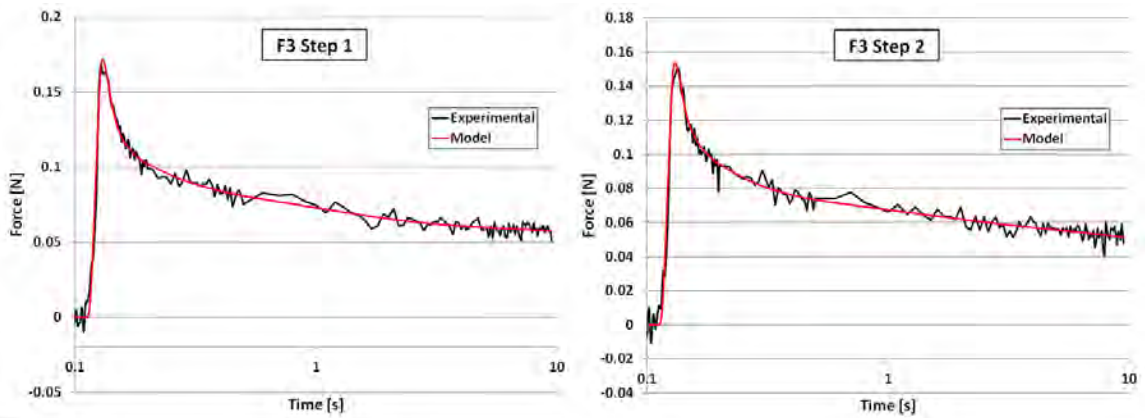
Figure A-8: Experimental data with model fit for F3 step tests.
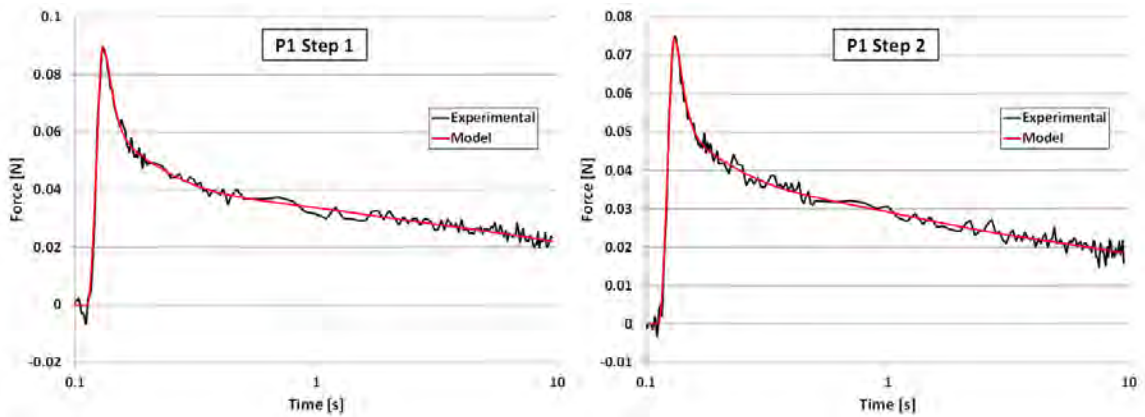
Figure A-9: Experimental data with model fit for P1 step tests.
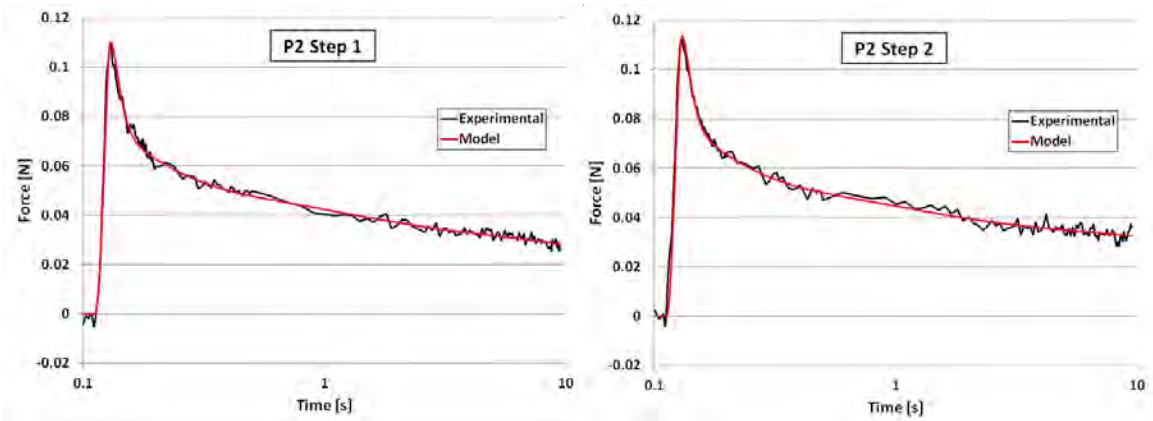
Figure A-10: Experimental data with model fit for P2 step tests.
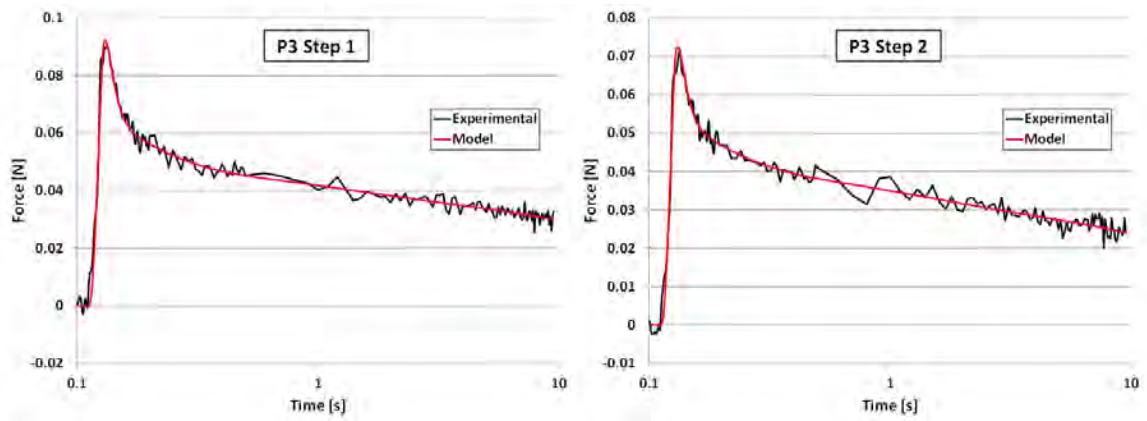
Figure A-11: Experimental data with model fit for P3 step tests.
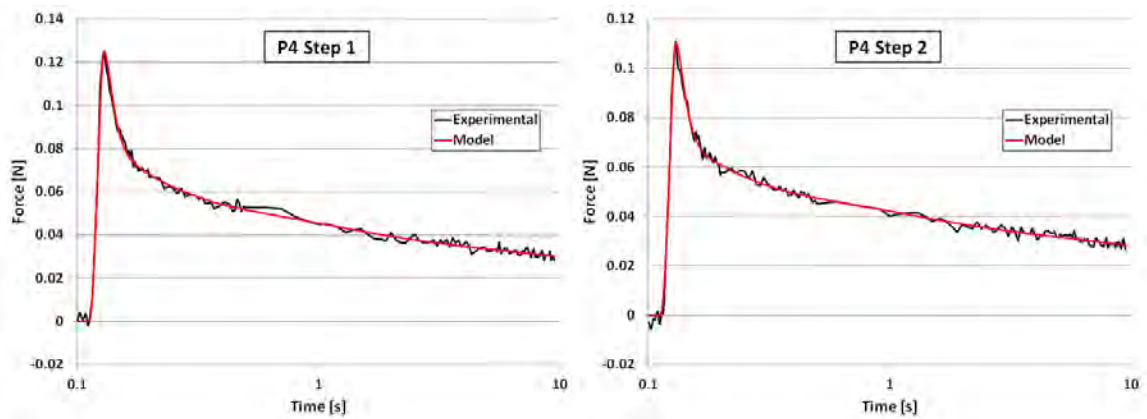
Figure A-12: Experimental data with model fit for P4 step tests.
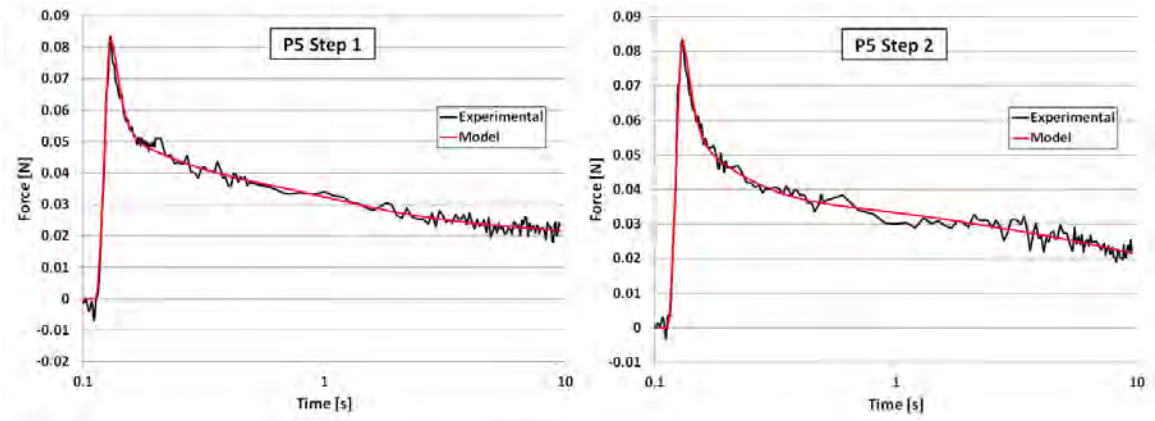
Figure A-13: Experimental data with model fit for P5 step tests.

Appendix B – Blast Pulmonary Test Conditions

Table B-1: Details of studies included in blast pulmonary injury modeling

	Species	Average Body Mass [kg]	Peak Incident Pressure [kPa]	Scaled Incident Pressure [kPa]	Duration [ms]	Scaled Duration [ms]	% Fatality
Bowen1968	Sheep	52.2	602.1	593.1	0.96	1.08	25.0%
		52.2	737.1	726.1	0.49	0.54	0.0%
		52.2	1118.5	1101.8	0.37	0.41	0.0%
		52.2	1395.6	1374.7	0.29	0.32	16.7%
		52.2	1460.0	1438.2	0.31	0.34	40.0%
		52.2	1778.6	1752.0	0.25	0.28	100.0%
Celander1955	Mouse	0.02	98.1	155.9	0.15	2.63	0.0%
		0.02	98.1	155.9	1.90	33.32	20.0%
		0.02	98.1	155.9	4.40	77.17	33.3%
		0.02	127.5	202.6	0.15	2.63	10.0%
		0.02	127.5	202.6	1.90	33.32	50.0%
		0.02	127.5	202.6	4.60	80.67	100.0%
		0.02	157.0	249.5	0.15	2.63	60.0%
		0.02	157.0	249.5	2.00	35.08	86.7%
		0.02	157.0	249.5	4.70	82.43	100.0%
		0.02	196.2	311.8	0.25	4.38	80.0%
		0.02	196.2	311.8	2.10	36.83	93.3%
		0.02	196.2	311.8	5.00	87.69	100.0%
Cernak2011	Mouse	0.025	68.0	108.1	6.00	97.03	3.9%
		0.025	76.0	120.8	6.00	97.03	27.7%
		0.025	105.0	166.9	7.00	113.20	42.4%
Clifford1984	Sheep	50	3.4	3.3	12.89	14.51	0.0%
		50	24.1	23.8	8.33	9.37	0.0%
		50	51.7	50.9	7.04	7.92	0.0%
		50	103.4	101.9	5.73	6.45	0.0%
Damon1964	Mouse	0.02	225.3	125.3	18.00	219.11	20.0%
		0.02	234.0	130.1	18.00	219.11	60.0%
		0.02	134.0	130.4	18.00	219.11	15.0%
		0.02	104.3	135.3	18.00	219.11	33.3%
		0.02	71.3	138.8	18.00	219.11	13.3%
		0.02	146.9	1430.0	18.00	219.11	60.0%

	Species	Average Body Mass [kg]	Peak Incident Pressure [kPa]	Scaled Incident Pressure [kPa]	Duration [ms]	Scaled Duration [ms]	% Fatality
		0.02	111.7	144.9	18.00	219.11	41.2%
		0.02	78.6	153.0	18.00	219.11	53.3%
		0.02	157.3	153.1	18.00	219.11	75.0%
		0.02	288.5	160.5	18.00	219.11	88.2%
		0.02	127.1	164.9	18.00	219.11	66.7%
		0.02	49.8	166.0	18.00	219.11	40.0%
		0.02	88.7	172.7	18.00	219.11	86.7%
		0.02	54.7	182.4	18.00	219.11	80.0%
		0.02	56.6	188.7	18.00	219.11	85.0%
Damon1966	Dog	17.1	142.2	118.8	36.00	65.33	20.0%
		17.1	150.5	125.7	36.00	65.33	25.0%
		17.1	158.2	132.1	36.00	65.33	36.4%
		17.1	161.2	134.6	36.00	65.33	50.0%
		18.7	64.6	138.7	36.00	39.48	16.7%
		17.5	111.6	139.8	36.00	52.91	40.0%
		18.7	67.5	145.0	36.00	39.48	35.0%
		18.7	69.8	149.9	36.00	39.48	80.0%
		17.5	123.7	155.0	36.00	52.91	50.0%
	Goat	21.7	57.9	123.0	36.00	37.47	30.0%
		21.7	59.6	126.6	36.00	37.47	50.0%
		21.7	61.5	130.6	36.00	37.47	60.0%
		31.2	132.3	131.1	36.00	48.29	33.3%
		21.7	65.2	138.5	36.00	37.47	87.5%
		31.2	148.3	147.0	36.00	48.29	100.0%
Damon1970	Dog	8.4	94.2	117.9	357.50	688.26	0.0%
	Sheep	37	47.9	57.7	160.00	181.07	0.0%
		41.2	95.7	115.3	160.00	174.87	0.0%
DASA1965	Goat	32.2	68.9	84.2	230.00	274.85	0.0%
		32.2	103.4	126.3	195.00	233.03	0.0%
		30.4	213.7	261.0	175.00	213.39	83.3%
		30.4	255.0	311.5	165.00	201.20	100.0%
		30.4	289.5	353.6	160.00	195.10	100.0%
		30.4	317.1	387.3	154.00	187.78	100.0%
		30.4	351.5	429.3	150.00	182.91	100.0%
		30.4	379.1	463.0	145.00	176.81	100.0%

	Species	Average Body Mass [kg]	Peak Incident Pressure [kPa]	Scaled Incident Pressure [kPa]	Duration [ms]	Scaled Duration [ms]	% Fatality
		30.4	399.8	488.3	142.00	173.15	100.0%
Dodd1989	Sheep	55	22.8	22.5	7.00	7.62	0.0%
		55	27.6	27.2	10.80	11.75	0.0%
		55	29.7	29.3	6.00	6.53	0.0%
		55	33.1	32.6	5.90	6.42	0.0%
		55	35.2	34.7	5.10	5.55	0.0%
		55	36.5	36.0	6.20	6.75	0.0%
		55	37.9	37.3	6.00	6.53	0.0%
		55	39.3	38.7	5.70	6.20	0.0%
		55	40.0	39.4	5.70	6.20	0.0%
		55	40.5	39.9	5.30	5.77	0.0%
		55	40.7	40.1	5.90	6.42	0.0%
		55	41.4	40.8	3.00	3.27	0.0%
		55	41.5	40.9	5.40	5.88	0.0%
		55	45.4	44.7	8.70	9.47	0.0%
		55	45.5	44.8	2.00	2.18	0.0%
		55	46.9	46.2	5.40	5.88	0.0%
		55	47.0	46.3	4.80	5.22	0.0%
		55	49.6	48.9	2.00	2.18	0.0%
		55	51.0	50.2	2.00	2.18	0.0%
		55	52.7	51.9	2.10	2.29	0.0%
		55	53.8	53.0	5.10	5.55	0.0%
		55	54.5	53.7	2.70	2.94	0.0%
		55	56.5	55.7	8.20	8.92	0.0%
		55	57.2	56.3	1.90	2.07	0.0%
		55	58.6	57.7	2.60	2.83	0.0%
		55	59.2	58.3	2.80	3.05	0.0%
		55	60.0	59.1	1.90	2.07	0.0%
		55	60.1	59.2	1.90	2.07	0.0%
		55	60.7	59.8	1.90	2.07	0.0%
		55	62.0	61.1	1.90	2.07	0.0%
		55	62.1	61.2	1.90	2.07	0.0%
		55	64.1	63.1	2.00	2.18	0.0%
		55	68.3	67.3	2.70	2.94	0.0%
		55	72.4	71.3	1.20	1.31	0.0%

	Species	Average Body Mass [kg]	Peak Incident Pressure [kPa]	Scaled Incident Pressure [kPa]	Duration [ms]	Scaled Duration [ms]	% Fatality
		55	73.1	72.0	1.20	1.31	0.0%
		55	75.2	74.1	1.20	1.31	0.0%
		55	82.7	81.5	0.80	0.87	0.0%
		55	85.5	84.2	0.80	0.87	0.0%
		55	86.9	85.6	0.80	0.87	0.0%
		55	90.3	88.9	0.80	0.87	0.0%
		55	100.0	98.5	0.80	0.87	0.0%
		55	101.5	100.0	1.10	1.20	0.0%
		55	103.4	101.9	1.10	1.20	0.0%
		55	103.6	102.1	0.80	0.87	0.0%
		55	105.5	103.9	1.00	1.09	0.0%
		55	111.0	109.3	1.00	1.09	0.0%
		55	113.8	112.1	1.10	1.20	0.0%
		55	115.8	114.1	1.00	1.09	0.0%
		55	120.0	118.2	1.10	1.20	0.0%
		55	121.1	119.3	1.40	1.52	0.0%
		55	127.6	125.7	1.00	1.09	0.0%
		55	142.7	140.6	0.90	0.98	0.0%
		55	148.9	146.7	0.80	0.87	0.0%
Mundie2000	Sheep	37.5	95.5	94.1	5.00	6.22	0.0%
		37.5	116.3	114.6	5.00	6.22	0.0%
		37.5	131.9	129.9	5.00	6.22	0.0%
		37.5	147.6	145.4	5.00	6.22	0.0%
Phillips1988	Sheep	38.2	46.3	45.6	14.30	17.69	0.0%
		38.2	84.3	83.0	15.60	19.30	0.0%
		38.2	103.2	101.7	15.20	18.80	0.0%
		38.2	133.9	131.9	14.40	17.81	100.0%
		38.2	136.4	134.4	13.60	16.82	33.3%
Richmond1961	Dog	15.1	101.3	125.1	375.20	584.88	0.0%
		15.1	114.4	141.3	383.80	598.29	10.0%
		15.1	122.0	150.7	390.90	609.36	60.0%
		15.1	131.0	161.8	399.60	622.92	100.0%
	Goat	20.5	115.1	140.6	385.20	539.37	20.0%
		20.5	125.5	153.3	396.80	555.61	40.0%
		20.5	133.7	163.3	406.50	569.20	60.0%

	Species	Average Body Mass [kg]	Peak Incident Pressure [kPa]	Scaled Incident Pressure [kPa]	Duration [ms]	Scaled Duration [ms]	% Fatality
		20.5	139.9	170.9	410.80	575.22	80.0%
	Mouse	0.022	70.3	134.9	353.85	5460.78	17.5%
		0.022	75.1	144.1	361.64	5581.00	60.0%
		0.022	77.2	148.2	356.86	5507.24	26.7%
		0.022	91.7	176.0	368.72	5690.27	90.0%
		0.022	124.1	238.2	395.63	6105.55	100.0%
	Rabbit	1.97	63.4	124.5	346.07	1102.64	5.0%
		1.97	72.4	142.2	353.32	1125.74	35.7%
		1.97	84.1	165.2	363.41	1157.89	66.7%
		1.97	90.3	177.4	370.49	1180.44	85.0%
		1.97	98.6	193.7	377.40	1202.46	100.0%
Richmond1962a	Mouse	0.021	22.1	42.3	3.50	54.99	0.0%
		0.021	46.9	90.0	3.50	54.99	0.0%
		0.021	64.1	123.0	3.50	54.99	7.5%
		0.021	78.6	150.8	3.50	54.99	10.0%
		0.021	81.3	156.1	3.50	54.99	63.3%
		0.021	100.0	191.8	3.50	54.99	100.0%
		0.021	104.8	201.1	3.50	54.99	90.0%
		0.021	111.0	213.0	3.50	54.99	96.7%
		0.021	119.3	228.9	3.50	54.99	100.0%
	Rabbit	1.81	24.8	40.4	3.50	12.63	0.0%
		1.81	48.3	78.5	3.50	12.63	0.0%
		1.81	69.6	113.2	3.50	12.63	0.0%
		1.81	73.1	118.8	3.50	12.63	0.0%
		1.81	80.7	131.2	3.50	12.63	14.3%
		1.81	91.0	148.0	3.50	12.63	0.0%
		1.81	91.0	148.0	3.50	12.63	100.0%
		1.81	100.6	163.7	3.50	12.63	0.0%
		1.81	100.6	163.7	3.50	12.63	100.0%
		1.81	107.5	174.9	3.50	12.63	91.7%
		1.81	111.0	180.5	3.50	12.63	100.0%
Richmond1962b	Mouse	0.0238	60.7	118.1	2.20	32.79	5.0%
		0.0238	82.7	131.4	1.30	21.45	30.0%
		0.0238	84.1	133.6	2.00	33.00	90.0%
		0.0238	73.1	142.2	2.10	31.30	20.0%

251

	Species	Average Body Mass [kg]	Peak Incident Pressure [kPa]	Scaled Incident Pressure [kPa]	Duration [ms]	Scaled Duration [ms]	% Fatality
		0.0238	90.3	143.5	1.40	23.10	50.0%
		0.0238	92.4	146.8	0.63	10.39	21.9%
		0.0238	79.3	154.3	2.10	31.30	63.3%
		0.0238	108.2	172.0	0.57	9.40	54.2%
		0.0238	115.1	182.9	1.20	19.80	95.0%
		0.0238	120.6	191.7	0.47	7.75	79.4%
		0.0238	127.5	202.6	0.50	8.25	85.0%
		0.0238	209.5	333.0	0.42	6.93	12.5%
		0.0238	264.7	420.6	0.38	6.27	53.3%
		0.0238	299.2	475.4	0.41	6.76	60.7%
		0.0238	318.5	506.1	0.43	7.09	55.6%
		0.0238	337.1	535.6	0.40	6.60	88.9%
	Rabbit	1.9	81.3	132.3	6.80	24.12	0.0%
		1.9	85.5	139.0	3.60	12.77	10.0%
		1.9	88.2	143.5	3.60	12.77	20.0%
		1.9	91.0	148.0	6.80	24.12	80.0%
		1.9	95.1	154.7	6.80	24.12	50.0%
		1.9	98.6	160.3	3.60	12.77	45.0%
		1.9	110.3	179.4	3.40	12.06	70.0%
		1.9	132.3	215.2	1.40	4.96	42.9%
		1.9	140.6	228.7	1.40	4.96	50.0%
		1.9	166.1	270.2	1.20	4.26	50.0%
		1.9	170.9	278.0	1.40	4.96	88.9%
		1.9	172.3	280.2	1.20	4.26	75.0%
		1.9	179.9	292.6	0.90	3.19	33.3%
		1.9	193.0	313.9	1.00	3.55	90.0%
Richmond1966	Dog	15.7	25.5	31.5	334.00	513.58	0.0%
		15.7	38.6	47.7	334.00	513.58	0.0%
		15.7	52.4	64.7	334.00	513.58	0.0%
		15.7	65.5	80.9	334.00	513.58	0.0%
		15.7	74.4	91.9	334.00	513.58	0.0%
		16.5	77.2	95.4	54.00	81.60	0.0%
		15.7	85.5	105.6	334.00	513.58	0.0%
		16.5	103.3	105.7	15.00	24.91	11.1%
		16.5	89.2	110.2	21.00	31.73	12.5%

252

Species	Average Body Mass [kg]	Peak Incident Pressure [kPa]	Scaled Incident Pressure [kPa]	Duration [ms]	Scaled Duration [ms]	% Fatality
	16.5	95.2	117.6	400.00	604.43	0.0%
	16.5	115.4	118.0	15.00	24.91	22.2%
	16.5	98.3	121.4	21.00	31.73	20.0%
	16.5	121.4	124.2	15.00	24.91	55.6%
	16.5	101.6	125.5	79.00	119.38	14.3%
	16.5	103.3	127.6	54.00	81.60	11.1%
	16.5	104.6	129.2	400.00	604.43	10.0%
	16.5	108.5	134.0	34.00	51.38	40.0%
	16.5	131.8	134.8	15.00	24.91	55.6%
	16.5	110.5	136.5	79.00	119.38	33.3%
	16.5	112.0	138.4	400.00	604.43	60.0%
	16.5	113.3	140.0	21.00	31.73	45.5%
	16.5	116.7	144.2	79.00	119.38	66.7%
	16.5	118.0	145.8	21.00	31.73	66.7%
	16.5	120.8	149.2	400.00	604.43	90.0%
	16.5	123.5	152.6	21.00	31.73	80.0%
	16.5	154.8	158.3	5.00	8.30	9.1%
	16.5	169.0	172.9	4.60	7.64	37.5%
	16	178.8	182.9	4.60	7.72	50.0%
	16.5	179.7	183.8	4.60	7.64	50.0%
	16.5	190.1	194.4	3.90	6.48	66.7%
	16.5	209.9	214.7	2.10	3.49	12.5%
	16.5	333.4	341.0	1.70	2.82	77.8%
	16.5	379.9	388.6	1.50	2.49	75.0%
Goat	21.9	122.9	124.3	17.00	25.56	20.0%
	21.9	106.1	129.6	400.00	547.26	20.0%
	21.9	128.9	130.3	17.00	25.56	50.0%
	21.9	111.1	135.7	40.00	54.73	16.7%
	21.9	137.5	139.0	17.00	25.56	83.3%
	21.9	118.0	144.1	400.00	547.26	40.0%
	21.9	119.4	145.8	62.00	84.82	30.0%
	21.9	146.9	148.6	17.00	25.56	100.0%
	21.9	125.1	152.8	40.00	54.73	50.0%
	21.9	127.7	156.0	400.00	547.26	60.0%
	21.9	130.6	159.5	40.00	54.73	71.4%

	Species	Average Body Mass [kg]	Peak Incident Pressure [kPa]	Scaled Incident Pressure [kPa]	Duration [ms]	Scaled Duration [ms]	% Fatality
		21.9	131.8	161.0	400.00	547.26	80.0%
		21.9	134.4	164.2	40.00	54.73	85.7%
		21.9	194.7	196.9	4.40	6.62	20.0%
		21.9	205.7	208.0	4.40	6.62	60.0%
		22.7	207.0	209.3	4.40	6.53	50.0%
		21.9	214.1	216.5	4.40	6.62	60.0%
		21.9	398.7	403.2	1.50	2.26	50.0%
	Mouse	0.0207	51.6	99.0	337.00	5313.45	5.0%
		0.0207	55.3	106.1	337.00	5313.45	20.0%
		0.0207	68.3	131.1	337.00	5313.45	42.5%
		0.0207	73.6	141.2	337.00	5313.45	42.5%
		0.0207	81.7	156.8	337.00	5313.45	85.0%
	Rabbit	3.7	53.0	104.1	352.00	898.99	0.0%
		3.7	55.1	108.2	352.00	898.99	0.0%
		3.7	59.4	116.7	352.00	898.99	25.0%
		3.7	68.3	134.1	352.00	898.99	75.0%
		3.7	82.9	162.8	352.00	898.99	87.5%
	Sheep	53.6	124.2	147.8	212.00	211.85	50.0%
		53.3	289.2	284.9	2.90	3.19	50.0%
		53.3	302.1	297.6	3.60	3.96	38.9%
Richmond1981	Sheep	45	8.6	8.5	4.00	4.67	0.0%
		42	8.6	8.5	10.50	12.56	0.0%
		42	16.6	16.4	10.50	12.56	0.0%
		45	23.2	22.9	10.00	11.68	0.0%
		45	25.4	25.0	4.00	4.67	0.0%
		45	26.2	25.8	11.70	13.66	0.0%
		42	28.7	28.3	10.50	12.56	0.0%
		45	45.4	44.7	10.00	11.68	0.0%
		45	48.3	47.6	8.50	9.93	0.0%
		45	51.7	50.9	9.70	11.33	0.0%
		42	54.9	54.1	10.50	12.56	0.0%
		45	64.8	63.8	4.30	5.02	0.0%
		42	68.3	67.3	10.50	12.56	0.0%
		45	68.9	67.9	2.30	2.69	0.0%
		45	69.6	68.6	8.60	10.04	0.0%

	Species	Average Body Mass [kg]	Peak Incident Pressure [kPa]	Scaled Incident Pressure [kPa]	Duration [ms]	Scaled Duration [ms]	% Fatality
		45	68.3	81.3	100.00	106.25	0.0%
		45	93.7	92.3	1.70	1.99	0.0%
		42	94.8	93.4	10.50	12.56	0.0%
		45	87.0	103.5	100.00	106.25	16.7%
		45	116.5	114.8	3.80	4.44	0.0%
		42	117.2	115.4	10.50	12.56	0.0%
		45	127.5	125.6	3.60	4.20	0.0%
		42	133.1	131.1	10.50	12.56	20.0%
		45	153.0	150.7	1.40	1.63	0.0%
		45	156.5	154.2	3.60	4.20	0.0%
		45	204.0	200.9	1.10	1.28	0.0%
		45	265.4	261.4	1.80	2.10	0.0%
Rubovitch2011	Mouse	0.035	17.2	27.3	3.65	52.60	0.0%
		0.035	37.9	60.2	3.01	43.37	4.8%
Woods2013	Mouse	0.0275	17.7	28.1	3.65	57.23	0.0%
		0.0275	42.6	67.7	3.01	47.27	0.0%
Yang1996	Sheep	28.8	18.0	17.7	8.11	11.08	0.0%
		28.8	21.0	20.7	7.83	10.69	0.0%
		28.8	27.8	27.4	7.37	10.07	0.0%
		28.8	29.1	28.7	7.29	9.96	0.0%
		28.8	30.4	29.9	7.23	9.87	0.0%
		28.8	39.2	38.6	10.00	13.66	0.0%
		28.8	40.9	40.3	6.79	9.27	0.0%
		28.8	65.3	64.3	6.12	8.36	0.0%
		28.8	73.6	72.5	5.95	8.13	0.0%
		28.8	100.5	99.0	5.02	6.86	0.0%
		28.8	107.4	109.7	39.30	52.70	0.0%
		28.8	114.5	112.8	5.13	7.01	0.0%
		28.8	122.1	124.7	38.93	52.21	0.0%
		28.8	130.1	128.2	4.90	6.69	0.0%
		28.8	146.0	149.2	40.50	54.31	0.0%
		28.8	196.1	193.2	3.97	5.42	0.0%
Young1985	Sheep	38.2	76.1	75.0	12.40	15.34	0.0%
		38.2	77.0	75.8	12.90	15.96	0.0%

Appendix C – Blast Apnea Test Data

Table C-1: Details of studies included in blast apnea injury modeling

	Species	M_{body} [kg]	Shock Tube	Peak Incident Pressure [kPa]	Δt [ms]	Anesthesia	Apnea ?
1	Mouse	0.0241	3″ cylinder	225.74	0.94	Induction: 4.3% Isoflurane with FiO2 of 30% for 90s within anesthesia induction box	N
2	Mouse	0.0251		246.37	0.93		N
3	Mouse	0.0252		248.23	0.95		N
4	Mouse	0.028		243.88	0.95		N
5	Mouse	0.0286		247.53	0.97		N
6	Mouse	0.0289		233.7	0.97		N
7	Mouse	0.0265		244.96	0.92		N
8	Mouse	0.0243		243.4	0.95		N
9	Mouse	0.0275		235.66	0.95		N
10	Mouse	0.0246		225.91	0.92	Maintenance: 1.6% Isoflurane via endotracheal tube	N
11	Mouse	0.0244		228.05	0.97		N
12	Mouse	0.0254		245.81	0.94		N
13	Mouse	0.0292		252.21	0.72		N
14	Mouse	0.0288		224.32	0.68		N
15	Mouse	0.029		243.99	0.7		N
16	Mouse	0.0269		226.81	0.65	Measure of Depth: Toe pinch	N
17	Mouse	0.0268		258.36	0.71		N
18	Mouse	0.0286		237.02	0.67		N
19	Mouse	0.0312		262.37	0.7		N
20	Mouse	0.0303		222.8	0.68		N
21	Mouse	0.0273		244.81	0.68		N
22	Mouse	0.0266		256.05	0.7		N
23	Mouse	0.0293		222.93	0.65		N
24	Mouse	0.0285		242.95	0.67		N
25	Mouse	0.0262		266.99	0.74		N
26	Mouse	0.0276		262.68	0.74		N
27	Mouse	0.0257		234.25	0.66		N
28	Mouse	0.0265		241.81	0.69		N
29	Mouse	0.024		254.74	0.73		N

	Species	M_{body} [kg]	Shock Tube	Peak Incident Pressure [kPa]	Δt [ms]	Anesthesia	Apnea?
30	Mouse	0.0267	3″ cylinder	254.5	0.72	Induction: 4.3% Isoflurane with FiO2 of 30% for 90s within anesthesia induction box	N
31	Mouse	0.0245		264.14	0.74		N
32	Mouse	0.0258		239.5	0.66		N
33	Mouse	0.026		270.74	0.73		N
34	Mouse	0.0252		260.82	0.71		N
35	Mouse	0.0249		237.6	0.7		N
36	Mouse	0.0234		261.06	0.73		N
37	Mouse	0.0263		241.31	0.71		N
38	Mouse	0.0276		264.41	0.73		N
39	Mouse	0.0269		261.87	0.72	Maintenance: 1.6% Isoflurane via endotracheal tube	N
40	Mouse	0.0258		264.03	0.73		N
41	Mouse	0.0251		262.55	0.73		N
42	Mouse	0.0289		259.63	0.72		N
43	Mouse	0.0298		262.8	0.73		N
44	Mouse	0.0262		256.8	0.72		N
45	Mouse	0.0247		266	0.73	Measure of Depth: Toe pinch	N
46	Mouse	0.0254		255.23	0.74		N
47	Mouse	0.0223		241.87	0.69		N
48	Mouse	0.0269		254.4	0.72		N
49	Mouse	0.0255		258.32	0.72		N
50	Mouse	0.028		257.32	0.72		N
51	Mouse	0.0249		232.51	0.66		N
52	Mouse	0.0273		261.16	0.71		N
53	Mouse	0.0287		252.66	0.71		N
54	Mouse	0.0258		247.88	0.69		N
55	Mouse	0.0248		307.87	0.83		N
56	Mouse	0.023		303.31	0.85		N
57	Mouse	0.0264		267.68	0.8		N
58	Mouse	0.0232		260.06	0.75		N
59	Mouse	0.0277		241.44	0.72		N
60	Mouse	0.0245		245.72	0.76		N
61	Mouse	0.0261		265.72	0.8		N

	Species	M_{body} [kg]	Shock Tube	Peak Incident Pressure [kPa]	Δt [ms]	Anesthesia	Apnea ?
62	Mouse	0.0244	3″ cylinder	248.63	0.77	Induction: 4.3% Isoflurane with FiO2 of 30% for 90s within anesthesia induction box	N
63	Mouse	0.0288		251.81	0.79		N
64	Mouse	0.025		234.72	0.75		N
65	Mouse	0.0237		257.97	0.79		N
66	Mouse	0.0268		240.68	0.76		N
67	Mouse	0.0245		256.54	0.78		N
68	Mouse	0.0265		238.17	0.77		N
69	Mouse	0.028		245.46	0.78		N
70	Mouse	0.0256		248.08	0.79	Maintenance: 1.6% Isoflurane via endotracheal tube	N
71	Mouse	0.0246		249.52	0.81		N
72	Mouse	0.0234		250.85	0.78		N
73	Mouse	0.0304		215.77	0.71		N
74	Mouse	0.0316		238.36	0.76		N
75	Mouse	0.0272		240.46	0.77		N
76	Mouse	0.0246		241.55	0.76		N
77	Mouse	0.0266		233.14	0.83	Measure of Depth: Toe pinch	N
78	Mouse	0.0288		238.21	0.78		N
79	Mouse	0.031		251.63	0.85		N
80	Mouse	0.0289		244.33	0.76		N
81	Mouse	0.0299		235.73	0.77		N
82	Mouse	0.0269		231.27	0.75		N
83	Mouse	0.0257		237.27	0.77		N
84	Mouse	0.027		236.81	0.76		N
85	Mouse	0.0293		242.31	0.76		N
86	Mouse	0.0284		235.32	0.75		N
87	Mouse	0.0305		227.41	0.77		N
88	Mouse	0.0317		235.23	0.77		N
89	Mouse	0.0325		237.85	0.74		N
90	Mouse	0.031		233.59	0.75		N
91	Mouse	0.0266		217.04	0.71		N
92	Mouse	0.0297		233.73	0.76		N
93	Mouse	0.0316		233.2	0.8		N

	Species	M$_{body}$ [kg]	Shock Tube	Peak Incident Pressure [kPa]	Δt [ms]	Anesthesia	Apnea ?
94	Mouse	0.0301	3″ cylinder	229.53	0.74	Induction: 4.3% Isoflurane with FiO2 of 30% for 90s within anesthesia induction box Maintenance: 1.6% Isoflurane via endotracheal tube Measure of Depth: Toe pinch	N
95	Mouse	0.0337		255.98	0.78		N
96	Mouse	0.0327		265.23	0.81		N
97	Mouse	0.0322		251.62	0.75		N
98	Mouse	0.0307		264.59	0.79		N
99	Mouse	0.0298		252.26	0.74		N
100	Mouse	0.0246		264.7	0.8		N
101	Mouse	0.0261		243.73	0.7		N
102	Mouse	0.0256		260.57	0.76		N
103	Mouse	0.0245		257.82	0.76		N
104	Mouse	0.0256		253.99	0.76		N
105	Mouse	0.0292		232.95	0.79		N
106	Mouse	0.0315		229.92	0.76		N
107	Mouse	0.0262		243.8	0.79		N
108	Mouse	0.0278		238.21	0.77		N
109	Mouse	0.0296		234.3	0.74		N
110	Mouse	0.0279		246.33	0.73		N
111	Mouse	0.0308		228.19	0.75		N
112	Mouse	0.024		221.38	0.74		N
113	Mouse	0.0313		217.41	0.76		N
114	Mouse	0.0275		226.72	0.81		N
115	Mouse	0.0314		243.28	0.78		N
116	Mouse	0.0279		238.6	0.79		N
117	Mouse	0.0282		246.91	0.81		N
118	Mouse	0.0267		220.46	0.78		N
119	Mouse	0.0262		234.38	0.76		N
120	Mouse	0.0277		227.82	0.75		N
121	Mouse	0.0284		234.89	0.78		N
122	Mouse	0.0283		233.69	0.75		N
123	Mouse	0.0237		188.6	0.65		N
124	Mouse	0.0289		242.94	0.78		N
125	Mouse	0.0274		278.79	0.97		Y

	Species	M_{body} [kg]	Shock Tube	Peak Incident Pressure [kPa]	Δt [ms]	Anesthesia	Apnea ?
126	Mouse	0.0271	3″ cylinder	285.72	1.03	Induction: 4.3% Isoflurane with FiO2 of 30% for 90s within anesthesia induction box

Maintenance: 1.6% Isoflurane via endotracheal tube

Measure of Depth: Toe pinch | Y |
127	Mouse	0.0245		251.85	0.95		Y
128	Mouse	0.0256		250.77	0.94		Y
129	Mouse	0.0256		249.21	0.93		Y
130	Mouse	0.0261		246.61	0.9		Y
131	Mouse	0.0262		242.69	0.92		Y
132	Mouse	0.0256		244.61	0.91		Y
133	Mouse	0.0272		244.58	0.95		Y
134	Mouse	0.0274		257.89	0.71		Y
135	Mouse	0.0267		315.34	0.91		Y
136	Mouse	0.0284		319.41	0.89		Y
137	Mouse	0.0248		325.31	0.88		Y
138	Mouse	0.0252		298.39	0.84		Y
139	Mouse	0.0228		310.86	0.84		Y
140	Mouse	0.025		332.63	0.86		Y
141	Mouse	0.024		297.45	0.84		Y
142	Mouse	0.0277		272.88	0.82		Y
143	Mouse	0.0253		284.21	0.81		Y
144	Mouse	0.022		265.13	0.75		Y
145	Mouse	0.0243		268.7	0.78		Y
146	Mouse	0.0273		268.63	0.76		Y
147	Mouse	0.0294		248.62	0.73		Y
148	Mouse	0.026		254.86	0.71		Y
149	Mouse	0.0233		257.09	0.79		Y
150	Mouse	0.0245		253.51	0.78		Y
151	Mouse	0.0279		239.06	0.79		Y
152	Mouse	0.0321		262.49	0.88		Y
153	Mouse	0.0286		289.81	0.88		Y
154	Mouse	0.0262		246	0.82		Y
155	Mouse	0.027		238.65	0.76		Y
156	Mouse	0.0267		249.54	0.81		Y
157	Mouse	0.028		249.37	0.82		Y

	Species	M_{body} [kg]	Shock Tube	Peak Incident Pressure [kPa]	Δt [ms]	Anesthesia	Apnea?
158	Mouse	0.0296	3″ cylinder	236.49	0.78	See Above	Y
159	Mouse	0.0305		252.04	0.82		Y
160	Mouse	0.0272		233.96	0.75		Y
161	Mouse	0.027		226.34	0.75		Y
162	Mouse	0.0235		226.75	0.74		Y
163	Mouse	0.0267		219.07	0.75		Y
164	Mouse	0.0285		233.91	0.75		Y
165	Mouse	0.0287		241.41	0.75		Y
166	Mouse	0.026		225.1	0.74		Y
167	Rabbit	3.45	8″ cylinder	171.68	0.86	Rafaels 2011	N
168	Rabbit	4		183.22	0.86		N
169	Rabbit	3.85		168.5	1.23	Induction: Sodium	N
170	Rabbit	4.35		174.46	1.23	Pentobarbital 25mg/kg	N
171	Rabbit	3.9		633.98	1.7		Y
172	Rabbit	4.5		706.86	1.81		Y
173	Rabbit	5.75		809.83	1.93	Maintenance:	Y
174	Rabbit	3.98		358.42	1.31	150mg/kg	Y
175	Rabbit	3.65		1006.19	2.39		Y
176	Rabbit	4		1084.65	2.39	Measure of Depth:	Y
177	Rabbit	4.2		788.81	2.04	Diminished	Y
178	Rabbit	4.25		729.23	1.93	palpebral	Y
179	Rabbit	4.1		835.62	1.93	reflex	Y
180	Ferret	1.18	8″ cylinder	99.74	0.68	Rafaels 2012	N
181	Ferret	1.27		613.18	1.06	Induction:	N
182	Ferret	1.32		232.98	3.72	Urethane	N
183	Ferret	1.3		99.74	0.68	1500mg/kg	N
184	Ferret	1.27		613.18	1.06	Maintenance: Urethane	N
185	Ferret	1		613.18	1.06	150mg/kg	N
186	Ferret	1		646.64	1.86	Measure of	N
187	Ferret	1		302.68	4.43	Depth: Jaw	N
188	Ferret	1		540.28	1.97	tension/toe	N
189	Ferret	1.1		233.46	3.72	pinch	N

	Species	M_{body} [kg]	Shock Tube	Peak Incident Pressure [kPa]	Δt [ms]	Anesthesia	Apnea ?
190	Ferret	0.9	8″ cylinder	429.95	1.56	Rafaels 2012	N
191	Ferret	1		486.41	0.95		N
192	Ferret	1.1		397.66	0.95	Induction:	N
193	Ferret	1.4		456.91	1.56	Urethane	N
194	Ferret	1.36		484.87	1	1500mg/kg	N
195	Ferret	1.36		559.14	1	Maintenance:	N
196	Ferret	1.45		132.63	2.51	Urethane	N
197	Ferret	1.36		134.04	2.51	150mg/kg	N
198	Ferret	1.36		240.23	0.9		N
199	Ferret	1.36		204.09	0.9	Measure of	N
200	Ferret	1.18		344.05	0.86	Depth: Jaw	N
201	Ferret	1.14		328.4	0.86	tension/toe	N
202	Ferret	1.27		156.46	2.51	pinch	N
203	Ferret	1.5		169.12	0.9		N
204	Ferret	1.45		430.78	1.56		N
205	Ferret	1.59		334.32	0.86		N
206	Ferret	1.41		423.55	0.95		N
207	Ferret	1.4		533.64	1		N
208	Ferret	1.4		537.55	1.05		N
209	Ferret	1.59		393.6	0.91		N
210	Ferret	1.6		419.29	0.91		N
211	Ferret	1.7		420.63	0.91		N
212	Ferret	1.6		451.68	0.95		N
213	Ferret	1.09		646.64	1.86		Y
214	Ferret	1		794.48	2.14		Y
215	Ferret	1		831.53	2.21		Y
216	Ferret	1.08		794.48	2.14		Y
217	Ferret	1.2		308.39	4.94		Y
218	Ferret	0.9		298.6	4.43		Y
219	Ferret	1		731.36	2.14		Y
220	Ferret	1.1		283.69	4.43		Y
221	Ferret	1		297.39	4.43		Y

	Species	M_{body} [kg]	Shock Tube	Peak Incident Pressure [kPa]	Δt [ms]	Anesthesia	Apnea ?
222	Ferret	0.9	8″ cylinder	308.39	4.94	Rafaels 2012	Y
223	Ferret	1		540.28	1.97		Y
224	Ferret	1		620.93	2.06	Induction: Urethane 1500mg/kg	Y
225	Ferret	0.9		540.28	1.97		Y
226	Ferret	0.8		620.93	2.06		Y
227	Ferret	1		435.14	2.06	Maintenance:	Y
228	Ferret	0.95		206.07	3.72	Urethane	Y
229	Ferret	0.86		302.68	4.43	150mg/kg	Y
230	Ferret	0.9		628.02	1.09		Y
231	Ferret	0.95		620.84	1.08	Measure of Depth: Jaw tension/toe pinch	Y
232	Ferret	0.9		549.38	1.06		Y
233	Ferret	1		621.59	1.86		Y
234	Ferret	0.97		698.45	1.11		Y
235	Ferret	0.9		754.43	1.11		Y
236	Ferret	1.36		485.11	1.05		Y
237	Ferret	1.36		575.99	1.05		Y
238	Ferret	1.25		503.33	1.03		Y
239	Ferret	1.27		539.17	1.03		Y
240	Ferret	1.5		509.9	1.03		Y
241	Ferret	1.5		683.73	1.05		Y
242	Ferret	1.64		678.85	1.08		Y
243	Ferret	1.45		720.73	1.09		Y
244	Ferret	1.64		774.55	1.11		Y

	Species	M_{body} [kg]	Shock Tube	Peak Incident Pressure [kPa]	Δt [ms]	Anesthesia	Apnea?
245	Ferret	1.5	8″ cylinder	339.1	1.3	Induction: Ketamine 5mg/kg, Dexmedet-omidine 80μg/kg Maintenance: Induction only Measure of Depth: Jaw tension/toe pinch	N
246	Ferret	1.63		339.1	1.3		N
247	Ferret	1.72		339.1	1.3		N
248	Ferret	1.7		339.1	1.3		N
249	Pig	61.4	12″ cylinder	182.91	2.04	Shridharani 2012 Induction: Telazol 4.4mg/kg, Xylazine 2.2mg/kg Maintenance: Propofol 4.8mg/kg/hr Measure of Depth: Diminished palpebral reflex	N
250	Pig	59		232.2	3.05		N
251	Pig	59		182.91	2.04		N
252	Pig	59		111.07	1.8		N
253	Pig	56.8		273.6	8.03		N
254	Pig	59		273.6	8.03		N
255	Pig	61.4		273.6	8.03		N
256	Pig	55.5		232.2	3.05		N
257	Pig	54.5		492.9	2.88		N
258	Pig	56		492.9	2.88		N
259	Pig	50		492.9	2.88		N
260	Pig	91		232.2	3.05		N
261	Pig	70.5		259.62	3.52		Y
262	Pig	70		823.6	3.44		Y
263	Pig	75		893.9	3.88		Y
264	Pig	56.8		259.62	3.52		Y
265	Pig	59		259.62	3.52		Y
266	Pig	57		273.6	8.03		Y

Appendix D – Blast Neurotrauma Test Data

Table D-1: Details of studies included in blast neurotrauma injury modeling

	Species	M$_{body}$ [kg]	Peak Incident Pressure [kPa]	Scaled Incident Pressure [kPa]	Duration [ms]	Scaled Duration [ms]	Fatality?
Garman 2011	Rat	0.388	241.3	394.3	4.00	27.57	N
			241.3	394.3	4.00	27.57	N
			241.3	394.3	4.00	27.57	N
			241.3	394.3	4.00	27.57	N
			241.3	394.3	4.00	27.57	N
			241.3	394.3	4.00	27.57	N
			241.3	394.3	4.00	27.57	N
			241.3	394.3	4.00	27.57	N
			241.3	394.3	4.00	27.57	N
			241.3	394.3	4.00	27.57	N
			241.3	394.3	4.00	27.57	N
			241.3	394.3	4.00	27.57	N
			241.3	394.3	4.00	27.57	N
			241.3	394.3	4.00	27.57	N
			241.3	394.3	4.00	27.57	N
			241.3	394.3	4.00	27.57	N
			241.3	394.3	4.00	27.57	N
			241.3	394.3	4.00	27.57	Y
			241.3	394.3	4.00	27.57	Y
			241.3	394.3	4.00	27.57	Y
			241.3	394.3	4.00	27.57	Y
Goldstein 2012	Mouse	0.02	77.0	151.4	4.80	68.50	N
			77.0	151.4	4.80	68.50	N
			77.0	151.4	4.80	68.50	N
			77.0	151.4	4.80	68.50	N
			77.0	151.4	4.80	68.50	N
			77.0	151.4	4.80	68.50	N
			77.0	151.4	4.80	68.50	N
			77.0	151.4	4.80	68.50	N
			77.0	151.4	4.80	68.49	N
			77.0	151.4	4.80	68.49	N

	Species	M_{body} [kg]	Peak Incident Pressure [kPa]	Scaled Incident Pressure [kPa]	Duration [ms]	Scaled Duration [ms]	Fatality?
Goldstein 2012	Mouse	0.02	77.0	151.4	4.80	68.49	N
			77.0	151.4	4.80	68.49	N
			77.0	151.4	4.80	68.49	N
			77.0	151.4	4.80	68.49	N
			77.0	151.4	4.80	68.49	N
			77.0	151.4	4.80	68.49	N
			77.0	151.4	4.80	68.49	N
			77.0	151.4	4.80	68.49	N
			77.0	151.4	4.80	68.49	N
			77.0	151.4	4.80	68.49	N
			77.0	151.4	4.80	68.49	N
			77.0	151.4	4.80	68.49	N
Rafaels 2011	Rabbit	3.85	168.5	248.0	1.23	5.63	N
		3.45	171.7	252.7	1.19	5.43	N
		4.35	174.5	256.9	1.23	5.63	N
		4	183.2	269.7	1.23	5.64	N
		3.9	634.0	933.2	1.70	7.75	N
		4.5	706.9	1040.5	1.81	8.28	N
		4.25	729.2	1073.3	1.93	8.81	Y
		4.2	788.8	1161.1	2.04	9.34	Y
		5.75	809.8	1192.0	1.93	8.80	N
		4.1	835.6	1229.9	1.93	8.81	Y
		3.65	1006.2	1481.1	2.39	10.91	Y
		4	1084.6	1596.5	2.39	10.92	Y
Rafaels 2012	Ferret	1.3	97.5	148.9	0.66	3.49	N
		1.18	97.5	148.9	0.66	3.49	N
		1.45	129.3	197.4	2.43	12.80	N
		1.36	130.3	198.9	2.42	12.75	N
		1.27	154.0	235.1	2.45	12.92	N
		1.5	164.9	251.7	0.87	4.59	N
		0.95	197.2	300.9	2.74	14.47	N
		1.36	197.6	301.6	0.87	4.58	N
		1.1	225.3	343.8	3.06	16.11	N
		1.32	225.5	344.2	3.60	18.96	N
		1.36	234.3	357.6	0.87	4.59	N

	Species	M_{body} [kg]	Peak Incident Pressure [kPa]	Scaled Incident Pressure [kPa]	Duration [ms]	Scaled Duration [ms]	Fatality?
Rafaels 2012	Ferret	1.1	275.8	421.0	4.27	22.52	N
		1	286.9	438.0	3.64	19.18	N
		0.9	289.1	441.2	4.28	22.58	Y
		0.86	291.0	444.1	3.38	17.85	Y
		0.9	297.6	454.2	4.05	21.36	Y
		1.2	303.6	463.3	4.82	25.41	Y
		1.14	320.2	488.8	0.83	4.40	N
		1.59	326.9	498.9	0.84	4.42	N
		1.18	335.5	512.1	0.83	4.40	N
		1.59	383.8	585.8	0.88	4.64	N
		1.1	384.9	587.6	0.92	4.83	N
		1.6	408.8	624.1	0.88	4.64	N
		1.7	410.2	626.0	0.88	4.64	N
		1.41	413.0	630.4	0.92	4.83	N
		0.9	413.3	630.9	1.19	6.27	N
		1	418.3	638.5	1.57	8.30	N
		1.45	421.2	642.9	1.51	7.97	N
		1.6	440.4	672.3	0.92	4.83	N
		1.4	445.5	680.0	1.50	7.93	N
		1.36	471.5	719.6	0.97	5.10	N
		1.36	471.7	720.0	1.01	5.31	N
		1	473.0	721.9	0.91	4.81	N
		1.25	491.3	749.9	0.99	5.24	N
		1.5	495.8	756.8	0.99	5.21	N
		1	513.3	783.5	1.36	7.15	N
		1	513.3	783.5	1.36	7.15	Y
		0.9	516.9	789.0	1.45	7.66	N
		1.4	518.9	792.0	0.97	5.10	N
		1.4	520.4	794.3	1.01	5.33	N
		0.9	523.7	799.3	0.75	3.97	N
		1.27	524.3	800.2	0.99	5.21	N
		1.36	545.2	832.2	0.97	5.12	N
		1.36	563.2	859.6	1.02	5.36	N
		1	591.9	903.4	1.46	7.69	Y
		1	593.6	906.0	1.03	5.41	N

	Species	M_{body} [kg]	Peak Incident Pressure [kPa]	Scaled Incident Pressure [kPa]	Duration [ms]	Scaled Duration [ms]	Fatality?
Rafaels 2012	Ferret	0.8	594.1	906.8	1.52	8.02	N
		0.95	596.8	911.0	0.82	4.34	N
		1	597.6	912.1	1.42	7.49	N
		1.27	597.9	912.6	1.03	5.42	N
		1.27	599.5	915.1	1.03	5.45	N
		0.9	603.7	921.5	0.83	4.40	N
		1	624.6	953.4	1.67	8.81	N
		1.09	628.8	959.7	1.79	9.45	N
		1.64	661.9	1010.4	1.04	5.50	N
		1.5	668.5	1020.4	1.02	5.36	N
		0.97	677.4	1034.0	1.07	5.62	N
		1.45	702.8	1072.7	1.06	5.57	N
		1	706.4	1078.3	1.92	10.14	N
		0.9	733.6	1119.7	1.07	5.62	N
		1.64	753.1	1149.6	1.07	5.62	N
		1	769.1	1173.9	2.07	10.91	N
		1.08	776.8	1185.7	2.08	10.97	N
		1	818.5	1249.3	2.16	11.39	Y
Shridharani 2012	Pig	59	107.0	134.3	1.21	2.96	N
		59	177.0	222.1	2.04	4.98	N
		59	177.0	222.1	2.53	6.18	N
		61	186.0	233.4	2.03	4.96	N
		59	227.0	284.9	2.53	6.18	N
		59	233.0	292.4	5.26	12.85	N
		90	234.0	293.7	2.53	6.18	N
		56	239.0	299.9	2.54	6.20	N
		70	242.0	303.7	3.51	8.57	N
		59	250.0	313.7	3.52	8.60	N
		57	260.0	326.3	3.53	8.62	N
		59	269.0	337.6	6.41	15.66	N
		61	272.0	341.4	6.40	15.63	N
		57	274.0	343.9	6.42	15.68	N
		57	278.0	348.9	6.43	15.70	N
		59	473.0	593.6	2.87	7.01	N
		51	501.0	628.7	2.88	7.03	N

	Species	M_{body} [kg]	Peak Incident Pressure [kPa]	Scaled Incident Pressure [kPa]	Duration [ms]	Scaled Duration [ms]	Fatality?
Shridharani 2012	Pig	55	501.0	628.7	2.89	7.06	N
		56	525.0	658.9	2.88	7.03	N
		70	741.0	929.9	3.44	8.40	N
Yu2012	Mouse	0.030	215.8	424.2	0.71	10.13	N
		0.027	217.0	426.7	0.71	10.13	N
		0.031	227.4	447.1	0.77	10.99	N
		0.030	229.5	451.3	0.74	10.56	N
		0.032	229.9	452.0	0.76	10.85	N
		0.027	231.3	454.7	0.75	10.70	N
		0.029	233.0	458.0	0.79	11.27	N
		0.027	233.1	458.4	0.83	11.84	N
		0.032	233.2	458.5	0.80	11.42	N
		0.031	233.6	459.3	0.75	10.70	N
		0.030	233.7	459.5	0.76	10.85	N
		0.025	234.7	461.5	0.75	10.70	N
		0.032	235.2	462.5	0.77	10.99	N
		0.028	235.3	462.7	0.75	10.70	N
		0.030	235.7	463.5	0.77	10.99	N
		0.027	236.8	465.6	0.76	10.85	N
		0.026	237.3	466.5	0.77	10.99	N
		0.033	237.9	467.6	0.74	10.56	N
		0.027	238.2	468.3	0.77	10.99	N
		0.029	238.2	468.3	0.78	11.13	N
		0.032	238.4	468.6	0.76	10.85	N
		0.028	239.1	470.0	0.79	11.27	Y
		0.027	240.5	472.8	0.77	10.99	N
		0.027	240.7	473.2	0.76	10.85	N
		0.025	241.6	474.9	0.76	10.85	N
		0.029	242.3	476.4	0.76	10.85	N
		0.026	243.7	479.2	0.70	9.99	N
		0.029	244.3	480.4	0.76	10.85	N
		0.028	245.5	482.6	0.78	11.13	N
		0.025	245.7	483.1	0.76	10.85	N
		0.026	248.1	487.8	0.79	11.27	N
		0.024	248.6	488.8	0.77	10.99	N

	Species	M$_{body}$ [kg]	Peak Incident Pressure [kPa]	Scaled Incident Pressure [kPa]	Duration [ms]	Scaled Duration [ms]	Fatality?
Yu2012	Mouse	0.025	249.5	490.6	0.81	11.56	N
		0.023	250.9	493.2	0.78	11.13	N
		0.032	251.6	494.7	0.75	10.70	N
		0.031	251.6	494.7	0.85	12.13	N
		0.029	251.8	495.1	0.79	11.27	N
		0.030	252.3	496.0	0.74	10.56	N
		0.025	253.5	498.4	0.78	11.13	Y
		0.026	254.0	499.4	0.76	10.85	N
		0.034	256.0	503.3	0.78	11.13	N
		0.025	256.5	504.4	0.78	11.13	N
		0.023	257.1	505.5	0.79	11.27	Y
		0.025	257.8	506.9	0.76	10.85	N
		0.024	258.0	507.2	0.79	11.27	N
		0.026	260.6	512.3	0.76	10.85	N
		0.031	264.6	520.2	0.79	11.27	N
		0.025	264.7	520.4	0.80	11.42	N
		0.033	265.2	521.5	0.81	11.56	N
		0.026	265.7	522.4	0.80	11.42	N

References

Alley, MD, Schimizze, BR and Son, SF. 2011. "Experimental modeling of explosive blast-related traumatic brain injuries." *NeuroImage* 54: S45-S54.

Anonymous. 1915. "An epitome of current medical literature: Rupture of lungs caused by bursting of a shell without external wound." *British Medical Journal* 1, 2834: E33-E44.

Arbogast, KB and Margulies, SS. 1997. "Regional differences in mechanical properties of the porcine central nervous system." Paper presented at 41st Stapp Car Crash Conference, Lake Buena Vista, FL, November 2007.

Arbogast, KB and Margulies, SS. 1998. "Material characterization of the brainstem from oscillatory shear tests." *Journal of Biomechanics* 31, 9: 801-07.

Armstrong, E. 1982. "A look at relative brain size in mammals." *Neuroscience Letters* 34, 2: 101-04.

Arun, P, Oguntayo, S, Alamneh, Y, Honnold, C, Wang, Y, Valiyaveettil, M, Long, JB and Nambiar, MP. 2012. "Rapid release of tissue enzymes into blood after blast exposure: potential use as biological dosimeters." *PloS ONE* 7, 4: e33798.

ASTM. 2007. *Standard Test Methods for Rubber Properties in Compression*. ASTM International,

Atay, SM, Kroenke, CD, Sabet, A and Bayly, PV. 2008. "Measurement of the Dynamic Shear Modulus of Mouse Brain Tissue In Vivo by Magnetic Resonance Elastography." *Journal of Biomechanical Engineering* 130, 2: 021013-13.

Azevedo, FA, Carvalho, LR, Grinberg, LT, Farfel, JM, Ferretti, RE, Leite, RE, Lent, R and Herculano-Houzel, S. 2009. "Equal numbers of neuronal and nonneuronal cells make the human brain an isometrically scaled-up primate brain." *Journal of Comparative Neurology* 513, 5: 532-41.

Bagalman, E. 2013. *Traumatic Brain Injury Among Veterans*. Congressional Reseach Service.

Bain, AC and Meaney, DF. 2000. "Tissue-Level Thresholds for Axonal Damage in an Experimental Model of Central Nervous System White Matter Injury." *Journal of Biomechanical Engineering* 122, 6: 615-22.

Baker, WE. 1973. *Explosions in air*. Austin, TX: University of Texas Press.

Bass, CR, Davis, M, Rafaels, K, Rountree, MS, Harris, RM, Sanderson, E, Andrefsky, W, DiMarco, G and Zielinski, M. 2005. "A methodology for assessing blast protection in explosive ordnance disposal bomb suits." *International Journal of Occupational Safety and Ergonomics* 11, 4: 347-61.

Bass, CR, Panzer, MB, Rafaels, KA, Wood, G, Shridharani, J and Capehart, B. 2012. "Brain Injuries from Blast." *Annals of Biomedical Engineering* 40, 1: 18.

Bass, CR, Planchak, CJ, Salzar, RS, Lucas, SR, Rafaels, KA, Shender, BS and Paskoff, G. 2007. "The Temperature-Dependent Viscoelasticity of Porcine Lumbar Spine Ligaments." *Spine* 32, 16: E436-E42.

Bass, CR, Rafaels, KA and Salzar, RS. 2008. "Pulmonary Injury Risk Assessment for Short-Duration Blasts." *The Journal of Trauma and Acute Care Surgery* 65, 3: 604-15.

Bell, MK. 2008. "Standardized model is needed to study the neurological effects of primary blast wave exposure." *Military Medicine* 173, 6: v-viii.

Bilston, LE, Liu, Z and Phan-Thien, N. 1997. "Linear viscoelastic properties of bovine brain tissue in shear." *Biorheology* 34, 6: 377-85.

Bogo, V, Hutton, R and Bruner, A. 1971. *The Effects of Airblast on Discriminated Avoidance Behavior in Rhesus Monkeys*. Lovelace Foundation for Medical Education and Research, Albuquerque, NM.

Bolander, R, Mathie, B, Bir, C, Ritzel, D and VandeVord, P. 2011. "Skull Flexure as a Contributing Factor in the Mechanism of Injury in the Rat when Exposed to a Shock Wave." *Annals of Biomedical Engineering* 39, 10: 2550-59.

Bowen, I and Fletcher, ER, DR. 1968. *Estimate of Man's Tolerance to the Direct Effects of Air Blast*. Lovelace Foundation for Medical Education and Research, Albuquerque, NM.

Bowen, I, Holladay, A, Fletcher, E, Richmond, D and White, C. 1965. *A Fluid-Mechanical Model of the Thoraco-Abdominal System with Applications to Blast Biology*. Lovelace Foundation for Medical Education and Research, Albuquerque, NM.

Boxenbaum, H. 1982. "Interspecies scaling, allometry, physiological time, and the ground plan of pharmacokinetics." *Journal of Pharmacokinetics and Pharmacodynamics* 10, 2: 201-27.

Boxenbaum, H. 1984. "Interspecies Pharmacokinetic Scaling and the Evolutionary-Comparative Paradigm." *Drug Metabolism Reviews* 15, 5-6: 1071-121.

Brands, DW, Bovendeerd, PH, Peters, GW, Wismans, JS, Paas, MH and van Bree, JL. 1999. "Comparison of the dynamic behavior of brain tissue and two model materials." Paper presented at 33rd Stapp Car Crash Conference, San Diego, CA

Brenner, LA, Ivins, BJ, Schwab, K, Warden, D, Nelson, LA, Jaffee, M and Terrio, H. 2010. "Traumatic Brain Injury, Posttraumatic Stress Disorder, and Postconcussive Symptom Reporting Among Troops Returning From Iraq." *The Journal of Head Trauma Rehabilitation* 25, 5: 307-12.

Brolén, P, Örtenwall, P, Österhed, H and Brändström, H. 2007. "KAMEDO Report 89: Terrorist Attack in Bali, 2002." *Prehospital and Disaster Medicine* 22, 03: 246-50.

Calder, WA. 1981. "Scaling of Physiological Processes in Homeothermic Animals." *Annual Review of Physiology* 43, 1: 301-22.

Capehart, B and Bass, D. 2012. "Review: managing posttraumatic stress disorder in combat veterans with comorbid traumatic brain injury." *Journal of Rehabilitation Resesearch and Development* 49, 5: 789-812.

Celander, H, Clemedson, C-J, Ericsson, UA and Hultman, HI. 1955a. "The Use of a Compressed Air Operated Shock Tube for Physiological Blast Research." *Acta Physiologica Scandinavica* 33, 1: 6-13.

Celander, H, Clemendson, C-J, Ericsson, UA and Hultman, HE. 1955b. "A Study on the Relation between the Duration of a Shock Wave and the Severity of the Blast Injury Produced by It." *Acta Physiologica Scandinavica* 33, 1: 14-18.

Cernak, I, Merkle, AC, Koliatsos, VE, Bilik, JM, Luong, QT, Mahota, TM, Xu, L, Slack, N, Windle, D and Ahmed, FA. 2011. "The pathobiology of blast injuries and blast-induced neurotrauma as identified using a new experimental model of injury in mice." *Neurobiology of Disease* 41, 2: 538-51.

Cernak, I, Savic, J, Ignjatovic, D and Jevtic, M. 1999. "Blast Injury from Explosive Munitions." *The Journal of Trauma and Acute Care Surgery* 47, 1: 96-103.

Cernak, I, Savic, J, Malicevic, Z, Zunic, G, Radosevic, P, Ivanovic, I and Davidovic, L. 1996. "Involvement of the Central Nervous System in the General Response to Pulmonary Blast Injury." *The Journal of Trauma and Acute Care Surgery* 40, 3S: 100S-04S.

Cernak, I, Wang, Z, Jiang, J, Bian, X and Savic, J. 2001a. "Cognitive deficits following blast injury-induced neurotrauma: possible involvement of nitric oxide." *Brain Injury* 15, 7: 593-612.

Cernak, I, Wang, Z, Jiang, J, Bian, X and Savic, J. 2001b. "Ultrastructural and Functional Characteristics of Blast Injury-Induced Neurotrauma." *The Journal of Trauma and Acute Care Surgery* 50, 4: 695-706.

Champion, HR, Holcomb, JB and Young, LA. 2009. "Injuries From Explosions: Physics, Biophysics, Pathology, and Required Research Focus." *Journal of Trauma and Acute Care Surgery* 66, 5: 1468-77.

Chatelin, S, Constantinesco, A and Willinger, R. 2010. "Fifty years of brain tissue mechanical testing: From in vitro to in vivo investigations." *Biorheology* 47, 5: 255-76.

Chavko, M, Koller, WA, Prusaczyk, WK and McCarron, RM. 2007. "Measurement of blast wave by a miniature fiber optic pressure transducer in the rat brain." *Journal of Neuroscience Methods* 159, 2: 277-81.

Chavko, M, Prusaczyk, WK and McCarron, RM. 2006. "Lung Injury and Recovery After Exposure to Blast Overpressure." *The Journal of Trauma and Acute Care Surgery* 61, 4: 933-42.

Chavko, M, Watanabe, T, Adeeb, S, Lankasky, J, Ahlers, ST and McCarron, RM. 2011. "Relationship between orientation to a blast and pressure wave propagation inside the rat brain." *Journal of Neuroscience Methods* 195, 1: 61-66.

Cheng, S, Clarke, EC and Bilston, LE. 2008. "Rheological properties of the tissues of the central nervous system: A review." *Medical Engineering & Physics* 30, 10: 1318-37.

Chua, W and Oyen, M. 2009. "Viscoelastic Properties of Membranes Measured by Spherical Indentation." *Cellular and Molecular Bioengineering* 2, 1: 49-56.

Clemedson, C-J. 1953. "Respiration and Pulmonary Gas Exchange in Blast Injury." *Journal of Applied Physiology* 6, 4: 213-20.

Clemedson, C-J and Pettersson, H. 1955. "Propagation of a High Explosive Air Shock Wave Through Different Parts of an Animal Body." *American Journal of Physiology -- Legacy Content* 184, 1: 119-26.

Clifford, C, Jaeger, J, Moe, J and Hess, J. 1984. "Gastrointestinal lesions in lambs due to multiple low-level blast overpressure exposure." *Military Medicine* 149, 9: 491.

Coats, B and Margulies, SS. 2006. "Material properties of porcine parietal cortex." *Journal of Biomechanics* 39, 13: 2521-25.

Cooper, GJ. 1996. "Protection of the Lung from Blast Overpressure by Thoracic Stress Wave Decouplers." *The Journal of Trauma and Acute Care Surgery* 40, 3S: 105S-10S.

Coronado, VG, Xu, L, Basavaraju, SV, McGuire, LC, Wald, MM, Faul, MD, Guzman, BR and Hemphill, JD. 2011. *Surveillance for traumatic brain injury-related deaths: United States, 1997-2007*. Atlanta, GA: US Department of Health and Human Services, Centers for Disease Control and Prevention.

Cripps, NPJ and Cooper, GJ. 1996. "The Influence of Personal Blast Protection on the Distribution and Severity of Primary Blast Gut Injury." *The Journal of Trauma and Acute Care Surgery* 40, 3S: 206S-11S.

Crosfill, ML and Widdicombe, JG. 1961. "Physical characteristics of the chest and lungs and the work of breathing in different mammalian species." *The Journal of Physiology* 158, 1: 1-14.

Dalle Lucca, JJ, Chavko, M, Dubick, MA, Adeeb, S, Falabella, MJ, Slack, JL, McCarron, R and Li, Y. 2012. "Blast-induced moderate neurotrauma (BINT) elicits early complement activation and tumor necrosis factor alpha (TNFα) release in a rat brain." *Journal of the neurological sciences* 318, 1: 146-54.

Damon, E, Yelverton, J, Luft, U, Mitchell, K and Jones, R. 1970. *The Acute Effects of Air Blast on Pulmonary Function in Dogs and Sheep*. Lovelace Foundation for Medical Education and Research, Albuquerque, NM.

Damon, EG, Gaylord, CS, Hicks, W, Yelverton, JT and Richmond, DR. 1966. *The Effect of Ambient Pressure on Tolerance of Mammals to Air Blast*. Lovelace Foundation for Medical Education and Research, Albuquerque, NM.

Damon, EG, Richmond, DR and White, CS. 1964. *The effects of ambient pressure on the tolerance of mice to air blast*. Lovelace Foundation for Medical Education and Research, Albuquerque, NM.

Darvish, K and al., e. 1999. "A Nonlinear Viscoelastic Model for Polyurethane Foams." *Journal of Materials and Manufacturing* 108: 209-15.

Darvish, KK and Crandall, J. 2002. "A parametric study on the effects of the peripheral cerebrospinal fluid on finite element model of brain injury." Paper presented at 21st Southern Biomedical Engineering Conference, Bethesda, MD

Darvish, KK and Crandall, JR. 2001. "Nonlinear viscoelastic effects in oscillatory shear deformation of brain tissue." *Medical Engineering and Physics* 23, 9: 633-45.

DASA. 1965. *Biomedical program 500-ton explosion*. Defense Atomic Support Agency, Washington, DC.

de Lanerolle, NC, Bandak, F, Kang, D, Li, AY, Du, F, Swauger, P, Parks, S, Ling, G and Kim, JH. 2011. "Characteristics of an Explosive Blast-Induced Brain Injury in an Experimental Model." *Journal of Neuropathology & Experimental Neurology* 70, 11: 1046-57.

Denes, A, Thornton, P, Rothwell, NJ and Allan, SM. 2010. "Inflammation and brain injury: Acute cerebral ischaemia, peripheral and central inflammation." *Brain, Behavior, and Immunity* 24, 5: 708-23.

Dickie, RA and Smith, TL. 1971. "Viscoelastic Properties of a Rubber Vulcanizate Under Large Deformations in Equal Biaxial Tension, Pure Shear, and Simple Tension." *Journal of Rheology* 15, 1: 91-110.

Dodd, K, Yelverton, J, Richmond, D, Morris, J and Ripple, G. 1989. *Nonauditory Injury Threshold for Repeated Intense Freefield Impulse Noise*. Walter Reed Army Institute of Research, Washington, DC.

Draeger, RH, Barr, JS and Sager, WW. 1946. "Blast Injury." *JAMA: The Journal of the American Medical Association* 132, 13: 762-67.

Elias, PZ and Spector, M. 2012. "Viscoelastic characterization of rat cerebral cortex and type I collagen scaffolds for central nervous system tissue engineering." *Journal of the Mechanical Behavior of Biomedical Materials* 12, 0: 63-73.

Elkin, BS, Azeloglu, EU, Costa, KD and Morrison, B, 3rd. 2007a. "Mechanical heterogeneity of the rat hippocampus measured by atomic force microscope indentation." *Journal of Neurotrauma* 24, 5: 812-22.

Elkin, BS, Ilankovan, A and Morrison, IIIB. 2009. "Age-Dependent Regional Mechanical Properties of the Rat Hippocampus and Cortex." *Journal of Biomechanical Engineering* 132, 1: 011010-10.

Elkin, BS, Ilankovan, AI and Morrison, B. 2011. "A Detailed Viscoelastic Characterization of the P17 and Adult Rat Brain." *Journal of Neurotrauma* 28, 11: 2235-44.

Elkin, BS and Morrison III, B. 2007b. "Region-specific tolerance criteria for the living brain." *Stapp Car Crash Journal* 51: 127-38.

Eppinger, R. 1976. "Prediction of thoracic injury using measurable experimental parameters." Paper presented at Sixth International Technical Conference on Experimental Safety Vehicles, NHTSA, Washington, DC

Eppinger, R, Sun, E, Bandak, F, Haffner, M, Khaewpong, N, Maltese, M, Kuppa, S, Nguyen, T, Takhounts, E and Tannous, R. 1999. *Development of improved injury criteria for the assessment of advanced automotive restraint systems–II*. National Highway Traffic Safety Administration, Washington, DC.

Eppinger, RH, Marcus, JH and Morgan, RM. 1984. *Development of dummy and injury index for NHTSA's thoracic side impact protection research program*. Society of Automotive Engineers, Warrendale, PA.

Estes, M and McElhaney, J. 1970. "Response of brain tissue to compressive loading." Paper presented at 4th ASME Biomechanics Conference

Fallenstein, GT, Hulce, VD and Melvin, JW. 1969. "Dynamic mechanical properties of human brain tissue." *Journal of Biomechanics* 2, 3: 217-26.

Faul, M, Xu, L and Coronado, V. 2010. *Traumatic Brain Injury in the United States: Emergency Department Visits, Hospitalizations, and Deaths*. CDC, Atlanta, GA.

Feng, Y, Clayton, EH, Chang, Y, Okamoto, RJ and Bayly, PV. 2013. "Viscoelastic properties of the ferret brain measured in vivo at multiple frequencies by magnetic resonance elastography." *Journal of Biomechanics* 46, 5: 863-70.

Finan, J, Elkin, B, Pearson, E, Kalbian, I and Morrison, B, III. 2012. "Viscoelastic Properties of the Rat Brain in the Sagittal Plane: Effects of Anatomical Structure and Age." *Annals of Biomedical Engineering* 40, 1: 70-78.

Findley, W and Onaran, K. 1989. *Creep and Relaxation of Nonlinear Viscoelastic Materials*. New York, NY: Dover Publications.

Fisher, R, Krohn, P and Zuckerman, S. 1941. *The relationship between body size and the lethal effects of blast*. Ministry of Home Security, London, UK.

Fung, Y. 1981. *Biomechanics: Mechanical Properties of Living Tissues*. New York: Springer-Verlag.

Funk, JR, Hall, GW, Crandall, JR and Pilkey, WD. 2000. "Linear and Quasi-Linear Viscoelastic Characterization of Ankle Ligaments." *Journal of Biomechanical Engineering* 122, 1: 15-22.

Galford, JE and McElhaney, JH. 1970. "A viscoelastic study of scalp, brain, and dura." *Journal of Biomechanics* 3, 2: 211-21.

Ganpule, S, Alai, A, Plougonven, E and Chandra, N. 2013. "Mechanics of blast loading on the head models in the study of traumatic brain injury using experimental and computational approaches." *Biomechanics and Modeling in Mechanobiology* 12, 3: 511-31.

Garman, RH, Jenkins, LW, Switzer, RC, 3rd, Bauman, RA, Tong, LC, Swauger, PV, Parks, SA, Ritzel, DV, Dixon, CE, Clark, RS, Bayir, H, Kagan, V, Jackson, EK and Kochanek, PM. 2011. "Blast exposure in rats with body shielding is characterized primarily by diffuse axonal injury." *Journal of Neurotrauma* 28, 6: 947-59.

Garo, A, Hrapko, M, van Dommelen, JAW and Peters, GWM. 2007. "Towards a reliable characterisation of the mechanical behaviour of brain tissue: The effects of post-mortem time and sample preparation." *Biorheology* 44, 1: 51-58.

Gefen, A, Gefen, N, Zhu, Q, Raghupathi, R and Margulies, SS. 2003. "Age-Dependent Changes in Material Properties of the Brain and Braincase of the Rat." *Journal of Neurotrauma* 20, 11: 1163-77.

Gefen, A and Margulies, SS. 2004. "Are in vivo and in situ brain tissues mechanically similar?" *Journal of Biomechanics* 37, 9: 1339-52.

Gent, AN and Meinecke, EA. 1970. "Compression, bending, and shear of bonded rubber blocks." *Polymer Engineering & Science* 10, 1: 48-53.

Glasstone, S. 1964. *The effects of nuclear weapons*. US Department of Defense, Washington, DC.

Goldstein, L, Fisher, A, Tagge, C, Zhang, XL, Velisek, L, Sullivan, J, Upreti, C, Kracht, J, Ericsson, M and Wojnarowicz, M. 2012. "Chronic traumatic encephalopathy (CTE) in blast-exposed US military veterans and a new blast neurotrauma mouse model." *Alzheimers & Dementia* 8, 4: P212-P13.

Gómez, AM, Domínguez, CJ, Pedrueza, CI, Calvente, RR, Lillo, VM and Canas, JM. 2007. "Management and analysis of out-of-hospital health-related responses to simultaneous railway explosions in Madrid, Spain." *European Journal of Emergency Medicine* 14, 5: 247-55.

Gondusky, JS and Reiter, MP. 2005. "Protecting military convoys in Iraq: an examination of battle injuries sustained by a mechanized battalion during Operation Iraqi Freedom II." *Military Medicine* 170, 6: 546-49.

Green, A and Rivlin, R. 1959. "The mechanics of non-linear materials with memory." *Archive for Rational Mechanics and Analysis* 4, 1: 387-404.

Hayda, R, Harris, RM and Bass, CD. 2004. "Blast Injury Research: Modeling Injury Effects of Landmines, Bullets, and Bombs." *Clinical Orthopaedics and Related Research*, 422: 97-108.

Hennessy, ER and Zielinski, MR. 2006. *Results of Benchmarking Ergonomics Evaluation of Explosive Ordnance Disposal (EOD) Personal Protective Equipment (PPE) Standard Program*. Army Natick Soldier Center, Natick, MA.

Ho, J and Kleiven, S. 2009. "Can sulci protect the brain from traumatic injury?" *Journal of Biomechanics* 42, 13: 2074-80.

Hofman, MA. 1983. "Energy Metabolism, Brain Size and Longevity in Mammals." *The Quarterly Review of Biology* 58, 4: 495-512.

Hofman, MA. 1985. "Size and Shape of the Cerebral Cortex in Mammals (Part 2 of 2)." *Brain, Behavior and Evolution* 27, 1: 35-40.

Hooker, DR. 1924. "PHYSIOLOGICAL EFFECTS OF AIR CONCUSSION." *American Journal of Physiology -- Legacy Content* 67, 2: 219-74.

Horgan, T and Gilchrist, MD. 2003. "The creation of three-dimensional finite element models for simulating head impact biomechanics." *International Journal of Crashworthiness* 8, 4: 353-66.

Hrapko, M, van Dommelen, JA, Peters, GW and Wismans, JS. 2008. "The Influence of Test Conditions on Characterization of the Mechanical Properties of Brain Tissue." *Journal of Biomechanical Engineering* 130, 3: 031003-03.

Hyde, D. 1991. *CONWEP, Conventional Weapons Effects Program*. US Army Engineers Waterways Experiment Station, Vicksburg, MS.

Iremonger, M. 1997. "Physics of detonations and blast waves". In *Scientific Foundations of Trauma*, edited by Cooper, G, 189-99. New York, NY: Butterworth-Heinemann.

Ji, S, Zhao, W, Li, Z and McAllister, T. 2014. "Head impact accelerations for brain strain-related responses in contact sports: a model-based investigation." *Biomechanics and Modeling in Mechanobiology* 13, 5: 1121-36.

Johnson, CL, McGarry, MDJ, Gharibans, AA, Weaver, JB, Paulsen, KD, Wang, H, Olivero, WC, Sutton, BP and Georgiadis, JG. 2013. "Local mechanical properties of white matter structures in the human brain." *NeuroImage* 79, 0: 145-52.

Kato, K, Fujimura, M, Nakagawa, A, Saito, A, Ohki, T, Takayama, K and Tominaga, T. 2007. "Pressure-dependent effect of shock waves on rat brain: induction of neuronal apoptosis mediated by a caspase-dependent pathway." *Journal of Neurosurgery* 106, 4: 667-76.

Kaur, C, Singh, J, Lim, MK, Ng, BL, Yap, EPH and Ling, EA. 1995. "The response of neurons and microglia to blast injury in the rat brain." *Neuropathology and Applied Neurobiology* 21, 5: 369-77.

Kim, J and Srinivasan, M. 2005. "Characterization of Viscoelastic Soft Tissue Properties from In Vivo Animal Experiments and Inverse FE Parameter Estimation". In *Medical Image Computing and Computer-Assisted Intervention*, edited by Duncan, J and Gerig, G, 599-606. Springer Berlin Heidelberg.

Kincaid, J. 1830. *Adventures in the Rifle Brigade: And, Random Shots from a Rifleman*. London: Mclaren and Company.

Kleiber, M and Rogers, T. 1961. "Energy metabolism." *Annual Review of Physiology* 23, 1: 15-36.

Koliatsos, VE, Cernak, I, Xu, L, Song, Y, Savonenko, A, Crain, BJ, Eberhart, CG, Frangakis, CE, Melnikova, T, Kim, H and Lee, D. 2011. "A Mouse Model of Blast Injury to Brain: Initial Pathological, Neuropathological, and Behavioral Characterization." *Journal of Neuropathology & Experimental Neurology* 70, 5.

Kovesdi, E, Kamnaksh, A, Wingo, D, Ahmed, F, Grunberg, NE, Long, JB, Kasper, CE and Agoston, DV. 2012. "Acute minocycline treatment prevents neurobehavioral impairment in a rat model of mild blast traumatic brain injury." *Frontiers in Neurology* 3.

Krohn, P, Whitteridge, D and Zuckerman, S. 1941. *The effect of blast on the heart and head*. UK Ministry of Home Security: Research and Experiments Department, London, UK.

Krohn, PL, Whitteridge, D and Zuckerman, S. 1942. "Physiological Effects of Blast." *The Lancet* 239, 6183: 252-59.

Larry, D-J. 1812. *Memories de Chirurgie Militaire, et Campagnes*. Paris, France: Smith and Buisson.

Lavery, GG and Lowry, KG. 2004. "Management of blast injuries and shock lung." *Current Opinion in Anesthesiology* 17, 2: 151-57.

Leonardi, AD, Bir, CA, Ritzel, DV and VandeVord, PJ. 2011. "Intracranial pressure increases during exposure to a shock wave." *Journal of Neurotrauma* 28, 1: 85-94.

Lindstedt, SL and Calder, WA, III. 1981. "Body Size, Physiological Time, and Longevity of Homeothermic Animals." *The Quarterly Review of Biology* 56, 1: 1-16.

Lion, A. "On the large deformation behaviour of reinforced rubber at different temperatures." *Journal of the Mechanics and Physics of Solids* 45, 11-12: 1805-34.

Lippert, SA, Rang, EM and Grimm, MJ. 2004. "The high frequency properties of brain tissue." *Biorheology* 41, 6: 681-91.

Liu, K, VanLandingham, MR and Ovaert, TC. 2009. "Mechanical characterization of soft viscoelastic gels via indentation and optimization-based inverse finite element analysis." *Journal of the Mechanical Behavior of Biomedical Materials* 2, 4: 355-63.

Lockey, DJ, MacKenzie, R, Redhead, J, Wise, D, Harris, T, Weaver, A, Hines, K and Davies, GE. 2005. "London bombings July 2005: The immediate pre-hospital medical response." *Resuscitation* 66, 2: ix-xii.

Long, JB, Bentley, TL, Wessner, KA, Cerone, C, Sweeney, S and Bauman, RA. 2009. "Blast overpressure in rats: recreating a battlefield injury in the laboratory." *Journal of Neurotrauma* 26, 6: 827-40.

Lu, J, Ng, KC, Ling, G, Wu, J, Poon, DJ, Kan, EM, Tan, MH, Wu, YJ, Li, P, Moochhala, S, Yap, E, Lee, LK, Teo, M, Yeh, IB, Sergio, DM, Chua, F, Kumar, SD and Ling, EA. 2012. "Effect of blast exposure on the brain structure and cognition in Macaca fascicularis." *Journal of Neurotrauma* 29, 7: 1434-54.

Lucas, SR, Bass, CR, Salzar, RS, Oyen, ML, Planchak, C, Ziemba, A, Shender, BS and Paskoff, G. 2008. "Viscoelastic Properties of the Cervical Spinal Ligaments Under Fast Strain-Rate Deformations." *Acta Biomaterialia* 4, 1: 117-25.

Lynnerup, N. 2001. "Cranial thickness in relation to age, sex and general body build in a Danish forensic sample." *Forensic Science International* 117, 1–2: 45-51.

Macosko, C. 1994. *Rheology: principles, measurement and applications*: VCH Publishers.

Margulies, SS and Thibault, LE. 1992. "A proposed tolerance criterion for diffuse axonal injury in man." *Journal of Biomechanics* 25, 8: 917-23.

Martin, EM, Lu, WC, Helmick, K, French, L and Warden, DL. 2008. "Traumatic Brain Injuries Sustained in the Afghanistan and Iraq Wars." *AJN The American Journal of Nursing* 108, 4: 40-47.

Masel, BE and DeWitt, DS. 2010. "Traumatic brain injury: a disease process, not an event." *Journal of Neurotrauma* 27, 8: 1529-40.

Maynard, R, Coppel, D and Lowry, K. 1997. "Blast injury of the lung". In *Scientific foundations of trauma*, edited by Cooper, G, 24. Oxford, UK: Butterworth-Heinemann.

Mekel, M, Bumenfeld, A, Feigenberg, Z, Ben-Dov, D, Kafka, M, Barzel, O, Michaelson, M and Krausz, MM. 2009. "Terrorist suicide bombings: lessons learned in Metropolitan Haifa from September 2000 to January 2006." *American journal of disaster medicine* 4, 4: 233-48.

Mellor, SG and Cooper, GJ. 1989. "Analysis of 828 servicemen killed or injured by explosion in Northern Ireland 1970–84: The hostile action casualty system." *British Journal of Surgery* 76, 10: 1006-10.

Melvin, JW. 1995. "Injury assessment reference values for the CRABI 6-month infant dummy in a rear-facing infant restraint with airbag deployment." Paper presented at SAE International Congress and Exposition

Merkle, A, Roberts, J and Wickwire, A. 2010. "Evaluation of the human surrogate test model response to ideal and complex blast loading conditions." Paper presented at Personal Armour Systems Symposium (PASS), Quebec, Canada

Mertz, H. 1985. "Biofidelity of the Hybrid III Head." *SAE*.

Metz, H, McElhaney, J and Ommaya, AK. 1970. "A comparison of the elasticity of live, dead, and fixed brain tissue." *Journal of Biomechanics* 3, 4: 453-58.

Miller, K and Chinzei, K. 1997. "Constitutive modelling of brain tissue: Experiment and theory." *Journal of Biomechanics* 30, 11–12: 1115-21.

Montanarelli, N, Hawkins, CE, Shubin, L, Army, UDot, Arsenal, E and America, USo. 1975. *Lightweight Body Armor for Law Enforcement Officers*. US Department of Justice, Washington, DC.

Moochhala, SM, Md, S, Lu, J, Teng, C-H and Greengrass, C. 2004. "Neuroprotective Role of Aminoguanidine in Behavioral Changes after Blast Injury." *The Journal of Trauma and Acute Care Surgery* 56, 2: 393-403.

Mordenti, J. 1985. "Pharmacokinetic scale-up: Accurate prediction of human pharmacokinetic profiles from animal data." *Journal of Pharmaceutical Sciences* 74, 10: 1097-99.

Mordenti, J. 1986. "Man versus beast: Pharmacokinetic scaling in mammals." *Journal of Pharmaceutical Sciences* 75, 11: 1028-40.

Moreland, JC, Wilkes, GL and Turner, RB. 1994. "Viscoelastic behavior of flexible slabstock polyurethane foams: Dependence on temperature and relative humidity. I. Tensile and compression stress (load) relaxation." *Journal of Applied Polymer Science* 52, 4: 549-68.

Moss, S, Huang, Y, Keer, T and Shah, B. 1997. "Development of An Advanced Finite Element Model Database of the Hybrid III Crash Test Dummy Family." *SAE*.

Moss, WC, King, MJ and Blackman, EG. 2009. "Skull flexure from blast waves: a mechanism for brain injury with implications for helmet design." *Physical Review Letters* 103, 10: 108702.

Mota, B and Herculano-Houzel, S. 2014. "All brains are made of this: a fundamental building block of brain matter with matching neuronal and glial masses." *Frontiers in Neuroanatomy* 8: 127.

Mott, F. 1916. "The Effects of High Explosives Upon the Central Nervous System." *The Lancet*, February 12, 1916: 8.

Mott, FW. 1919. *War neuroses and shell shock*. New York, NY, US: Oxford University Press.

Mott, P and Roland, C. 2001. "Aging of Natural Rubber in Air and Seawater." *Rubber Chemistry and Technology* 74: 79-88.

Mundie, TG, Dodd, KT, Lagutchik, MS, Morris, JR and Martin, D. 2000. "Effects of Blast Exposure on Exercise Performance in Sheep." *The Journal of Trauma and Acute Care Surgery* 48, 6: 1115-21.

Nelson, TJ, Clark, T, Stedje-Larsen, ET, Lewis, CT, Grueskin, JM, Echols, EL, Wall, DB, Felger, EA and Bohman, HR. 2008. "Close proximity blast injury patterns from improvised explosive devices in Iraq: a report of 18 cases." *Journal of Trauma and Acute Care Surgery* 65, 1: 212-17.

Nicolle, S, Lounis, M and Willinger, R. 2004. "Shear properties of brain tissue over a frequency range relevant for automotive impact situations: New experimental results." *Stapp Car Crash Journal* 48: 239-58.

Nie, X, Sanborn, B, Weerasooriya, T and Chen, W. 2013. "High-rate bulk and shear responses of bovine brain tissue." *International Journal of Impact Engineering* 53, 0: 56-61.

Northcutt, RG. 2002. "Understanding Vertebrate Brain Evolution." *Integrative and Comparative Biology* 42, 4: 743-56.

Nyein, MK, Jason, AM, Yu, L, Pita, CM, Joannopoulos, JD, Moore, DF and Radovitzky, RA. 2010. "In silico investigation of intracranial blast mitigation with relevance to military traumatic brain injury." *Proceedings of the National Academy of Sciences* 107, 48: 20703-08.

Ogden, RW. 1972. "Large Deformation Isotropic Elasticity - On the Correlation of Theory and Experiment for Incompressible Rubberlike Solids." *Proceedings of the Royal Society of London. Series A, Mathematical and Physical Sciences* 326, 1567: 565-84.

Ommaya, AK and Hirsch, AE. 1971. "Tolerances for cerebral concussion from head impact and whiplash in primates." *Journal of Biomechanics* 4, 1: 13-21.

Ommaya, AK, Hirsch, AE, Yarnell, P and Harris, EH. 1967. *Scaling of experimental data on cerebral concussion in sub-human primates to concussion threshold for man*. David W Taylor Naval Ship Research and Development Center, Bethesda, MD.

Owens, BD, Kragh Jr, JF, Wenke, JC, Macaitis, J, Wade, CE and Holcomb, JB. 2008. "Combat wounds in operation Iraqi Freedom and operation Enduring Freedom." *Journal of Trauma* 64, 2: 295.

Panzer, A, Capehart, B, Wood, G and Bass, C. 2012a. "Lethal Consequences of Missed TBI Diagnosis: Execution by World War I Firing Squad." Paper presented at National Neurotrauma Society Annual Meeting, Phoenix, AZ

Panzer, M and Bass, C. 2012b. "Human results from animal models: Scaling laws for blast neurotrauma." Paper presented at National Neurotrauma Society Annual Meeting, Phoenix, AZ, July.

Panzer, M, Myers, B, Capehart, B and Bass, C. 2012c. "Development of a Finite Element Model for Blast Brain Injury and the Effects of CSF Cavitation." *Annals of Biomedical Engineering* 40, 7: 1530-44.

Panzer, MB. 2012. "Numerical Simulation of Primary Blast Brain Injuries." PhD diss., Duke University.

Panzer, MB, Bass, CR, Rafaels, KA, Shridharani, J and Capehart, BP. 2012d. "Primary blast survival and injury risk assessment for repeated blast exposures." *The Journal of Trauma and Acute Care Surgery* 72, 2: 454-66.

Panzer, MB, Cameron, R, Rafaels, KA, Shridharani, J and Capehart, BP. 2012e. "Primary blast survival and injury risk assessment for repeated blast exposures." *Journal of trauma and acute care surgery* 72, 2: 454-66.

Panzer, MB, Myers, BS and Bass, CR. 2013. "Mesh considerations for finite element blast modelling in biomechanics." *Computer methods in biomechanics and biomedical engineering* 16, 6: 612-21.

Panzer, MB, Wood, GW and Bass, CR. 2014. "Scaling in neurotrauma: How do we apply animal experiments to people?" *Experimental Neurology* 261, 0: 120-26.

Pare, A and Buon, G. 1585. *Les Ouevres d'Ambrose Pare Conseiller et Permier Chirugien de Roy*. Paris: Chez Gabrael Buon.

Pellman, EJMD, Viano, DCDm, Ph.D., Tucker, AMMD, Casson, IRMD and Waeckerle, JFMD. 2003. "Concussion in Professional Football: Reconstruction of Game Impacts and Injuries." *Neurosurgery October* 53, 4: 799-814.

Pervin, F and Chen, WW. 2009. "Dynamic mechanical response of bovine gray matter and white matter brain tissues under compression." *Journal of Biomechanics* 42, 6: 731-35.

Phillips, YY, Mundie, TG, Yelverton, JT and Richmond, DR. 1988. "Cloth ballistic vest alters response to blast." *Journal of Trauma* 28, 1 Suppl: S149-52.

Pipkin, AC and Rogers, TG. 1968. "A non-linear integral representation for viscoelastic behaviour." *Journal of the Mechanics and Physics of Solids* 16, 1: 59-72.

Plazek, DJ. 1965. "Temperature Dependence of the Viscoelastic Behavior of Polystyrene." *The Journal of Physical Chemistry* 69, 10: 3480-87.

Prange, MT, Meaney, DF and Margulies, SS. 2000. "Defining brain mechanical properties: effects of region, direction, and species." *Stapp Car Crash Journal* 44: 205-13.

Pun, PB, Kan, EM, Salim, A, Li, Z, Ng, KC, Moochhala, SM, Ling, EA, Tan, MH and Lu, J. 2011. "Low level primary blast injury in rodent brain." *Frontiers in Neurology* 2: 19.

Purves, D, Augustine, G, Fitzpatrick, D, Hall, W, LaMantia, A, McNamara, J and White, L. 2008. *Principles of Cognitive Neuroscience*. Sunderland, MA: Sinauer Associates.

Rafaels, K, Bass, CR, Salzar, RS, Panzer, MB, Woods, W, Feldman, S, Cummings, T and Capehart, B. 2011. "Survival risk assessment for primary blast exposures to the head." *Journal of Neurotrauma* 28, 11: 2319-28.

Rafaels, KA, Bass, CR, Panzer, MB and Salzar, RS. 2010. "Pulmonary Injury Risk Assessment for Long-Duration Blasts: A Meta-Analysis." *The Journal of Trauma and Acute Care Surgery* 69, 2: 368-74.

Rafaels, KA, Cameron, R, Panzer, MB, Salzar, RS, Woods, WA, Feldman, SH, Walilko, T, Kent, RW, Capehart, BP and Foster, JB. 2012. "Brain injury risk from primary blast." *The Journal of Trauma and Acute Care Surgery* 73, 4: 895-901.

Raftenberg, MN, Scheidler, MJ and Moy, P. 2004. *Transverse compression response of a multi-ply Kevlar vest*. Army Research Laboratory, Aberdeen, MD.

Ramasamy, A, Harrisson, SE, Clasper, JC and Stewart, MPM. 2008. "Injuries From Roadside Improvised Explosive Devices." *The Journal of Trauma and Acute Care Surgery* 65, 4: 910-14.

Readnower, RD, Chavko, M, Adeeb, S, Conroy, MD, Pauly, JR, McCarron, RM and Sullivan, PG. 2010. "Increase in blood–brain barrier permeability, oxidative stress, and activated microglia in a rat model of blast-induced traumatic brain injury." *Journal of Neuroscience Research* 88, 16: 3530-39.

Richmond, D, Goldizen, V, Clare, V, Pratt, D, Sherping, F, Sanchez, R, Fischer, C and White, C. 1962a. "The biologic response to overpressure. III. Mortality in small animals exposed in a shock tube to sharprising overpressures of 3 to 4 msec duration." *Aerospace medicine* 33: 1-27.

Richmond, D, Goldizen, V, Clare, V and White, C. 1962b. *The Overpressure-Duration Relationship and Lethality in Small Animals*. Lovelace Foundation for Medical Education and Research, Albuqueruqe, NM.

Richmond, D, SANCHEZ, R, Goldizen, V, CLARE, V, WHITE, C and PRATT, D. 1961. "Biological Effects of Overpressure II: A shock tube utiliized to produce sharp-rising overpressures of 400 milliseconds duration and its employment in biomedical experiments." *Aerospace Medicine* 32, 11: 997.

Richmond, D, Yelverton, J, Fletcher, E, Phillips, Y and Jaeger, J. 1982. *Damage-risk criteria for personnel exposed to repeated blasts*. Lovelace Foundation for Medical Education and Research, Albuquerque, NM.

Richmond, DR, Damon, EG, Bowen, IG, Fletcher, ER and White, CS. 1966. *Air-blast studies with eight species of mammals*. Lovelace Foundation for Medical Education and Research, Albuquerque, NM.

Richmond, DR, Damon, EG, Fletcher, ER, Bowen, IG and White, CS. 1968. "The Relationship between Selected Blast-Wave Parameters and the Response of Mammals Exposed to Air Blast." *Annals of the New York Academy of Sciences* 152, 1: 103-21.

Richmond, DR, Wetherbe, M, Taborelli, R, Sanchez, R and Sherping, F. 1959. *Shock Tube Studies of the Effects of Sharp-Rising, Long-Duration Overpressures on Biological Systems*. Lovelace Foundation for Medical Education and Research, Albuquerque, NM.

Richmond, DR and White, CS. 1962c. *A Tentative Estimation of Mans Tolerance to Overpressures from Air Blast*. Lovelace Foundation for Medical Education and Research, Albuquerque, NM.

Richmond, DR, Yelverton, JT and Fletcher, ER. 1981. *The biological effects of repeated blasts*. Lovelace Foundation for Medical Education and Research, Albuquerque, NM.

Richmond, DR, Yelverton, JT, Fletcher, ER and Phillips, YY. 1985. *Biologic response to complex blast waves*. Lovelace Foundation for Medical Education and Research, Albuquerque, NM.

Risling, M, Plantman, S, Angeria, M, Rostami, E, Bellander, BM, Kirkegaard, M, Arborelius, U and Davidsson, J. 2011. "Mechanisms of blast induced brain injuries, experimental studies in rats." *NeuroImage* 54, Supplement 1, 0: S89-S97.

Risling, M, Suneson, A, Skold, M, Lai, L, Abo, M, Chen, Z and Bjelke, B. 2002. *Evaluation of Diffuse Brain Injury with Magnetic Resonance Imaging: Technical Report for the Swedish Defence Research Agency*. Swedish Defence Research Agency, Stockholm, Sweden.

Rodoplu, Ü, Arnold, JL, Tokyay, R, Ersoy, G, Cetiner, S and Yücel, T. 2004. "Mass-Casualty Terrorist Bombings In Istanbul, Turkey, November 2003: Report of the Events and the Prehospital Emergency Response." *Prehospital and Disaster Medicine* 19, 02: 133-45.

Rubovitch, V, Ten-Bosch, M, Zohar, O, Harrison, CR, Tempel-Brami, C, Stein, E, Hoffer, BJ, Balaban, CD, Schreiber, S, Chiu, W-T and Pick, CG. 2011. "A mouse model of blast-induced mild traumatic brain injury." *Experimental Neurology* 232, 2: 280-89.

Rupert, NL, Green, WH, Wells, JM and Doherty, KJ. 2001. *Damage Assessment in TiB2 Ceramic Armor Targets*. Army Research Laboratory, Aberdeen, MD.

Saljo, A, Arrhen, F, Bolouri, H, Mayorga, M and Hamberger, A. 2008. "Neuropathology and pressure in the pig brain resulting from low-impulse noise exposure." *Journal of Neurotrauma* 25, 12: 1397-406.

Saljo, A, Bao, F, Haglid, KG and Hansson, HA. 2000. "Blast exposure causes redistribution of phosphorylated neurofilament subunits in neurons of the adult rat brain." *Journal of Neurotrauma* 17, 8: 719-26.

Säljö, A, Bao, F, Hamberger, A, Haglid, KG and Hansson, H-A. 2001. "Exposure to short-lasting impulse noise causes microglial and astroglial cell activation in the adult rat brain." *Pathophysiology* 8, 2: 105-11.

Saljo, A, Bao, F, Jingshan, S, Hamberger, A, Hansson, HA and Haglid, KG. 2002. "Exposure to short-lasting impulse noise causes neuronal c-Jun expression and induction of apoptosis in the adult rat brain." *Journal of Neurotrauma* 19, 8: 985-91.

Saljo, A, Bolouri, H, Mayorga, M, Svensson, B and Hamberger, A. 2010. "Low-level blast raises intracranial pressure and impairs cognitive function in rats: prophylaxis with processed cereal feed." *Journal of Neurotrauma* 27, 2: 383-9.

Sasser, SM, Sattin, RW, Hunt, RC and Krohmer, J. 2006. "Blast Lung Injury." *Prehospital Emergency Care* 10, 2: 165-72.

Savage, VM, Allen, AP, Brown, JH, Gillooly, JF, Herman, AB, Woodruff, WH and West, GB. 2007. "Scaling of number, size, and metabolic rate of cells with body size in mammals." *Proceedings of the National Academy of Science* 104, 11: 4718-23.

Schapery, RA. 2000. "Nonlinear viscoelastic solids." *International Journal of Solids and Structures* 37, 1–2: 359-66.

Seal, KH, Cohen, G, Waldrop, A, Cohen, BE, Maguen, S and Ren, L. 2011. "Substance use disorders in Iraq and Afghanistan veterans in VA healthcare, 2001–2010: Implications for screening, diagnosis and treatment." *Drug and Alcohol Dependence* 116, 1–3: 93-101.

Sharma, SP and Wilson, GJ. 1996. "Computations of axisymmetric flows in hypersonic shock tubes." *Journal of Thermophysics and Heat Transfer* 10, 1: 169-76.

Shergold, OA, Fleck, NA and Radford, D. 2006. "The uniaxial stress versus strain response of pig skin and silicone rubber at low and high strain rates." *International Journal of Impact Engineering* 32, 9: 1384-402.

Shier, D, Butler, J and Lewis, R. 2007. *Hole's human anatomy & physiology*. New York, NY: McGraw-Hill.

Shridharani, J, Wood, G, Panzer, M, Matthews, K, Perritt, C, Masters, K and Bass, C. 2012a. "Blast effects behind ballistic protective helmets." Paper presented at Personal Armor Systems Symposium, Nuremberg, Germany

Shridharani, JK, Wood, GW, Panzer, MB, Capehart, BP, Nyein, MK, Radovitzky, RA and Dale'Bass, CR. 2012b. "Porcine head response to blast." *Frontiers in Neurology* 3.

Shuck, LZ and Advani, SH. 1972. "Rheological Response of Human Brain Tissue in Shear." *Journal of Fluids Engineering* 94, 4: 905-11.

Shulyakov, AV, Cenkowski, SS, Buist, RJ and Del Bigio, MR. 2011. "Age-dependence of intracranial viscoelastic properties in living rats." *Journal of the Mechanical Behavior of Biomedical Materials* 4, 3: 484-97.

SIAD. "SIAD Independent Panel on the Safety and Security of UN Personnel in Iraq." Retrieved 7/16/11, from http://www.un.org/News/dh/iraq/safety-security-un-personnel.iraq.pdf.

Smith, DH and Meaney, DF. 2000. "Axonal Damage in Traumatic Brain Injury." *The Neuroscientist* 6, 6: 483-95.

Song, B, Chen, W and Cheng, M. 2004. "Novel model for uniaxial strain-rate-dependent stress-strain behavior of ethylene-propylene-diene monomer rubber in compression or tension." *Journal of Applied Polymer Science* 92, 3: 1553-58.

Stahl, WR. 1967. "Scaling of respiratory variables in mammals." *Journal of Applied Physiology* 22, 3: 453-60.

Statistics, DoDPaMC. 2012. *Global war on terrorism - Casualty summary by reason: October 7, 2001 through May 7, 2012*. Department of Defense, Washington, DC.

Stein, M and McAllister, T. 2009. "Exploring the Convergence of Posttraumatic Stress Disorder and Mild Traumatic Brain Injury." *American Journal of Psychiatry* 166, 7: 768-76.

Stuhmiller, JH, Santee, W and Friedl, K. 2008. "Blast injury, translating research into operational medicine." *Military Quantitative Physiology: Problems and Concepts in Military Operational Medicine*: 267-302.

Suneson, A, Axelsson, H, Hjelmqvist, H, Medin, A and Persson, J. 2000. *Physiological changes in pigs exposed to a blast wave from a detonating high-explosive charge*. Association of Military Surgeons, Bethesda, MD.

Svetlov, SI, Prima, V, Kirk, DR, Gutierrez, H, Curley, KC, Hayes, RL and Wang, KKW. 2010. "Morphologic and Biochemical Characterization of Brain Injury in a Model of Controlled Blast Overpressure Exposure." *The Journal of Trauma and Acute Care Surgery* 69, 4: 795-804.

Taber, K, Warden, D and Hurley, R. 2006. "Blast-related traumatic brain injury: what is known?" *The Journal of neuropsychiatry and clinical neurosciences* 18, 2: 141-45.

Takhounts, EG, Crandall, JR and Darvish, K. 2003. "On the importance of nonlinearity of brain tissue under large deformations." *Stapp Car Crash Journal* 47: 79-92.

Tanielian, TL and Jaycox, L. 2008. *Invisible wounds of war: Psychological and cognitive injuries, their consequences, and services to assist recovery*. Santa Monica, CA: Rand Corporation.

Taylor, PA and Ford, CC. 2009. "Simulation of Blast-Induced Early-Time Intracranial Wave Physics leading to Traumatic Brain Injury." *Journal of Biomechanical Engineering* 131, 6: 061007-07.

Thibault, KL and Margulies, SS. 1998. "Age-dependent material properties of the porcine cerebrum: effect on pediatric inertial head injury criteria." *Journal of Biomechanics* 31, 12: 1119-26.

Treloar, LRG, Hopkins, HG, Rivlin, RS and Ball, JM. 1976. "The Mechanics of Rubber Elasticity [and Discussions]." *Proceedings of the Royal Society of London. Series A, Mathematical and Physical Sciences* 351, 1666: 301-30.

Trudeau, D, Anderson, J, Hansen, L, Shagalov, D and Schmoller, J. 1998. "Findings of Mild Traumatic Brain Injury in Combat Veterans With PTSD and a History of Blast Concussion." *The Journal of Neuropsychiatry and Clinical Neurosciences* 10, 3: 308-13.

Urbanczyk, CA, Palmeri, ML and Bass CR. 2015. "Material Characterization of in Vivo and in Vitro Porcine Brain Using Shear Wave Elasticity." *Ultrasound in Medicine & Biology* 41, 3: 713-23.

van Dommelen, J, Jolandan, M, Ivarsson, B, Millington, S, Raut, M, Kerrigan, J, Crandall, J and Diduch, D. 2006. "Nonlinear Viscoelastic Behavior of Human Knee Ligaments Subjected to Complex Loading Histories." *Annals of Biomedical Engineering* 34, 6: 1008-18.

van Dongen, P. 1998a. "Brain Size in Vertebrates". In *The Central Nervous System of Vertebrates*, edited by Nieuwenhuys, R, 2099-134. Berlin: Springer.

Van Dongen, P. 1998b. "Neocortex: Quantitative Aspects and Folding". In *The Central Nervous System of Vertebrates*, edited by Nieuwenhuys, R, 2008-23. Berlin: Springer.

VandeVord, P, Bolander, R, Sajja, V, Hay, K and Bir, C. 2012. "Mild Neurotrauma Indicates a Range-Specific Pressure Response to Low Level Shock Wave Exposure." *Annals of Biomedical Engineering* 40, 1: 227-36.

Vappou, J, Breton, E, Choquet, P, Willinger, R and Constantinesco, A. 2008. "Assessment of in vivo and post-mortem mechanical behavior of brain tissue using magnetic resonance elastography." *Journal of Biomechanics* 41, 14: 2954-59.

Viano, D, Aldman, B, Pape, K, Hoof, Jv and Holst, Hv. 1997. "Brain kinematics in physical model tests with translational and rotational acceleration." *International Journal of Crashworthiness* 2, 2: 191-206.

Walley, SM, Field, JE, Pope, PH and Safford, NA. 1989. "A Study of the Rapid Deformation Behaviour of a Range of Polymers." *Philosophical Transactions of the Royal Society of London. Series A, Mathematical and Physical Sciences* 328, 1597: 1-33.

Wang, HC and Wineman, AS. 1972. "A mathematical model for the determination of viscoelastic behavior of brain in vivo—I Oscillatory response." *Journal of Biomechanics* 5, 5: 431-46.

Wang, Y, Wei, Y, Oguntayo, S, Wilkins, W, Arun, P, Valiyaveettil, M, Song, J, Long, JB and Nambiar, MP. 2011. "Tightly coupled repetitive blast-induced traumatic brain injury: development and characterization in mice." *Journal of Neurotrauma* 28, 10: 2171-83.

Wang, Y, Ye, Z, Hu, X, Huang, J and Luo, Z. 2010. "Morphological changes of the neural cells after blast injury of spinal cord and neuroprotective effects of sodium β-aescinate in rabbits." *Injury* 41, 7: 707-16.

Warden, D. 2006. "Military TBI During the Iraq and Afghanistan Wars." *The Journal of Head Trauma Rehabilitation* 21, 5: 398-402.

Wei, YT, Nasdala, L, Rothert, H and Xie, Z. 2004. "Experimental investigations on the dynamic mechanical properties of aged rubbers." *Polymer Testing* 23, 4: 447-53.

White, CS, Jones, RK, Damon, EG, Fletcher, ER and Richmond, DR. 1971. *The biodynamics of air blast*. Lovelace Foundation for Medical Education and Research, Albuquerque, NM.

Wood, G, Panzer, M, Shridharani, J, Matthews, K, Capehart, B, Myers, B and Bass, C. 2012. "Attenuation of blast pressure behind ballistic protective vests." *Injury Prevention* 19:19-25.

Woods, AS, Colsch, B, Jackson, SN, Post, J, Baldwin, K, Roux, A, Hoffer, B, Cox, BM, Hoffer, M, Rubovitch, V, Pick, CG, Schultz, JA and Balaban, C. 2013. "Gangliosides and Ceramides Change in a Mouse Model of Blast Induced Traumatic Brain Injury." *ACS Chemical Neuroscience* 4, 4: 594-600.

Wright, D, Kellerman, A, McGuire, L, Chen, B and Popovic, T. 2013. "CDC grand rounds: reducing severe traumatic brain injury in the United States." *MMWR. Morbidity and mortality weekly report* 62, 27: 549.

Wu, JD and Liechti, KM. 2000. "Multiaxial and Time Dependent Behavior of a Filled Rubber." *Mechanics of Time-Dependent Materials* 4, 4: 293-331.

Wu, JZ, Dong, RG, Smutz, PW and Schopper, AW. 2003. "Nonlinear and viscoelastic characteristics of skin under compression: experiment and analysis." *Bio-Medical Materials and Engineering* 13, 4: 373-85.

Yang, K and Le, J. 1992. "Finite Element Modeling of Hybrid III Head-Neck Complex." *SAE*.

Yang, KH, Hu, J, White, NA, King, AI, Chou, CC and Prasad, P. 2006. "Development of numerical models for injury biomechanics research: a review of 50 years of publications in the Stapp Car Crash Conference." *Stapp Car Crash Journal* 50: 429-90.

Yang, Z, Wang, Z, Tang, C and Ying, Y. 1996. "Biological Effects of Weak Blast Waves and Safety Limits for Internal Organ Injury in the Human Body." *Journal of Trauma and Acute Care Surgery* 40, 3S: 81S-84S.

Yeoh, S, Bell, ED and Monson, KL. 2013. "Distribution of blood–brain barrier disruption in primary blast injury." *Annals of biomedical engineering* 41, 10: 2206-14.

Young, AJ, Jaeger, JJ, Phillips, YY, Yelverton, JT and Richmond, DR. 1985. "The influence of clothing on human intrathoracic pressure during airblast." *Aviation, Space, and Environmental Medicine* 56, 1: 49-53.

Yu, A, Bigler, B, Wood, G, Panzer, M, Meaney, D, Morrison III, B and Bass, C. 2014. "In vs. Out: Controversies in shock tube blast experiments." Paper presented at National Neurotrauma Society Annual Meeting, San Francisco, CA

Yu, A, Wang, H, Matthews, K and Bass, C. 2012. "Mouse Lethality Risk and Intracranial Pressure During Exposure to Blast." Paper presented at Biomedical Engineering Society National Meeting, Atlanta, GA, October 2012.

Zatzick, DF, Rivara, FP, Jurkovich, GJ and et al. 2010. "MUltisite investigation of traumatic brain injuries, posttraumatic stress disorder, and self-reported health and cognitive impairments." *Archives of General Psychiatry* 67, 12: 1291-300.

Zhang, L, Yang, KH, Dwarampudi, R, Omori, K, Li, T, Chang, K, Hardy, WN, Khalil, TB and King, AI. 2001. "Recent advances in brain injury research: a new human head model development and validation." *Stapp Car Crash Journal*, 45: 369-94.

Zhang, M, Zheng, YP and Mak, AFT. 1997. "Estimating the effective Young's modulus of soft tissues from indentation tests—nonlinear finite element analysis of effects of friction and large deformation." *Medical Engineering & Physics* 19, 6: 512-17.

Zuckerman, S. 1940. "Experimental study of blast injuries to the lungs." *The Lancet* 236, 6104: 219-24.

Zuckerman, S. 1941. "Discussion on the problem of blast injuries." *Proceedings of the Royal Society of Medicine* 34: 171-88.

Biography

Garrett Wayne Wood

Born: Mint Hill, NC on April 1, 1986

EDUCATION:

Ph.D. Biomedical Engineering   April, 2015
     Duke University, Durham, NC, United States
B.S.E. Biomedical and Mechanical Engineering   May, 2008
     Duke University, Durham, NC, United States

PUBLICATIONS:

Wood, G.W., Panzer, M.B., Bass, C.R., Myers, B.S. (2010). Viscoelastic Properties of Hybrid III Head Skin. *SAE International Journal of Materials and Manufacturing. 3*(1):186-193.

Bass, C.R., Panzer, M.B., Rafaels, K.A., **Wood, G.W.**, Shridharani, J.K., Capehart, B.P (2011). Brain injuries from blast. *Annals of Biomedical Engineering*. 40(1):1-18.

Shridharani, J.K., **Wood, G.W**., Panzer, M.B., Capehart, B.P., Nyein, M.K., Radovitzky, R.A., Bass, C.R. (2012). Porcine head response to blast. *Frontiers in Neurology. 3*.

Wood, G.W., Panzer, M.B., Shridharani, J.K., Matthews, K.A., Capehart, B.P., Myers, B.S., Bass, C.R. (2012). Attenuation of blast pressure behind ballistic protective vests. *Injury Prevention.* 19:19-25.

Panzer, M.B., **Wood, G.W.**, Bass, C.R. (2014). Scaling in neurotrauma: how do we apply animal experiments to people? *Experimental Neurology*. 261:120-126.